Identification of substrates of the *Drosophila* F-Box protein Skp2 by flow cytometric and biochemical assays

DISSERTATION ZUR ERLANGUNG DES
DOKTORGRADES DER NATURWISSENSCHAFTEN (DR. RER. NAT.)
DER FAKULTÄT FÜR BIOLOGIE UND VORKLINISCHE MEDIZIN
DER UNIVERSITÄT REGENSBURG

vorgelegt von
Thomas Rössler

aus
Regensburg

im Jahr
2019

Das Promotionsgesuch wurde eingereicht am

Die Arbeit wurde angeleitet von
Prof. Dr. Frank Sprenger

Unterschrift

Table of Contents

1 Abstract

Proteasomal degradation of proteins is one of many ways for a cell to regulate different processes to achieve cell homeostasis and correct functioning. It is especially important for cell cycle regulation, since it allows for timely, rapid degradation of proteins. Key players of proteasomal degradation are E3 ubiquitin ligases that transfer ubiquitin molecules to the respective substrate proteins, which ultimately lead to recognition by the proteasome and degradation of said proteins. A prominent E3 ubiquitin ligase that also has important tasks in cell cycle regulation is the SCF-complex. One part of the SCF-complex, the F-Box proteins, fulfill the role of substrate recognition subunits.

Skp2 is one of the most characterized F-Box proteins in higher eukaryotes, with a broad range of different substrates. Perhaps the most important are p21, p27 and p57, cyclin dependent kinase inhibitors (CKI) that are responsible for inhibition of the activity of the CycE/Cdk2 complex. These CKIs are thereby exerting a regulatory function in the transition from G1- to S-Phase. In the cell cycle, SCF^{Skp2} does target the three CKIs for ubiquitination and subsequent proteasomal degradation, resulting in CycE/Cdk2 activity and beginning of S-Phase. Other substrates of Skp2 are for example Cdt1, necessary for the licensing of origin of replications and ordered DNA replication, or CycE, which activates the Cyclin dependent kinase 2. Skp2 in *Drosophila melanogaster* is poorly characterized, in comparison. Only one substrate has been proposed up to date, the p21, p27 and p57 homologue Dacapo, although the data availability is not definite in this case.

This thesis centers on the characterization of Skp2 in *Drosophila* Schneider cells and the search for new Skp2 interaction partners in the fly. This was achieved by analysis of the cell cycle distribution, live cell imaging experiments, biochemical interaction assays, mass-spectrometric analysis of Skp2 binding partners and protein stability analysis by flow cytometry, which was developed in the Sprenger group.

Skp2 overexpression resulted in a longer G1-Phase, knockdown in faster transition from G1 to S. This result together with the impassivity of Dap stability upon modulation of Skp2 levels, the inconclusive interaction between Skp2 and Dap and the outcome that Skp2 enhanced the Dap cell cycle phenotype makes it highly unlikely that Dap is negatively regulated by Skp2. Instead, experiments showed that Cdt1 is probably a substrate of SCF^{Skp2} in *Drosophila*. The results also hinted that Cdt1 has to be phosphorylated for this interaction and experiments were undertaken to identify the responsible phosphorylation sites in Cdt1. For CycE on the other hand it was not possible to determine regulation of protein stability by Skp2 with certainty even though biochemical interaction could be seen. The mass-spectrometric analysis of Skp2 binding partners did not identify new substrates of Skp2.

In opposition to the state of knowledge, Dap seems to be not a substrate of the SCF^{Skp2} ubiquitin ligase. Cdt1 on the other hand seems to be a new target of Skp2 in *D. melanogaster* and further work will reveal the phosphorylation sites necessary for this relationship. These results shed new light on the role that Skp2 has on the *Drosophila* cell cycle.

2 Kurzzusammenfassung

Der proteasomale Abbau von Proteinen ist einer von vielen Wegen, wie eine Zelle die verschiedensten Prozesse für ein physiologisches Gleichgewicht und den korrekten Ablauf lenken kann. Insbesondere spielt er für die Regulation des Zellzyklus eine wichtige Rolle, da es dadurch möglich wird, Proteine zeitgenau und schnell abzubauen. Hauptbestandteil des proteasomalen Abbaus sind E3-Ubiquitin Ligasen, die Ubiquitin-Moleküle auf die entsprechenden Proteinsubstrate übertragen, was schlussendlich dazu führt, dass das Proteasom diese erkennt und abbaut. Eine bekannte E3-Ubiquitin Ligase, die auch wichtige Aufgaben während des Zellzyklus erfüllt, ist der SCF-Komplex. Ein Teil des SCF-Komplexes, die F-Box Proteine, sind verantwortlich für die Erkennung der Substrate.

Skp2 ist eines der am besten untersuchten F-Box Proteine in höheren Eukaryoten und hat eine große Bandbreite an Substraten. Vielleicht die wichtigsten Substrate sind p21, p27 und p57, Inhibitoren von Cyclin-abhängigen Kinasen (CKI), die sich verantwortlich zeichnen für die Inhibierung der Aktivität des CycE/Cdk2 Komplexes. Diese CKIs üben dabei eine regulatorische Funktion beim Übergang von der G1- in die S-Phase aus. Während des Zellzyklus sorgt SCF^{Skp2} für die Ubiquitinierung und anschließendem proteasomalen Abbau, was zu Aktivität von CycE/Cdk2 und Beginn der S-Phase führt. Andere Substrate von Skp2 sind zum Beispiel Cdt1, notwendig für die Lizensierung von Replikations-Origins und geordneter DNA Replikation, oder CycE, welches die Cyclin-abhängige Kinase 2 aktiviert. Im Vergleich dazu ist Skp2 in *Drosophila melanogaster* nur wenig beschrieben. Bis jetzt ist nur Dacapo als Substrat vorgeschlagen, das Homolog zu p21, p27 und p57, jedoch ist in diesem Fall die Datenlage nicht eindeutig.

In dieser Doktorarbeit werden die Effekte von Skp2 in *Drosophila* Schneider Zellen untersucht und neue Interaktionspartner von Skp2 ermittelt. Eingesetzt wurden hierzu Untersuchungen zur Zellzyklusverteilung, Live Cell Imaging Experimente, Untersuchungen zur biochemischen Interaktion, massenspektrometrische Analyse von Skp2 Bindungspartnern und Untersuchungen der Proteinstabilität mittels Durchflusszytometrie, ein Ansatz, der in der Arbeitsgruppe Sprenger entwickelt wurde.

Überexpression von Skp2 resultierte in einer verlängerten G1-Phase, der Knockdown hingegen in einem schnelleren Übergang von G1 nach S. Dieses Ergebnis, zusammen mit der Erkenntnis, dass die Dap Stabilität unempfindlich gegenüber Veränderungen der Skp2 Level war, dass die Interaktion zwischen Skp2 und Dap nicht eindeutig bestimmbar war und das Skp2 den Zellzyklusphänotyp von Dap verstärkte, zeigt, dass ein negativer Effekt von Skp2 auf Dap sehr unwahrscheinlich ist. Stattdessen zeigte sich, dass Cdt1 in Fliegen wahrscheinlich ein neues Substrat von SCF^{Skp2} sein könnte. Die Ergebnisse deuteten auch darauf hin, dass Cdt1 für diese Interaktion phosphoryliert sein muss und Experimente wurden ausgeführt um die verantwortlichen Phosphorylierungsstellen zu identifizieren. Für CycE hingegen war es nicht möglich eine Regulation der Proteinstabilität mit Sicherheit festzustellen, obwohl eine biochemische Interaktion ermittelt werden konnte. Die massenspektrometrische Analyse von Skp2 Bindungspartnern konnte keine neuen Substrate von Skp2 identifizieren.

Im Gegensatz zum derzeitigen Wissensstand scheint Dap kein Substrat von SCF^{Skp2} zu sein. Auf der anderen Seite scheint Cdt1 als ein neues Substrat von Skp2 in *D. melanogaster* identifiziert worden zu sein. Weitere Experimente werden zeigen, welche Phosphorylierungsstellen in diesem Zusammenhang wichtig sind. Diese Ergebnisse werfen ein neues Licht auf die Rolle, die Skp2 im Zellzyklus von *Drosophila* spielt.

3 Introduction

3.1. Principles of cell cycle regulation

The cell cycle is a fundamental process in biology. Its purpose is to multiply the number of cells of organisms. After a cell receives an internal or external signal to start the division process, a molecular machinery is set into motion and the cell runs through a well ordered program which consists of certain distinct phases, typically G1-, S- and G2-Phase (combined also called interphase) and M-Phase (Figure 1). The cell cycle can show great plasticity, however. For example, during *Drosophila melanogaster* larval development, G1- and G2-Phases are absent in the beginning and the cell cycle only consists of alternating M- and S-Phases (Morgan, 2007). In the end, two daughter cells will emerge that are identical on the DNA level. If cells divide symmetrically, the two daughter cells will receive the same set of RNAs and proteins. If asymmetrical cell division occurred, the daughter cells will differ in their RNA and protein setting. This has great influence on the destiny of the two cells (Knoblich, 2010; Roubinet and Cabernard, 2014). After the cell cycle is completed, cells may directly undergo another round of replication, increasing the cell number further, or may exit the cell cycle by entering the so-called G0-state. Cells either stay in G0 until another division signal arrives or exit the cell cycle permanently for differentiation. Consequently, the cell cycle plays the most fundamental role in many different processes, from development and growth to wound healing and homeostasis (Morgan, 2007).

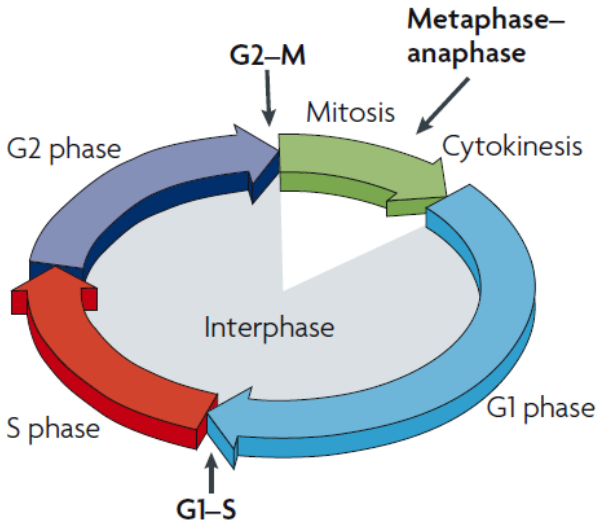

Figure 1 General model of the cell cycle
The prototypical model of the cell cycle consists of G1-, S-, G2- and M-Phase. Three important checkpoints are also marked: G1-S transition, G2-M transition and the transition from metaphase to anaphase (Hochegger et al., 2008).

The processes of the cell cycle have to be strongly regulated to guarantee correct development and survival of organisms. For example, cells have to ensure that DNA replication occurs only once during the cycle. If some part or even the whole of the genome is replicated more than once during S-Phase, the molecular architecture of the daughter cells will be tremendously disturbed. Therefore, diverse control mechanisms exist for the different proteins that play important roles in the replication machinery.

Besides DNA replication, many more aspects during the cell cycle have to be regulated. The beginning of a new cell cycle, the process of DNA replication itself, DNA damage control, the transition from G2 to M,

the assembly of the spindle during mitosis and the separation of sister chromatids are all monitored closely. Different checkpoints exist to control these processes. Checkpoints are molecular mechanisms in the cell cycle that monitor if certain requirements are met. If not, the checkpoint sends out molecular signals that first for all stop the cell cycle. Repair mechanisms may also be activated that remove the deficiencies. If this is not possible because the damage cannot be repaired, cell apoptosis is activated.

The failing of checkpoints has severe consequences for single cells and the whole organism. DNA damage can accumulate, since DNA repair systems are unable to start working, leading up to severe mutations. Furthermore, the cell cycle itself may become unregulated, resulting in developmental deficiencies and the formation of tumors. Indeed, mutated cell cycle regulators are typical for cancer (Heo et al., 2016). Two of the most important aspects that cells have to regulate are the start of a new cell cycle, especially the transition from G1- to S-Phase, and the molecular regulation of DNA replication, especially the prevention of rereplication.

3.2. The start of a new cell cycle and transition from G1 to S

The cell cycle is unidirectional: once started, it is impossible to reverse this decision. Therefore, the start of a new cell cycle has to be regulated intensively. The so called “restriction point” (or “start” in the yeast system) is responsible for regulation of the beginning of a new cycle and the transition from G1- to S-Phase (Bertoli et al., 2013; Morgan, 2007).

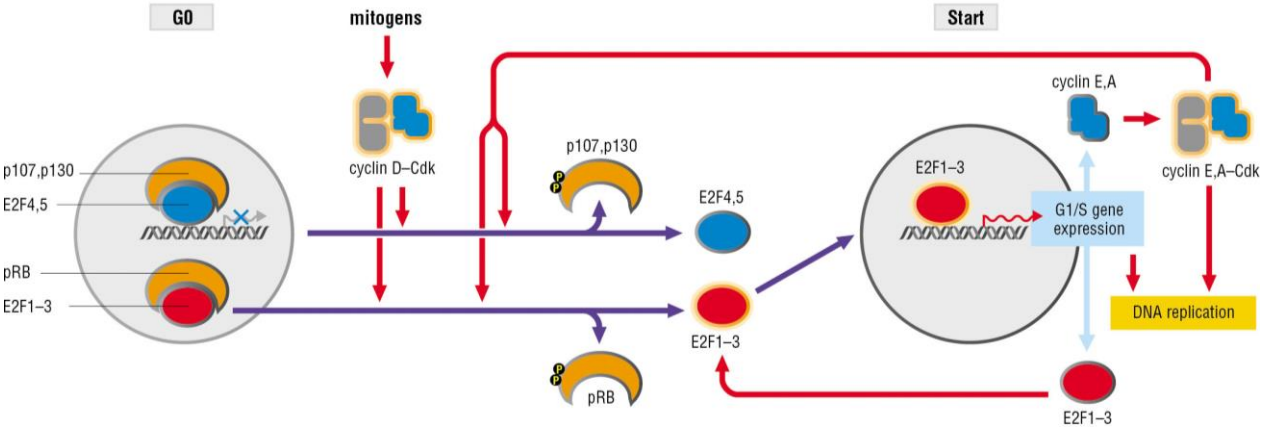

Figure 2 The start of a new cell cycle

A new cell cycle starts if mitogens give the signal to activate Cyclin D/Cdk4, 6. This leads to phosphorylation of members of the pRB protein family and consequently either deactivation or activation of the respective E2F proteins. E2F1-3 serve as transcription factors, leading to G1/S gene expression, for example Cyclins E and A, and consequent Cdk activity. This results in a positive feedback loop by further phosphorylation of pRB proteins and enhanced G1/S gene expression. Finally, the transition to S-Phase and activation of DNA replication takes place (Morgan, 2007).

The start of a new cell cycle (Figure 2) is set in motion by the appearance of external signals, called mitogens, or internal signals. These signals are leading to expression of the Cyclin D protein. Cyclin D binds to two Cyclin dependent kinases (Cdks), Cdk4 and Cdk6 and activates their kinase activity, thereby (Morgan, 2007). The primary target of Cyclin D/Cdk4 or 6 are members of the pocket protein family, specifically p107, p130 and pRB, which are regulators of the E2F protein family members. Proteins of the E2F family are either transcriptional inhibitors or activators of genes important for G1-Phase progression and consequently transition to S-Phase (Dyson, 1998). Unphosphorylated p107 and p130 can bind to E2F4

and E2F5 and thereby anchor both proteins in the nucleus where they act as inhibitors of G1 gene expression. Phosphorylation of p107/p130 leads to release of both E2Fs and consequently to their nuclear export, which obstructs their inhibitory effect (Bertoli et al., 2013). pRB on the other side, binds E2F1, E2F2 and E2F3 (Lees et al., 1993) and inhibits their activity as G1 gene expression activators. Phosphorylation of pRB leads to release and DNA binding of E2F1-3 and ultimately expression of G1 genes (Dyson, 1998; Rubin et al., 2005).

Perhaps the most important gene that is dependent on the E2F proteins is Cyclin E (Duronio et al., 1996; Helin, 1998; Ohtani et al., 1995; Sherr and Roberts, 1999). Cyclin E binds and activates Cdk2 and the Cyclin E/Cdk2 complex is in the center of the transition from G1 to S. First, CycE/Cdk2 kinase activity leads to a positive feedback with the pocket proteins, resulting in more phosphorylated p107, p130 and pRB and consequently a stronger Cyclin E expression and Cdk2 activity. The second important task of CycE/Cdk2 is phosphorylation of many different proteins, for example histone H1, p27, ORC6 and others, which culminates in the onset of DNA replication (Rizzardi and Cook, 2012; Sherr and Roberts, 1999).

Thus, activity of CycE/Cdk2 is regulated by E2F dependent gene expression of Cyclin E and the complex formation of this protein with Cdk2. So-called cyclin dependent kinase inhibitors (CKI) accomplish an additional level of regulation. While cyclins are positive regulators of Cyclin-dependent kinases, CKIs are in analogy negative regulators. In mammals, three CKIs are regulating the activity of the CycE/Cdk2 complex and consequently the G1-S transition: p21, p27 and p57 (Harper et al., 1993; Matsuoka et al., 1995; Polyak et al., 1994). p21 has an important role in the DNA damage response, p27 is among other things responsible for cell cycle exit and p57 is essential for embryonic development (Starostina and Kipreos, 2012). These CKIs have to be inactivated and degraded for progression into S-Phase.

The first step of CKI depletion is performed by a non-catalytic function of CycD/Cdk4. p21 and p27 are bound to CycE/Cdk2 in G1-Phase. However, CycD/Cdk4 is able to bind both CKIs and diminish thereby their grip on CycE/Cdk2. As a result, the Cdk2 activity starts to rise and since the two CKIs are themselves substrates of CycE/Cdk2 activity they are being phosphorylated (Polyak et al., 1994), which serves as a signal for ubiquitination and proteasomal degradation. This feedback loop results in lowered p21/p27 concentration in G1 and increasing Cdk2 activity, leading to Cdk2 dependent gene expression of S-Phase genes and beginning of S-Phase. In S-Phase, an alternative degradation pathway for the CKIs by $CRL4^{Cdt2}$ starts, resulting in enhanced proteasomal degradation and maximized cyclin/Cdk activity. Section 3.7.3 will deal further with the function and regulation of the CKIs.

3.3. Regulation of DNA replication

DNA replication, the process of doubling the genetic material of the cell, is the defining step of S-Phase. DNA replication starts at specific sites in the genome, the so-called origins of replication. While bacteria and *Saccharomyces cerevisiae* possess origins with a defined base sequence, in higher eukaryotes the surrounding DNA sequence and structure is the crucial aspect (Masai et al., 2010). Nonetheless, the general steps at the origin to start DNA replication are conserved.

During telophase, the second to last step of mitosis, the origin recognition complex (ORC) starts to bind to the origins of replication. ORC stays at the origin during cytokinesis and G1 and serves as a binding site for the Cdc6 protein (Pozo and Cook, 2016). During G1-Phase the protein Cdt1 (Cdc10 dependent transcript 1) accumulates in the cell (Nishitani et al., 2000; Nishitani et al., 2001). Cdt1 binds and transports the MCM-complex (mini chromosome maintenance) to ORC-Cdc6 (Masai et al., 2010), which results in the so-called licensing of the origins. The ORC-Cdc6-Cdt1-MCM complex is also called the pre-replication complex. After

Cdt1-MCM is transported and bound to ORC-Cdc6, Cdc6 hydrolysis ATP, leading to binding of the MCM to DNA and release of Cdt1 from the pre-RC. Cdc6 is likewise released after ATP hydrolyzation (Randell et al., 2006). MCM is the DNA helicase responsible for the unwinding of the DNA double strand, leading to the recruitment of the members of the DNA replication machinery. MCM alone is not active however, phosphorylation of S-Phase Cdks and Cdc7-Dbf4 lead to the recruitment of different factors, forming the pre-initiation complex. This complex is able to melt the DNA and start the synthesis of the two new strands (Masai et al., 2010; Morgan, 2007).

It is crucial that during the cell cycle, DNA is only replicated once; re-firing of origins has to be prohibited. Tight control mechanisms for ORC, Cdc6, MCM and Cdt1 exist, ensuring that origins are not firing more than once. Cdc6 for example is phosphorylated by S-Phase cyclins and thereby exported from the nucleus, preventing ORC binding (Saha et al., 1998). Another example would be hOrc1, the biggest component of the ORC, which is strongly degraded in S-Phase (Mendez et al., 2002). The member of the pre-RC that is most regulated is probably Cdt1, underlining its importance and central status in DNA replication. Cdt1 is regulated by transcription, by proteasomal degradation and by binding to an inhibitory protein (see 3.7.4).

3.4. Principal means of cell cycle regulation

On a molecular level, cell cycle regulation is reduced to activity of different proteins at specific time points or time spans and specific locations. Regulation of protein abundance, activity and localization is the most basic task of cell cycle control.

The above described mechanisms of two critical steps, the start of a new cell cycle and the licensing of replication origins, demonstrate the many ways of protein regulation during the cycle. The first way of protein regulation is of course gene expression. For example, S-Phase genes can only be transcribed if transcription factors are present that are themselves activated only during G1. Another example would be Cdc20, one of two important substrate recognition subunits for the APC/C. This protein is at least partly regulated by its expression pattern. Cdc20 mRNA accumulates in G2 and is degraded in G1, in agreement with its protein function as APC/C activator during mitosis (Fang et al., 1998).

Localization is the second way for regulating protein activity. For example, the inhibitor E2F4 is localized in the nucleus upon binding to p130 and p107. This binding is interrupted through phosphorylation and E2F4 is shuttled in the cytoplasm, were it can no longer perform its inhibitory function (Gaubatz et al., 2001).

The third way for cell cycle regulation is the modification of enzymes and the resulting change in activity. The most important modification is probably phosphorylation or dephosphorylation. For example, MCM alone is not able to perform its DNA helicase activity. First, it has to be phosphorylated, which leads to recruitment of Cdc45 and GINS, a prerequisite of replication (Sheu and Stillman, 2006). Besides change of protein activity, phosphorylation can also play an important role in protein stability. As discussed below (see 3.7), phosphorylation is at least in some cases a necessary precondition for the substrate recognition of E3 ubiquitin ligases and their ubiquitin dependent proteasomal degradation.

At the core of the cell cycle, regulation takes place with the help of small regulating molecules, which is the fourth regulatory mechanism. The most important of these molecules are cyclins that are only present at specific time spans in the cell and are positive regulators of cyclin dependent kinases (Morgan, 1995). Thus, Cdk activity is restricted to these specified time points. Another example would be the aforementioned cyclin dependent kinase inhibitors that have the reverse effect. CKIs are inhibitors of

Cyclin/Cdk complexes; binding to these complexes prevents the kinase activity. For example, both CycD/Cdk4 and 6 and CycE/Cdk2 are inhibited by various different CKIs, allowing for a tight control of the beginning of a new cell cycle (Sherr and Roberts, 1999).

The last mechanism is the degradation of cell cycle proteins by the Ubiquitin-Proteasome system. Different proteins are degraded by this system at specific time points in the course of the cell cycle, making it one of the major means of cell cycle regulation in all steps (Bassermann et al., 2014). Among other things, the ubiquitin-proteasome system is responsible for the regulation of the sister chromatid separation after the connection of the spindle apparatus to all chromosomes (Peters, 2002). This is crucial for the even distribution of the chromosomes. Ubiquitination is also important for the degradation of cyclins after the cell cycle is completed (Glotzer et al., 1991). In addition, it is crucial for the transition from G1- to S-Phase (Rizzardi and Cook, 2012). Therefore, Ubiquitin-dependent regulation is essential for cell cycle control.

3.5. The ubiquitin-proteasome system of degradation

The ubiquitin-proteasome system is perhaps the most important mechanism for a cell to dispose of proteins. It enables cells to target only specific proteins for degradation at specific time points. Targeted protein degradation is a crucial step in numerous different cell tasks, therefore the scope of this system has a wide span, ranging from stress-response, ribosomal biogenesis, DNA repair mechanisms, embryonal development, immune response and of course cell division and control of the cell cycle (Jentsch et al., 1991; Schulman and Harper, 2009).

In principal, proteins are marked by ubiquitin through a cascade of three enzyme reactions. Afterwards, ubiquitin marked proteins are recognized, shuttled to the proteasome and disassembled. While the principal steps of this pathway are conserved, great variety exists regarding the proteins that are involved. The central molecule, ubiquitin, is a small polypeptide consisting of 76 amino acids with a molecular mass of 8.5 kDa that was discovered in 1975. It was named after the fact that it is present in most eukaryotic cells (Goldstein et al., 1975; Wilkinson, 2005). The most recognized function of ubiquitin is marking proteins for proteasomal degradation. A chain of polyubiquitin has to be formed on the target protein for this task.

On a molecular level, the first step of ubiquitination is activation of ubiquitin through the activity of a Ubiquitin-activating enzyme E1. E1 forms a thioester bond with a ubiquitin molecule under consumption of ATP. E1 interacts with a ubiquitin conjugating enzyme (E2) and transfers the ubiquitin thereby. Ubiquitin-loaded E2 enzymes bind to the E3 ubiquitin ligases, the last family of enzymes in the cascade. The purpose of the E3 enzymes is to ligate the ubiquitin molecule to the respective substrates. Therefore, E3s can bind both the E2 enzymes and the substrates (Schulman and Harper, 2009). Different E3 ubiquitin ligases are responsible for different sets of substrates. After the substrate received the ubiquitin molecule, it stays at the ubiquitin ligase and more ubiquitin molecules are connected to it, often at the already attached ubiquitin. A ubiquitin chain is produced that serves as an internal mark for the cell on how to proceed further with the protein.

The fate of the protein is dependent on how the single ubiquitin molecules of the chain are interconnected (Figure 3). The ubiquitin molecule has seven Lysine residues to which other ubiquitins could be attached. For example, a chain of Lys63 connected ubiquitins plays a part in signal transduction, receptor endocytosis and DNA repair mechanisms. Mixed chains of Lys29/Lys33 on the other hand have a role in the regulation of AMPK-related kinases by blocking their activation (Ikeda and Dikic, 2008). The most well-known function of ubiquitin is the degradation via the proteasome though. Ubiquitin chains that are interconnected on

their Lys48 are recognized by UBA-proteins (Saeki, 2017) and shuttled to the 26S proteasome were the target proteins are disassembled into amino acids and recycled for new protein synthesis.

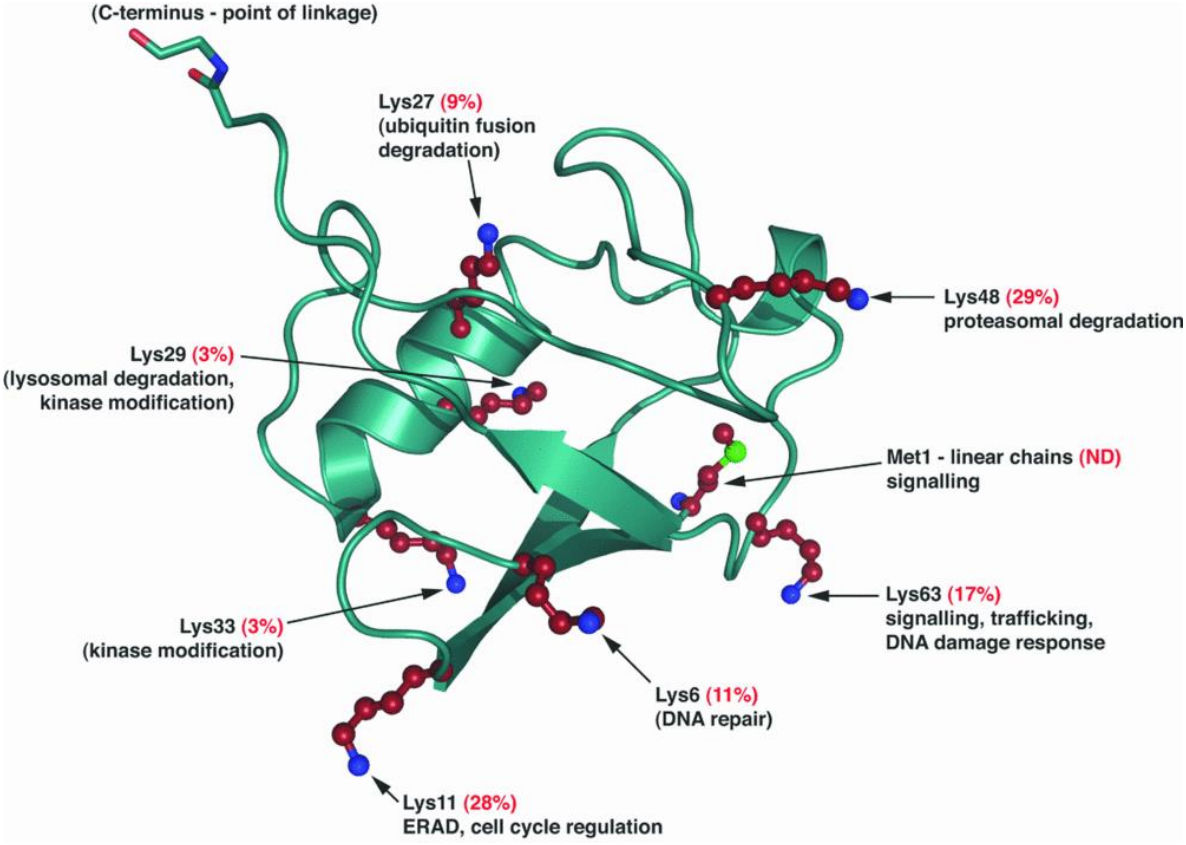

Figure 3 The fate of a substrate of a ubiquitin ligase in dependency of the ubiquitin linkage
E3 ubiquitin ligases are marking their substrates with a chain of ubiquitin. The interlinkage of the ubiquitin molecules of the chain is deciding the fate of the substrate. The majority of ubiquitin molecules are linked together on Lys48, a signal for proteasomal degradation. The linkage between other lysines has different effects on the substrate protein (Komander, 2009).

Eight E1 enzymes are proposed to exist in humans, their shared characteristic feature is an adenylation domain responsible for the binding of ubiquitin (Schulman and Harper, 2009). In *Drosophila melanogaster*, at least Uba1 is identified as an E1 (Schulman and Harper, 2009).

The molecular domains that define the function of E2 ubiquitin conjugating enzymes are the HPN motif and conserved cysteine, proline and tryptophan at positions 87, 67 and 95 respectively. Proline and tryptophan are flanking the active center of the enzyme, thereby (Cottee et al., 2006). At least 40 proteins are considered E2s in humans (Ye and Rape, 2009), whereas it is thought that *D. melanogaster* has 25 different E2 enzymes (Jones et al., 2002).

Although the task of the different E3 ubiquitin ligases is altogether identical, this class of proteins is very variable regarding their structure. Two different families of E3 enzymes exist: the HECT and RING family. The HECT (homologous to E6-AP C-terminus) ubiquitin ligases are actively binding ubiquitin. After the E2-ubiquitin complex binds to the HECT E3, ubiquitin is transferred to the HECT-domain of the E3-ligase and is forming a thioester intermediate with the cysteine in the active center of the HECT E3 (Metzger et al., 2012). From there, it is attached to the respective substrate that is also bound on the HECT E3. Structurally,

HECT E3s are characterized by the HECT domain, located at the C-terminus, and consisting of two lobes. The N-terminal N-lobe interacts with the E2 ubiquitin conjugating enzyme, whereas the C-lobe, positioned at the C-terminus, contains the cysteine that is used for attachment of the ubiquitin (Huang et al., 1999). Around 30 HECT E3 ubiquitin ligases exist in mammals (Metzger et al., 2012).

The larger group of E3 ubiquitin ligases are the members of the RING (really interesting new gene) family, with at least 600 genes encoding for an E3 RING ubiquitin ligase (Li et al., 2008). The difference to HECT E3s lies in the mode of ubiquitin transfer. Unlike HECT ubiquitin ligases, RING E3s do not bind ubiquitin themselves. Instead, their role is to bring the E2-ubiquitin complex and the respective substrate in spatial vicinity to each other and to catalyze the transfer of ubiquitin coming from E2 to the substrate. The motif responsible for E2 binding is a zinc-finger (Metzger et al., 2012). Because of their great number, RING E3s have a broader role in cells, including cell cycle control. Three of the most important RING E3s in this regard are the APC/C, the CRL4 and the SCF complex.

3.6. Important members of the RING E3 ubiquitin ligase family

Because of their great number and their different substrates, RING E3 ubiquitin ligase complexes exhibit large variability in their structure. Nonetheless, all ligases have certain elements that fulfill similar roles. There always is a scaffold protein, which serves as an interaction platform for all the other components. A protein with a zinc-finger motif is responsible for the connection with the respective E2 ubiquitin conjugating enzyme. An adapter protein binds to a so-called substrate recognition subunit (SRS). The SRS is responsible for substrate binding. Some of the RING E3 ubiquitin ligases are rather simple structured, for example CRL4 and the SCF complex (Figure 4). APC/C on the other hand is a large multi protein complex, consisting of 19 proteins in humans (Sivakumar and Gorbsky, 2015).

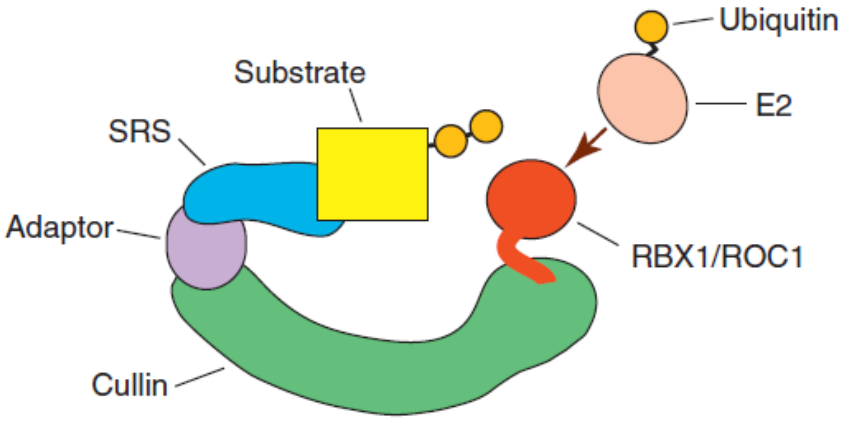

Figure 4 Schema of Cullin RING ligases
Cullin RING ligases are relatively simple constructed. They are built up of only four different proteins: a cullin scaffold, an RBX1 RING finger and an adapter protein to which the substrate recognition subunit binds (Starostina and Kipreos, 2012).

3.6.1. Anaphase Promoting Complex/Cyclosome

The APC/C (anaphase promoting complex/cyclosome) is an unusual ubiquitin ligase because of its size. Whereas normally cullin RING ubiquitin ligases consist of around four different proteins, APC/C has 19 subunits (see Figure 5), consisting of 14 different proteins, five of which are present in two copies each. The overall mass of the APC/C is 1.22 MDa (Sivakumar and Gorbsky, 2015). Why the APC/C consists of so

many subunits is still not clear and open for discussion. In principal, the complex is comprised of three domains. The platform subcomplex serves as a scaffold and interaction platform. The catalytic core subcomplex is responsible for ubiquitin-transfer if substrate and E2 is bound. The tetratricopeptide repeat subcomplex does also have scaffolding function and is also important for APC/C assembly and interaction with regulatory proteins (Sivakumar and Gorbsky, 2015). The co-activators of APC/C are either Cdc20 or Cdh1, which also play a role in substrate recruitment. The respective homologues in *D. melanogaster* are fizzy (fzy) and fizzy-related (fzr).

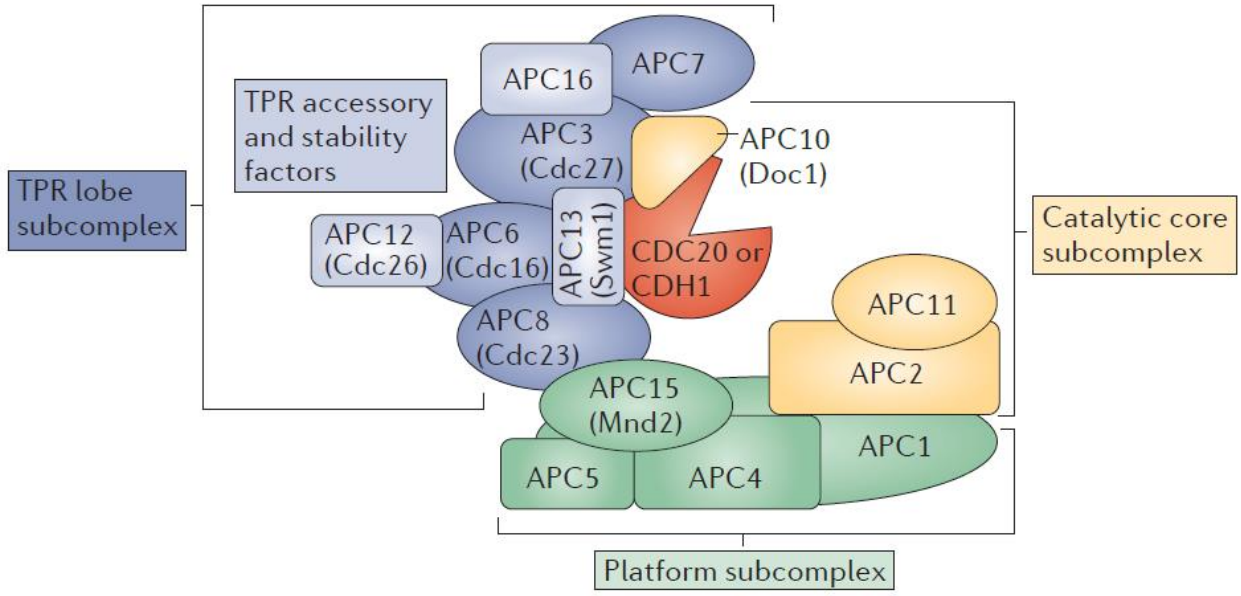

Figure 5 Structure of the APC/C
The APC/C is composed of 14 different proteins that can be subdivided in three different complexes. The platform subcomplex serves as a scaffold, the catalytic core subcomplex is responsible for the ubiquitin ligase activity and the TPR (tetratricopeptide repeat) lobe subcomplex has important functions in APC/C assembly and regulation (Sivakumar and Gorbsky, 2015).

Cdc20 is responsible for APC/C activity from the beginning of the mitosis onwards to the end of metaphase. One of the prime substrates of APC/C^{Cdc20} during metaphase is securin. After chromosome condensation, the sister chromatids are hold together by a protein complex called cohesin. For successful distribution of the sister chromatids, it is essential that cohesin is degraded before anaphase. Separase is the enzyme that is responsible for cohesin degradation. Since preliminary activity of separase would deeply disturb mitosis, it has to be thoroughly regulated. Securin is inhibiting separase activity. In *Saccharomyces cerevisiae*, APC/C^{Cdc20} ubiquitinates securin, marking it for degradation and unleashing separase activity. This function of APC/C^{Cdc20} is also present in vertebrates. However, the majority of cohesin is dissociated by another pathway in prophase and pro-metaphase in this case. Nonetheless, centromeric cohesin is not affected by this pathway and has to be removed upon APC/C^{Cdc20}-mediated ubiquitination of securin and subsequent activation of separase in anaphase in homology to the events in *S. cerevisiae* (Peters, 2002).

Cdh1 is responsible for APC/C activity from anaphase until the end of G1-Phase. Cdc20 is a substrate of the APC/C^{Cdh1} complex; thereby the APC/C is regulating itself to switch to other targets in the end of mitosis and the beginning of G1. Some of the most important targets of APC/C^{Cdh1} are cyclins. Cyclin degradation

abolishes Cdk activity, which is necessary for the beginning of another cell cycle or quiescence (McLean et al., 2011). Cdk activity at the end of G1-Phase leads to Cdh1 phosphorylation, which prevents the binding to APC/C. Therefore, APC/C activity is shut off in S-Phase. Cdh1 is degraded by the proteasome in S-Phase.

Both Cdc20 and Cdh1 use WD40 repeats as their substrate recognition motifs that form to a β-propeller and are able to interact with other proteins. APC/C substrates have conserved degron motifs that allows Cdc20 or Cdh1 to recruit them to the APC/C. In most cases this is either the D-Box or the KEN-Box (Sivakumar and Gorbsky, 2015).

3.6.2. CRL4^{Cdt2}

CRL4^{Cdt2} (see Figure 6) is a cullin RING ligase that is specifically active in S-Phase and among other things responsible for ubiquitination and disposal of important regulators of G1-S transition. Cullin4 (Cul4) serves as the scaffold protein, its C-terminus is binding to the RING finger protein Rbx1. The E2-Ub complex is using Rbx1 as its docking site. The adapter-protein DDB1 binds to the N-terminus of Cul4. As already mentioned, adapter-proteins are the juncture of the substrate recognition subunit with the E3 ubiquitin ligase scaffold. Cdt2 is the SRS in CRL4^{Cdt2}, responsible for recruitment of the substrates to the complex were ubiquitination takes place (Havens and Walter, 2011).

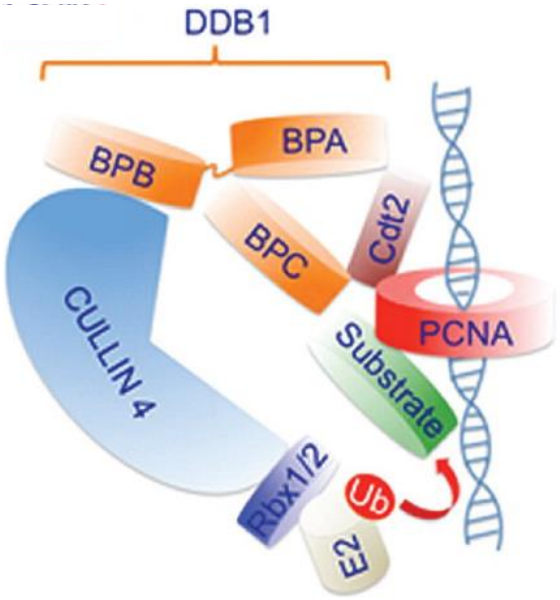

Figure 6 Schema of CRL4^{Cdt2}
CRL4^{Cdt2} consists of the scaffold protein Cullin 4, the RING protein Rbx1 that binds the E2 and the adapter protein DDB1 to which the SRS Cdt2 binds. Substrates of CRL4^{Cdt2} have to be bound to the PCNA during S-Phase to be recognized by this complex. Picture adapted from Abbas and Dutta (2011).

One peculiarity of the CRL4^{Cdt2} complex is its mode of substrate recognition. All substrates possess a PIP (PCNA interacting protein) degron, which enables them to bind to the proliferating cell nuclear antigen (PCNA) where they are recognized by CRL4^{Cdt2}. The PCNA is a complex necessary for efficient DNA synthesis. DNA polymerases are not capable of DNA strand synthesis alone, since they are falling off the template strand easily. The ring-like structure of the PCNA enables them to bind to DNA efficiently and move freely on the strand. Therefore, the falling off is prevented and the efficiency of DNA replication

elevated (Morgan, 2007). PCNA is loaded onto DNA exclusively in S-Phase or if DNA damage occurred, thereby restricting the function of $CRL4^{Cdt2}$ also to these incidences (Havens and Walter, 2009). Though there are variations, the PIP degron consists in principal of three elements. A PIP box is a conserved amino acid sequence that leads to recruitment onto the PCNA. The binding to the PCNA via the PIP-box is only weak though. Therefore, most but not all PIP degrons have additionally a threonine-aspartame motif that leads to high affinity binding. Lastly, there also exists a basic amino acid four residues downstream of the PIP-Box, responsible for $CRL4^{Cdt2}$ binding (Havens and Walter, 2011). This rather special way of substrate recognition allows $CRL4^{Cdt2}$ to mark its substrates efficiently for degradation in the beginning of S-Phase.

$CRL4^{Cdt2}$ has a number of substrates. For example, after transition to S-Phase, E2F1 is degraded via its PIP Box, since expression of G1 genes has to be prevented (Shibutani et al., 2008). The CKIs p21 and p27 are likewise degraded by the proteasome in S-Phase and though there are more regulatory mechanisms, they are also substrates of $CRL4^{Cdt2}$ (Havens and Walter, 2011). This is also true for the respective homologue of p21 and p27 in *Drosophila*, the protein Dacapo (Dap) (Higa et al., 2006; Swanson et al., 2015). Another example is Cdt1 that is highly regulated in S-Phase since otherwise, re-replication would occur (Liu et al., 2007). This regulation is performed at least partly by PIP degron mediated degradation (Havens and Walter, 2011). Dap and *Drosophila* Cdt1 will be discussed in greater length below (3.7.3.2 and 3.7.4.2).

3.6.3. Skp1, Cullin, F-Box protein (SCF) complex

The Skp1, Cullin, F-Box protein (SCF) complex has important roles in cell cycle regulation from G1 through S-Phase and up to G2. The reason for this broad role is the wide variety of different substrate recognition subunits that make the SCF highly versatile. The SCF was first discovered in yeast; its name is derived by some of its components, namely Skp1, Cullin1 and the F-Box protein (Feldman et al., 1997; Skowyra et al., 1997). Cullin1 (Cul1) is the scaffold protein. Rbx1 is the RING protein and binds to Cul1. As already described, the task of the RING protein is to interact with the E2 ubiquitin conjugating enzyme loaded with ubiquitin and recruit it to the E3 (Willems et al., 2004). Skp1 is the adapter protein that binds a specific substrate recognition subunit. These subunits are called F-Box proteins in the case of the SCF-complex (see 3.7).

The SCF complex is tightly regulated. Assembly of the SCF is prevented by binding of the sequestration factor CAND1 to Cul1. CAND1 prevents the binding of Skp1 and the F-Box protein to Cul1, effectively disabling SCF activity. NEDD8 has to be attached to Cul1 to release it from its CAND1 inhibition. Furthermore, NEDD8 binding also increases the ubiquitin ligase activity of the SCF-complex, changes the structure to facilitate the attachment of the ubiquitin and allows the E2 enzyme wider access to the growing polyubiquitin chain (Skaar and Pagano, 2009). Besides, the presence or absence of respective F-Box proteins also determines the ability of the SCF-complex to bind and ubiquitinate certain substrates.

SCF subunits are overall highly conserved. Indeed, it is possible to rescue deficiencies of Skp1, Cul1 and Rbx1 in yeast with the respective human versions of the SCF-complex (Deshaies, 1999). The high conservation can also be observed in *D. melanogaster*. *Drosophila* Cul1 has 62% identity to the human homologue, *Drosophila* SkpA (homologue of Skp1) and Rbx1 have 76% and 91% respectively (Bocca et al., 2001). The interaction of fly SCF was investigated by Yeast Two Hybrid and *in vitro* interaction assays in the same studies. In fact, it was accomplished to rescue yeast Rbx1 deficiency with expression of fly Rbx1, which also demonstrates the similarity between components of the SCF in different organisms.

F-Box proteins of the SCF are of special interest, since they allow one protein complex to regulate a large number of different proteins. Indeed, faulty regulation of cell cycle F-Box proteins is often a cause of cancer

(Heo et al., 2016). This underlines that the regulation of F-Box proteins, their way of substrate recognition and especially their target substrates are important aspects for proper cell cycle progression.

3.7. The F-Box protein Skp2 and its substrates

3.7.1. Skp2 in mammals and humans

The first F-Box protein that was identified is Cyclin F in 1994 (Kraus et al., 1994). This is also were the name of this protein class is derived from. All F-Box proteins have in common that they share a conserved, so called F-Box motif through which they can bind to the adapter protein of SCF-complexes (Kipreos and Pagano, 2000). F-Box proteins can be divided in three classes according to their way of substrate binding. The Fbxw proteins have WD40 repeats that are responsible for binding to their substrates. The Fbxl proteins possess leucine rich repeats that are fulfilling this role. Fbxo proteins on the other hand have various different sequence motifs for substrate binding (Heo et al., 2016). F-Box proteins may have a number of functions independently from the Ubiquitin-Proteasome pathway (Nelson et al., 2013); their main task is nonetheless the recruitment of substrates to the SCF (Skowyra et al., 1997). Therefore, they play a central role in regulation of proteins through the ubiquitin-proteasome system. A peculiarity of F-Box proteins is that recognition of their substrates is primarily regulated by modification. This can happen in many different ways. For example, it may be necessary that a cofactor has to be bound on the substrate for recognition. Another possibility is that the degron motifs on the substrates have to be made accessible first. The most important mechanism is phosphorylation though, meaning that the phosphorylation status of the substrates are determining if they can be recognized and regulated by F-Box proteins (Skaar et al., 2013).

Around 69 proteins are considered F-Box proteins in humans, whereas it is estimated that *D. melanogaster* possess 27 (Skaar et al., 2009). Many F-Box proteins play important roles in cell cycle regulation (Zheng et al., 2016). Perhaps the most known F-Box protein in this regard is the S-Phase kinase associated protein 2 (Skp2), a member of the Fbxl family. SCF^{Skp2} is extensively studied in the human system, since it is of importance for the regulation of several crucial cell cycle proteins.

Skp2 was discovered in 1995 in a study that identified two interaction partners of Cyclin A/Cdk2 (Zhang et al., 1995). In 1998, it was found that Skp2 is in fact an F-Box protein of the SCF-complex, regulating the protein stability of Cyclin D and of the CKI p21 (Yu et al., 1998). This implies that Skp2 has an important part in the transition from G1- to S-Phase. Skp2 is regulated by several ways. A number of different transcription factors are supposed to be responsible for gene expression of Skp2, including, among others, E2F1 (Chan et al., 2010). On the other side, Skp2 is disposed of by APC/C^{Cdh1} ubiquitination and subsequent proteasomal degradation (Bashir et al., 2004; Wei et al., 2004). Skp2 accumulates in late G1-Phase and is degraded in late M-Phase by APC/C^{Cdh1} activity (Bashir et al., 2004; Kurland and Tansey, 2004; Wei et al., 2004). Besides expression and degradation, Skp2 is also regulated by its localization and failures in this respect have severe consequences. While Skp2 resides in the nucleus under normal conditions, it was shown that phosphorylation by AKT/protein kinase B leads to nuclear export and accumulation in the cytoplasm (Lin et al., 2009b). The same study suggested that this is one reason of Skp2 dependent cancer formation. Indeed, it was also found that Skp2 is localized in the cytoplasm in aggressive lymphomas (Lim et al., 2002). Besides AKT signaling, evidence exists that links TGFβ-signaling to the localization of Skp2 in the nucleus, where it is targeted by APC/C^{Cdh1} mediated proteasomal degradation (Hu et al., 2011). The protein Connexin 50 does also seem to have a role in the Skp2 localization. Connexin 50 binds and masks the Skp2 NLS sequence, which also leads to cytosolic accumulation. In this case, it was also found that Skp2

possesses auto-ubiquitination capability in these circumstances and takes care of its own degradation (Shi et al., 2015).

There also seems to exist an unknown pathway of degradation. Application of the drug lovastatin results in a depletion of Skp2 protein levels. This drug has the ability to deplete the geranylgeranyl-isoprenoid intermediates of the cholesterol biosynthesis. It was speculated that consequently an unknown regulator of Skp2 could no longer be geranylgeranylated, which leads to Skp2 degradation. This pathway is dependent upon the N-terminus of Skp2 (Vosper et al., 2015).

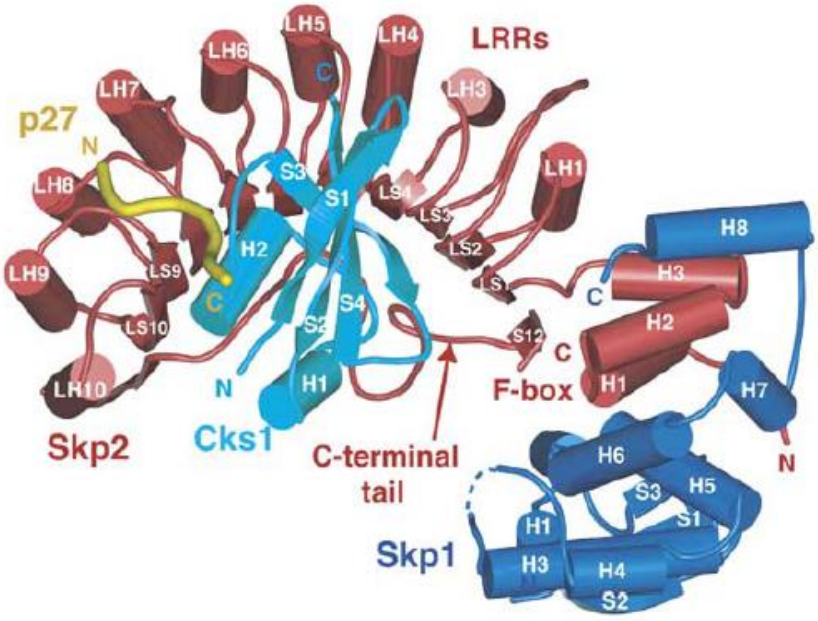

Figure 7 Atomic structure of Skp2
Skp2 (red) is sickle shaped, whereupon the F-Box domain builds the handle and the leucine rich repeats the blade. The F-Box domain binds to Skp1 (dark blue) thereby forming the SCF^{Skp2} complex. Cks1 (light blue) associates to the blade and supports the binding of the substrate p27 (yellow, only partly depicted). Picture adapted from Hao et al. (2005).

Another factor that is important for Skp2 activity is the small molecule Cks1. As already mentioned, some F-Box proteins require a cofactor for efficient substrate binding (Skaar et al., 2013). Cks1 is the cofactor that is at least in some cases essential for Skp2 activity. Cks1 is necessary for the recognition of the CKI p27 by Skp2 *in vivo* and *in vitro* (Ganoth et al., 2001; Spruck et al., 2001).

The atomic structure of Skp2 is described as sickle shaped. The handle of the sickle is thereby comprised of the F-Box motif and responsible for interaction with Skp1 and consequent recruitment of the protein to the SCF. The leucine rich repeats (LRR), the motif responsible for the binding of the substrates, are forming the blade of the sickle (Schulman et al., 2000). The role of Cks1 was elucidated by determining the atomic structure of both complexes (Figure 7). Cks1 binds to the LRR blade of Skp2 and supports the binding and recognition of p27 (Hao et al., 2005).

Skp2 is extensively studied because of its role in cancer development. Indeed, it was shown that Skp2 levels are increased in tissue samples of breast, colon and colorectal cancers (Fujita et al., 2008). Likewise, the knockdown of Skp2 led to reduced proliferation and invasiveness of osteosarcoma cells (Ding et al., 2017). Skp2 is also considered a prognostic marker in cancer outcome; high levels are correlated with poor

prognosis in various different tumors, for example breast cancer (Zhang et al., 2016), gastric cancer (Wei et al., 2013), lung cancer (Zhu et al., 2004) and nasopharyngeal carcinoma (Wang et al., 2014). Skp2 was also already proposed as an object of cancer therapy (Bassermann et al., 2014). Indeed, many different medications are already tested that target Skp2 for cancer treatment (Chan et al., 2013; Ding et al., 2017). The reason for the importance in cancer research is the array of substrates that Skp2 regulates by ubiquitination.

Skp2 has a multitude of different substrates in mammals (Heo et al., 2016). For example, TRUSS, one of the substrate recognition subunits of CRL4 (see 3.6.2), is a substrate of SCF^{Skp2}. TRUSS is a regulator of the gene expression factor Myc, and disruption of the Skp2 dependent regulation does lead to cancer (Jamal et al., 2015). LKB1, an important kinase for the regulation of different functions in the cell is also the aim of Skp2 dependent ubiquitination. Quite unusually though, in this case the ubiquitination does not lead to proteasomal degradation but to activation of LKB1 (Lee et al., 2015). Another Skp2 substrate in humans is E2F1, one of the important transcription regulators for the start of a new cell cycle (Marti et al., 1999). Furthermore, Cyclin E, important for G1/S gene expression is targeted for degradation by Skp2 (Nakayama et al., 2000). The human ORC1 protein, the biggest subunit of the ORC complex, is another example for Skp2 mediated ubiquitination (Mendez et al., 2002). This shows that Skp2 has also important roles in replication control and the prevention of re-replication. The fact that Skp2 is also responsible for Cdt1 ubiquitination underlines this result (Li et al., 2003). However, the function that is considered the most essential is the regulation of the three CKIs p21, p27 and p57 (Lu and Hunter, 2010). Skp2 is performing a direct control of the transition from G1-Phase to S-Phase therefore, a step that is extremely critical for the cell and the prevention of cancer development.

3.7.2. Skp2 in *Drosophila melanogaster*

Although Skp2 is studied extensively in mammals for its importance in cell cycle control and cancer research, not much is known about the homologue in flies. *Drosophila* Skp2 was discovered and described in 2011 together with Cks85A, the homologue of Cks1 (Ghorbani et al., 2011). According to this source, *Drosophila* Skp2 has 23% identity and 41% similarity in comparison to the human version. These percentages increase if the comparison is restricted to the functional parts of the protein, the F-Box and the LRRs (33% identity and 59% similarity). The role of Skp2 that the authors saw is maintenance of diploidy and growth promotion. Reducing the levels of Skp2 in flies has several different outcomes. Skp2 knockout leads to a delayed development in *D. melanogaster* larvae and ultimately to death early in the pupal phase. Growth is negatively affected as the number and ploidy of cells in salivary glands is reduced. Another effect was seen in larval brains. If Skp2 is eliminated, the overall size of the brains become smaller. At the same time, cells become larger and polyploid. Polyploidy is also seen in eye imaginal discs and wing imaginal discs if Skp2 is knocked out. Additionally, wing imaginal discs do also show increased apoptosis under these circumstances. These effects could be also seen in adult wings since Skp2 knockdown results in an increased distance between the wing hairs. The authors saw that the effects of Cks85A knockdown are comparable to Skp2 knockdown. This observation led to their consideration that both proteins work together. Indeed, they also saw biochemical interaction between Skp2 and Cks85A. In addition, they could show genetical interaction between both proteins in eye imaginal discs. It seems that Cks85A has a role in the substrate recognition process of Skp2. This is in accordance with mammalian SCF^{Skp2}, where Cks1 also enables or at least supports Skp2 function. Co-IP experiments also showed an interaction between Skp2 and SkpA, the homologue of Skp1 in *D. melanogaster*, demonstrating that Skp2 is indeed part of an SCF-complex. Furthermore, interaction with Cyclin-dependent kinase 1 and 2 could also be detected. Although

it was not the focus of this paper, it was also tested if Skp2 knockout influenced the amount of Double parked (Dup, homologue of Cdt1, see 3.7.4) and Dacapo (Dap, homologue of p21, p27 and p57, see 3.7.3). Dup protein levels are not changed upon Skp2 knockout, which led the authors to assume that it is not a substrate in *Drosophila*. Dacapo levels are also not positively influenced by Skp2 knockout. It has to be said though that these Western analyses are only hints and cannot give definitive statements if Dup and Dap are targets of Skp2 ubiquitination, especially since both proteins are strongly regulated in the cell cycle by other mechanisms.

The relationship between Skp2 and Dacapo was analyzed more thoroughly two years later (Dui et al., 2013). Dui et al. (2013) proposed that Dacapo is a substrate of Skp2. They performed different biochemical assays, Western Blots, Co-IPs and ubiquitination assays, as well as genetical approaches on eye and wing development. Their result was that Skp2 ubiquitinates Dap for subsequent proteasomal degradation. However, one caveat of this study is that the authors did not consider the role of the PIP box mediated degradation of Dap and its cell cycle function. At least some of their results can also be explained by cell cycle shifts caused by altered Skp2 or Dap levels and consequent regulation by $CRL4^{Cdt2}$. Up to now, these two sources represent the only serious studies that focus on Skp2 in *D. melanogaster*. Since their results differ regarding Dap being a substrate of Skp2, one of the starting points of this thesis was to clarify this issue.

The overall topic of this work was to figure out if *Drosophila* Skp2 is responsible for the regulation of the fly homologues of p21, p27, p57, Cdt1 and CycE. These potential substrates will be discussed in greater detail in the next sections.

3.7.3. Function and regulation of the G1-S CKIs

3.7.3.1. Characterization of p21, p27 and p57 and their regulation by Skp2

p21, p27 and p57 are members of the CIP/KIP (CDK interacting protein/kinase inhibitory protein) family of CKIs and responsible for inhibition of Cdk1 or Cdk2 activity in mammalians and thereby important for G1- to S-Phase transition. All three are well known substrates of the SCF^{Skp2} complex.

p21 was discovered in 1993 in human cells as a potent inhibitor of the Cdk2 complex. Overexpression of p21 leads to disappearance of Cdk2 activity and consequently the transition from G1 to S does no longer take place (Harper et al., 1993). p21 can be activated under stress conditions, for example DNA damage or oxidative stress, and is thereby exerting an important function in cell homeostasis (Abbas and Dutta, 2009). SCF^{Skp2} is responsible for ubiquitination of p21 in *vivo* in G1-Phase (Yu et al., 1998) and *in vitro* (Bornstein et al., 2003). An important finding of this study is that addition of both Cks1 and CycE/Cdk2 is necessary for the ubiquitination of p21 by Skp2. The CycE/Cdk2 complex seems to have two tasks in this case. First, the authors could demonstrate that CycE/Cdk2 is necessary for the phosphorylation of p21. This phosphorylation facilitates the recognition through SCF^{Skp2} in accordance with the fact that Skp2 binds preferably to phosphorylated substrates. However, this general function of CycE/Cdk2 is not a prerequisite in this case, ubiquitination could still happen efficiently without phosphorylation. Nonetheless, CycE/Cdk2 has to be present for the regulation of p21. Therefore, the second task of CycE/Cdk2 seems to be to build a physical interaction with p21, which is necessary for the recognition by Skp2. Besides ubiquitination through SCF^{Skp2}, p21 is also a target of $CRL4^{Cdt2}$, which regulates this protein in S-Phase (Abbas et al., 2008; Kim et al., 2008; Nishitani et al., 2008). Although p21 levels drop in S-Phase, the protein reaccumulates in G2 and M (Dulic et al., 1998). The reason is that p21 inhibits the activity of Cdk1, thereby delaying mitosis.

The authors speculated that this gives the cell time to integrate the signals of G2 checkpoints that are important for start of mitosis, thereby assuring proper control of the beginning of M-Phase. However, p21 has to be degraded for complete Cdk1 activity and upkeep of the spindle assembly checkpoint in prometaphase (Amador et al., 2007). The same study showed that APC/C^{Cdc20} is responsible for p21 ubiquitination in mitosis.

p27 was also discovered as an inhibitor of CycE/Cdk2 (Polyak et al., 1994). It is considered to be an intrinsically unstructured protein (Bienkiewicz et al., 2002). The crystal structure of p27 in complex with CycA/Cdk2 gave a general insight into how the CKIs are able to inhibit the function of cyclin dependent kinases (Russo et al., 1996). In the beginning, p27 binds to the CycA protein. After binding to CycA, a helix of p27 is becoming structurally unordered. If this helix is getting close to Cdk2, its structure is restored and binds the N-terminus of Cdk2. Consequently, parts of p27 that are mimicking the structure of ATP are occupying the catalytical center of the CycA/Cdk2 complex. This has two effects: already bound ATP is driven away from the Cyclin-Cdk complex and further ATP binding is abolished. Besides, since p27 also interacts with CycA, recruitment of phosphorylation targets is also prevented.

Just like p21, SCF^{Skp2} also targets p27 for ubiquitination and consequent proteasomal degradation (Carrano et al., 1999). The same study also showed that p27 has to be phosphorylated at threonine 187 for interaction with Skp2. This phosphorylation is performed by Cdk2 activity (Sheaff et al., 1997). It was also observed that p27, just like p21, has to physically interact with CycE/Cdk2 for recognition by SCF^{Skp2} (Montagnoli et al, 1999). Later on, it was shown that Skp2 is not able to bind to p27 without the addition of Cks1 *in vitro* (Ganoth et al., 2001) and *in vivo* (Spruck et al., 2001), underlining the importance of Cks1 as a supporter molecule. p27 level are also rising under Skp2 knockout conditions in mouse cells and tissues, another hint that SCF^{Skp2} regulates p27 protein stability (Nakayama et al., 2000).

Besides Skp2, p27 is regulated in multiple other ways. It was shown in rabbit reticulocyte lysates that the E3 ubiquitin ligase KPC is also responsible for ubiquitination of p27 in G1-Phase (Kamura et al., 2004). Furthermore, a knockdown of Cul4 or DDB1 also results in accumulation of p27, hinting to a possible regulation by $CRL4^{Cdt2}$ via a PIP degron (Higa et al., 2006).

p57 was discovered in a two-hybrid screen for interaction partners with cyclins and Cdks (Matsuoka et al., 1995). The authors could show p57 binding to cyclin/Cdk complexes that are essential for the G1-S transition, for example CycE/Cdk2. Consequently, overexpression of p57 leads to a stop of the cell cycle in SAOS-2 cells. In the same publication, it was also observed that p57 expression is restricted to certain organs. This is a difference to p21 and p27 that are expressed in all tissues and organs. The authors also speculated that the task of p57 is to prevent restart of the cell cycle after cells become differentiated. Just like the other two CKIs, p57 is regulated by proteasomal degradation and SCF^{Skp2} is responsible for the ubiquitination. Phosphorylation does also have an important part in this regulation, since p57 has to be phosphorylated on a threonine at the C-terminus for Skp2 recognition (Kamura et al., 2003).

3.7.3.2. Dacapo and the regulation by Skp2 in flies

Instead of three CKIs that prevent the transition from G1 to S, *D. melanogaster* possesses only one, the protein Dacapo. Upon its discovery, it was shown that Dap bears sequence similarities to rat p21 (de Nooij et al., 1996). Furthermore, it was also shown that Dap could inhibit the activity of Cyclin E/Cdk2 *in vitro*. It does also prevent S-Phase *in vivo* in dependency of Cyclin E. The interaction with CycE/Cdk2 is specific, since Dap does not seem to interact with CycB/Cdk1 or CycA/Cdk1 (Lane et al., 1996).

One of the functions of Dap seems to be the prevention of cells from re-entering the cell cycle during embryonal development. Embryonic epidermal cells go through 16 complete cell cycles and arrest afterwards in the G1-Phase of cycle 17. A loss-of-function mutation of Dap seems to lead to an additional full cycle, resulting in a drastic increase of the embryonic cell number (de Nooij et al., 1996; Lane et al., 1996). Conversely, overexpression of Dap results in a premature stop of the embryonic cell cycle after completion of mitosis 16 (Lane et al., 1996). Additionally, null mutants of Dap are lethal, underlining its importance in the fly development (de Nooij et al., 1996). In accordance with the inhibitory effect of Dap on CycE/Cdk2 activity, overexpression of Dap leads to G1 accumulation of wing imaginal disc cells as seen by flow cytometric analysis (Reis and Edgar, 2004). This effect was also seen in *Drosophila* Schneider cells in the Sprenger group (Bauer, 2011). According to this, Dap plays a prominent role in the transition from G1- to S-Phase in *D. melanogaster* and the corresponding cell lines.

Just like the three mammalian CKIs, Dacapo has to be tightly regulated for correct cell proliferation control. While Dacapo should exercise its inhibitory function during G1-Phase, it would hinder the proper course of the cell cycle at the end of G1 and in S. Western Blot analysis showed that Dap levels are dependent upon the activity of CUL4, the scaffold protein of the $CRL4^{Cdt2}$ E3 ubiquitin ligase (Higa et al., 2006). Indeed, it was shown that Dacapo does not only possess a PIP degron but that it is also degraded in S-Phase (Swanson et al., 2015). In case of F-Box mediated degradation, a PhD thesis in the Sprenger Group observed that Dap stability is negatively affected by activity of the F-Box protein Rca1 (Regulator of cyclin A1), the fly homologue to human Emi1 (Kies, 2017). This connection was seen by analysis of protein stability with flow cytometric methods, by Co-IP assays and by MS analysis.

Although the binding and ubiquitination of the three CKIs is considered the essential function of Skp2 in mammals, this interaction is not studied well in flies. As already mentioned, the only two publications that deal with this topic come to different results. Ghorbani et al. (2011) could not see an increase of protein levels under Skp2 knockout conditions in larvae or brain/imaginal disc cells. However, Dui et al. (2013) came to different results. Among other things, Dap shows robust biochemical interaction with Skp2 and simultaneous Cks85A overexpression does increase this interaction further. Dap levels are also sensitive to modulation of Skp2 levels and overexpressing Skp2 leads to an enhanced portion of ubiquitinated Dap. These assays are neglecting some indirect effects, however and a final answer if Skp2 is really a regulator of Dap is not satisfactorily given, yet.

3.7.4. Cdt1, an essential factor in DNA replication

3.7.4.1. Cdt1 and its regulation

As already mentioned (see 3.3), Cdt1 has the important responsibility to recruit the MCM helicase to the DNA, thereby completing the pre-replication complex. The formation of the pre-RC is a prerequisite for subsequent start of DNA replication. Cdt1 was first discovered in fission yeast as a protein that is dependent on Cdc10 for its expression, thereby making it cell cycle regulated (Hofmann and Beach, 1994). The primary function of recruiting the MCM was described later (Nishitani et al., 2000). Since Cdt1 has essential function in DNA replication, homologues can be found in *S. cerevisiae* (Devault et al., 2002), *D. melanogaster* (Whittaker et al., 2000), *Xenopus laevis* (Maiorano et al., 2000) and *Homo sapiens* (Wohlschlegel et al., 2000). All of these homologues have in common that they are essential for DNA replication (Morgan, 2007).

DNA replication is a critical step in the cell cycle, since mistakes can lead to severe effects and deregulation of cell division. Therefore, Cdt1 expression, activity and stability must be controlled and regulated by cells. Indeed, Cdt1 levels are increased in several cancer cell lines and cells overexpressing Cdt1 can induce tumor growth if injected in mice (Arentson et al., 2002). The authors of this study conclude that Cdt1 is an oncogene. They also showed that cells enter S-Phase faster if Cdt1 is overexpressed, which is in accordance with its biological function. The effects of Cdt1 overexpression are dependent on the used cell line however. It was found that Cdt1 overexpression leads to re-replication only in certain tumor cell lines. It seems that the effect of Cdt1 overexpression in these cases is increased recruitment of MCM to the DNA. This ends up in erroneous DNA replication resulting in the creation of ssDNA, which is a signal for activation of the DNA damage response system (Liu et al., 2007).

Not all cell lines do react to the overexpression of Cdt1. However, a combined overexpression of Cdt1 together with ORC1 and Cdc6, other members of the pre-replicative complex, results in overreplicating cells, regardless of the cell line (Sugimoto et al., 2009). This effect could also be seen in mouse embryonic stem cells, where the combined overexpression leads to origin re-firing, re-replication and DNA damage (Munoz et al., 2017).

Cdt1 overexpression effects also the whole organism. Overexpression in mice results in increased cell numbers in mesenteric nodes and in rarer cases in massive adenopathy (Seo et al., 2005). The same study also performed Cdt1 overexpression experiments combined with p53 knockdown to prevent the activation of the DNA damage response system. Under these circumstances, mice fall ill on thymic lymphoblastic lymphomas and die prematurely. This suggests that Cdt1 is responsible for cell proliferation. Mouse embryos react to a combined overexpression of Cdt1 and Cdc6 with slowed development or even with degeneration and embryonic liver cells show an increase in DNA content. The same study also found that Cdt1 and Cdc6 overexpression leads to changes in the gastrointestinal tract, bone marrow, spleen and thymus, leading to morbidity and reduced life span in adult mice (Munoz et al., 2017).

Cdt1 activity and regulation does also play an important role in many different kinds of cancers. Cdt1 is a factor of tumor development from the first stages of cancer formation. While initial Cdt1 overexpression activates cell protection systems, prolonged overexpression circumvents these mechanisms and leads to genomic instability and the enhancement of aggressive properties of cells (Liontos et al., 2007). Cdt1 does also play a role in the formation of lung cancer, since its mRNA and protein levels are increased in lung cancer tissue. In addition, overexpressed Cdt1 and Cdc6, together with mutated p53, results in poor prognosis for lung cancer patients (Karakaidos et al., 2004). Another example is breast cancer, where higher Cdt1 levels result in reduced survival time of patients and Cdt1 mRNA and protein levels are increased in breast cancer cell lines (Mahadevappa et al., 2017).

Since Cdt1 stands in the center of DNA replication, it is not surprising that its activity and stability is thoroughly regulated in the course of the cell cycle. There are several mechanisms to regulate Cdt1. The protein Geminin binds to Cdt1 *in vivo* and *in vitro* and inhibits its ability to recruit MCM to the ORC-Cdc6 complex (Wohlschlegel et al., 2000). Furthermore, Cdt1 is also degraded by proteasomal degradation. In *C. elegans* it was found that knockdown of Cul4, the scaffold protein of the $CRL4^{Cdt2}$ ubiquitin ligase, leads to an arrest in S-Phase, because Cdt1 could no longer be removed from S-Phase cells (Zhong et al., 2003). Indeed, it could be shown that $CRL4^{Cdt2}$ is responsible for ubiquitination of Cdt1, leading to proteasomal degradation (Nishitani et al., 2006). The finding that PCNA is required for this degradation and the locating of the PIP degron at the beginning of the N-terminus are in accordance with this finding (Senga et al., 2006). It seems that this regulatory mechanism is conserved. In *Schizosaccharomyces pombe* two PIP

degrons are responsible for the proteasomal degradation of Cdt1 (Guarino et al., 2011). In addition, the original PIP degron was actually found and described in the *X. laevis* Cdt1 (Havens and Walter, 2009).

Finally, Cdt1 is also a substrate of SCF^{Skp2}, which regulates it in S- and G2-Phase (Li et al., 2003; Nishitani et al., 2006). Cdt1 needs to be phosphorylated to be recognized by Skp2 as well (Li et al., 2003), which is in concordance with substrate modification being the signal for Skp2 mediated degradation. Subsequent studies found that the CycA/Cdk1 and CycA/Cdk2 complexes are responsible for Cdt1 phosphorylation, priming it for ubiquitination by SCF^{Skp2} (Sugimoto et al., 2004). In addition, it was possible to identify the phospho-sites that need to be phosphorylated for Skp2 binding, a threonine at position 29 (Takeda et al., 2005) and presumably also the serine at position 31 (Nishitani et al., 2006). It has to be noted however that investigations differ in the importance of the Skp2 mediated degradation. Takeda et al. (2005) saw that a Cdt1 mutant that is no longer able to bind to Skp2 is still degraded like wild type Cdt1, speaking against a strong impact of SCF^{Skp2} regarding Cdt1 regulation. On the other hand, both Senga et al. (2006) and Nishitani et al. (2006) found that Skp2 mediated degradation is redundant and independent from $CRL4^{Cdt2}$, underlining the importance of this mechanism.

There also seems to exist a certain cross talk between Geminin and the proteasomal degradation of Cdt1. Association of Geminin to Cdt1 results in an increase of Cdt1 stability and a model was created were Geminin binding protects Cdt1 in S-, G2- and M-Phase from proteasomal degradation, at least to a certain extent. This mechanism ensures the persistence of basal Cdt1 levels in S-Phase and takes care of the re-accumulation of Cdt1 during G2- and M-Phase, which makes origin licensing from telophase onwards possible (Ballabeni et al., 2004). Indeed, it was found that Geminin protects Cdt1 explicitly from degradation by SCF^{Skp2} during mitosis (Tsunematsu et al., 2013).

3.7.4.2. The Cdt1 homologue in *D. melanogaster*

The homologue of Cdt1 in *Drosophila* is called Dup (double parked), since mutation of this gene not only results in a disablement of DNA replication but also in mitotical arrests during embryogenesis, thereby "parking" at two different points of the cell cycle (Whittaker et al., 2000). Dup shares sequence homology to other Cdt1 homologues, specifically to *S. pombe*, *Arabidopsis thaliana*, *C. elegans* and mouse and human versions. Another observation in this study was that Dup co-localizes with the ORC complex, in accordance with the behavior of its homologue. Furthermore, mutation of Dup results in a number of defects that are all linked to malfunctioning DNA replication. For example, DNA replication fails in S-Phase of embryonic cycle 16 if Dup is mutated (Whittaker et al., 2000). While maternal factors take care of correct progression of the DNA replication machinery, they are depleted after cycle 15 and the mutated version of Dup is unable to recruit the *Drosophila* MCM helicase to the DNA. Astonishingly, these cells are still capable of entering mitosis 16 where the cell cycle then stops. Ultimately, this results in embryonic death. The authors also used a second mutation of Dup that does not result in embryonic lethality and it was possible to investigate effects in adult individuals. It seems that this Dup version leads to reduced DNA amplification during oogenesis. Conversely, a simple overexpression of Dup does not lead to critical defects in fly development. Ubiquitous Dup overexpression leads to normal fly development and overexpression exclusively in the *Drosophila* eye leads only to a weak rough eye phenotype (Lee et al., 2010).

Regulation of Dup seems to be similar to Cdt1 in mammals for the most part. The *Drosophila* version of Geminin is able to interact biochemically and genetically with Dup (Quinn et al., 2001) and leads to prevention of re-replication in S-Phase caused by Cdt1 over activity (Mihaylov et al., 2002). Besides protein inhibition, Dup is also regulated by degradation. It was shown that two independent mechanisms are

responsible. The first mechanism does not rely on Dup phosphorylation for its degradation, the second mechanism only takes care of phosphorylated Dup, which is performed by CycE/Cdk2 (Thomer et al., 2004).

Later on, it became clear that in homology to Cdt1 the phosphorylation independent mechanism is based upon $CRL4^{Cdt2}$ degradation with the help of a PIP degron. Knockout of Cul4, the scaffold protein of CRL4, results in higher levels of Cdt1 in follicle cells (Lin et al., 2009a). Geminin knockdown results not only in re-replication but also in degradation of Cdt1 in *Drosophila* S2 cells (Hall et al., 2008). The authors speculated that both effects are connected. Increased re-replication leads to DNA damage and activation of the DNA damage checkpoint, which also targets Dup via the PIP degron. The PIP degron may be the main mechanism for Dup regulation. While overexpression of Dup alone does not show prominent effects, ubiquitous overexpression of a PIP degron deleted version results in embryonic death and in severe developmental effects in the eye, when expressed there (Lee et al., 2010). This indicates that cells are able to cope with an excessive amount of Dup, as long as the S-Phase degradation is still intact.

The protein responsible for the phosphorylation dependent pathway of Dup degradation is not known yet. It was already shown that CycE/Cdk2 potentially targets 10 phosphorylation sites in the Dup protein, since mutations of all of these sites results in a Dup version with increased stability (Thomer et al., 2004). In analogy to higher eukaryotes, it is possible that this mechanism is proteasomal degradation after ubiquitination by SCF^{Skp2}. As already mentioned, Cdt1 is a substrate of SCF^{Skp2} in other species and needs to be phosphorylated for this procedure. Furthermore, the phenotype of Dup overexpression – increased size of the nucleus and increased amount of apoptosis (Thomer et al., 2004) – is similar to some of the effects of Skp2 knockout (Ghorbani et al., 2011). Although Ghorbani et al. (2011) could not detect an increased amount of Dup under Skp2 knockout conditions, they exclusively concentrated on the endogenous protein, which is still under the control of its PIP-degron. This leaves the possibility of Skp2 regulation open, especially if it is not the main mechanism. Another hint is that the knockdown of Skp2 in plasmatocytes resulted in an accumulation of the Cdt1 signal, determined by fluorescence imaging (Kroeger et al., 2013). However, this study is solely based on fluorescence signals and fluorescence microscopy. A thorough investigation of Cdt1 stability in dependency of Skp2 with different methods did not happen, yet.

3.7.5. Cyclin E, an important regulator in G1- and S-Phase

3.7.5.1.Cyclin E in humans and mammals

The protein Cyclin E (CycE), has important regulatory function during G1- and S-Phase. Right from the start of its discovery, it was seen that CycE is capable of binding to Cdk1 and Cdk2 and in accordance with the conventional function of a cyclin is able to activate the kinase activity (Koff et al., 1991). In this publication, signs for high conservation of Cyclin E, at least regarding its function, were also observed. For example, human Cyclin E can interact with Cdc28 the *S. cerevisiae* homologue of Cdk1. Subsequent research identified Cdk2 as the main interaction partner for CycE (Koff et al., 1992). Therefore, it is an important regulator of S-Phase transition (see 3.2). Surprisingly, in contrast to other species, CycE/Cdk2 activity is not necessary for the progression of the cell cycle of continuously cycling cells (Geng et al., 2003). Indeed, these authors showed that mice with CycE knockout are developing largely normal and cell proliferation does also happen without problems. It was found however, that CycE/Cdk2 activity is necessary for quiescent cells to reenter the cell cycle.

A change in Cyclin E activity exercises dramatic effects in the control and regulation of the cell cycle. Overexpression of CycE results in less G1 cells, whereas S and G2 cell number is increased. The reason for this change in cell cycle distribution is a drastically shortened G1-Phase (Ohtsubo and Roberts, 1993). Overexpression of CycE also leads to changes in the number of chromosomes in rat embryo fibroblasts and human breast epithelial cells (Spruck et al., 1999). It seems that this increase in chromosomal instability is linked to the longer S-Phase, associated with CycE overexpression, since failures in the replication of the chromosomes occur. This links CycE to the formation and development of tumors.

Cyclin E/Cdk2 activity targets many proteins during the cell cycle for phosphorylation (Siu et al., 2012). Cyclin E dependent phosphorylation is not only regulating the expression of S-Phase genes but also stability of different proteins in G1- and S-Phase. For example, as already mentioned, it plays a role in the phosphorylation and ubiquitination of the three CKIs p21, p27 and p57 (see 3.7.3.1). The human Orc1 protein was also identified as a substrate for phosphorylation by CycE/Cdk2, though a direct consequence for protein stability was not found in this case (Mendez et al., 2002). The authors speculated that CycE marks Orc1 for recognition by Skp2, but that other F-Box proteins are also able to interact with Orc1 regardless of its phosphorylation status. An interesting case for Cyclin E dependent regulation is Cdc6 in quiescent cells. Phosphorylation by CycE/Cdk2 protects Cdc6 from ubiquitination through APC/C^{Cdh1} and proteasomal degradation. This allows Cdc6 to accumulate and is one factor that allows cells reentering of the cell cycle (Mailand and Diffley, 2005). Interestingly, it seems that besides its Cdk2 activating role, Cyclin E does also possess other activity, since a kinase dead mutation was still able to stimulate cell cycle reentering. Kinase dead CycE is able to bind to DNA, which would give a starting point to explain this observation (Geng et al., 2007).

Expression of CycE is regulated by E2F1 (Ohtani et al., 1995). As already described (see 3.2), there exists a positive feedback loop: mitogen-signaling results in initial phosphorylation of pRB and E2F1 activity, which leads among other things to CycE expression. CycE activity leads to hyperphosphorylation of pRB and consequently to stronger E2F1 activity and CycE expression.

Cyclin E is degraded during S-Phase by several mechanisms. It was observed that CycE/Cdk2 has auto-phosphorylating activity, resulting in phosphorylation of CycE at threonine 380. Eventually, this leads to ubiquitination and proteasomal degradation in S-Phase (Won and Reed, 1996). Furthermore, it seems that only free, unbound Cyclin E is susceptible to ubiquitination. Binding to Cdk2 protects CycE from proteasomal degradation (Clurman et al., 1996).

Later on, it was realized that a second phosphorylation site (threonine 62) is also important for ubiquitination and that the SCF^{Fbxw7} complex is responsible for this ubiquitination (Koepp et al., 2001; Strohmaier et al., 2001). These results are confirmed by experiments regarding CycE stability in knockin mice that also show that both phosphorylation sites are necessary for the regulation by Fbxw7 (Minella et al., 2008). Fbxw7 is not the only F-Box protein that regulates CycE stability however. Experiments showed that Skp2 is also able to recognize and ubiquitinate Cyclin E, resulting in its proteasomal degradation. In accordance with the data regarding Fbxw7, Skp2 can only target free CycE. Cdk2 binding seems to protect CycE from degradation also in this case (Nakayama et al., 2000).

3.7.5.2. Cyclin E function and regulation in *Drosophila melanogaster*

Just like its mammalian counterpart, *Drosophila* CycE does also interact with and activate Cdk2. However, unlike CycE in higher eukaryotes, it seems to be directly responsible for entry into S-Phase in *D. melanogaster* (Knoblich et al., 1994). This makes *Drosophila* CycE one of the most important regulators for

the transition of G1 to S. Another important function of CycE in flies is the regulation of endocycles. Endocycling cells and tissues, for example salivary glands, depend upon the oscillation of E2F1 and CycE. While E2F1 is responsible for CycE expression, CycE brings cells into S-Phase where E2F1 is degraded by $CRL4^{Cdt2}$, which resets the system for the next endocycle (Zielke et al., 2011).

The regulation of CycE in *D. melanogaster* is for the most part similar to that in higher eukaryotes. Expression of Cyclin E is also regulated by the activity of the E2F1 fly homologue (Duronio et al., 1996). In case of the degradation of CycE, it was seen that the F-Box protein Archipelago (Ago), the fly version of Fbxw7, is also responsible for CycE ubiquitination, leading to proteasomal degradation. Loss of Ago increases the number of cells in S- and G2/M-Phase and stabilizes Cyclin E in fly eyes (Moberg et al., 2001). Stabilization of CycE after Ago knockdown is also seen in *Drosophila* S2 cells (Koepp et al., 2001). Evidence exist that the protein Minus plays a supporting role in the binding of CycE through Ago (Szuplewski et al., 2009), something that is not known in mammals. This Ago dependent degradation links CycE regulation with the cell response to metabolic stress. The reduction of ATP-levels in cells leads ultimately to activation of p53 and expression of Ago, resulting in CycE instability and stop of the cell cycle in G1, which prevents cells from proliferation if growth conditions are not ideal (Mandal et al., 2010). Interestingly a study found hints that CycE stability is also connected to the presence of Cul4 in *Drosophila* (Higa et al., 2006). Since Cul4 is the scaffold protein of the CRL4 complex, this opens up the possibility of further, unknown regulation. Indeed, regarding the importance of Cyclin E in *Drosophila* for the beginning of S-Phase, it seems probable that its stability is not only regulated by SCF^{Ago} but by a number of different mechanisms. One of these candidates could be Skp2.

3.8. Aim of the thesis

The aim of this thesis was to obtain a deeper insight into the substrates and tasks of the F-Box protein Skp2 in *Drosophila melanogaster*. Since current literature does not give a final answer to the question if the CKI Dacapo is a substrate of SCF^{Skp2} this will be the first potential substrate that is analyzed. Special care will be taken to concentrate specifically on the effects of Skp2 on Dap. All disturbing factors, namely the G1 stop that Dap exerts when overexpressed and the degradation in S-Phase by $CRL4^{Cdt2}$, will be excluded by use of mutations that do not show these effects any longer. A thorough investigation, that incorporates Dap effects and alternative degradation mechanisms, has not happened in *Drosophila* yet and will hopefully help to clarify the role of Skp2 regarding Dap.

The second potential substrate that will be investigated is *Drosophila* Cdt1. Just like with Dap, mutations will be designed and created that exclude cell cycle effects and degradation by $CRL4^{Cdt2}$ in S-Phase. Again, the aim is to focus solely on the effects that Skp2 has on Cdt1 stability. Since Cdt1 is a crucial factor in DNA replication it is of interest to completely understand its regulation during the cell cycle. Experiments that focus specifically on Skp2 regulating Cdt1 have not happened yet and they will give further insight into the regulation of this important member of the origin licensing machinery.

The last potential substrate will be CycE, where first experiments regarding its regulation by SCF^{Skp2} will be performed. In these experiments, it will be tried to minimize the dramatic effect of CycE overexpression on the cell cycle to exclude indirect effects on stability that these shifts might have. CycE is a decisive factor for the transition into S-Phase in *D. melanogaster* and it is important to learn about its regulation for a better understanding of cell cycle regulation.

Besides these targeted approaches, an MS-analysis of Skp2 binding partners will also be performed to find new, unconsidered substrates for ubiquitination by the SCF^{Skp2} complex.

The first experiments however will be conducted to learn about the phenotypes of Skp2 overexpression and knockdown, primarily in Schneider cells. A Skp2 mutant, lacking the F-Box will also be investigated. The effects of these treatments on the cell cycle distribution will be important for the assessment of new substrates for Skp2. An experiment will also be performed to investigate if stability changes of potential substrates upon Skp2 overexpression or knockdown are caused directly or indirectly.

Methodically, this thesis will focus on a new approach developed in the Sprenger group to measure relative protein stability in living cells during the cell cycle by flow cytometry. This method has the advantage to measure protein stability in a relatively uncomplicated way in a massive number of cells. Besides, changes of cell cycle distribution, rescue experiments, live cell imaging and co-immunoprecipitations for analysis of biochemical interaction will also be applied.

Skp2 is one of the most intensive studied F-Box proteins in mammals. In comparison, the state of knowledge in *D. melanogaster* is relatively meager. Finding new targets for Skp2 in flies will give greater insight into the *Drosophila* model system regarding cell cycle and DNA replication control and may reveal new aspects of the F-Box protein Skp2.

4 Material and Methods

4.1. Material

4.1.1. Chemicals

Table 1 Chemicals

Chemical	Distributor
Molecular Biology	
1 kb Gene ruler DNA Ladder Mix	Thermo Fischer Scientific
Ampicillin	Carl Roth GmbH + Co. KG
ATP (100 mM)	New England Biolabs
Bacto Agar	BD Bioscience
Bacto Trypton	BD Bioscience
Bacto Yeast Extract	BD Bioscience
CTP (100 mM)	New England Biolabs
dNTP mix (dATP, dCTP, dGTP, dTTP)	New England Biolabs
DTT (1,4-dithiothreitol)	AppliChem GmbH
EDTA (ethylenediaminetetraacetic acid)	Fluka
Ethanol	Carl Roth GmbH + Co. KG
Ethidium bromide	SERVA Electrophoresis
Glycerol	Carl Roth GmbH + Co. KG
GTP (100 mM)	New England Biolabs
Hydrochlorid acid	Merck KGaA
Isopropanol	Merck KGaA
Kanamycin	AppliChem GmbH
Potassium Acetat	Merck KGaA
Purple Loading Dye (6x)	New England Biolabs
Restriction buffers 10x	New England Biolabs
Sodium chloride	Carl Roth GmbH + Co. KG
Sodium dihydrogen phosphate	Fluka
Sodium hydrogen phosphate	Fluka

Sodium hydroxide	Gerbu Trading GmbH
Spermidine	Sigma-Aldrich Chemie GmbH
T4 ligase buffer 10x	New England Biolabs
Tris (tris(hydroxymethyl)aminomethane)	Carl Roth GmbH + Co. KG
Ultrapure Agarose	Invitrogen GmbH
UTP (100 mM)	New England Biolabs
Cell Culture	
$CuSO_4$	AppliChem GmbH
FBS	PAN Biotech
FuGENE HD	Promega Corporation
Penicillin 100X	Invitrogen GmbH
Schneider`s *Drosophila* medium	Invitrogen, PAN Biotech
Sodium chloride	Carl Roth GmbH + Co. KG
Sodium dihydrogen phosphate	Fluka
Sodium hydrogen phosphate	Fluka
Streptomycin 100X	Invitrogen GmbH
Trypan Blue	Sigma-Aldrich Chemie GmbH
Trypsin/EDTA (ethylenediaminetetraacetic acid)	PAN Biotech
FACS	
EDTA	Fluka
Hoechst 33342	Sigma-Aldrich Chemie GmbH
Sodium azide	Sigma-Aldrich Chemie GmbH
Sodium chloride	Carl Roth GmbH + Co. KG
Sodium dihydrogen phosphate	Fluka
Sodium hydrogen phosphate	Fluka
Trypsin	SERVA Electrophoresis GmbH
Tween20	Carl Roth GmbH + Co. KG
Co-IP/SDS-PAGE/Western Blot	
Acetic acid	Merck KGaA
Acrylamide 30%/bisacrylamide	Carl Roth GmbH + Co. KG
APS (ammonium persulfate)	Merck KGaA

beta-Mercaptoethanol	Fluka
Bromphenol blue	SERVA Electrophoresis GmbH
Coomassie Brilliant Blue	Sigma-Aldrich Chemie GmbH
EDTA	Fluka
EGTA (ethylene glycol tetraacetic acid)	Sigma-Aldrich Chemie GmbH
Gloria skimmed milk powder	Nestle
Glycerol	Carl Roth GmbH + Co. KG
Glycine	AppliChem GmbH
HEPES (2-[4-(2-hydroxyethyl)piperazin-1-yl]ethanesulfonic acid)	AppliChem GmbH
Methanol	Carl Roth GmbH + Co. KG
Precision Plus Protein All Blue Prestained Protein Standard	Bio-Rad Laboratories, Inc.
Protease inhibitor cocktail	Bimake.com
SDS (Sodium dodecyl sulfate)	Carl Roth GmbH + Co. KG
Sodium acetate	Merck KGaA
Sodium chloride	Carl Roth GmbH + Co. KG
Sodium dihydrogen phosphate	Fluka
Sodium fluoride	Fluka
Sodium hydrogen phosphate	Fluka
TEMED (tetramethylethylenediamine)	Fluka
Tris (tris(hydroxymethyl)aminomethane)	Carl Roth GmbH + Co. KG
Triton X-100	Fluka
Mass spectrometric analysis	
Acetonitrile	Sigma-Aldrich Chemie GmbH
Ammonium bicarbonate (NH_4HCO_3)	Fluka
Liquid nitrogen	AG Schneuwly (University of Regensburg)
Trypsin Gold, Mass Spectrometry Grade	Promega Corporation
Fly Experiments	
Dpx	Sigma-Aldrich Chemie GmbH

4.1.2. Kits

Table 2 Kits

Kit	Distributor	Purpose
FLAG Immunoprecipitation Kit	Sigma-Aldrich Chemie GmbH	Co-IP for Mass Spec
Invisorb Spin DNA Extraction Kit	Stratec Biomedical AG	Clean Up PCRs
MSB Spin PCRapace	Stratec Biomedical AG	Clean Up Gel Fragments
PureYield Plasmid Midiprep system	Promega Corporation	Midi Preparations

4.1.3. Solutions and buffers

Table 3 Solutions and buffers

Solution/Buffer	Components	Concentration
Ampicillin stock solution	Ampicillin in 50 % ethanol	50 mg/ml
APS solution 10 %	APS in H_2O	10 % (w/v)
Coomassie staining solution	Coomassie Brilliant Blue G250 Methanol Glacial acetic acid in H_2O	0.01% 50% 10%
dNTP mix (2mM each)	dNTP mix in H_2O	2 mM
Easy Prep buffer	Tris, pH 8.0 EDTA, pH 8.0 Sucrose Lysozyme RNase A	10 mM 1 mM 150 mg/ml 2 mg/ml 0.2 mg/ml

	BSA	0.1 mg/ml
	in H_2O	
IP Lysis buffer	HEPES, pH 7.5	50 mM
	NaCl	150 mM
	EGTA	1 mM
	NaF	10 mM
	Triton X-100	1 % (v/v)
	Glycerol	10 % (v/v)
	in H_2O	
	For use, Protease inhibitor mix is freshly added.	
IP Washing buffer	HEPES, pH 7.5	50 mM
	NaCl	150 mM
	Triton X-100	1 % (v/v)
	Glycerol	10 % (v/v)
	in H_2O	
Kanamycin stock solution	Kanamycin	50 mg/ml
	in H_2O	
Laemmli running buffer 10X	Tris	250 mM
	Glycin	9.46 M
	SDS	10 g/l
	in H_2O	
LSB 2X	Tris, pH 6.8	120 mM
	SDS	4 % (w/v)
	Glycerol	20 % (v/v)
	Bromophenol blue	0.04 % (w/v)
	beta-Mercaptoethanol	10 % (v/v)
	in H_2O	
LSB 2X, non-reducing	Tris, pH 6.8	120 mM

	SDS	4 % (w/v)
	Glycerol	20 % (v/v)
	Bromophenol blue	0.04 % (w/v)
	in H_2O	
Milk powder solution	Skim milk powder	5 % (m/v)
	Sodium azide	0.01 % (m/v)
	in PBS	
MS Trypsin Solution	Trypsin Gold, Mass Spectrometry Grade	30 % (v/v)
	in 50 mM NH_4HCO_3	
MS Washing Solution I	AcN	25 % (v/v)
	in 50 mM NH_4HCO_3	
MS Washing Solution II	AcN	50 % (v/v)
	in 50 mM NH_4HCO_3	
MS ioadacetamide solution	Iodacetamide	5 mg/ml
	in 50 mM NH_4HCO_3	
MS DTT	DTT for MS	1 mg/ml
	in 50 mM NH_4HCO_3	
NTP mix (25 mM each)	NTP mix	25 mM
	in H_2O	
PBS	NaCl	130 mM
	Na_2HPO_4	7 mM
	NaH_2PO_4	3 mM
	pH	7.2
	in H_2O	
PBT	Tween 20	0.1 % (v/v)

	in PBS	
Phusion HF Buffer	not specified	5x

Resolving gel (SDS PAGE) For 10 ml resolving gel:

Gel	H_2O (ml)	Acrylamide 30%/ Bisacrylamide (µl)	1.5 M Tris/HCl pH 8.8 (µl)	10 % SDS (µl)	10 % APS (µl)	TEMED (µl)
8 %	4.7	2.7	2.5	0.1	100	10
12%	3.4	4.0	2.5	0.1	100	10
15%	2.4	5.0	2.5	0.1	100	10

SDS solution 10 %	SDS	10 % (w/v)
	in H_2O	

Stacking gel (SDS PAGE) For 10 ml stacking gel:

Gel	H_2O (ml)	Acrylamide 30%/ Bisacrylamide (µl)	1.5 M Tris/HCl pH 6.8 (µl)	10 % SDS (µl)	10 % APS (µl)	TEMED (µl)
4%	6.1	1.3	2.5	0.1	100	10

Stacking gel was stored as 50 ml stock solution without APS and TEMED.

TAE buffer	Tris, pH 8.0	40 mM
	EDTA	10 mM
	in H_2O	
Transcription buffer 5X (T7)	HEPES, pH 7.5	80 mM
	Spermidine	2 mM

	DTT	10 mM
	NTPs (ATP, CTP, GTP, UTP)	3 mM
	$MgCl_2$	12 mM
	in H_2O	
Transfer buffer 3 (Western blot)	Methanol	20 % (v/v)
	Tris, pH 7.5	40 mM
	EDTA, pH 8.0	2 mM
	Sodium acetate	20 mM
	SDS	0.05 % (v/v)
	in H_2O	
Trypsin/EDTA in PBS	Trypsin	0.05%
	EDTA	0.02%
	in PBS	0.1 M

All solutions and buffers in kits were used as described in the respective manuals.

4.1.4. Proteins and Enzymes

Table 4 Proteins and enzymes

Proteins	Distributor	Purpose
Phusion DNA polymerase	AG Thomm (homemade)	PCR
Restriction endonucleases	New England Biolabs	Restriction (cloning)
RNase A	AppliChem GmbH	EasyPrep buffer
RNase Inhibitor	AG Medenbach (homemade)	In vitro transcription
Shrimp Alkaline Phosphatase (rSAP)	New England Biolabs	Dephosphorylation (cloning)
T4 DNA Ligase	New England Biolabs	Ligation
T7 RNA polymerase	Thermo Scientific	In vitro transcription

4.1.5. Media and agar plates

Table 5 Media and agar plates

Medium/Agar Plate	Components	Concentration
LB agar plate	Bacto Agar In LB medium (autoclaved) Solution is boiled for casting plates. Before adding any antibiotic, the solution is first cooled down to 50°C.	1.7 % (w/v)
LB medium (autoclaved)	BactoTrypton Bacto Yeast Extract NaCl pH in H_2O	10 g/l 5 g/l 10 g/l 7.2
Schneider's *Drosophila* complete medium	GIBCO FBS Penicillin/Streptomycin in Schneider's *Drosophila* Medium	10 % (v/v) 1% (v/v)

Ampicillin was used as 100 µg/ml; Kanamycin was used as 50 µg/ml.

4.1.6. Antibodies

Table 6 Primary antibodies for Co-IP and Western Blot analysis

Antigen	Number	Source	Western Blot	Co-IP	Distributor	Purpose
FLAG	374	Mouse	1:5000	1:300	Sigma	Precipitation, analysis
HA	373	Mouse	1:2000	1:300	Covance	Precipitation, analysis

Table 7 Secondary antibodies for Co-IP and Western Blot analysis

Antigen	Number	Source	Fluorochrome	Dilution	Distributor	Purpose
Mouse	367	Goat	IRDye 800	1:5000	Li-Cor, Inc.	analysis

4.1.7. Oligonucleotides

Oligonucleotides used for cloning and sequencing are not listed but can be found in the database of the Sprenger Group. Amplification of DNA for dsRNA production was performed with SPO_288 (Sequence: 5'TAGGCCTTAATACGACTCACTATAGGG3').

4.1.8. Plasmids

Table 8 Plasmids

Plasmid	Name	Promotor	Nickname	Purpose
pFSR-0092	pBSII Bluescript KS+	-	Bluescript	3
pFSR-0400	MtPro-HA-NLS-GFP(G)	MtPro	HA-NLS-GFP(G)	9
pFSR-0419	MtPro-HA-CycE	MtPro	HA-CycE	1
pFSR-0804	T7-Skp2-T7	-	-	2
pFSR-0814	MtPro-4XFLAG-DmSkp2	MtPro	4XFLAG-Skp2	9
pFSR-0845	T7-hygromycin-T7	-	-	2
pFSR-0859	T7-Amp-T7	-	-	2
pFSR-0864	MtPro-HA-NLS-Cdt1_Del-102-609-3XCHE	MtPro	Cdt1-1-101_3XCHE	9

pFSR-0871	MtPro-GFP(G)-Skp2	MtPro	GFP(G)-Skp2	9
pFSR-0951	MtPro-3xHA-Cks85A-SV40UTR	MtPro	3xHA-Cks85A	1
pFSR-0952	PubPro-4xFLAG-Skp2-ryUTR	PubPro	4xFLAG-Skp2	1, 5, 6, 7
pFSR-0967	ActPro-GFP(G)-Dap-GloACUTR	actPro(S)	GFP-Dap	1
pFSR-1004	pUbPro-HA-Dap-ryUTR	PubPro	HA-DAP	1, 5
pFSR-1023	PubPro-Cks85A-ryUTR	PubPro	-	1
pFSR-1069	PubPro-Skp2 4xFLAG ryUTR	PubPro	-	1
pFSR-1071	actPro 3xChe MtPro-GFP-CycE SV40 UTR	actPro	-	7
pFSR-1072	actPro(L)-mChe-dT2A-HA-NLS-GFP(G)-GloACUTR	actPro(L)	CHE-T2A-HA-NLS-GFP	1
pFSR-1077	PubPro-4xFLAG-Skp2_Del-175-223-ryUTR	PubPro		1
pFSR-1150	actPro(L)-mChe-dT2A-HA-NLS-GFP(G)-Cdt1_Del-601-743-GloACUTR	actPro(L)	CHE-T2A-GFP-Cdt1 15-600	1
pFSR-1179	actPro(L)-HA-NLS-BamHI-XbaI-CHE-ddT2A-HA-NLS-GFP	actPro(L)	BX-CHE-ddT2A-GFP	1
pFSR-1180	actPro(L)-HA-NLS-CHE-BamHI-XbaI-ddT2A-HA-NLS-GFP	actPro(L)	-	1
pFSR-1185	actPro-CHE-CycE-T2A-HA-NLS-GFP	actPro(L)	-	1
pFSR-1194	PubPro-Skp2-1-500-hairpin	PubPro	Skp2 Hairpin	1
pFSR-1204	actPro(L)-HA-NLS -GFP-ddT2A-HA-NLS-CHE-BamHI-XbaI	actPro(L)	GFP-ddT2A-CHE-BX	1
pFSR-1214	actPro(L)-HA-NLS -GFP-ddT2A-HA-NLS-BamHI-XbaI-CHE	actPro(L)	GFP-ddT2A-BX-CHE	1
pFSR-1222	pUbPro-HA-Cdt1-1-600-ryUTR	PubPro	-	6
pFSR-1238	actPro(L)-HA-NLS-GFP-ddT2A-HA-NLS- CHE-Dap-dCDI	actPro(L)	GFP-ddT2A-CHE-Dap-dCDI	1
pFSR-1247	actPro(L)-HA-NLS-Che-Cdt1_Del-1-15-Del-301-743-	actPro(L)	Che Cdt1 15-300	1

	T2A-HA-NLS-GFP(G)-GloACUTR			
pFSR-1248	MtPro-Hygro-Hairpin	MtPro	Hygro Hairpin	1
pFSR-1270	actPro(L)-HA-NLS-CHE-CycE-ddT2A-HA-NLS-GFP	actPro(L)	CHE-CycE-ddT2A-GFP	1
pFSR-1275	pUbPro-HA-Slmb-vhh-GFP-ryUTR	PubPro		1
pFSR-1281	T7 Cdt1 nt1406-nt1800-T7	-	Cdt1 dsRNA	2
pFSR-1282	actPro(L)-HA-NLS-CHE-Cdt1_Del1-15_Del601-742-ddT2A-HA-NLS-GFP	actPro(L)	Che Cdt1 15-600	1
pFSR-1283	actPro(L)-HA-NLS-CHE-Cdt1_Del1-15_Del_226-743-ddT2A-HA-NLS-GFP	actPro(L)	Che Cdt1 15-225	1
pFSR-1284	actPro(L)-HA-NLS-CHE-Cdt1_Del1-15_Del264-743-ddT2A-HA-NLS-GFP	actPro(L)	Che Cdt1 15-263	1
pFSR-1285	actPro(L)-HA-NLS-CHE-Cdt1_Del1-169_Del301-743-ddT2A-HA-NLS-GFP	actPro(L)	Che Cdt1 170-300	1
pFSR-1288	actPro(L)-HA-NLS-GFP-ddT2A-HA-NLS-CHE-Dap	actPro(L)	-	1
pFSR-1300	actPro(L)-HA-NLS-CHE-Cdt1_Del1-15_Del264-743_S111A-ddT2A-HA-NLS-GFP	actPro(L)	Che Cdt1 15-263 S111A	1
pFSR-1301	actPro(L)-HA-NLS-CHE-Cdt1_Del1-15_Del264-743_T158A-ddT2A-HA-NLS-GFP	actPro(L)	Che Cdt1 15-263 T158A	1
pFSR-1302	actPro(L)-HA-NLS-CHE-Cdt1_Del1-15_Del264-	actPro(L)	Che Cdt1 15-263 S168A	1

	743_S168A-ddT2A-HA-NLS-GFP			
pFSR-1303	actPro(L)-HA-NLS-CHE-Cdt1_Del1-15_Del264-743_S226A-ddT2A-HA-NLS-GFP	actPro(L)	Che Cdt1 15-263 S226A	1
pFSR-1310	actPro(L)-Cdt1-mCHE-dT2A-Deopt-HA-NLS-GFP	actPro(L)	-	1
pFSR-1319	actPro(L)-Cdt1-15-763-mCHE-dT2A-Deopt-HA-NLS-GFP	actPro(L)	-	1
pFSR-1363	actPro(L)-HA-NLS-GFP-ddT2A-HA-NLS-Che-Dap_Del-38-44-RAR-_Del-103-150-G_Del-184-188-SV40UTR	actPro(L)	-	1
pHT-013	HA-SkpA in RmHARW2	MtPro	HA SkpA	5,6,7
pOT-233	pUC-19	-	-	8

1) FACS cell cycle and stability analysis

2) *in vitro* transcription of dsRNA

3) empty DNA for transfection

4) Mass spectrometric analysis of Skp2 binding partners

5) Co-IP between Skp2 and Dap

6) Co-IP between Skp2 and Cdt1 fragments

7) Co-IP between Skp2 and CycE

8) Intermediate cloning

9) Live cell imaging

4.1.9. Bacterial strains

Table 9 Bacterial strains

Strain	Genotype
DH5 α	F^- *endA1 glnV44 thi-1 recA1 relA1 gyrA96 deoR nupG purB20* ϕ80d*lacZ*ΔM15 Δ(*lacZYA-argF*)U169, hsdR17($r_K^- m_K^+$), λ^-

4.1.10. Eukaryotic cell lines

Drosophila Schneider cells (S2R+) were used for cell cycle analysis, flow cytometric stability analysis, co-immunoprecipitations and MS-analysis.

4.1.11. Fly Strains

Table 10 Fly Strains

Strain	Information
UAS-HA-Skp2	Skp2 overexpression
en::gal4	engrailed driver line
attp-86F	Control cross

4.1.12. Equipment

Table 11 Equipment

Equipment	Distributor
µ-Slide 8 Well	ibidi GmBH
Acrylamide gel apparatus	Bio-Rad Laboratories, Inc.
Agarose gel electrophoresis apparatus HE33	Hoefer, Inc.
Anti-FLAG Affinity Gel	bimake.com
Axio Observer.Z1 (inverted)	Zeiss
AxioCam MRm Rev3	Zeiss
Axygen 200 µl Maxymum Recovery pipette tips	Corning Inc.
Axygen MCT-060-L-C Microcentrifuge Tube 0.6 ml	Corning Inc.
Caps with holes for 0.5 ml Axygen Cups	selfmade
Caps with holes for 1.5 ml Cups	selfmade
CaptiveSpray nanoflow electrospray source	Bruker Daltonics
Cell culture incubator	Hereaus
Cell culture roller TC-7	New Brunswick Scientific
Centrifuge 5418 (on the bench)	Eppendorf
Centrifuge 5402 (for Co-IPs)	Eppendorf
Centrifuge Heraeus Multifuge 1S (for midi preps)	Thermo Scientific

Centrifuge RotoFix 32A (for cell culture)	Hettich
Clean bench	Ceag Schirp Reinraumtechnik
Clean bench Mars Safety Class 2	SCANLAF
Electrophoresis power supply EPS 200	Pharmacia Biotech
Electrophoresis power supply EPS 300	Pharmacia Biotech
Electroporation apparatus Easyject Prima	Equibio
FastPette V2 Pipette Controller	Labnet
Flow cytometer CyFlow space	Partec
Freezer C760	New Brunswick Scientific
Fuchs-Rosenthal Counting chamber (16 mm², 0.2 mm cell depth)	Hausser Scientific
Halogen lamp 100 W	
Heating block (Digital Dry Bath, dual position)	Benchmark Scientific
Heating System	ibidi GmBH
HT 200	ibidi GmBH
I-3020	Applied Scientific Instrumentation
Incubator Heraeus B 5050 E	Heraeus
Incubator Sanyo MIR-153	Sanyo
Inverted microscope CKX41 (equipped with Reflected Fluorescence System with Light Source X-Cite 120Q)	Olympus
MaXis plus UHR-QTOF System	Bruker Daltonics
MF-Millipore Membrane	Merck KGaA
NuPAGE 4-12% Bis-Tris Protein Gels	Thermo Fischer Scientific
Odyssey Infrared Imaging system	LI-COR
PerfectBlue Semi-Dry Electro Blotter	Peqlab
Plan-APOCHROMAT 20X	Zeiss
Protein G Plus-Agarose Beads	Santa Cruz
Sieve (2 cm² diameter)	Own production
SimplyBlue SafeStain	Thermo Fischer Scientific
Spectrophotometer / Fluorometer DS-11 FX+	DeNovix
Spinning disk unit (CSU-X1)	Yokogawa

Thermocycler GTC96S Cleaver	Scientific Ltd
ThermoMixer F1.5	Eppendorf
Tube 3.5 ml, 55 x 12 mm, PS (FACS sample tube)	Sarstedt AG & Co. KG
UV Crosslinker	Stratalinker
UVP GelStudio PLUS	Analytik Jena AG
Water purification system	ELGA

All other used equipment and consumables (e.g. beakers, reaction tubes, freezers, …) were considered non-critical and are not mentioned.

4.1.13. Lasers and Light Sources

Table 12 Lasers and Light Sources

Name	Wavelength [nm]	Power	Fluorescent dyes
Flow Cytometer			
UV-LED	365	-	Hoechst
Sapphire 488-20 Laser	488	20 mW	GFP
Sapphire 561-100-CW Laser	561	100 mW	Cherry
Spinning Disk Microscope			
OPSL Laser	488	100 mW	GFP
Diode Laser	561	40 mW	Cherry

4.1.14. Filters

Table 13 Filters

Filters	Fluorescence	Equipment
Bandpass-Filter BP527/30	GFP	flow cytometer
Bandpass-Filter BP455/50	Hoechst 33342	flow cytometer
Bandpass-Filter BP488	FSC/SSC	flow cytometer
Longpass-Filter LP590	mChe	flow cytometer
ET Bandpass 605/70	mChe	Spinning disk microscope

4.1.15. Software

Table 14 Software

Software	Developer	Source	Application
Canvas Version 11	ACD Systems of America, Inc	n.a.	Figures
ContigExpress	Invitrogen	n.a.	Sequencing analysis
dsCheck	n.a.	Naito et al., 2005	Check for off targets of dsRNA
Endnote X7.5	Thomson Reuters	n.a.	Citation
FCS Express 4.07	De Novo Software	n.a.	FACS data analysis
FileMaker Pro 15	FileMaker, Inc.	n.a.	Data base management
ImageJ	n.a.	Schneider et al., 2012	Image analysis
Origin 2017 (64-bit)	Origin Lab Corporation	n.a.	Figures, statistics
PAST	n.a.	Hammer et al., 2001	statistics
Vector NTI Advance 11.5.4	Invitrogen	n.a.	Plasmid design

4.2. Methods

4.2.1. Cloning Methods

4.2.1.1. PCR

PCR was used for DNA amplification. Table 15 shows the used PCR reaction mix.

Table 15 PCR Reaction Mix

Component	Volume/Amount
DNA	100 ng
Forward Primer (100 pmol/l)	1 µl
Reverse Primer (100 pmol/l)	1 µl
5xHF Phusion Buffer	10 µl
dNTPs (2mM)	5 µl
Phusion Polymerase (2U/µl)	0.5 µl
H_2O	-> add 50 µl

Table 16 shows the PCR program.

Table 16 PCR program

Step	Temperature	Time	Cycles
Initial Denaturation	96°C	30 sec	
Denaturation	96°C	10 sec	
Annealing	Variable	20 sec	25
Extension	72°C	Variable	
Final extension	72°C	5 min	
Storage	4°C	∞	

Annealing Temperature was chosen according to the primer base composition and calculated with the online tool "Tm calculator" from ThermoFischer Scientific (https://www.thermofisher.com/de/de/home/brands/thermo-scientific/molecular-biology/molecular-biology-learning-center/molecular-biology-resource-library/thermo-scientific-web-tools/tm-calculator.html, retrieving date: 24.05.2018).

Extension time was chosen in dependency of the length of the PCR product according to the speed of Phusion-Polymerase, which was estimated as 40 seconds per kilobase.

4.2.1.2. DNA Clean Up

DNA Clean Up was used for purification of PCRs or for enrichment of low concentrated plasmids. The *MSB Spin PCRapace* was used.

50 µl DNA (for example the PCR reaction mix) was mixed well with 250 µl binding buffer. The sample was transferred to a Spin Filter and centrifuged 2 min at 11000 g. The filtrate was removed and the sample was centrifuged again for 3 minutes to remove excess buffer. The Spin Filter was placed in a new tube and the desired volume of H_2O (e.g. 30 µl for PCR clean ups) was added directly to the filter. After 1 minute of incubation at room temperature, the DNA was eluted by centrifugation for 1 min at 11000 g.

4.2.1.3. Restriction for cloning

DNA vectors and inserts were restricted with enzymes overnight at 37°C. Up to 5000 ng of vector and insert DNA was used for restriction. 1 µl of each restriction enzyme and 3 µl of the correct buffer was added to the DNA. The reaction was filled-up with H_2O to 30 µl.

If the insert was a PCR product, it was purified (see 4.2.1.2) and afterwards the whole 30 µl were used for restriction. The complete restriction setup had a volume of 35 µl in this case.

4.2.1.4. Dephosphorylation

To minimize the number of religated vectors during cloning, dephosphorylation was used after restriction in some cases.

1.5 µl of shrimp alkaline phosphatase (rSAP) was added to the digest after restriction was finished. The reaction was incubated at 37°C for 30 min and then heat inactivated at 65°C for 5 min.

4.2.1.5. Agarose gel electrophoresis

Agarose gel electrophoresis was used for separation of DNA bands, which was necessary for gel fragment isolation (see 4.2.1.6), screening of Kochlysates (see 4.2.1.11) and quantification of DNA bands (see 4.2.1.7 and 4.2.1.13).

Gels were casted by heating up 40 ml of TAE buffer together with 0.4 g of agarose in a microwave. 40 µl of ethidium bromide (EtBr, concentration 10 mg/ml) was added and gels were cast in the gel sleds. Samples were mixed with 6x Loading Dye and pipetted in the gel pockets. 5 µl of 1 kb Gene ruler Mix was also loaded on one gel lane. The gel run was performed for 45 min at 90 V. If necessary, documentation was performed at UVP GelStudio PLUS. Images were saved digitally for later analysis (e.g. quantification).

4.2.1.6. DNA Gel extraction

For isolation of digested DNA fragments, the restricted DNA was separated by agarose gel electrophoresis (see 4.2.1.5). The desired band was cut out with a scalpel, transferred in a reaction tube and weighed.

DNA Gel extraction was performed with the *Invisorb Spin DNA Extraction Kit*. 500 µl Gel solubilizer was added to the agarose fragment (in case the weight of the fragment exceeded 150 mg, 1000 µl were added instead). The tube was heated at 50°C until the gel was completely solubilized. 250 µl (or respectively 500 µl) of Binding Enhancer were added to the reaction. The whole sample was loaded onto a Spin Filter and centrifuged for 2 min at 11000 g. The filtrate was discarded and 500 µl Wash Buffer were pipetted on the filter. After another centrifugation (1 min at 11000 g) the filtrate was discarded. This washing step was repeated once. For removal of last traces of Wash Buffer, centrifugation was performed for 4 min at full speed. Afterwards the Spin Filter was put into a Receiver Tube, 30 µl of water was put on the center of the filter and incubated for 5 min at room temperature. For eluting the DNA, the Spin Filter was centrifuged for 1 min at 11000 g.

4.2.1.7. Quantification of vector and insert

Concentration of vector and insert DNA was determined by agarose gel quantification. One tenth of the eluted DNA was mixed with loading dye and loaded onto a gel. After the gel run and documentation (see 4.2.1.5) the digital images were analyzed with ImageJ. The intensities of the vector and insert DNA bands were quantified with the help of the intensity of the DNA ladder bands as a reference.

4.2.1.8. Ligation

A typical ligation setup consisted of 2 µl of Ligation buffer, 1 µl of T4 DNA Ligase and vector and insert DNA. A molar ratio of vector to insert of 1:3 was used. Up to 100 ng of vector DNA and the equivalent amount of insert DNA was inserted into the ligation. If necessary, water was added to a volume of 20 µl. To estimate the number of self-ligating vector later, a control ligation was also set up, with no insert DNA in it. This was necessary for the estimation of the number of colonies to be screened.

Incubation was performed at room temperature for at least 2.5 hours. If incubation was performed over night or over the weekend, the ligations were put on 18°C. Afterwards, transformation was conducted (see 4.2.1.10).

4.2.1.9. Site directed mutagenesis

Site directed mutagenesis (Weiner et al., 1994) was used for introducing point mutations in proteins. A PCR was performed as described in 4.2.1.1 with a mutagenesis primer. These primers contained the desired mutation.

After PCR, a DpnI restriction was performed. DpnI is a four cutter and exclusively cuts methylated DNA. Therefore, most of the un-mutated PCR template was removed. 1 µl of DpnI was added to the PCR and the sample was incubated at 37°C for one hour.

To remove the high amount of salt that would disturb the following transformation (see 4.2.1.10), dialysis against water was conducted. The sample was pipetted onto a dialysis membrane in a petri dish filled with de-ionized water. After one hour, the sample was removed and transformation was conducted.

4.2.1.10. Transformation

Electroporation was used for transforming *Escherichia coli* with cloned plasmids. The *E. coli* strain DH5α was used for transformation, aliquots (100 µl each) of which were stored at -80°C. The bacteria were slowly thawed on ice and diluted with 100 µl of H_2O. 100 µl of the bacterial suspension was mixed with 1 µl of the ligation mix and transferred in an electroporation cuvette. All steps were performed on ice. Before putting the cuvette in the electroporator, it was dried. Electroporation took place with 2500 V. Directly afterwards 1 ml of LB_0 was applied to the transformed bacteria.

If the plasmid contained Ampicillin resistance, cells were directly platted on LB_{Amp} plates. If the resistance was Kanamycin, cells were put at 37°C for one hour, since in this case it was necessary that the resistance is developed before platting.

In either case, 100 µl were platted on LB plates. Incubation was performed overnight at 37°C.

4.2.1.11. Screening of colonies with Kochlysates

Colonies were screened for successful cloning with the Kochlysate method (Berghammer and Auer, 1993). Colonies were picked from the plate and transferred to 2 ml of LB_{Amp}- or LB_{Kan}-Medium. These Kochlysate cultures were incubated at 37°C over night.

On the next day, 1.5 ml of the bacterial culture was transferred in a reaction tube and centrifuged with full speed for 4 min. The supernatant was discarded and the cell pellet was resuspended with 50 µl of Easy Prep Buffer. Afterwards, lysis was performed by putting the reaction tubes for 1 min at 100°C. After that, samples were immediately cooled down by putting them on ice for 1 min. In a final step, centrifugation took place for 15 min at full speed. Plasmid DNA was now in the supernatant.

A test digest with fitting restriction enzymes revealed if the colony was positive or negative. 5 µl of the plasmid DNA was mixed with 1 µl buffer, 0.5 µl of each restriction enzyme and 3 µl H_2O. Incubation took place for 1 hour at 37°C. The digest was analyzed by gel electrophoresis (see 4.2.1.5).

4.2.1.12. Midi Preps

Midi preps were performed for receiving highly concentrated, clean DNA. The *PureYield Plasmid Midiprep system* from Promega was used. Midi cultures, at least 50 ml of LB with fitting antibiotics, were inoculated with 100 µl of the positive Kochlysate culture. If Ampicillin was the antibiotic, it was necessary to wash the Kochlysate culture with LB_{Amp} before inoculation. Otherwise, traces of β-Lactamase originating from transformed *E. coli* and responsible for the resistance of the bacteria against Ampicillin, would end up in the Midi culture, which would lower the selection pressure and significantly reduce the DNA yield. Therefore, cells were centrifuged at 4000 rpm for 4 min, the supernatant was discarded and 1 ml of LB_{Amp} was applied to the cell pellet. Centrifugation was repeated, the supernatant again discarded and the pellet resolved in 100 µl of LB_{Amp}, which was used for inoculation. Since Kanamycin worked in a different fashion, this procedure was not necessary and inoculation happened right away. In either case, incubation took place at 37°C overnight.

On the next morning, the Midi culture was transferred to a 50 ml reaction tube and spun down at 4500 rpm for 10 min. The supernatant was discarded and the pellet was resuspended in 3 ml of Cell Resuspension Solution. For cell lysis, 3 ml of Cell Lysis Solution was applied, the sample was inverted 5 times and incubated for 3 min. Directly afterwards, 5 ml of Neutralization Solution was pippeted into the reaction tube and mixed by inverting 5 times. The mix was centrifuged at 4500 rpm for 25 min for precipitation, the plasmid DNA was in the supernatant afterwards.

The supernatant was filtered through a sieve to get rid of cell debris. Thereafter, the sample was loaded onto a binding column which was attached to a vacuum pump. Vacuum was applied, the sample was sucked through the column, whereby the DNA stuck to the binding membrane. The DNA was washed by applying 20 ml of Wash Buffer. The vacuum was again applied until the column was completely dry. To ascertain that the ethanol completely vanished, the column was transferred in a fresh 50 ml reaction tube and centrifuged for 1500 g for 1 min.

To elute the DNA, the column was again transferred in a new 50 ml reaction tube. 600 µl of sterile water was applied to the volume. Elution took place by centrifugation at 1500 g for 2 min. The DNA was now ready for quantification. In the end, samples were stored at -20°C upon usage.

4.2.1.13. Quantification of Plasmid DNA

Two methods were used for DNA quantification: a photometric quantification with the *Spectrophotometer/Fluorometer DS-11 FX+* and gel quantification.

For the photometric quantification, 1 µl of DNA was used. The photometer analyzed the quality of the DNA (the 260 to 280 ratio) and the concentration.

If a plasmid was only used for further cloning, only the photometric concentration was used. If, however, the plasmid was to be used in transfection, the more thorough quantification method by an agarose gel was applied. Since it is only possible to quantify DNA fragments precisely, the first step was to digest the new plasmid. If possible, restriction enzymes were chosen, which produce an 1100 bp band that was used for quantification. Around 50 – 100 ng of plasmid DNA (according to the photometric quantification) was used for digestions together with 1 µl buffer and 1 µl of each enzyme. H_2O was used to fill up the volume to 10 µl. Restriction took place at 37°C for at least 1 hour. After gel electrophoresis (see 4.2.1.5) the digital gel image was analyzed with ImageJ.

The principal quantification was done with the intensity of the DNA ladder as reference (as in 4.2.1.7.) However, since the plasmid was bigger than the quantified DNA band alone, a correction factor had to be implemented. The size of the whole plasmid in basepairs was divided by the size of the quantified fragment. This ratio was multiplied with the quantified concentration of the fragment. The result was the concentration of the whole plasmid that was later used for transfection (see 4.2.3.5).

4.2.1.14. Blunt end cloning

In certain cases, direct cloning did not work for unspecified reasons. In these cases, an intermediate cloning step was performed. As a result, the insert was present in an intermediate plasmid in high purity and concentration. Subsequent cloning with this intermediate plasmid was generally successful.

After PCR for amplification of the insert (see 4.2.1.1), a DpnI digest was performed (as described in 4.2.1.9). The restriction was purified by the DNA Clean Up procedure (see 4.2.1.2); elution took place in 25 µl H_2O.

For the actual blunt end cloning reaction, 3 µl of the DpnI digested, purified PCR insert was mixed with 2 µl pOT-233 (already cut with SmaI), 2 µl Cutsmart Buffer, 2 µl 10mM ATP, 0.5 µl of SmaI and T4-DNA Ligase and 10 µl H_2O. Ligation took place for 2 hours at 24°C. SmaI creates blunt ends in the digest. Likewise,

phusion polymerase creates PCR products with blunt ends. In the above reaction, the PCR insert attached to the SmaI cutted vector and the T4 ligase ligated them together. However, the ligase also religated the cutted vector. To prevent a high amount of religations, SmaI was also present in the reaction. Every religated vector was immediately cut open by SmaI. This did not affect the desired plasmids, since the SmaI site vanished if the insert was ligated to the vector.

In the end, the PCR product was cloned efficiently into an intermediate vector. Subsequent steps were transformation (see 4.2.1.10), screening by Kochlysates (see 4.2.1.11), Midi prep (see 4.2.1.12) and quantification (see 4.2.1.13).

Afterwards the intermediate vector was used for subsequent cloning.

4.2.1.15. Sequencing

The success of cloning was controlled by sequencing. Sequencing was performed at Microsynth Seqlab or Eurofins Genomics.

Table 17 shows reaction setups for both companies.

Table 17 Reaction for sequencing

	Microsynth Seqlab	Eurofins Genomics
Plasmid DNA	1200 ng	500 ng
Primer	0.3 µl	0.3 µl
H_2O	to 15 µl	to 10 µl

4.2.2. *in vitro* transcription (IVT)

Gene knockdown could be achieved either by transfecting hairpin constructs or by applying dsRNA to the cells. *in vitro* transcription was used for synthesizing dsRNA.

For *in vitro* transcription, a gene fragment was cloned to a vector that contained a T7 Promotor upstream and downstream of the fragment. A PCR with primer SPO-288 was conducted (see 4.2.1.1). This resulted in amplification of a piece of DNA containing the fragment and both T7 sites. After clean up (see 4.2.1.2) the *in vitro* transcription was started. The reaction consisted of 10 µl of the purified PCR, 10 µl of T7 Transcription buffer, 1.5 µl of the RNAse inhibitor, 5 µl of NTPs, 22 µl of H_2O and 1.5 µl of T7 RNA Polymerase. The reaction took place overnight at 37°C.

The samples were quantified as described in 4.2.1.7, as were the corresponding PCR products. The quantified band of the IVT sample consisted of DNA from the PCR product and dsRNA of the IVT. To obtain only the dsRNA concentration, the gel concentration of the PCR product was subtracted from the IVT sample. Samples were stored at -20°C upon usage.

4.2.3. Cell culture

4.2.3.1. Cell Cultivation

Drosophila S2R+-cells were grown in 75 cm^2 cell culture flasks, containing 12 ml Schneider's *Drosophila* complete medium. Incubation took place at 27°C, cells were split twice a week (see 4.2.3.2).

4.2.3.2. Cell Split

To prevent overgrowth and ensure constant, optimal proliferation conditions, cell split took place twice a week. Old cell medium was discarded and cells were washed once with 5 ml of PBS. For loosening the cells from the flask bottom, 5 ml of Trypsin/EDTA solution was applied to them and incubated for 2 min. Trypsin/EDTA solution was resuspended until the cells were detached. The cell suspension was transferred in a 15 ml reaction tube and centrifuged at 1200 rpm at 2 min. Trypsin/EDTA solution was discarded and the cell pellet was resuspended in 8 ml Schneider's *Drosophila* complete medium. 2 ml were used for inoculating a new cell culture flask. The rest was used for seeding 12-well or 6-well plates (see 4.2.3.4).

4.2.3.3. Determining cell concentration

Since it was necessary to seed always a constant number of cells, cell concentration had to be determined, for which the Fuchs Rosenthal cell counting chamber was used. 20 µl of cell suspension was mixed with 80 µl of Trypan Blue, to exclude all dead cells (living cells are not stained by Trypan Blue and appear white under the microscope).

The counting chamber consisted of 256 squares. The number of living cells in 16 of these squares was counted under the microscope. For determination of the cell concentration, the average cell number of the 16 squares was multiplied with 0.32. The result was the concentration of cells in 10^6 cells/ml.

4.2.3.4. Cell seeding

Cells were seeded after the concentration determination (see 4.2.3.3) in either 12-well plates (for FACS analysis and live cell imaging) or 6-well plates (for Co-IP studies and the MS analysis). For 12-well plates 140000 cells were seeded in 1.5 ml Schneider's *Drosophila* complete medium per well. For 6-well plates 600000 cells were seeded in 3.0 ml Schneider's *Drosophila* complete medium per well.

4.2.3.5. Transfection

Transfection of cells was done one day after seeding (see 4.2.3.4). For a 12 well plate, a total amount of 200 ng was transfected. In most cases, 50 ng was used from every plasmid that should be transfected. If the 200 ng were not reached (for example because only three plasmids were transfected), pFSR-0092, which is an empty vector without promoter site, was used to compensate the difference. This was necessary to ensure constant transfection efficiencies. In case of 6-well plates, 600 ng of DNA was used in total, the amount of the single plasmids varied usually between 200-300 ng in dependency of the used construct.

According to their concentration (see 4.2.1.7), the volume of each plasmid was calculated and pipetted to Schneider's *Drosophila* medium (without FBS and Pen/Strep). For 12-well plates, the transfection had a total volume of 75 µl and for 6-well plates 150 µl. FuGENE HD was used as the transfection reagent, 0.7 µl were used for transfecting a 12-well and 2 µl for a 6-well. Transfection mixes were vortexed for around 7 seconds directly after addition of FuGENE. After 15 minutes of incubation time, the transfection mix was pipetted into the respective wells. The plate was lightly shaken after transfection for dispersion of the transfection mixture.

4.2.3.6. Induction with $CuSO_4$

If plasmids contained Metallotheonine-Promotors, expression had to be induced by exposition to heavy metals, e.g. $CuSO_4$. $CuSO_4$ was applied to the cells to a final concentration of 500 µM directly after transfection.

4.2.3.7. Applying dsRNA for knockdown experiments

For gene knockdown experiments, either plasmids with a hairpin construct or in vitro transcribed dsRNA (see 4.2.2) was used. Hairpin plasmids were transfected as described above (see 4.2.3.5); dsRNA on the other hand was applied directly to the cells. For FACS analysis (see 4.2.6), dsRNA was applied directly after transfection to the cells. For live cell imaging experiments (see 4.2.7), dsRNA was put to the cells directly before the start of the microscope run. For the analysis of the phenotype of a prolonged Skp2 knockdown (see 5.1.4), dsRNA was added twice, once directly after transfection, and a second time 3 days later. In this case, incubation lasted 3 days longer. In all cases, dsRNA was used to an end concentration of 5 nM.

4.2.4. Co-IP and Western Blots

4.2.4.1. Co-Immunoprecipitation (Co-IP)

Co-IPs were performed to test for biochemical interaction between potential binding partners. They were carried out roughly 48 hours after transfection. To preserve potential binding between proteins, all steps were performed on ice, or at 4°C respectively.

To receive enough cell material, transfections (see 4.2.3.5) were always performed twice in two wells of a 6-well plate. The bait protein was tagged with a 4xFLAG, 3xHA or HA epitope, the target protein was tagged accordingly with FLAG or HA. A Co-IP setup consisted always of a negative control (the target protein without the bait), a positive control (the bait protein and a confirmed interaction partner) and the actual test sample (bait and target protein together). If possible, bait and target protein were under polyubiquitin promotors, for strong expression.

As a first step, cell medium was removed from the 6-well plates and 500 µl of cold PBS was applied on every well. Cells were removed from the bottom with a cell scratcher and transferred in 2 ml reaction tubes, identical samples were pooled in the same tube. Samples were centrifuged for 10 min at 2000 rpm. Afterwards, the supernatant was discarded and cells were resuspended in IP lysis buffer, containing a protease inhibitor mix. Incubation took place 20 min, after 10 min, reaction tubes were inverted once for stirring. Afterwards, 100 µl of the supernatant was saved at 4°C for later Western Blot analysis (see 4.2.4.2 and 4.2.4.3). This was the input, which confirmed that the proteins were expressed. The remaining 900 µl of the supernatant was used for the actual Co-IP.

Two kinds of agarose beads were used for the protein precipitation: Protein G Beads and FLAG-tagged beads. The FLAG-tagged beads were used for Dap pull down for example, since it turned out that precipitation of Dap worked only with these beads efficiently.

In case of Protein G beads, FLAG or HA antibody was given to the Co-IP in a dilution of 1:300 (see Table 6). The samples were incubated under rotation for 30 min at 4°C. This led to antibodies bound to the bait protein. This was not necessary for the FLAG-tagged beads, since the antibodies were already present on the beads in this case.

The Protein G beads had to be washed before application to the Co-IP. For washing, 30 µl beads per sample were mixed with 1 ml of IP Lysis buffer. After centrifugation (1000 rpm for 30 sec), the supernatant was discarded completely. This step was repeated once. Finally, beads were resuspended in IP lysis buffer (including protease inhibitors), in 30 µl per sample.

After the antibody was bound to the bait proteins, 30 µl of beads were applied to the Co-IP. This led to binding of the bait protein – antibody complex to the beads since protein Protein G binds antibodies efficiently. If the target protein interacted biochemically with the bait protein, it will have been also located at the beads, therefore. Incubation took place for 1.5 – 2 hours at 4°C under rotation. To get rid of unbound

proteins, a washing step was performed in the end. Samples were centrifuged at 1000 rpm for 30 sec, the supernatant was completely discarded and the beads resuspended in IP Washing buffer. This step was repeated once. Finally, 40 µl of 2xLSB was applied to the beads and 100 µl directly to the input. All samples were boiled for 5 min at 100°C. This led to protein denaturation and, in case of the Co-IP, elution from the beads. Samples were either directly analyzed on a Western Blot (see 4.2.4.2 and 4.2.4.3) or stored at -20°C.

In case of FLAG tagged beads, it was not necessary to incubate samples with antibodies since they were already linked to the beads. After washing the beads, they were applied directly to the samples and all steps were performed as described above. It was possible to minimize IgG band background in the Western Blot analysis in this case. Co-IPs were incubated with 20 µl of 2xLSB without β-Mercaptoethanol and boiled for 5 min at 100°C. This led to elution of proteins from the beads. Antibodies were still co-eluted from the beads, but to a lesser amount. The samples were centrifuged for 30 sec at 1000 rpm and the supernatant, including the proteins, were transferred in new reaction tubes. Now, 20 µl of 2xLSB with β-Mercaptoethanol was pipetted to the samples and the boiling was repeated, this led to protein denaturation.

4.2.4.2. SDS-PAGE

To separate protein samples, SDS-polyacrylamide gel electrophoresis was used. Gels were casted and ran in a PAGE Gel System by BioRad, in which 7 ml of resolving gel and 3 ml of stacking gel was used. Electrophoresis was performed at 200 V. The gel percentage and running time varied depending on protein size, since it had to be avoided that IgG-bands of the used antibodies (see 4.2.4.1) would mask important protein bands. Normally, gels were either 8% or 12% and ran for 60 – 70 min.

4.2.4.3. Western Blot analysis

Western Blot was used for transferring proteins on a nitrocellulose membrane and subsequent antibody staining was used for making them visible.

A semi-dry blotting system was used. A blotting sandwich was built in the blotting chamber. This sandwich consisted of a Whatman Paper (approx. 5.5 – 8.5 cm) as the lowest layer. A nitrocellulose membrane (5.5 – 8.5 cm) was put on top. The SDS-PAGE Gel was the next layer and finally another Whatman Paper completed the sandwich. Whatman Paper and membrane were soaked in Western Transfer Buffer 3. Blotting was performed at 70 mA per blotting sandwich for 90 minutes.

After blotting, blots had to be blocked to prevent unspecified antibody binding later on. Blots were transferred to Blocking Buffer and incubated for at least 1 hour shaking at room temperature. Blots were washed two times with PBS-T. Subsequent antibody staining took place in 5 ml PBS-T. The antibodies were used in an appropriate dilution (see Table 6), incubation took place overnight at 4°C on a shaker. On the next day the primary antibody was discarded and blots were again washed two times with PBS-T. Again, 5 ml PBS-T were used for staining with the secondary antibody. The IR Dye 800 anti-mouse from Licor was used in a dilution of 1:5000 (see Table 7). Incubation took place for 2 hours at room temperature in the dark on a shaker. Afterwards, the secondary antibody was discarded and the blots were washed again two times with PBS-T. Blots were put into 5 ml PBS-T and shaken for 30 min at room temperature to minimize antibody background. Finally, blots were stored in PBS-T at 4°C and scanned on a Licor odyssey scanner.

ImageJ was used for visual processing of the blots.

4.2.5. MS analysis of Skp2 binding partners

4.2.5.1. Sample Preparation

Mass spectrometric analysis was performed to obtain a broader idea of Skp2 binding partners. 4xFLAG Skp2 was overexpressed in Schneider cells and precipitated, using the same protocol as in the Co-IP studies (see 4.2.4.1). In this case, however, the Lysis and Wash Buffers of the *Flag immonuprecipitation kit* was used since these buffers were optimized for FLAG precipitation. Furthermore, FLAG tagged beads were used as described in 4.2.4.1. It was checked that 4xFLAG Skp2 was expressed and precipitated by Western Blot analysis (see 4.2.4.3). Schneider cell lysate without Skp2 overexpression was used as a control, to eliminate hits that only bound unspecifically to the beads.

For protein separation, a commercial NuPAGE 4-12% Bis-Tris gradient gel was used to reach optimal separation.

Coomasie-staining was used for making the proteins visible before gel extraction. The gel was washed 3 times for 5 minutes shaking in H_2O and stained for 1 hour shaking in SimplyBlue SafeStain Coomasie G-250 solution (Thermo Fischer Scientific). The stained gel was destained by washing 3 times for five minutes shaking in H_2O and by incubation in H_2O shaking over night at room temperature.

A sterile scalpel was used to cut bands out of the gel. Fragments were transferred to 2 ml Eppendorf Reaction Tubes and washed with 2 ml NH_4HCO_3 shaking for 1 hour. Gel pieces were dried by incubating them with 1 ml MS washing buffer 1 and 2 for 30 minutes each and with 200 µl of Acetonitrile (AcN) for 10 minutes. In all steps, samples were shaken and the supernatant discarded. Finally, the gel fragments were lyophilized for 30 minutes.

For reduction of cysteine, gel fragments were incubated with 200 µl of MS DTT at 56°C for 35 minutes. This step was performed to ascertain complete digestion of the proteins through trypsin later on. Blocking of reduced cysteine was achieved by incubation with MS Iodacetamide solution at room temperature in the dark for 35 minutes. Another drying of the gel pieces was done as described above.

In-gel protein digest was performed by applying MS Trypsin solution and incubation for 10 minutes at room temperature. Either 20 or 40 µl Trypsin was added, until the fragments got transparent. 20 or 50 µl of NH_4HCO_3 were applied to the fragments respectively, and the digest was conducted overnight at 37°C.

The supernatant, containing the digested proteins, was collected in fresh 0.5 ml Axygen reaction tubes for every sample. The gel fragments were washed twice with 100 µl NH_4HCO_3 at 37°C for 1 hour each. The supernatant was transferred in the same tubes as above. Finally, fragments were washed with 100 µl of MS washing buffer 2 at 24°C for 20 min and the supernatant was again pooled into the Axygen Cups. For all the above steps, Axygen low binding tips were used since they were optimized for minimal contamination of the tip material.

The supernatant was lyophilized overnight and afterwards stored at -20°C until mass spectrometric analysis. For lyophilization, reaction tubes with self-made holes in the tube cap was used. Sample preparation was done in the lab of Dr. Astrid Bruckmann, which also took care of primary sample analysis. Mass spectrometric data was compared with the Uniprot KB data base.

4.2.5.2. Analysis of mass spectrometric data

After the MS run, the obtained data had to be organized and adjusted. Two protein lists were created: all the protein hits found in the Skp2 precipitation sample and in the control sample. The hits were ordered

by an automatically calculated score value. Every sample with a score below 100 was discarded from further analysis, since it was deemed as not reliably detected.

The proteins in the Skp2 list were verified with the control list to exclude proteins that bound unspecifically to the beads or were a contamination during the sample preparation (e.g. keratin). All proteins that were found solely in the Skp2 list were considered real hits, as were proteins that were in both lists, but had a score 300 points higher in the Skp2 list in comparison to the control list.

4.2.6. Flow cytometric analysis of the cell cycle and protein stability

4.2.6.1. Principal Idea

Flow cytometry was used to analyze cell cycle distribution of Schneider cells and potential changes upon protein overexpression and knockdown. Furthermore, an assay developed in the lab (Polz, 2017) was used to determine protein stability by flow cytometry. With this assay, stability changes of hypothesized Skp2 substrates were observed by either Skp2 overexpression or knockdown. If stability would be diminished or increased respectively, this would be a clear hint for a Skp2 regulation of the mentioned substrate.

4.2.6.2. Sample preparation

After transfection (see 4.2.3.5), cells were incubated two to three days before analysis. It was assumed that stability experiments would show the same results after both time spans. Nonetheless, to exclude this source of variability, all Cdt1 related experiments were analyzed after roughly 48 hours and all Dap experiments after roughly 72 hours.

In most cases, cell cycle distribution was visualized, either for observation of the effects of the treatments or for analyzing protein stability in the three distinct cell cycle phases, G1, S and G2/M. Hoechst staining was used for the visualization. Hoechst binds to the DNA and is stimulated by the UV LED in the flow cytometer. The more DNA a cell possesses, the stronger is the Hoechst signal, making a distinction between G1-, S- and G2/M-Phase possible. 6 µl of Hoechst stock solution was pipetted to every well. The plate was incubated for 15 minutes at 27°C afterwards. The medium was discarded and a mixture consisting of 1 ml Trypsin/EDTA solution and 6.4 µl Hoechst was applied to every well. This led to removal of the cells from the well bottom and insured constant Hoechst staining at the same time. Cells were resuspended in the well for complete removal and transferred to FACS sample tubes.

4.2.6.3. Fluorescence activated cell scanning (FACS)

For the actual measurement, sample tubes were inserted into the flow cytometer. Schneider cells were separated from cell debris by their forward and side scatter. Excitation and detection of fluorescence was done by lasers, filters and fluorescence detectors (see Table 12 for specifications). Samples were analyzed with a speed of 800-900 events per second. It was counted until 270000 events were recorded or, if this was not possible, until the whole sample was analyzed.

4.2.6.4. Cell cycle analysis and export of stability data with FCS Express

Visualization and primary analysis of FACS data was performed with the program FCS Express (Version 4.07.0020). Two tasks were fulfilled: first, the cell cycle distribution was visualized and analyzed by calculating the ratio of G1 to G2 cells. Second, data for protein stability determination was prepared and exported for analysis in Origin (see 4.2.6.5).

It was necessary to process the data, since strictly speaking, the flow cytometer was only measuring events which consisted of air bubbles, cell debris, cell cluster and actual cells. Events were selected and filtered

by using gates. In this way, only non-clustered *Drosophila* cells were analyzed. The cell cycle distribution of gated cells was visualized and the number of cells in certain areas were determined by markers. In this way, the ratio of G1 to G2 cells was calculated.

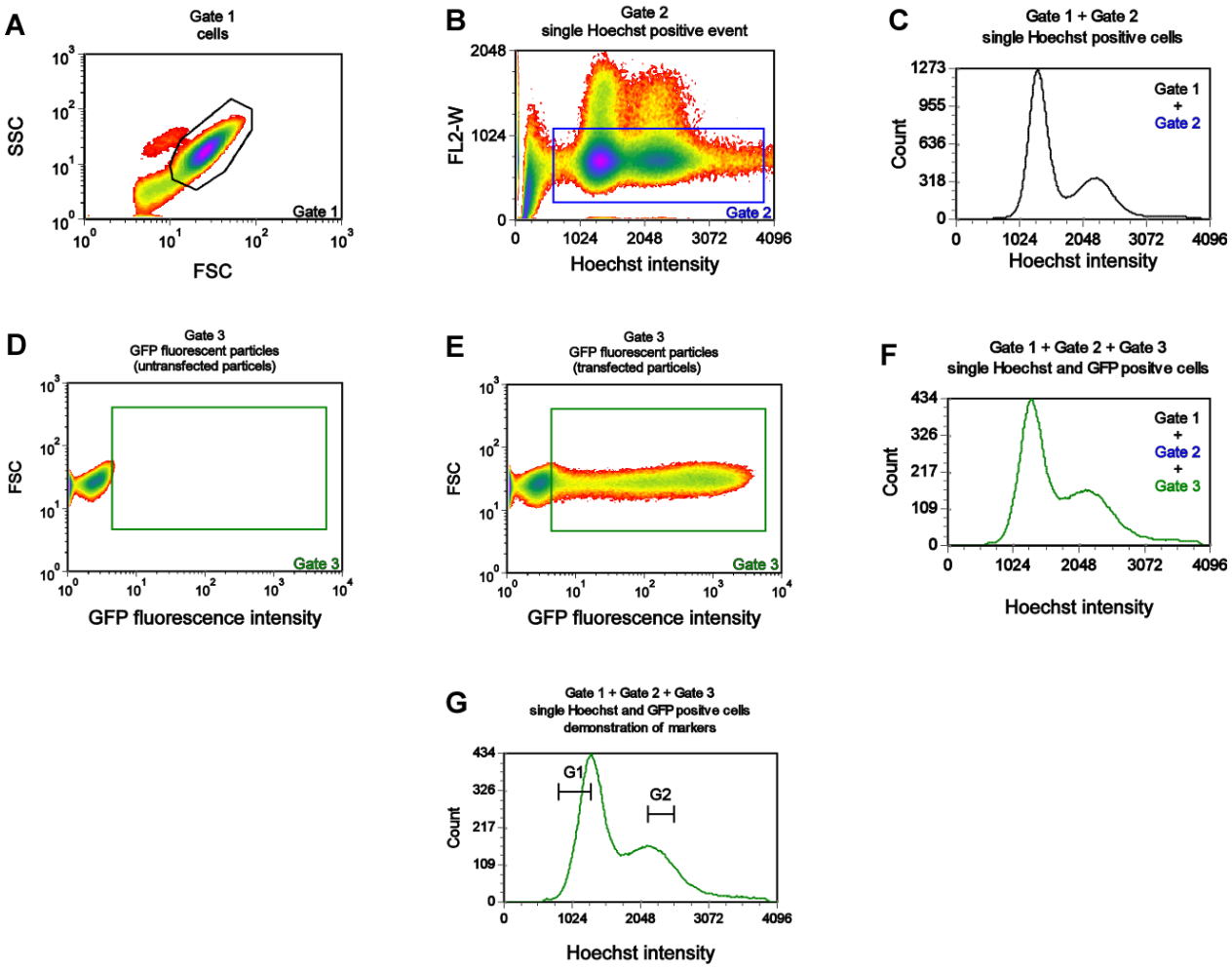

Figure 8 Analysis of flow cytometry data with FCS Express

Gates and markers that were used to analyze cell cycle distribution and preparation of samples for Origin analysis. *Drosophila* S2R+-cells were transfected with a T2A control vector, expressing both GFP and mChe (not shown). **(A)** Density plot of FSC against SSC. Gate 1 shows the population of S2R+-cells. **(B)** Density plot of Hoechst intensity (FL2) against width of events in the Hoechst channel (FL2-W). Gate 2 is used to isolate single cell events. Gates 1 and 2 are used to determine the cells for exportation to Origin. **(C)** Histogram of cells that were in Gate 1 and Gate 2, showing the cell cycle profile of all single cells in the sample. **(D)** Density plot of GFP intensity against FSC. Shown here are untransfected cells to determine the GFP background (not more than 0.5% of GFP background events are in Gate 3). **(E)** Same as D but shown with transfected cells. Gate 3 determines GFP positive cells, equivalent to transfected cells. **(F)** Histogram of cells that are in Gate 1, Gate 2 and Gate 3, showing the cell cycle profile of all single GFP positive cells in the sample. This histogram was used to analyze the cell cycle profile of transfected cells if GFP was used as a transfection control (same procedure was performed if mCherry was the control, with a mChe gate). **(G)** G1 and G2 markers to determine the number of cells in G1 and G2/M-Phase. FSC: forward scatter; SSC: side scatter.

Figure 8 shows the process in an example. In plot A, the forward scatter (FSC) is plotted against the side scatter (SSC). This diagram was used to separate Schneider cells from cell debris with Gate 1. Figure 8B shows the Hoechst signal in relation of the FL2-W paramater (width of signal of events in the Hoechst channel). Gate 2 was used to separate single cells from cell doublets or clusters. Both gates combined

delivered all single *Drosophila* cells, which were used for analysis (see Figure 8C as an example of cell cycle distribution). For protein stability analysis, the collected data of these cells, especially the fluorescence intensity of GFP, mCherry (mCh) and Hoechst, was exported as a comma-separated value file (.csv) and afterwards processed in Origin (see 4.2.6.5).

For cell cycle analysis, separation from transfected and untransfected cells had to be performed. Every experiment had one fluorescence protein that served as a transfection control. As an example, in Figure 8 GFP is the control. A GFP gate (Gate 3) was used to get rid of untransfected cells. The gate was set so that no more than 0.5% of all cells were inside if the untransfected cells were viewed. Figure 8D shows this procedure, the signals were background, originating from either Hoechst staining or the laser itself. Plot E shows the same gate, but with transfected cells. A combination of Gate 1, Gate 2 and Gate 3, depicted as a histogram against the Hoechst fluorescence intensity showed the cell cycle distribution of all single, transfected cells (Figure 8F).

S-Phase in Schneider cells is not resolved well. Therefore, a clear separation of G1 and G2 cell peaks is not possible. Consequently, the starting point of the G1 marker was set at the maximum turning point of the G1-peak, the end point was the minimal turning point of the S-Phase. This marker was shifted, so that the end point landed on the maximum turning point of G1. Likewise, the starting point of the G2 marker was the minimal turning point of S-Phase, whereas the end was the maximum turning point of G2/M. Shifting the marker forward to the maximum turning point of the G2/M-peak resulted in the determination of the G2/M cells (see Figure 8G). Since the distribution of the G1- and G2-peaks are symmetrical, these two markers consisted of half of the cells in G1 and G2/M, from which the G1/G2 ratio was calculated.

For analysis of the cell cycle distribution, the ratio of G1/G2 was calculated for all replications. Data was depicted as boxplots.

4.2.6.5. Relative protein stability analysis with Origin

Protein stability analysis based upon comparison of fluorescence intensities of GFP and mCherry in cells. The flow cytometer can detect the fluorescence intensities of every single cell. Therefore, it is possible to determine the ratio of GFP and mCh fluorescence intensity of every transfected cell in a well. It is known that GFP and mCh alone are stable in the cell cycle, hence the ratio of GFP and mCh fluorescence is constant if the correct expression system is used. If a protein of interest that is degraded in the course of the cell cylce is tagged with either GFP or mCh, the respective fluorescence intensity will be decreased. The intensity of the other fluorophore will be unaffected and can serve as the reference.

For example, if the protein of interest (“X”) is tagged with mCh, the ratio of the logarithmic intensity of the mCh fluorescence to the logarithmic intensity of the GFP fluorescence can be calculated as $\frac{\log(Intensity\ mCh\ X)}{\log(Intensity\ GFP)}$. Since the GFP intensity is not affected, this ratio is representative for the relative protein stability of the protein of interest “X”. It is possible to identify substrates of Skp2 with this assay. The supposed substrates are the proteins of interest (“X”) in the above example. If Skp2 is responsible for the ubiquitination, an overexpression will lead to an increased degradation of “X” and consequently a decreased intensity of mCh. As a result, the ratio will be smaller under these overexpression conditions in comparison to normal Skp2 levels. Likewise, Skp2 knockdown should lead to the contrary effect: less degradation of “X” and increased intensity of mCh resulting in a greater ratio.

In a first step, FCS Express was used to identify cells and filter out cell debris, cell clusters and air bubbles in the data gathered by the flow cytometer (see 4.2.6.4). However, FCS Express is not capable of a direct comparison of single cell fluorescent intensities, so Origin 2017 was used since this software could perform the necessary computer calculations. After the .csv files were loaded into Origin, the software determined a background GFP or mCh threshold according to the untransfected cells. Every cell above this threshold

was considered transfected and taken into analysis. This was necessary, since the export of data described above did not eliminate any background events. Upon this threshold, all cells were divided into positive and negative cells. The transfection efficiency was calculated by dividing the number of positive cells through the complete cell number. If transfection efficiencies were under 10 %, the sample was considered as not fit for analysis and excluded.

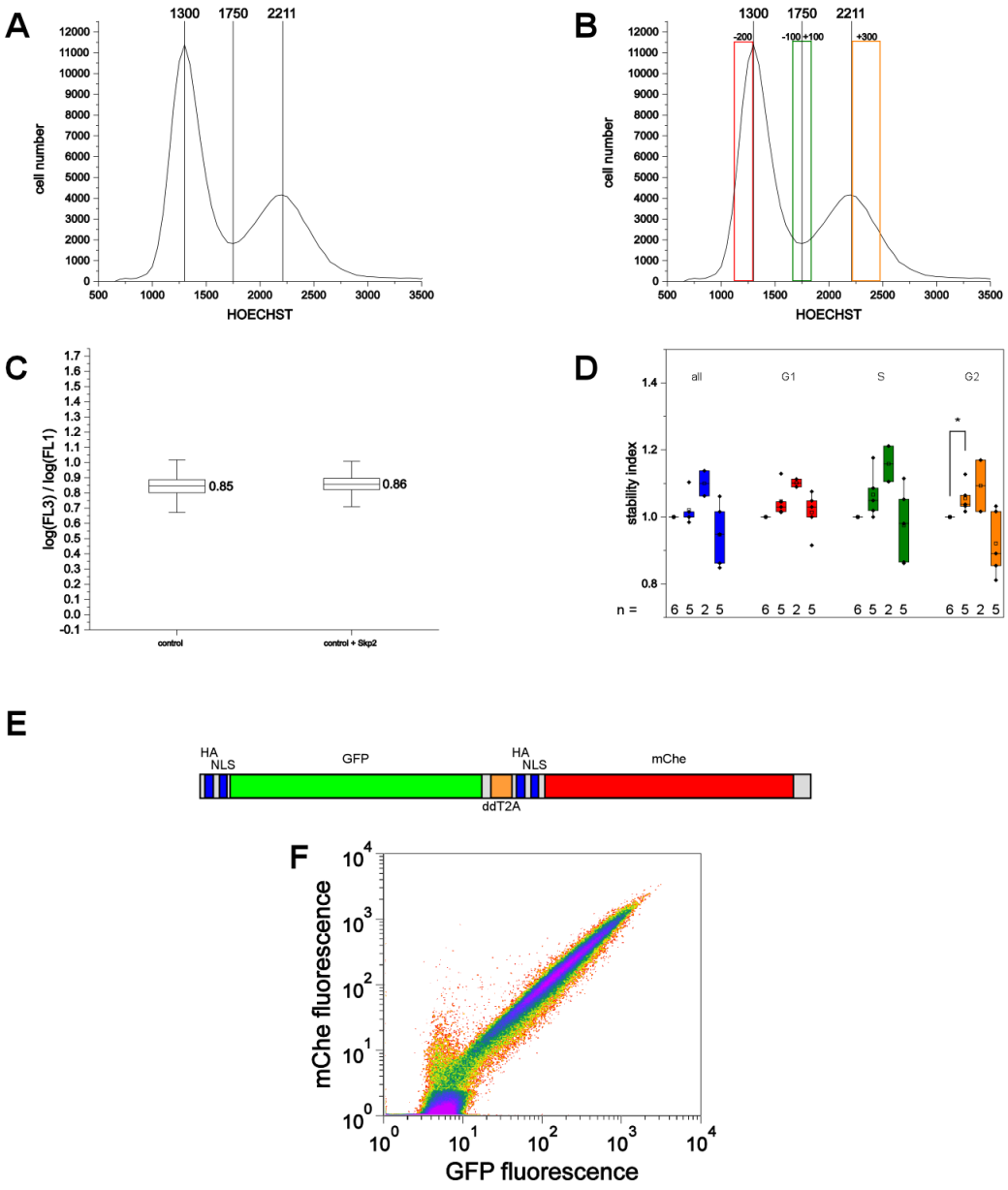

Figure 9 Analysis of relative protein stability data by Origin

Principles of relative protein stability analysis of flow cytometric data with Origin. **(A)** Determination of G1-, S- and G2/M-Phase. Cell cycle distribution of fluorescent negative cells of a sample. Origin determines the two maxima and the minimum. These values are adjusted manually if necessary. **(B)** Depending on the values in A, cells are sorted as G1 (red area), S (green area) and G2/M (yellow area). **(C)** Origin calculates the ratio of mChe ("FL3") and GFP ("FL1") fluorescent intensity for every transfected cell in the sample and displays it as a boxplot. The line inside the box and the number indicates the mean value of the sample, which was used as an index of stability. **(D)** Stability indices of the reproductions were recorded, statistically analyzed and also displayed as boxplots. Analysis was conducted on all transfected cells, G1, S and G2/M (called "G2" for simplicity) cells respectively, according

to the areas in B. Values were normalized on the stability of the protein of interest. **(E)** Schema of a T2A construct. GFP and mChe are translated under one promotor in a stoichiometric ratio, since the T2A site leads to ribosome skipping. Proteins of interest can be tagged with GFP or mChe either N- or C-terminally. **(F)** Ratio of GFP and mChe fluorescence intensity remains stable using the T2A system.

In most cases, it was desired to analyze protein stability in the different cell cycle phases. Therefore, it was necessary to determine the G1- and G2/M-peak and the S-phase valley. The software created cell cycle profiles of the untransfected cells of every sample as a reference (see Figure 9A) and automatically determined and marked the two maximum and the one minimum turning points. Every profile was inspected and manually corrected if the positioning was not correct. Origin sorted the transfected cells according to these three values in a G1, S and G2 (comprising of G2- and M-Phase cells) population, whereas G1 was set between 200 Hoechst fluorescent units before the G1-peak and the peak itself. S was defined as the region +/- 100 Hoechst fluorescent units around the minimum, and G2 started at the G2/M-peak and ended 300 Hoechst fluorescent units after the peak (see Figure 9B). As already described, the G1, S and G2/M cell distributions are symmetrical. Therefore, the defined populations were considered representative and are called G1-, S- and G2-phase from now on.

Stability analysis was performed on "all" cells, meaning all transfected cells in a well, regardless of the cell cycle phase they were in, and on the G1-, S- and G2-Phase. An exception was the analysis of direct or indirect effects of F-Box protein overexpression and knockdown effects (see 5.2). In this case, Hoechst could not be used, since it created high background in the GFP channel, which impeded stability analysis if the protein of interest was GFP tagged, as it was the case here. In this case, cell cycle analysis was not possible and stability was determined only for all transfected cells, regardless of their cell cycle phase.

Origin depicted the stability data as box plots, in which every box plot represented one sample and every data point of a box plot was one measured cell. For a more detailed explanation of the method and the used macros, see Polz (2017). Origin calculated for every boxplot the average value of the fluorescence intensity ratios of every transfected cell in the sample (see Figure 9C). This average was used as the stability index. Reproductions were performed in the same week and over several weeks. The stability indices of the different treatments (for example Skp2 overexpression, CycE overexpression, combined Skp2 and CycE overexpression, Skp2 knockdown, …) were recorded and statistical analysis (see 4.2.9) was performed on them, in order to identify potential influences of the treatments on the protein stability. This data was also depicted as boxplots (see Figure 9D). The box represented the interquartile range (all data points between the 25^{th} and 75^{th} percentile). The whiskers represented the last data point that was in between the so called Upper and Lower Inner Fence. These fences were defined as the 75^{th} percentile plus 1.5 times the interquartile range or as the 25^{th} percentile minus 1.5 times the interquartile range respectively. The line represented the median, the square the average. For reasons of comparability, all stability indices were normalized. In case of the controls, samples were normalized to the control plasmid alone (e.g. mChe stability), in case of the test, normalization was performed on the stability of the protein of interest (e.g. mChe Dap), or in some cases to the protein of interest under CycE overexpression conditions for experimental reasons (see the result sections for details).

One important aspect of this method was that it depended strongly on constant expression of GFP and mCherry. The T2A system was used for expressing the fluorescent proteins in these kinds of experiments. This system allowed expression of two different proteins on one plasmid under only one promotor. A T2A sequence resided in between two DNA sequences (see Figure 9E). If the ribosome reaches the T2A sequence, translation stops and the first protein is released, without the ribosome leaving the RNA. Afterwards, the ribosome starts translating the second protein. As a result, the expression of GFP and mChe is in a stoichiometric proportion and the ratio of fluorescence intensity remained reliably stable for

the controls (see Figure 9F). A caveat of this method is that proteins are slightly changed in this process. 17 aa of the T2A sequence are fused on the C-terminus of the protein upstream of the T2A sequence and 1 aa (a proline) on the N-terminus of the protein downstream. All proteins of interest were cloned into T2A plasmids specifically designed for flow cytometric stability analysis (Polz, 2017), allowing for determination of their relative protein stability. The proteins of the different treatmens were not expressed by the T2A system, but resided on independent plasmids (see Table 8) that were co-transfected.

Previous results hinted that the T2A expression system becomes unreliable with expression levels either too low or too high. In these cases, the ratio of upstream and downstream protein is no longer stoichiometric and protein stability analysis becomes impossible. Therefore, these boundary conditions were excluded from the analysis. Expression levels were determined by analysis of the fluorescence intensity of the reference protein. In general, an expression level between 100 and around 560 ($10^{2.00}$ – $10^{2.75}$) fluorescence units was deemed as fitting for analysis. If not otherwise mentioned, all stability data layed in this range. However, in case of the Cdt1 project (see 5.4) it turned out that results varied strongly if a different range was used. In case of these results, two expression level ranges are shown, the usual range and a much lower expression level range between around 17 and 100 ($10^{1.25}$ – $10^{2.00}$) fluorescent units. This phenomenon was solely seen in the Cdt1 project, in all other cases, the analysis of the high and the low level showed similar results.

In all experiments, controls were performed to exclude the possibility that the overexpression or knockdown of proteins were influencing the GFP or mChe stability. Therefore, any stability changes on the protein of interest was solely caused by protein overexpression or knockdown.

4.2.7. Live cell imaging

Live cell imaging was used to determine the length of the G1-Phase at Skp2 overexpression or knockdown conditions.

4.2.7.1. Preparation of cells

Cells were seeded and transfected as described in 4.2.3. After around 48 hours, cells were trypsinized, transferred in an IBIDI well plate and put under the microscope. For knockdown experiments, dsRNA was applied at this point to the cells.

An IBIDI heating system was used to incubate the cells at constant 27°C. Cells were observed for around 96 hours.

4.2.7.2. Handling of the microscope

For live cell imaging, the Axio Observer Z1 microscope (Carl Zeiss) was used, with a plan-apochromat objective (20x magnification). GFP was detected with an OPSL-Laser at 488 nm and 100 mW, Cherry with a diode laser at 561 nm with 40 mW. A spinning disk laser system (Yokogawa Electric Corporation) was used to minimize photo bleaching.

An automatic table made multi position images possible. Pictures were taken every 15 minutes with transmitted light, and the GFP and mCherry lasers. For each picture, three z-stacks were recorded. It was checked if the cells were still in focus on the morning of the day after the start of the experiment. If needed, the focus was adjusted.

Images were processed with ImageJ for analysis.

4.2.7.3. Determination of G1 length with cell cycle markers

G1 length was determined by overexpression of a cell cycle marker, being a protein that is degraded on a defined time point during the cell cycle but does no longer have an effect on the cell cycle. This marker is tagged with a fluorescence protein, which makes the degradation and re-accumulation visible.

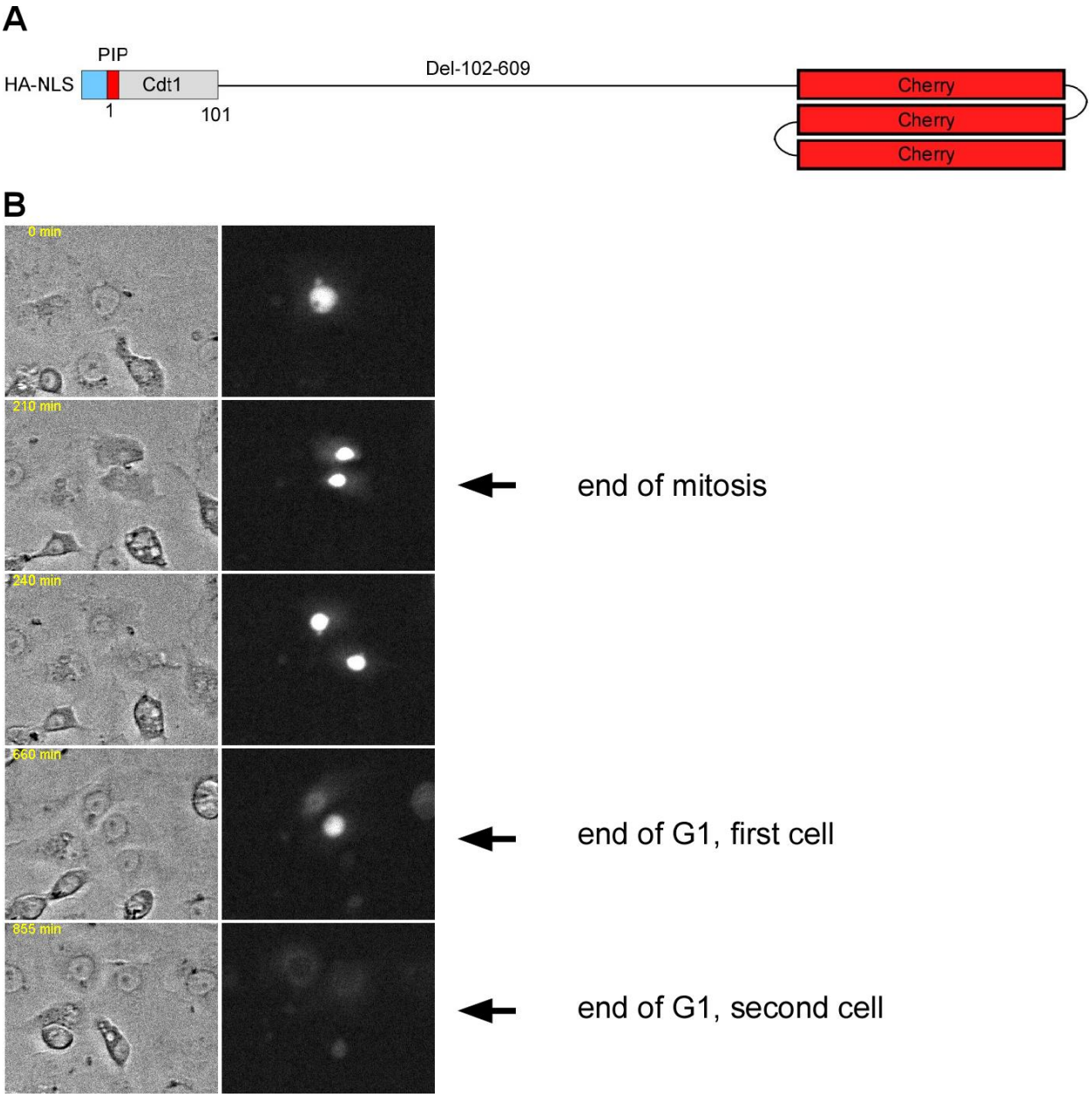

Figure 10 Determination of G1 length with a cell cycle marker

Principle of determining G1 length with live cell imaging and Cdt1 1-101 3xCherry as a cell cycle marker. (A) Schema of Cdt1 1-101 3xCherry. Because of the deletion, this marker does not affect the cell cycle. However, it is still degraded in S-Phase because of the PIP-degron. 3xCherry makes it visible under a microscope. (B) Images from live cell imaging. Anaphase was easily recognized and determined as the end of mitosis (row 2). S-Phase starts when Cdt1 1-101 3xChe is degraded (rowes 4 and 5). The difference in both time points is the length of G1-Phase.

As a cell cycle marker, Cdt1 1-101 3xCherry was used (see Figure 10). This marker did not have any cell cycle effects because of the deletion, but still contained the PIP-degron, which leads to rapid degradation in S-Phase (Havens and Walter, 2009).

For this experiment, anaphase was defined as the end of mitosis since it could be easily recognized in the images. Consequently, cells were observed from anaphase until the vanishing of the Cherry signal, equivalent to Cdt1 1-101 degradation and onset of S-Phase (see Figure 10). The number of frames in between were counted. Since a frame was taken every 15 minutes, this number, multiplied by 15 gave the length of G1 in minutes. As with FACS protein stability analysis, the data was pictured as box plots as described in 4.2.6.5.

4.2.8. Fly Experiments

4.2.8.1. Fly rearing and crossing

Flies were reared in food vials with fly food (containing cornmeal, agar, soy meal, molasses, malt flour, yeast and nipagin as a fungicide). For optimal growth conditions, flies were kept at 24°C, a relative humidity of 65% and a 12-hour light/dark cycle. Vials were sealed with a rubber foam plug. Flies were flipped twice a week in fresh food vials.

Crosses were performed to combine genetically elements of two different fly strains. Virgins and males of both strains were collected and pooled in a fresh vial. Offspring hatched after ca. 9 days and could be screened and analyzed or crossed further. Offspring was collected until 18 days after the cross, since from this point on, the F2 generation hatched and the genotype of flies could not be determined safely.

4.2.8.2. UAS/Gal4 system

The UAS/Gal4 system was used for ectopic gene expression restricted to certain tissues, e.g. wings or eyes. Driver lines, e.g. eng:Gal4, expressed the Gal4 protein only in specific tissues. These lines were crossed with flies that expressed the construct under a UAS ("upstream activating sequence") promotor. UAS is normally not active but is activated upon presence of Gal4. Therefore, tissue specific expression was possible.

4.2.8.3. Wing preparation

The eng:Gal4 driver line was used for expression in fly wings. Crosses were performed and the wings of the offspring dissected in EtOH. Only wings of male individuals were used. Wings were transferred to microscopic slides. Mounting was performed with Dpx. After drying overnight, samples were ready for microscopic imaging.

A CKX41 microscope (Olympus) with a CCD camera was used for imaging. Images were taken with a 2.5x magnification for overview and a 5x magnification for details.

4.2.9. Statistical analysis

Statistical analysis was performed with PAST (Hammer et al., 2001). All data was tested for normal distribution with the Shapiro-Wilk test. If normal distribution was fulfilled, a two-tailed t-test was used for testing of significant differences. If not, the Mann-Whitney U-Test was used instead.

An exception was the analysis of FACS protein stability data (see 4.2.6.5) of the respective Skp2 substrates. The Mann-Whitney U-Test was to imprecise to detect significant changes. This was seen by analyzing the stability of Dap dCDI with CycE overexpression. This Dap version still contains a functioning PIP-degron. Simultaneous CycE overexpression should lead to an enhanced degradation of this construct since cells

shift strongly in S-Phase. Nonetheless, the Mann-Whitney U-Test showed a non-significant difference. Therefore, the t-test, which is much sharper, was used in analyzing these experiments regardless of normal distribution.

5 Results

5.1. Skp2 phenotypes in Schneider cells and flies

5.1.1. Overview

The F-Box protein Skp2 has many substrates in the mammalian organism, ranging for example from the cyclin dependent kinase inhibitors (CKI) p21 (Bornstein et al., 2003; Yu et al., 1998), p27 (Carrano et al., 1999; Nakayama et al., 2000; Sutterluty et al., 1999) and p57 (Kamura et al., 2003) to cyclins (e.g. Cyclin E (Nakayama et al., 2000)) and E2F1 (Marti et al., 1999) and even to parts of the replication machinery (Li et al., 2003; Mendez et al., 2002). Hence, Skp2 is an important part of various different cellular processes. The *Drosophila melanogaster* Skp2 is poorly studied in contrast. The gene was characterized with knock out/knockdown studies in *Drosophila* larvae salivary glands, brains, eyes and wings (Ghorbani et al., 2011; Dui et al., 2013). Up to date, only one substrate, Dacapo (Dap), the homologue of p21 and p27, is proposed as a substrate in flies (Dui et al., 2013).

For identifying new substrates and thereby illuminating the role of Skp2 in the cell cycle, the phenotypes of Skp2 knockdown and overexpression was studied in *Drosophila* Schneider S2R+-cells. The effect on the cell cycle of Skp2 overexpression and knockdown was analyzed by flow cytometric analysis. A Skp2 mutant with a deleted F-Box was analyzed the same way. A closer look was given to the cause of the observed cell cycle effects by performing live cell imaging experiments. Finally, it was tried to reproduce a polyploidy phenotype in Schneider cells that is already described in wing discs (Ghorbani et al., 2011).

5.1.2. Skp2 overexpression leads to more G1 cells caused by a prolonged G1-Phase

Transient Skp2 overexpression in S2R+-cells was analyzed by flow cytometry. Cells were cotransfected with a GFP and mCherry control. In this case, the mCherry protein was used as a transfection control. Hoechst was used for DNA staining. Cells showed a characteristic distribution with two peaks. The first peak represents cells with lower DNA content and most of these cells will reside in G1 or early S-Phase. For simplicity, this will be referred to as “G1-peak”. The second peak represents cells with doubled DNA content, meaning late S-, G2- and M-Phase cells. This peak will be referred to as the “G2-peak” since most of these cells will reside in G2. Cells in S-Phase are not well resolved in Schneider cells, there is no distinct S plateau visible between the G1 and G2/M-peak (Figure 11A)

Overexpression of 4xFLAG Skp2 led to an accumulation of cells in G1-Phase. Transfected cells showed a higher G1-peak and consequently a G2/M-peak with less cells (Figure 11B). This effect was quantified by calculating the G1 to G2 ratio of the respective cells (see 4.2.6.4). Indeed, the accumulation of G1 cells was statistically significant (Figure 11C, t-test for unequal variances, $p < 0.01$).

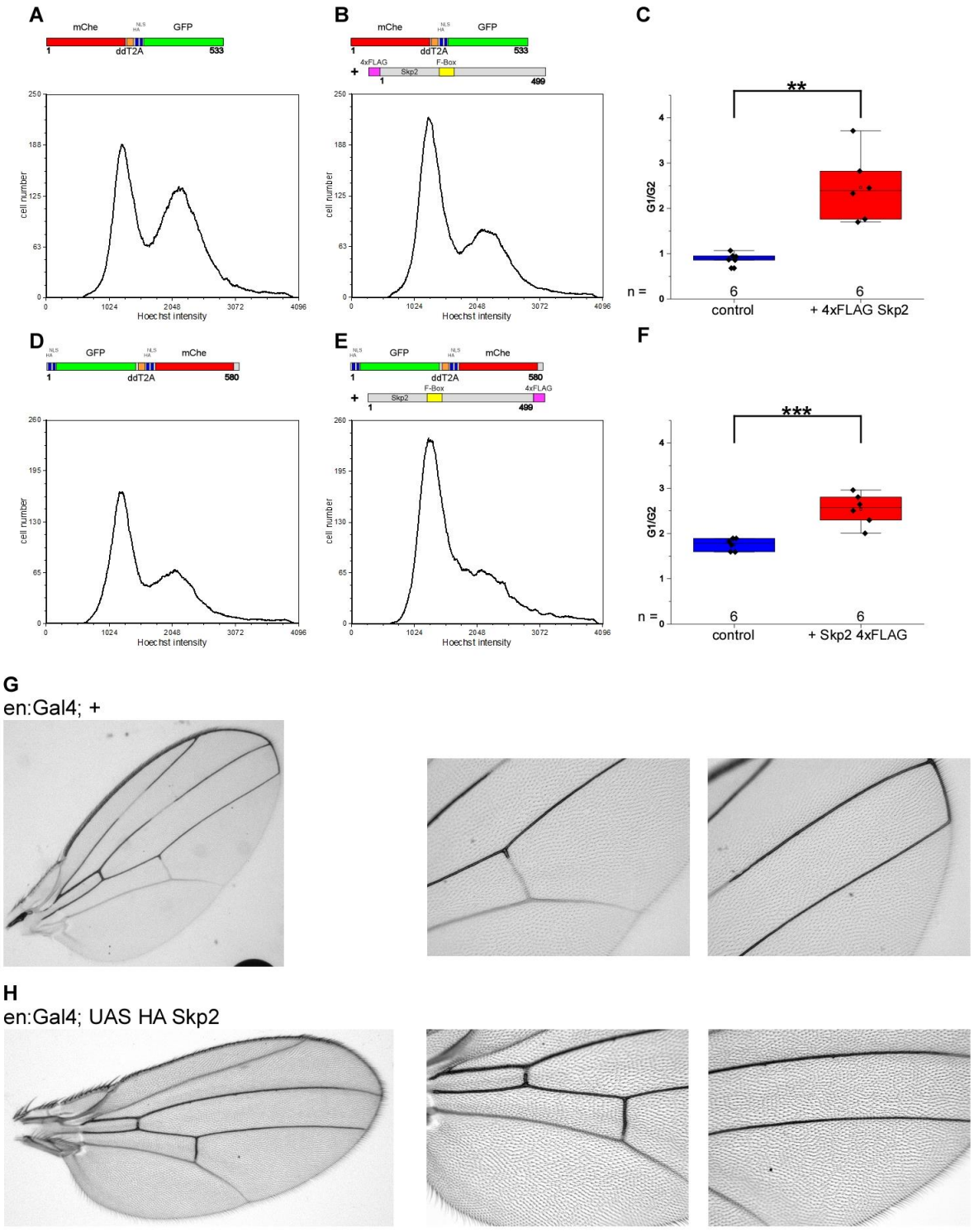

Figure 11 Skp2 overexpression in Schneider cells and wings

Phenotypic effects of Skp2 overexpression in S2R+-cells and wings. *Cells:* mChe serves as the transfection control, only mChe positive cells are shown. (A, D) Cell cycle profile of cells transfected with a construct that results in expression of GFP and mCherry (mCHE-T2A-GFP). (B) Cell cycle profile of cells cotransfected with mCHE-T2A-GFP and 4xFLAG Skp2, leading to a G1 shift. (C) Quantification of G1/G2 ratio of control and Skp2 overexpression cells. (E) Cell cycle profile of cells cotransfected with mCHE-T2A-GFP and Skp2 4xFLAG, also showing an accumulation in G1. (F) Quantification of the associated G1/G2 cell cycle profile. All presented cell cycle distributions are representative. *Wings:* (G) Wing morphology of control cross en:Gal4; + (H) Wing morphology

of UAS-driven Skp2 overexpression in the posterior part of the wing using en:Gal4. Representative pictures are shown. ** = p < 0.01; *** = p < 0.001; t-test for unequal variances. Non-significant changes are not indicated.

A biochemical interaction between Skp2 and Dap was reported (Dui et al., 2013) although in this case, the 4xFLAG tag was located C-terminally in Skp2. Therefore, Skp2 4xFLAG was also cloned and effects on the cell cycle were analyzed. As with the other construct, Skp2 4xFLAG also led to a visible shift of cells into G1-Phase in comparison to the control (Figure 11D and E). Calculation of G1/G2 ratios showed that this effect was also statistically significant (Figure 11F, t-test for unequal variances, p < 0.001).

In contrast to the effects seen in cells, Skp2 overexpression in *Drosophila* wings did not show any visible phenotype. Skp2 overexpression by the UAS-Gal4 system with the engrailed driver showed no change in wing morphology in comparison to the control cross, en:GAL4 crossed with w- flies (Figure 11G and H, 11 wings for each treatment were recorded, representative pictures are shown).

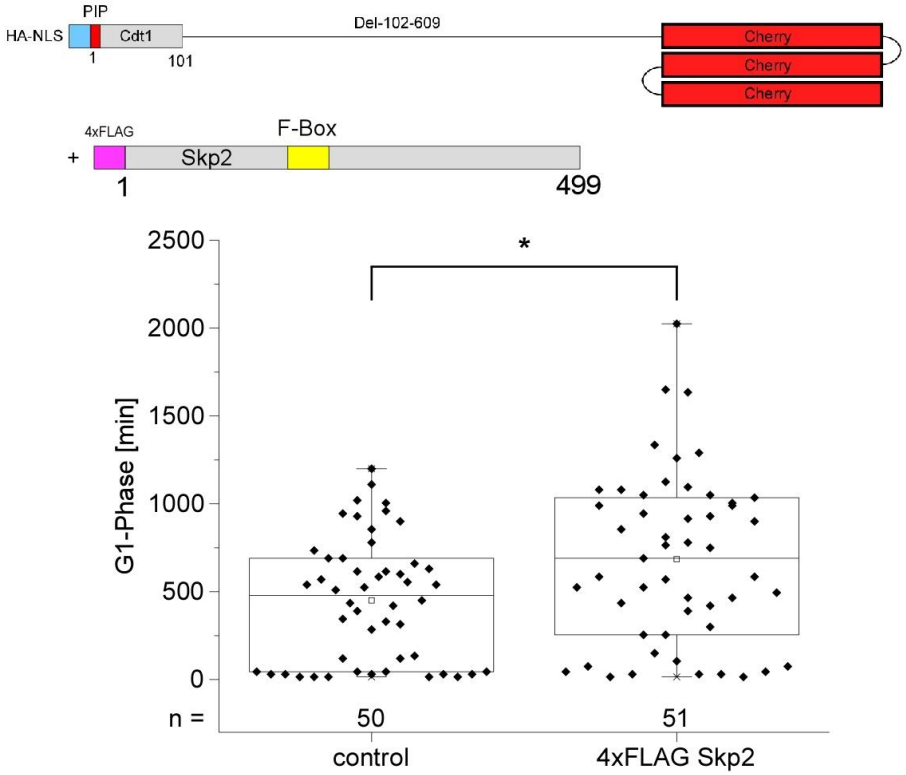

Figure 12 Measurement of G1 length by Skp2 overexpression
Quantification of G1 length of Schneider cells with and without 4xFLAG Skp2 overexpression by live cell imaging. Cdt1 1-101 serves as a G1 cell cycle marker. The line inside the box is the median, the square the average. * = p < 0.05; Mann-Whitney U-Test.

A continuative analysis of the cause of this phenotype was done by live cell imaging. The length of the G1 cell cycle phase was measured to find out if the accumulation of G1 cells could be explained by a prolonged G1-Phase. It was assumed that every cell that was positive for the cell cycle marker (Cdt1 1-101) had also been cotransfected with Skp2. Analysis of the G1 length showed that 4xFLAG Skp2 overexpression led to a statistically significant prolongation of G1-Phase (Figure 12, Mann-Whitney U-Test, p < 0.05).

5.1.3. Changes in cell cycle distribution require the F-Box in Skp2

Although the overexpression of Skp2 did show cell cycle effects, it was unclear if these effects were caused by its function as an F-Box protein or if it played further roles in the cell cycle. Therefore, a version of Skp2, called Skp2 dF-Box, was created that lacked the whole F-Box domain, but was otherwise identical to 4xFLAG Skp2.

A Co-IP was performed to ensure that Skp2 dF-Box lost its ability to bind to the SkpA-Cul1-Rbx1 complex. 4xFLAG Skp2 or 4xFLAG Skp2 dF-Box was precipitated and the binding to HA SkpA was controlled, since SkpA is the adapter protein of SCF, connecting Skp2 to the SCF via the F-Box (see Figure 4). Skp2 dF-Box had a smaller molecular weight, which was in concordance with its missing F-Box (Figure 13A, left blot). Precipitation of both Skp2 versions worked well. Expression of HA SkpA was weak, yet bands could be observed (Figure 13A, right blot). HA SkpA showed the strongest signal when 4xFLAG Skp2 was also overexpressed. It turned out that HA SkpA bound unspecifically to the Protein G beads (Figure 13A, right blot). Yet, simultaneous overexpression of 4xFLAG Skp2 led to a stronger HA SkpA signal, indicating biochemical interaction of 4xFLAG Skp2 and HA SkpA. It can be ruled out that the stronger band intensity solely stemmed from the higher expression level of HA SkpA, since the relatively moderate increase in band strength in the Input could not explain the drastic effect when co-precipitatd with 4xFLAG Skp2. On the other hand, precipitation of 4xFLAG Skp2 dF-Box did not show a stronger signal in the HA-blot in comparison to the negative control. This is consistent with the notion that this Skp2 version was unable to form a complex with the SkpA-Cul1-Rbx1 complex.

The cell cycle effect of Skp2 dF-Box was also studied. Overexpression of 4xFLAG Skp2 showed the already described shift in G1-Phase (Figure 13B, middle). Overexpression of 4xFLAG Skp2 dF-Box showed no G1 shift (Figure 13B, right). Cell cycle distributions were again quantified by calculation of the G1/G2 ratio. The G1 shift of 4xFLAG Skp2 overexpression was statistically significant (Figure 13C, t-test for unequal variances, $p < 0.01$) in comparison to the control cells. The cell cycle effects of Skp2 and Skp2 dF-Box also differed significantly (t-test for unequal variances, $p < 0.05$). 4xFLAG Skp2 dF-Box showed no significant effect in comparison to the control (Figure 13C, t-test for unequal variances, $p > 0.05$), another indication that Skp2 dF-Box was no longer a part of a SCF-complex.

Another advantage of this construct was that it also made another way of searching for Skp2 substrates possible. One way to establish that a protein is targeted by a certain SCF-complex is to analyze if a delta F-Box version of the F-Box protein does exercise a dominant-negative effect on the potential substrate (Carrano et al., 1999). An F-Box protein without the F-Box will still bind to its respective substrates; however, it is no longer able to recruit these substrates to the SCF-complex because of the deletion. The substrates are therefore protected from proteasomal degradation and still functional. Overexpression of Skp2 dF-Box should consequently lead to protein stabilization of actual substrates.

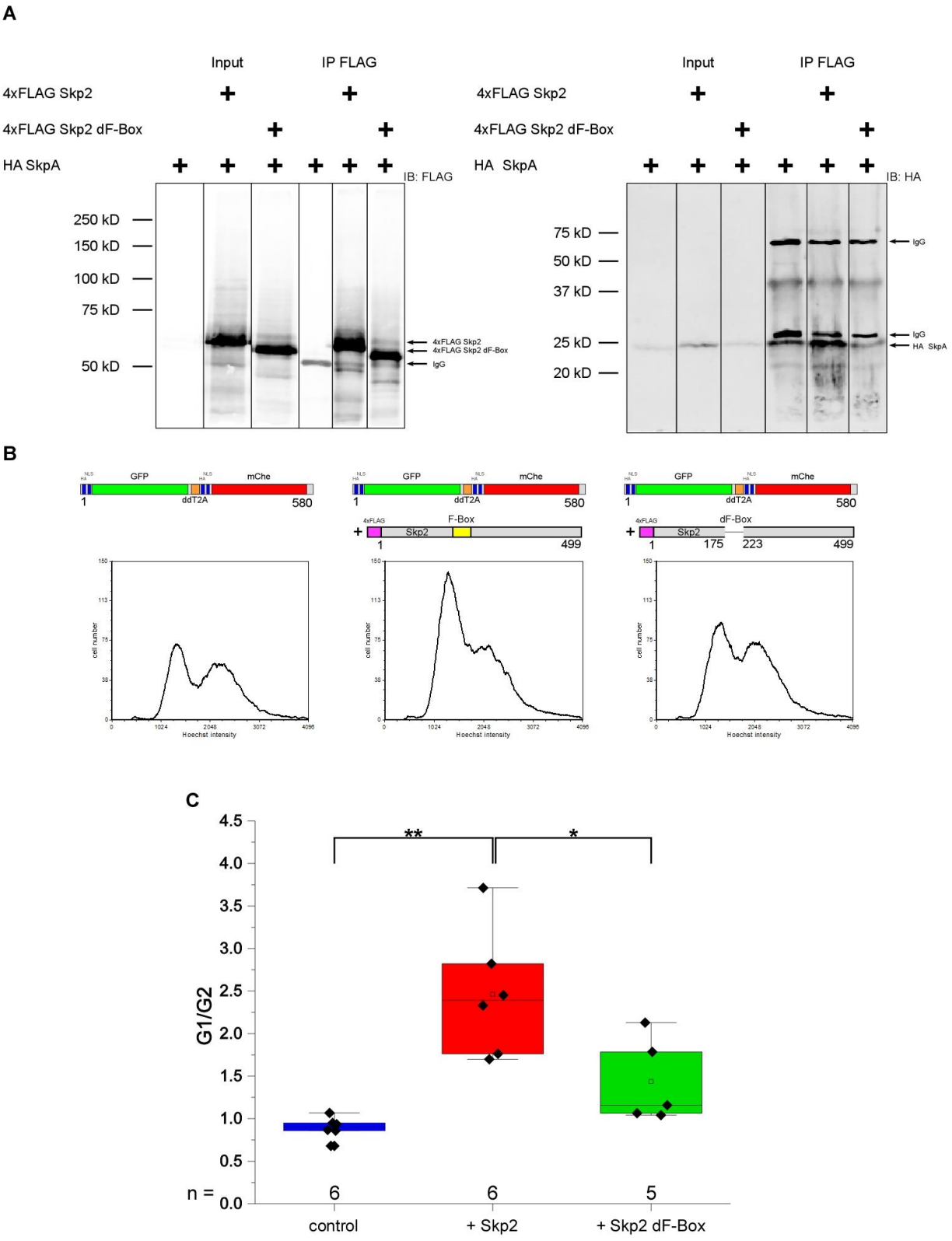

Figure 13 Skp2 dF-Box phenotypes

Co-IP experiment for interaction of Skp2 dF-Box with SkpA-Cul1-Rbx1 complex and phenotypic effects of Skp2 dF-Box in S2R+-cells. (A) Co-IP of 4xFLAG Skp2 and 4xFLAG Skp2 dF-Box with HA SkpA. Precipitation was performed with FLAG antibody, FLAG or HA antibody was used for detection respectively. Skp2 dF-Box is no longer interacting with SkpA. (B) Phenotypic effect of 4xFLAG

Skp2 and 4xFLAG Skp2 dF-Box on cell cycle distribution in S2R+-cells. mChe serves as the transfection control, only mChe positive cells are shown. (C) Quantification of the G1/G2 ratio of control, Skp2 and Skp2 dF-Box overexpression. The line inside the box is the median, the square the average. * = $p < 0.05$; ** = $p < 0.01$; t-test for unequal variances. Non-significant changes are not indicated. All presented cell cycle distributions are representative.

5.1.4. Skp2 knockdown leads to a G2 shift in Schneider cells, caused by a shortened G1-Phase

After establishing that Skp2 overexpression led to a shift in G1-Phase (see 5.1.2), it was also of interest to determine the phenotype of Skp2 knockdown. Schneider cells were transfected with a GFP and mCherry control and incubated with Skp2 double-stranded RNA.

Since it is necessary in knockdown experiments to ensure that activity of the Dicer/RISC system alone does not have any effect, incubation with a nonsense dsRNA was also performed. dsRNA against a fragment of β-Lactamase (the enzyme responsible for Ampicillin resistance in *Escherichia coli*, therefore called Amp dsRNA) was synthesized as a control. Incubation with Schneider cells showed a shift in G1-Phase in this case (see Figure 14A,B) but quantification of various replications showed that this effect was not significant (Figure 14D, t-test for unequal variances, $p > 0.05$). The second control was Hygro dsRNA (against a fragment for the hygromycin-resistance gene). Hygro dsRNA did also show no significant changes in cell cycle distribution (t-test for unequal variances, $p > 0.05$, Figure 14E,F,G). Both controls were usable, therefore.

Skp2 dsRNA on the other hand caused a drastic effect. Schneider cells showed a strong change in cell cycle distribution with an accumulation of cells in G2 (Figure 14C). This shift was significant in comparison to cells without treatment (Figure 14D, t-test for unequal variances, $p < 0.01$) and to Amp dsRNA control knockdown (t-test for unequal variances, $p < 0.01$). Functionality of the Skp2 dsRNA, especially that it was directed against Skp2, was tested beforehand (Jan Polz, 6-week internship).

Again, live cell imaging was used to analyze the cause of this shift into G2-Phase. G1 length was again measured but this time with Skp2 knockdown. Through preliminary experiments, it was estimated that dsRNA needed about 50 hours to unfold its full effect (data not shown). For this reason, cells were analyzed after 50 hours of dsRNA application. In case of the Hygro dsRNA control treatment, data was recorded both before and after this mark to ensure that the dsRNA did not have any effect over the complete time span. There was no significant difference detectable in G1 length after Hygro dsRNA application before and after 50 hours (Figure 15**,** Mann-Whitney U-Test, $p > 0.05$). Skp2 knockdown on the other hand led to a significant shorter G1-Phase, resulting in the described shift into G2-Phase (Figure 15**,** Mann-Whitney U-Test, $p < 0.001$).

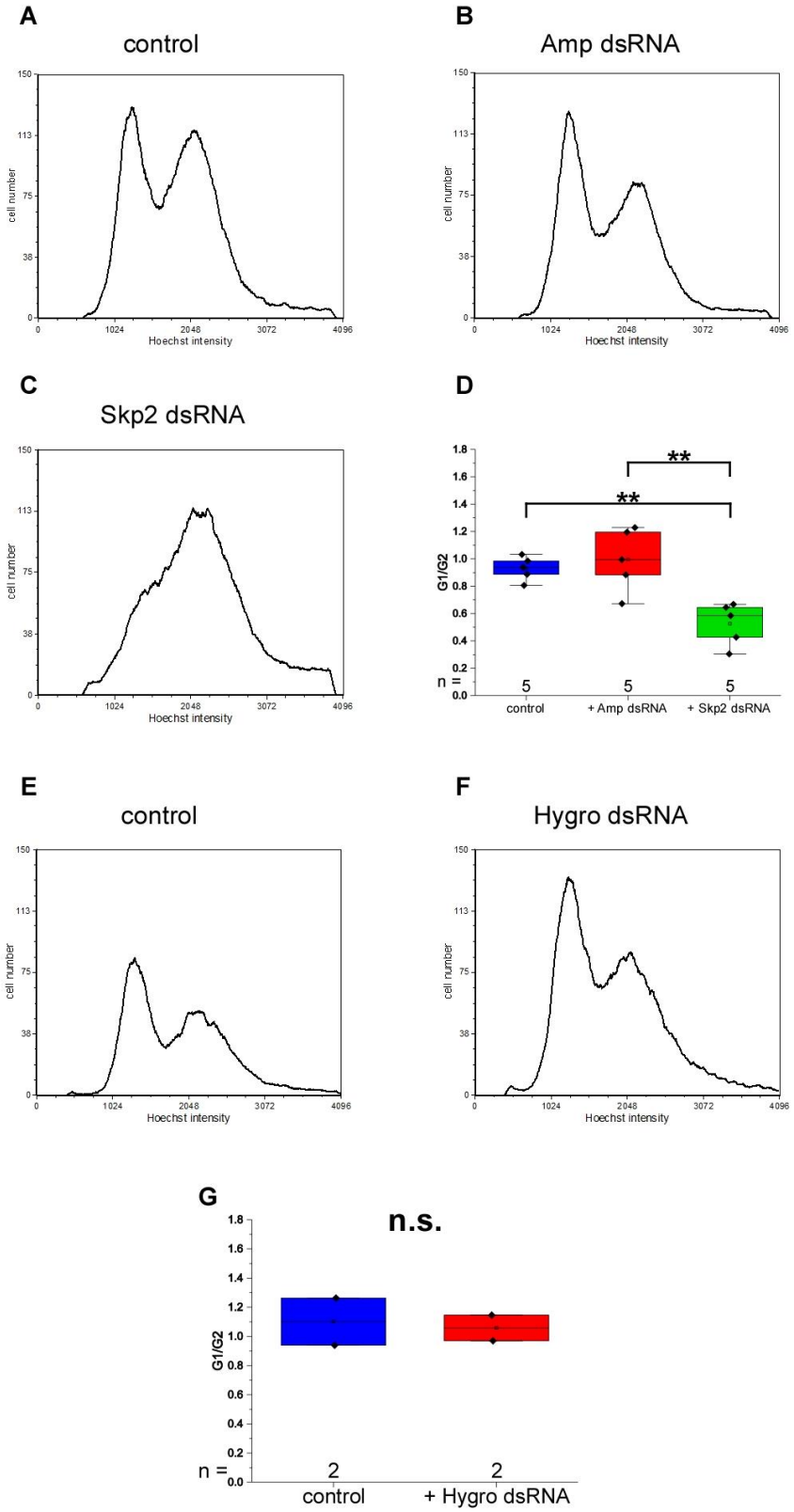

Figure 14 Skp2 knockdown effect

Phenotypic effect of Skp2 dsRNA on cell cycle distribution. mChe serves as the transfection control, only mChe positive cells are shown. (A, E) Cell cycle distribution of S2R+-cells. (B) Amp dsRNA has no significant effect on cell cycle distribution. (C) Skp2 dsRNA leads to a strong G2 shift. (D) Quantification of G1/G2 ratio upon application of Skp2 and Amp dsRNA. (F) Hygro dsRNA has no

effect on cell cycle distribution. (G) Quantification of G1/G2 ratio upon application of Hygro dsRNA. n.s = p > 0.05; ** = p < 0.01; t-test for unequal variances. Non-significant changes are not indicated. All depicted cell cycle distributions are representative.

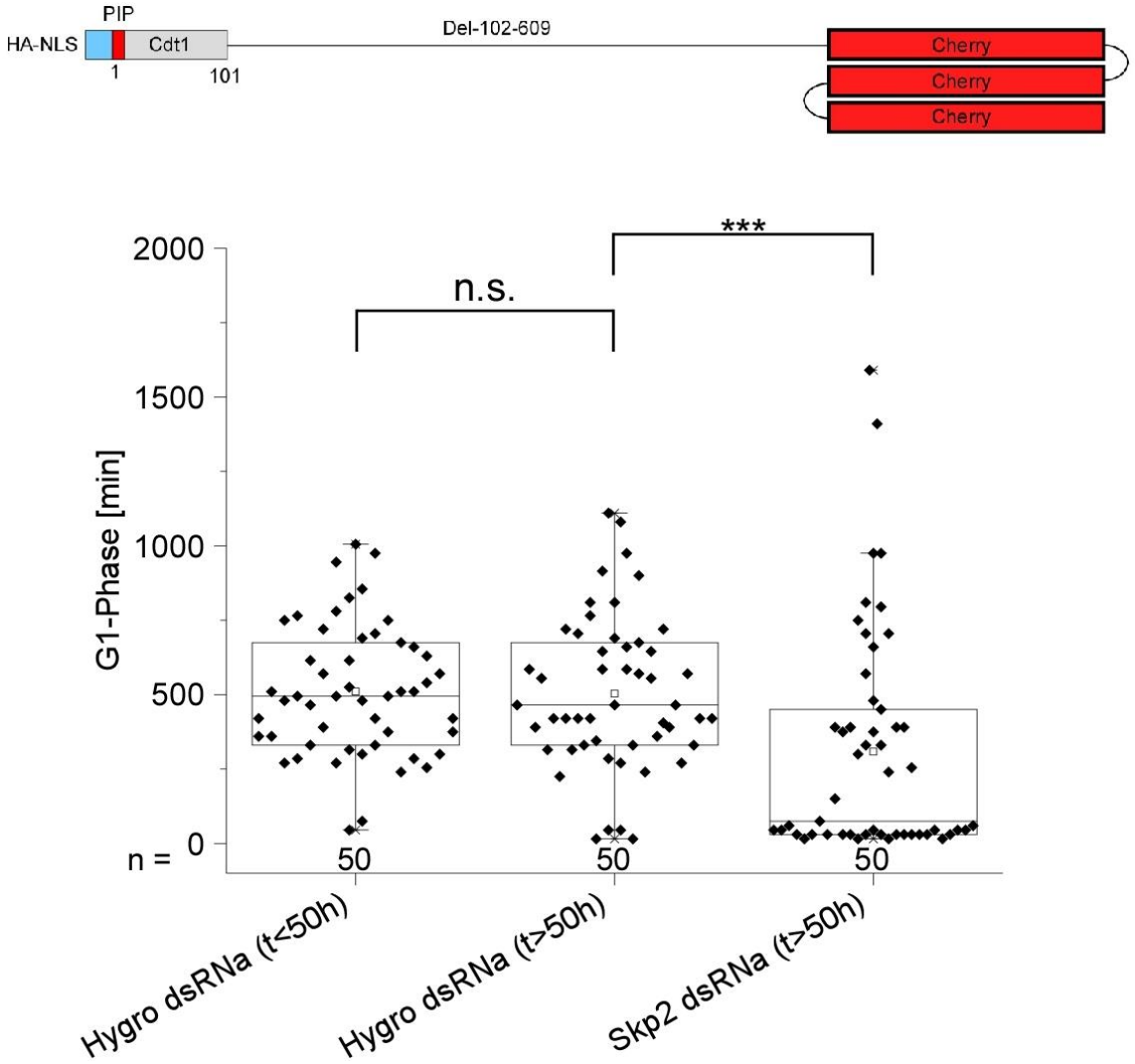

Figure 15 Length of G1-Phase upon Skp2 knockdown

Measurement of G1 length in Schneider cells upon Skp2 knockdown with dsRNA. Double stranded RNA needs around 50 hours incubation time to cause an effect. Impact of control Hygro dsRNA was analyzed before and after this mark to rule out any effect. Effect of Skp2 dsRNA was only analyzed in cells with an incubation time longer than 50 hours. Cdt1 1-101 serves as a G1 cell cycle marker. The line inside the box is the median, the square the average. n.s = p > 0.05; *** = p < 0.001; Mann-Whitney U-Test.

Knockdown by Skp2 dsRNA showed strong effects. Nonetheless, a disadvantage of this method was that it affected all cells in a well. This was problematic for flow cytometric protein stability analysis, since untransfected cells served here as a control to sort the cells in G1-, S- and G2-Phase (see 4.2.6.5). Double stranded RNA would have led to shifts in this control, which would made comparison between different knockdowns unreliable.

To overcome this obstacle, hairpin constructs were created. These constructs consisted in principal of two identical sequences of the gene of interest that should be downregulated, with one fragment in the usual orientation and the other in a 3' to 5' direction. Because of this reverse complement sequence, the transcribed RNA will anneal and build a hairpin structure after transcription that activates the Dicer/RISC system and knocks down the gene of interest. In this case though, only transfected cells showed this effect.

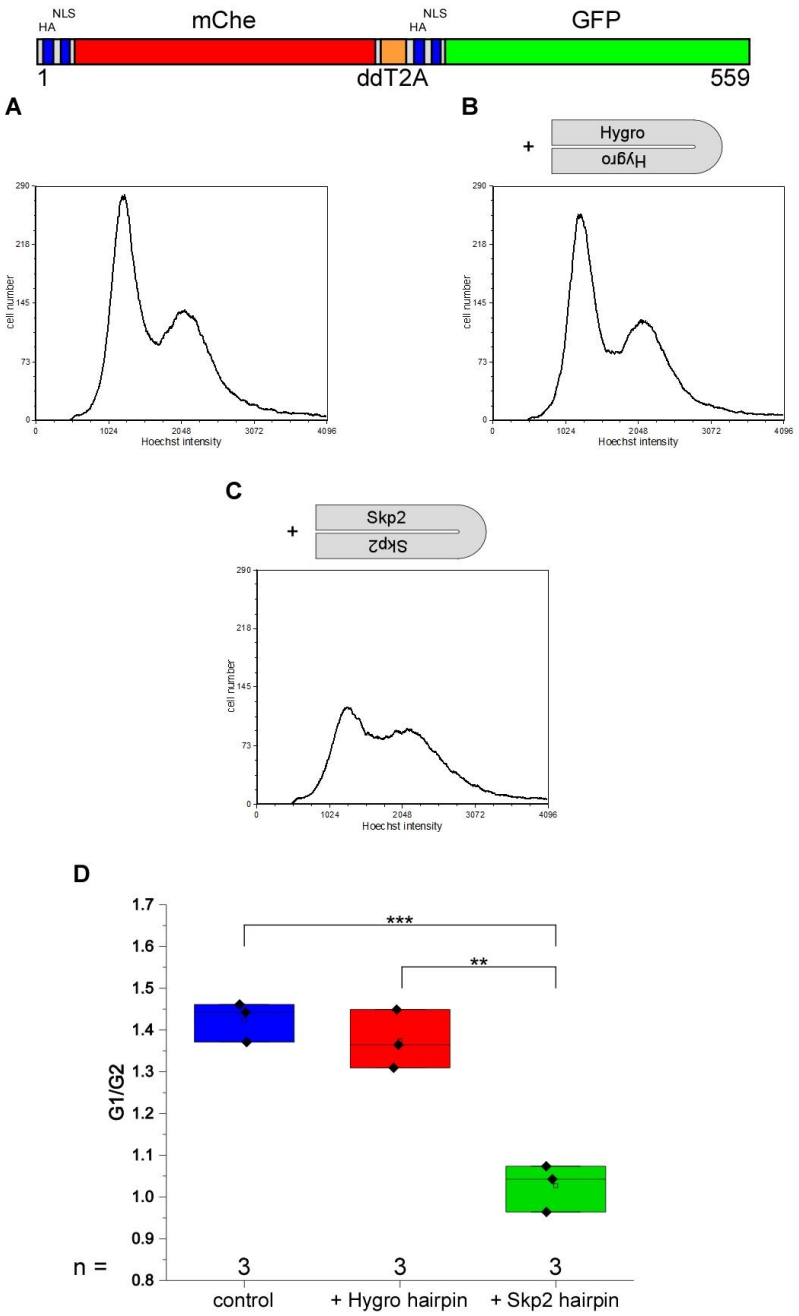

Figure 16 Cell cycle effects of the hairpin constructs

Phenotypic effects on cell cycle distribution of hairpin constructs. mChe serves as the transfection control, only Che positive cells are shown. (A) Cell cycle of S2R+-cells. (B) Effect of Hygro hairpin, serving as a control knockdown. (C) Effect of Skp2 hairpin. (D) Quantification of G1/G2 ratio of S2R+-cells alone and after transfection of Hygro and Skp2 hairpin. ** = $p < 0.01$; *** = $p < 0.001$; t-test for unequal variances. Non-significant changes are not indicated. All presented cell cycle distributions are representative.

Besides Skp2 hairpin, a Hygro hairpin construct was also created as a control and the cell cycle effects of both constructs were analyzed. Expression of the Hygro hairpin construct did not lead to a visible difference in cell cycle distribution (Figure 16A,B,D, t-test for unequal variances, $p > 0.05$). On the other hand, the Skp2 hairpin construct led to a shift into G2/M-Phase (Figure 16C) that was also statistically significant in comparison to S2R+-cells (Figure 16D, t-test for unequal variances, $p < 0.001$) and the control knockdown with Hygro hairpin (t-test for unequal variances, $p < 0.01$). This effect was weaker than the G2 shift caused by Skp2 dsRNA.

5.1.5. Skp2 knockdown over a prolonged time period leads to overreplication

It is already known that knockdown of Skp2 leads to overreplicating cells in wing imaginal discs (Ghorbani et al., 2011). This was not seen in S2R+-cells, which only showed a shift in G2-Phase, albeit a strong one if dsRNA was used (Figure 14C). A possible explanation for this discrepancy was that cells might first accumulate in G2 and only after a prolonged time span under knockdown conditions start to overreplicate. To find out if Skp2 knockdown can cause overreplication in S2R+-cells, Amp and Skp2 dsRNA incubation was performed for six instead of only three days. Cell cycle distribution was analyzed afterwards.

Schneider cells without any knockdown showed a strong shift into a G2 population after six days of incubation in a well (Figure 17A). This was expected, since prolonged time of growth results in cells that are overcrowding leading to an accumulation in G2. Incubation with Amp dsRNA showed a similar effect (Figure 17B). However, Skp2 dsRNA after six days led to an even stronger G2 shift and importantly to a higher number of cells beyond the G2-peak, corresponding with overreplicating cells (Figure 17C). Note also that the overall cell number in the experiment with Skp2 dsRNA was profoundly lower in comparison with the two controls (compare the two y-axes). All cell cycle distributions are overlaid in Figure 17D and normalized to the G2-peak.

Overreplication inevitably leads to cells bigger than normal. Therefore, cell size between all three treatments was also compared. The forward scatter (FSC) is a parameter for cell size, the higher the FSC signal, the bigger are the cells. Amp dsRNA treatment for six days did not lead to cells with a greater size in comparison to control cells. In fact, Amp dsRNA led to smaller cells, though the difference was only marginal. Skp2 knockdown however resulted in bigger cells (Figure 17E). Also note that the x-axis of this figure is logarithmic. Hence, the difference between Skp2 dsRNA and the two control treatments may seem modest, but it represents in fact an increase of around 300 units.

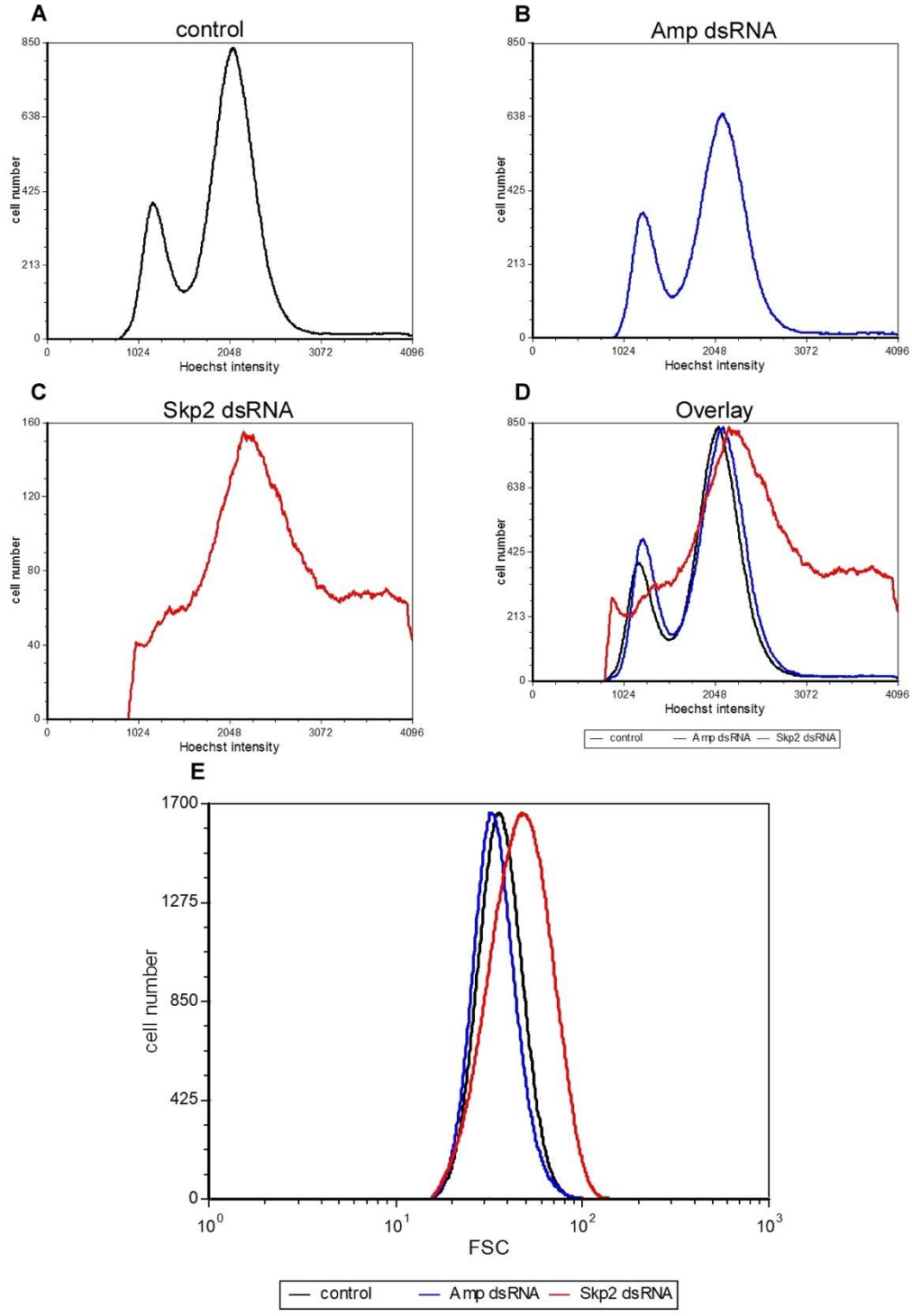

Figure 17 Overreplication of Schneider cells after prolonged Skp2 knockdown

Cell cycle distribution and cell size after six days of incubation with dsRNA. (A) Schneider cells show a G2 shift after six days of incubation. (B) Treatment with Amp dsRNA does not lead to obvious changes in comparison to untreated cells (C) Treatment with Skp2 dsRNA for six days leads to an enhanced G2 shift and a decreased cell number, overreplicating cells occur. (D) Overlay of the cell cycle distributions of control, Amp dsRNA and Skp2 dsRNA cells. Histograms are normalized to the G2-peak. (E) Comparison of forward scatter (FSC) between Schneider cells, Amp dsRNA and Skp2 dsRNA treatment as a parameter of cell size. Skp2 dsRNA leads to bigger cells in comparison. Histograms are normalized. All depicted graphs are representative.

5.2. Skp2 overexpression or knockdown does not lead to indirect changes of protein stability

Overexpression or knockdown of proteins can lead to tremendous changes in a cell. Not all of these changes have to be a direct effect mediated by enhanced or diminished protein activity. Instead, some of them could be side effects by flooding the cell with a protein or depleting it. Overexpression and knockdown studies – used extensively in this thesis – should therefore always consider and monitor these indirect effects.

Overexpression of Skp2, or any other F-Box protein, might be problematic if abundance of the SkpA-Cul1-Rbx1 complex (SC-complex) is a rate-limiting factor. In this case, overexpression of Skp2 will lead to a pronounced formation of the SCF^{Skp2} complex, other F-Box proteins will be pushed aside from SkpA-Cul1-Rbx1 and their substrates will no longer be ubiquitinated. Knockdown of Skp2 on the other side will lead to a greater amount of free SC-complex that is ready to receive other F-Box proteins. An enhanced ubiquitination of the substrates of these F-Box proteins is the result. These indirect effects may result in wrong conclusions of cell cycle effects and substrates of Skp2.

An assay was developed to sort out if modulation of Skp2 levels has any unwanted indirect effects. Determination of GFP stability by flow cytometry and targeted degradation of GFP by slmb-vhhGFP4 was combined for this assay. Slmb-vhhGFP4 is a fusion construct consisting of the F-Box domain of the Slmb F-Box protein and the sequence of the vhhGFP4 nanobody. Nanobodies are antibodies consisting only of a monomeric heavy chain. Vhh is a nanobody derived from camels (Arbabi Ghahroudi et al., 1997) and vhhGFP4 is specifically directed against GFP. Therefore, slmb-vhhGFP4 is specifically developed for ubiquitination and consequent degradation of GFP-fusion proteins (Caussinus et al., 2011). This system was used in this thesis to mimic the degradation of a substrate by means of ubiquitination through an F-Box protein. Simultaneous overexpression, respectively knockdown of Skp2 can elucidate indirect effects, since Skp2 is not targeting GFP.

Figure 18A shows the principle of this assay. Slmb-vhh and GFP will be overexpressed in Schneider cells. If enough free SkpA-Cul1-Rbx1 complex will be present, $SCF^{slmb\text{-}vhh}$ will be formed and ubiquitinate GFP resulting in GFP degradation (Figure 18A, middle). Depletion of Skp2 could lead to a greater amount of free SC-complex that could be inhabitated by slmb-vhh. As a result, GFP would be more unstable (Figure 18A, left side). Skp2 overexpression on the other hand could lead to more competition for the SC-complex in this case. Less $SCF^{slmb\text{-}vhh}$ is built and hence, GFP gets stabilized (Figure 18A, right side). If Skp2 and slmb-vhh are not competing for the SkpA-Cul1-Rbx1 complex, a change in Skp2 levels should not result in varying GFP stability.

GFP protein stability was measured by flow cytometric analysis. Since the protein of interest was GFP, the ratio between GFP fluorescence and mCherry fluorescence was calculated. This ratio served as the stability index. Since the data was normalized, a stability index lower than 1 is synonymous to protein destabilization and an index higher than 1 means stabilization. Statistical analysis revealed, if changes of the stability index upon the various treatments were significant. Analysis was performed on all transfected cells. For detailed information, see 4.2.6.5.

A control experiment showed that neither Skp2 overexpression nor knockdown did have any significant effect on GFP stability (Figure 18B, left, Mann-Whitney U-Test, $p > 0.05$). Hygro knockdown served as a control for the knockdown experiment and did likewise not have any statistically significant effect (Mann-Whitney U-Test, $p > 0.05$).

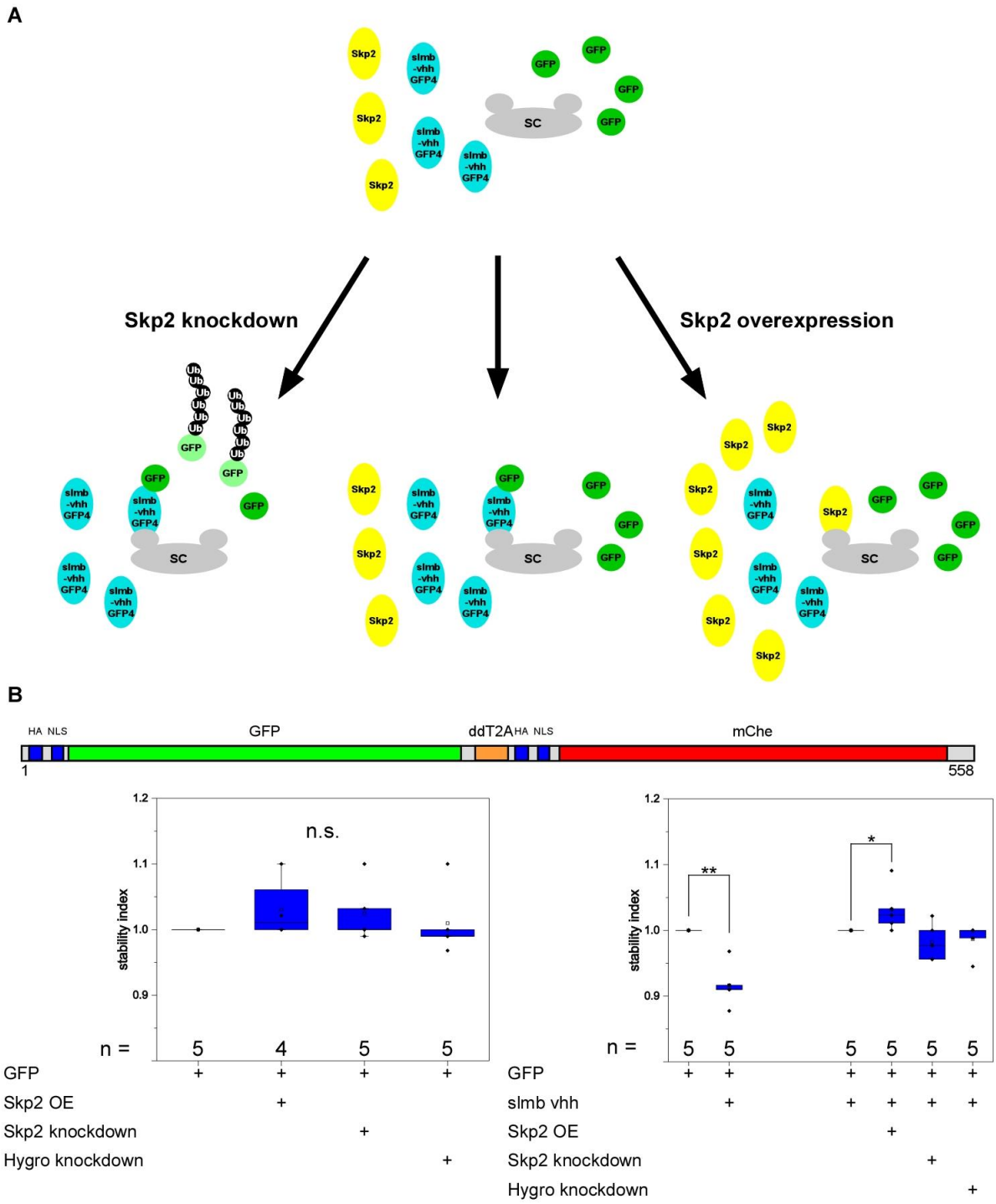

Figure 18 Test of indirect effects of Skp2 overexpression or knockdown

Principle and result of the assay for direct or indirect effects of changing Skp2 levels. (A) Principle of the assay. Slmb-vhh degrades GFP. If slmb-vhh competes with Skp2 for binding to the SkpA-Cul1-Rbx1 complex (SC-complex), Skp2 depletion should lead to stronger GFP degradation (left). Likewise, Skp2 overexpression, re-enacting the massive overexpression of two F-Box proteins, could lead to displacement of slmb-vhh and GFP stabilization (right). (B) Left: Skp2 overexpression (OE), Skp2 knockdown and Hygro knockdown alone does not have a significant effect on GFP-stability. Right: GFP is degraded upon overexpression of slmb vhh. Overexpression of two F-Box proteins (slmb-vhh and Skp2) leads to GFP stabilization. Skp2 knockdown and Hygro knockdown does not alter the ability of slmb-vhh to degrade GFP. n.s. = $p > 0.05$, * = $p < 0.05$, ** = $p < 0.01$, Mann-Whitney U-Test.

Degradation of GFP by slmb-vhh in this setup was significant, underlining that the assay was functional (Figure 18B, right, Mann-Whitney U-Test, $p < 0.01$). Indeed, this test showed that substrates are degraded by overexpression of an F-Box protein. For the remaining assays, all data was normalized to GFP stability with slmb-vhh already overexpressed. Combined overexpression of slmb-vhh and Skp2 did indeed increase GFP stability significantly (Figure 18B, right, Mann-Whitney U-Test, $p < 0.05$). Contrary, Skp2 knockdown and Hygro knockdown did not have an effect of the GFP stability (Mann-Whitney U-Test, $p > 0.05$, for more detailed information about the display of the data, see 4.2.6.5).

According to these findings, any effect seen in Skp2 overexpression or knockdown studies were direct and not caused by competition of Skp2 and other F-Box proteins for the SkpA-Cul1-Rbx1 complex, excluding this source for misinterpretation. Competition between F-Box proteins can occur, but according to the results only under extreme conditions when two F-Box proteins were overexpressed under strong promotors. This effect was probably not occurring in the experiments presented in the rest of this thesis.

5.3.Dacapo is not destabilized by SCF^{Skp2} activity

5.3.1. Overview

Skp2 targets p21, p27 and p57 for degradation in mammalians (Heo et al., 2016). Though it seems only logical that this would also be the case in *D. melanogaster*, the literature is not clear in this respect. While at first it was found that the fly homologue Dacapo (Dap) is not a substrate of SCF^{Skp2} (Ghorbani et al., 2011), a later analysis indeed did reveal the ability of SCF^{Skp2} to mark Dap for degradation (Dui et al., 2013). The results of this publication are questionable however and could be explained by side effects of the used assays and not directly by Skp2. Therefore, the influence of SCF^{Skp2} on Dap is still not well resolved.

To illuminate the answer to this question, Dacapo stability was assayed by flow cytometric analysis. In contrast to the former publications, not only wild type Dacapo was used but in addition versions that did no longer have the ability to alter the cell cycle, thereby excluding any effect on stability that purely resulted by shifts into certain cell cycle phases. Furthermore, the alternative degradation pathway in S-Phase via $CRL4^{Cdt2}$ was also shut off. Co-immunoprecipitation studies were also performed to analyze biochemical interaction between Skp2 and Dap. Finally, rescue experiments were undertaken to analyze changes in the Dap overexpression phenotype if Skp2 was overexpressed.

5.3.2. Cell cycle effects of different Dacapo mutants

The cell cycle effects of the different Dacapo versions used in this thesis will be shown first. These versions were created and characterized by former group members. Cell cycle effects of mCHE-tagged Dap versions are shown that are representative of the effects of all tested Dap versions regardless of their respective tag.

Overexpression of Dap full length in a T2A vector led to a G1 shift of the cell cycle in comparison to the control T2A construct (Figure 19, compare A and B, C is an overlay of both), which was also seen by other researchers (Frank, 2013; Swanson et al., 2015). Dap dCDI (Figure 19E) contained deletions that prevented the interaction with CycE/Cdk2, resulting in an unaltered cell cycle in comparison to the control (compare D and E, F is an overlay of both). Dap dCDI dPIPa (Figure 19H) further contained a deletion in the PIP-Box region, preventing it from degradation by $CRL4^{Cdt2}$. This Dap version also did not have any influence on the cell cycle (compare G and H, I is an overlay of both). All shown cell cycle distributions are representative for all experiments. Overlaid distributions are normalized to the G1-peak.

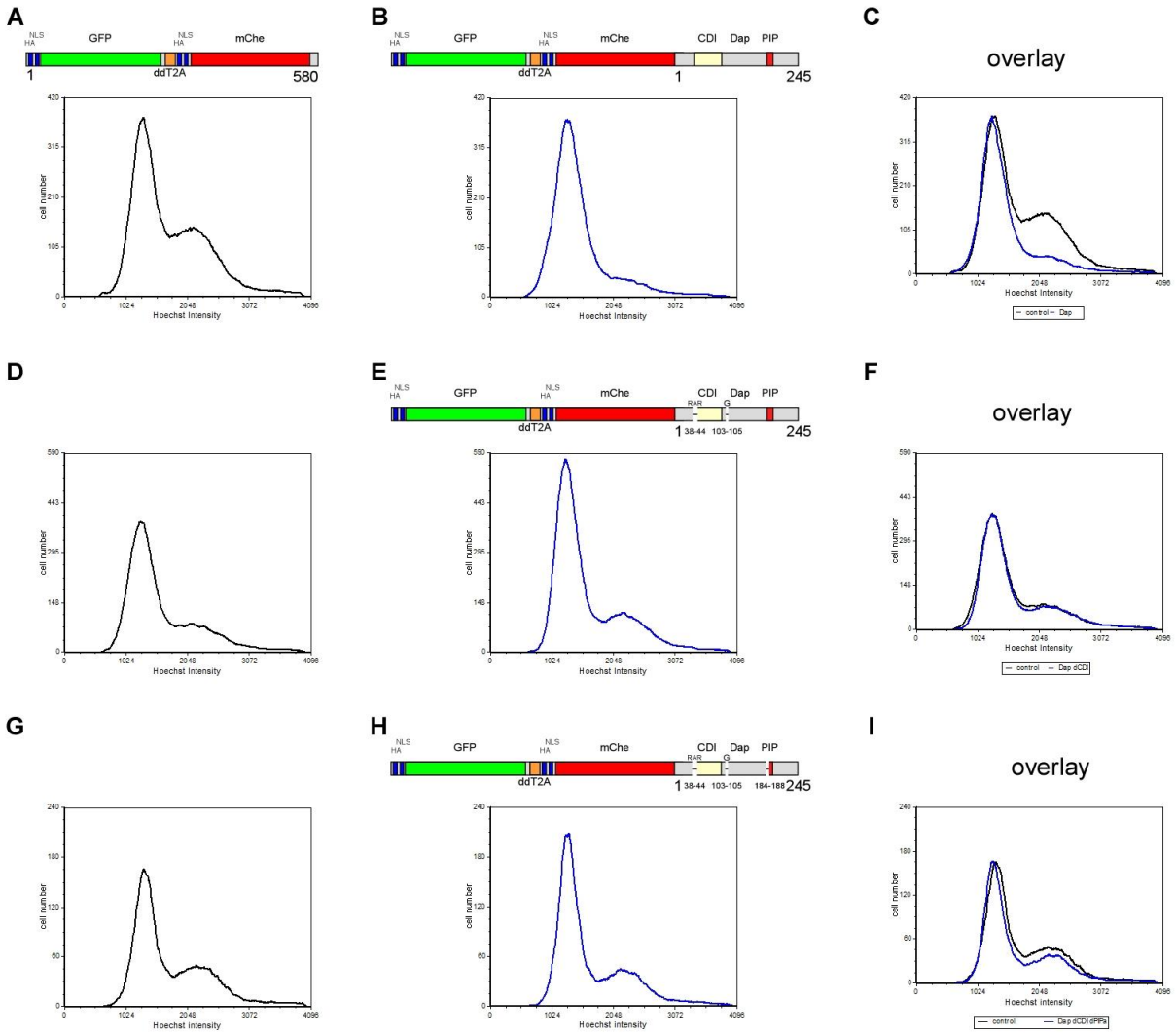

Figure 19 Cell cycle effects of different Dacapo versions

Cell cycle distributions of cells transfected with different Dacapo versions. GFP serves as the transfection control, only GFP cells are shown. (A,D,G) Cell cycle distribution of the control T2A construct. (B) Overexpression of Dap leads to more cells in G1-Phase. (C) Overlay of A and B. (E) Dap dCDI does not have any visible effect on the cell cycle. (F) Overlay of D and E. (H) Dap dCDI dPIPa overexpression also has no visible effect. (I) Overlay of G and H. For all overlays, histograms are normalized to the G1-peak. All depicted cell cycle distributions are representative.

5.3.3. Dacapo stability remains constant with changing Skp2 levels

Flow cytometric stability analysis for Dap was performed with overexpression of different Skp2 versions. Stability was analyzed for all transfected cells, regardless of their cell cycle stage, and for the three distinct cell cycle phases (G1, S and G2), determined by Hoechst staining. Since results became unreliable if the T2A system is expressed either too weak or too strong, only cells with a medium expression level range were analyzed that were determined by the fluorescent level of the reference protein (in this case the range of the logarithmic GFP fluorescence values between 2.00 and 2.75, see 4.2.6.5 for more details). All

stability data was normalized to the stability of the tested Dacapo constructs. Influence of the overexpressed components on GFP and mCherry was checked in all cases; it was found that no overexpression changed the mCherry stability (data not shown) except for the Cks85A overexpression (Figure 20C).

In the beginning, the influence of Skp2 overexpression on Dap full length stability was investigated. Surprisingly, Skp2 overexpression did lead in all cases to a slight stabilization of the Dacapo protein. Destabilization of Dap was not observed by Skp2 overexpression. Yet, it has to be said that these changes were not significantly different (Figure 20A, one sample t-test, $p > 0.05$), with the notable exception of the G2-Phase. In this case, the stabilization of Dap was significant (one sample t-test, $p < 0.05$).

It is well known that substrates of Skp2, for example the Dap homologue p27, need to be phosphorylated to be recognized (Montagnoli et al., 1999). Overexpressing Dacapo does not automatically ensure that it is phosphorylated in the cell and thereby marked for Skp2 binding. Since phosphorylation may be a critical factor, it was also incorporated in the assay. For this reason, CycE overexpression was also applied. An excess amount of CycE leads to an increased formation of the CycE/Cdk2 complex, since the amount of Cdk2 is higher than CycE, resulting in a portion of unbound, inactive Cdk2 molecules (Arooz et al., 2000). CycE overexpression results in binding of this inactive Cdk2 population and enhanced activity. This can be seen by the marked change in the cell cycle profile. The increased CycE/Cdk2 activity, in analogy to the human system, should result in intensified phosphorylation of Dap as well (de Nooij et al., 2000; de Nooij et al., 1996).

CycE overexpression, and subsequent Dap phosphorylation, did lead to higher stability of Dap. Yet, all these changes were statistically not significant. Therefore, CycE alone was not influencing Dap stability to a great extent (Figure 20A, one sample t-test, $p > 0.05$).

Combined overexpression of Skp2 and CycE should lead to a degradation of Dap. Indeed, it can be observed that Dap stability was diminished in this case. Yet, all changes were again not significant and an effect of Skp2 on Dap stability could not be seen (one sample t-test, $p > 0.05$).

Biochemical interaction between Skp2 and Dap was already shown by Co-IP studies and published (Dui et al., 2013). In this case, Skp2 4xFLAG was used; it may well be that an N-terminal FLAG tag is preventing interaction between Skp2 and Dap. Therefore, the experiment was repeated with Skp2 4xFLAG overexpression.

Overexpression of Skp2 4xFLAG had a slightly different effect in comparison to the N-terminal tag. The modest, non-significant stabilization seen before vanished and Dap stability was indifferent in comparison to Dacapo alone. As before, no significant difference could be observed (Figure 20B, one sample t-test, $p > 0.05$). Again, Dap stability was analyzed with CycE overexpression alone. In this case, Dap was actually significantly stabilized for all cells (one sample t-test, $p < 0.05$). Broken down into the distinct cell cycle phases, no significant difference could be observed. Just like above, combined overexpression of Skp2 4xFLAG and CycE did not show any significant change in Dap overexpression (one sample t-test, $p > 0.05$).

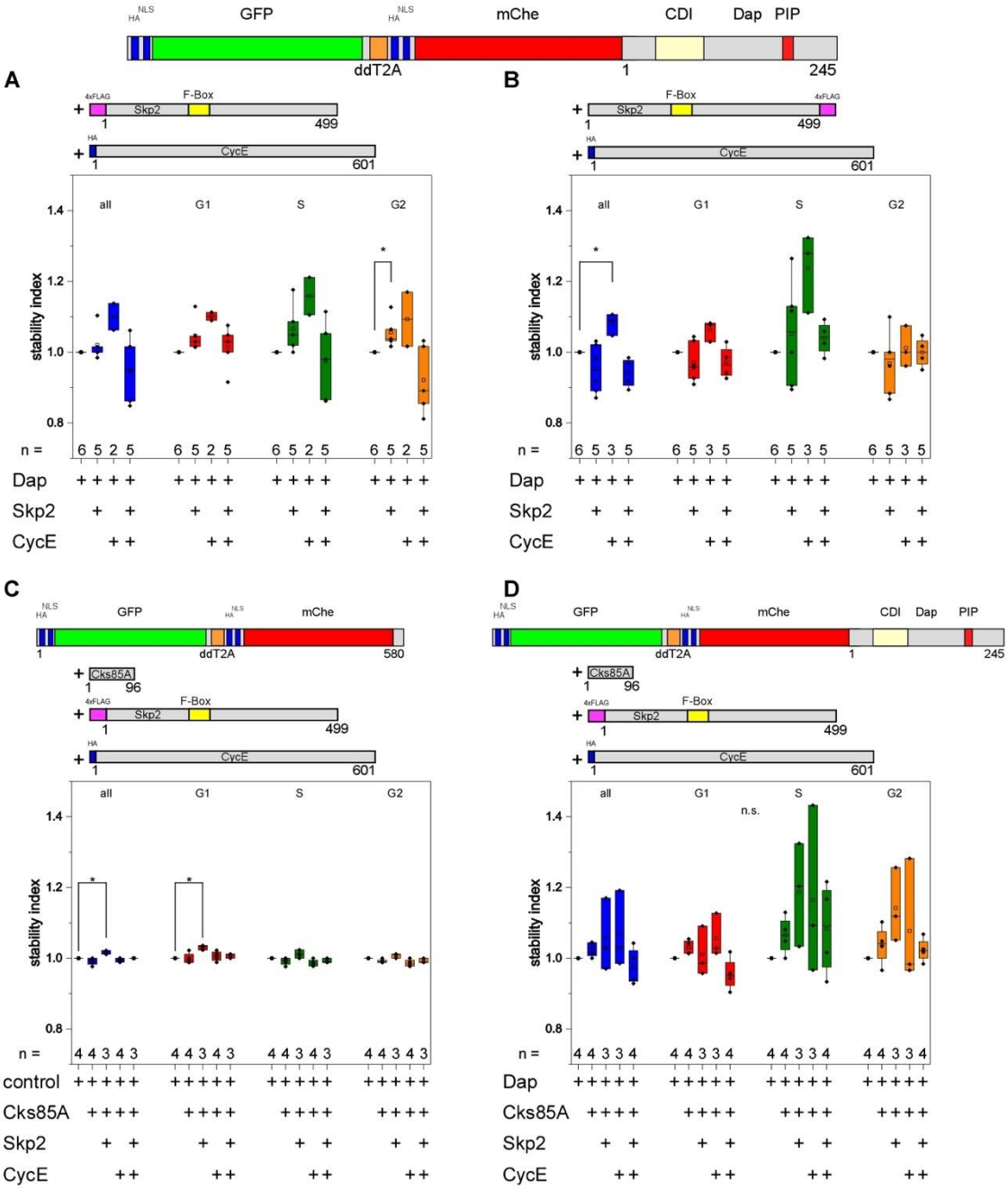

Figure 20 Dacapo stability upon overexpression of different Skp2 versions plus CycE and Cks85A

Results of the Dacapo protein stability analysis with flow cytometry. (A) Dap stability is not significantly altered by overexpression of 4xFLAG Skp2 or/and CycE. Only Skp2 overexpression leads to stabilization in G2-Phase. (B) Dap stability is not significantly influenced by Skp2 4xFLAG or/and CycE, with the exception of CycE overexpression in all cells where it is stabilized. (C) Overexpression of Cks85A and 4xFLAG Skp2 does result in stabilization of mCherry in all and G1 cells. (D) Dap stability is not significantly influenced by overexpression of 4xFLAG Skp2, CycE or/and Cks85A. n.s. = $p > 0.05$, * = $p < 0.05$, one-sample t-test. Only significant changes are indicated.

Another factor that may influence Skp2 substrate binding is the availability of Cks85A. Cks85A supports Skp2 by binding its substrates, indeed the homologue Cks1 is necessary for Skp2 mediated degradation of p27 (Ganoth et al., 2001; Spruck et al., 2001). This is in concordance with the fact that Skp2 precipitates Dap more efficiently with a simultaneous overexpression of Cks85A (Dui et al., 2013). Cks85A may therefore be a limiting factor and overexpression may influence Dap stability in combination with Skp2 and CycE.

Surprisingly, Cks85A overexpression did significantly alter the stability of mCherry in all and G1 if combined with Skp2 overexpression (Figure 20C, one sample t-test, $p < 0.05$). This was not observed in the other experiments with Dap full length.

Overexpression of Cks85A did not have a significant effect on Dap stability (Figure 20D, one sample t-test, $p > 0.05$). Moreover, even simultaneous overexpression of Skp2, CycE or both combined did not lead to any significant change in protein stability (one sample t-test, $p > 0.05$). Importantly, all observed tendencies were hinting to a stabilization of Dap by overexpression of the various components. Instability was never observed.

Additionally, the effect of Skp2 dF-Box was also tested. A missing F-Box should have prevented Skp2 from binding to the SkpA-Cul1-Rbx1 complex. Yet, this construct still had the capability to bind its substrates, since the leucine rich repeats, responsible for substrate binding, were not touched by this deletion. Substrate binding to the dF-Box version should therefore lead to protection, since intact F-Box proteins could no longer bind them. A dominant negative effect should be visible. However, neither Skp2 nor Skp2 dF-Box overexpression led to a significant change in Dap stability (Figure 21, one sample t-test, $p > 0.05$).

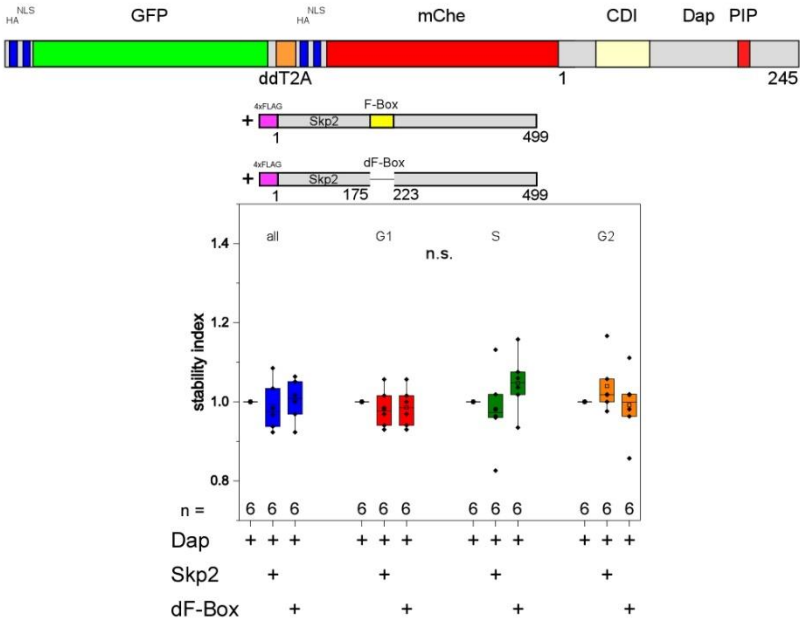

Figure 21 Dacapo stability upon overexpression of Skp2 dF-Box
Results of the flow cytometric analysis of Dap protein stability. Stability is not significantly influenced by either overexpression of Skp2 or Skp2 dF-Box. n.s. = $p > 0.05$, one-sample t-test.

In conclusion, Dacapo full-length stability was for the most part not affected by different overexpression treatments. Furthermore, any significant effects seen showed stabilization of Dap, destabilization was never seen on a statistically significant level. Dap stability seemed to be indifferent concerning Skp2 overexpression.

It was also analyzed what happened to Dacapo full-length if Skp2 was downregulated by hairpin constructs. A Skp2 hairpin construct was used for the knockdown. The Hygro hairpin construct served as the control. Neither Skp2 hairpin nor Hygro hairpin had a significant effect on GFP and mCherry alone (data not shown). In case of this experiment, the difference between Dap stability with Skp2 knockdown and the control Hygro knockdown was analyzed.

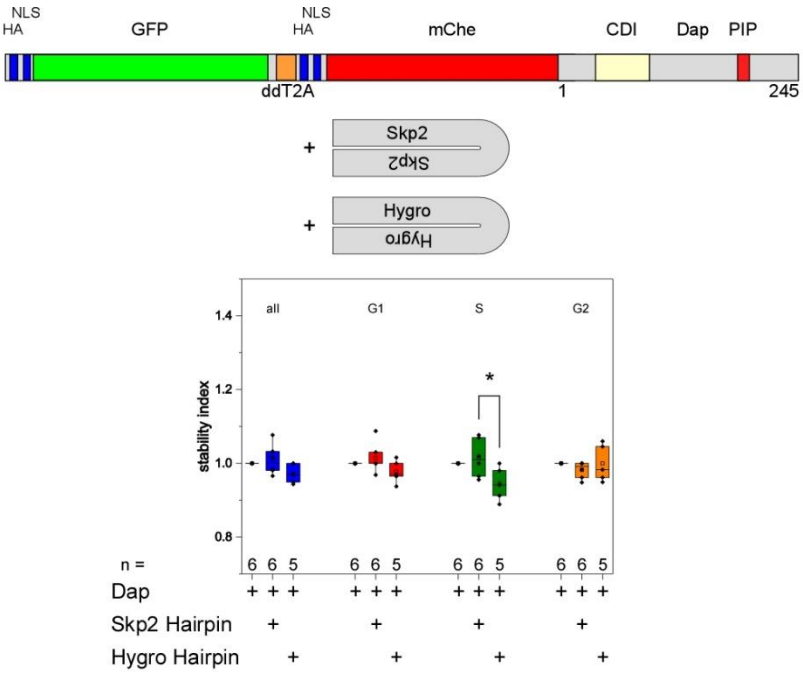

Figure 22 Dacapo stability upon Skp2 knockdown
Dacapo full length protein stability measured by flow cytometry under Skp2 knockdown conditions. Skp2 knockdown does lead to Dap stabilization in S-Phase cells in comparison to Hygro control knockdown. In all other cases, Skp2 knockdown does not have an effect. * = $p < 0.05$, t-test for equal variances. Only significant changes are indicated.

Skp2 knockdown did not significantly change the stability of Dap in comparison to the control Hygro knockdown in all, G1 or G2 cells (Figure 22, t-test for equal variances, $p > 0.05$). The knockdown led to significant stabilization in S-Phase, however (t-test for equal variances, $p < 0.05$).

So far, Dacapo did not seem to be prominently influenced by changing Skp2 levels. This held true even if Skp2 substrate recognition was enhanced in theory by CycE and Cks85A overexpression. According to these assays, full length Dacapo was not a substrate for SCF^{Skp2}, yet it has to be said that this Dap version still contained another mechanism for degradation by a PIP-degron and led also to a shift in the cell cycle when overexpressed, which may have obscured any Skp2 related effects.

5.3.4. Dap is not regulated by Skp2, regardless of its impact on the cell cycle

Though Dacapo seemed to be not influenced by Skp2 overexpression (even combined with CycE and Cks85A overexpression) or knockdown, one has to consider the cell cycle effects of this protein. As already demonstrated Dap full-length overexpression did lead to a stop in G1-Phase (Figure 19B). This was disadvantageous for experiments, since the cell cycle was deeply disturbed in this case. Indirect effects may lead to wrong interpretation of results and furthermore, Skp2 dependent degradation may well be hindered in this case. Therefore, Dap dCDI stability was analyzed. Dap dCDI contained deletions, primarily in the CDI domain, that made the binding to CycE/Cdk2 impossible. Though still degraded like wild type Dap, this construct did have no longer an effect on the cell cycle (Figure 19D,E).

Dap dCDI was significantly stabilized upon 4xFLAG Skp2 overexpression in all, G1- and S-Phase cells (Figure 23A, one sample t-test, $p < 0.05$). There seemed to be no effect in G2-Phase (one sample t-test, $p > 0.05$). Likewise, CycE overexpression did lead to a significant decrease in protein stability (one sample t-test, $p < 0.05$ or $p < 0.01$) with the exception of the G2-Phase (one sample t-test, $p > 0.05$). Combined overexpression of both, 4xFLAG Skp2 and CycE, resulted in Dacapo protein stability that was not significantly changed (one sample t-test, $p > 0.05$), excepting G2-Phase where it was significantly stabilized (one sample t-test, $p < 0.05$).

Similar effects could also be observed when Skp2 4xFLAG was used. Overexpression of Skp2 4xFLAG led to a significant stabilization of the Dap dCDI protein in the four analyzed cell cycle states (Figure 23B, one sample t-test, $p < 0.001$ or $p < 0.05$). CycE overexpression (a direct reproduction of the experiments in Figure 23A) showed a similar result, a significant destabilization of Dap dCDI in all and G1 (one sample t-test, $p < 0.05$), however, unlike in the first experiment, CycE was not influencing protein stability in S-Phase (one sample t-test, $p > 0.05$). Combined overexpression did only have a stabilizing effect in G2-Phase (one sample t-test, $p < 0.05$) in concordance with the previous result.

The effect of Cks85A overexpression was also measured. Cks85A led to a significant stabilization of Dap dCDI in S- and G2-Phase (Figure 23C, one sample t-test, $p < 0.05$), stability in all and G1 cells remained unaffected (one sample t-test, $p > 0.05$). Simultaneous overexpression of Skp2 did lead to more stable Dap dCDI in all, S and G2 cells but not in S-Phase. However, note that this experiment was only performed once, results are not reliable and statistical analysis could not be performed therefore. Cks85A and CycE overexpression did lead to a change in stability: while it got unstable in all and G1 cells (one sample t-test, $p < 0.05$ or $p < 0.01$), it did show no effect in S-Phase cells (one sample t-test, $p > 0.05$) and even stabilization in G2-Phase (one sample t-test, $p < 0.05$). Overexpression of all three components did not affect Dap dCDI stability in all and G1 cells (one sample t-test, $p > 0.05$), yet it led to stabilization in S- and G2-Phase (one sample t-test, $p < 0.01$ or $p < 0.05$).

Dap dCDI stability was also tested with Skp2 dF-Box overexpression. In this set of experiments, Skp2 overexpression showed the same stabilizing effect as already observed in Figure 23A. In this case, though Dap dCDI was stabilized even in G2 (Figure 23D, one sample t-test, $p < 0.01$ or $p < 0.05$). Skp2 dF-Box did also lead to protein stabilization (one sample t-test, $p < 0.01$, $p < 0.001$ or $p < 0.05$), with the exception of G1-Phase were stability remained indifferent (one sample t-test, $p > 0.05$).

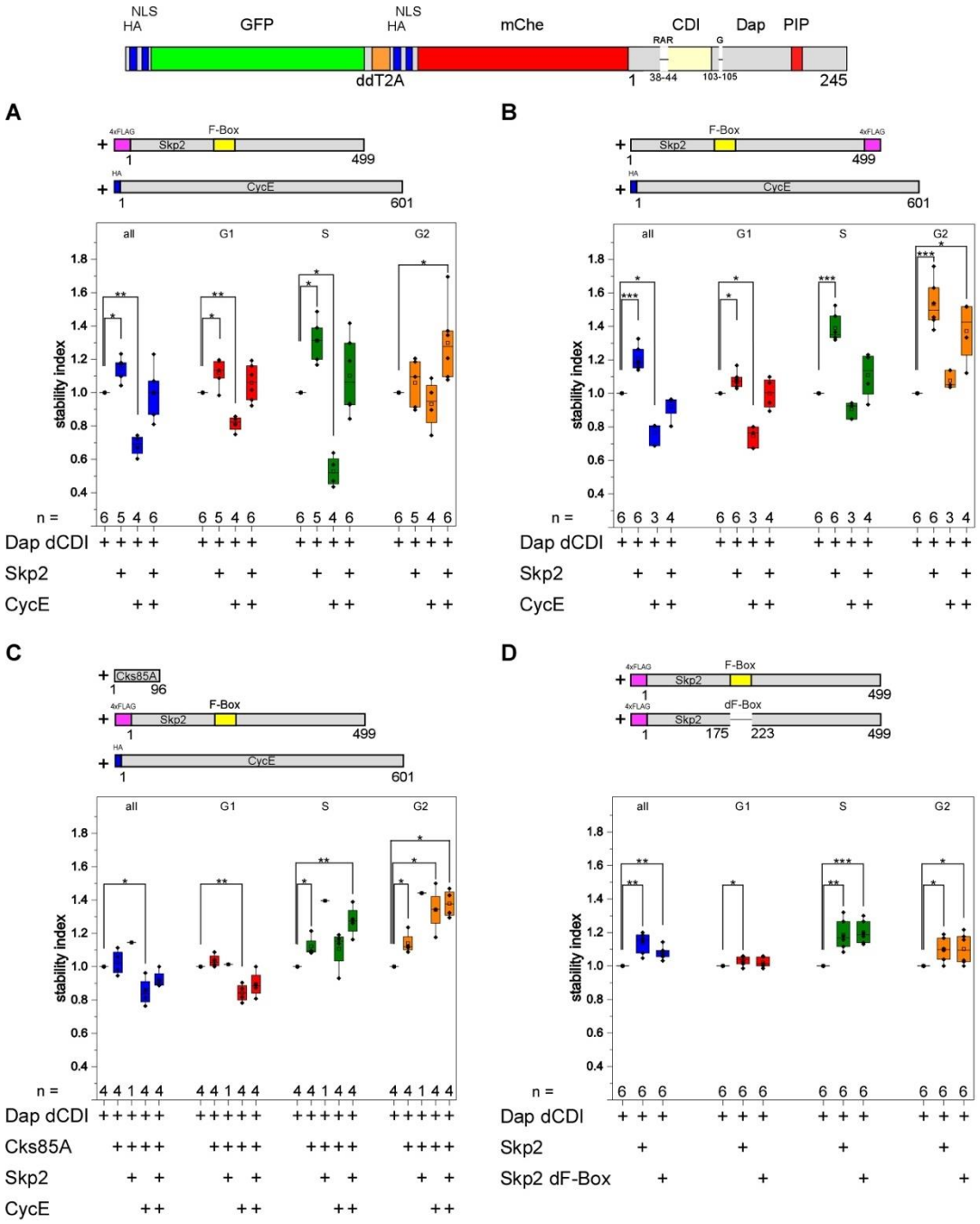

Figure 23 Dacapo dCDI stability upon overexpression of different Skp2 versions plus CycE and Cks85A
Results of the Dacapo dCDI protein stability analysis with flow cytometry. (A) Dap dCDI stability is significantly stabilized by 4xFLAG Skp2 and destabilized by CycE overexpression in all, G1- and S-cells. Combined overexpression leads to stabilization only in G2. (B) Overexpression of Skp2 4xFLAG and CycE does lead to similar results as in A. (C) Overexpression of 4xFLAG Skp2, CycE and Cks85A does lead to Dap dCDI stabilization in S and G2. (D) Overexpression of either Skp2 dF-Box or 4xFLAG Skp2 does lead to stabilization * = $p < 0.05$, ** = $p < 0.01$, *** = $p < 0.001$, one-sample t-test. Only significant changes are indicated.

Just like before, knockdown studies were also performed. Dap dCDI showed no reaction to the Skp2 knockdown in comparison to the control knockdown (Figure 24, t-test for equal variances, $p > 0.05$).

To conclude this section, Dap dCDI showed significant changes of stability by overexpression of Skp2, CycE and Cks85A. It was degraded by CycE overexpression; yet, it was never observed that Dap dCDI was degraded by Skp2 overexpression. Indeed, the opposite was true: Skp2 overexpression seemed to stabilize this mutant. This effect was also observed by Skp2 dF-Box overexpression. Dap dCDI showed also no effect upon Skp2 knockdown.

Using Dap dCDI eliminated any influences of cell cycle changes that are inevitable by performing overexpressions with Dap full length. Yet this Dap version is still degraded efficiently by another E3 ubiquitin ligase ($CRL4^{Cdt2}$) in S-Phase by its PIP-degron motif (Swanson et al., 2015). This PIP dependent degradation pathway may have disguised any effects that Skp2 may had on Dap, especially if the Skp2 mediated degradation was not the main way of Dacapo degradation.

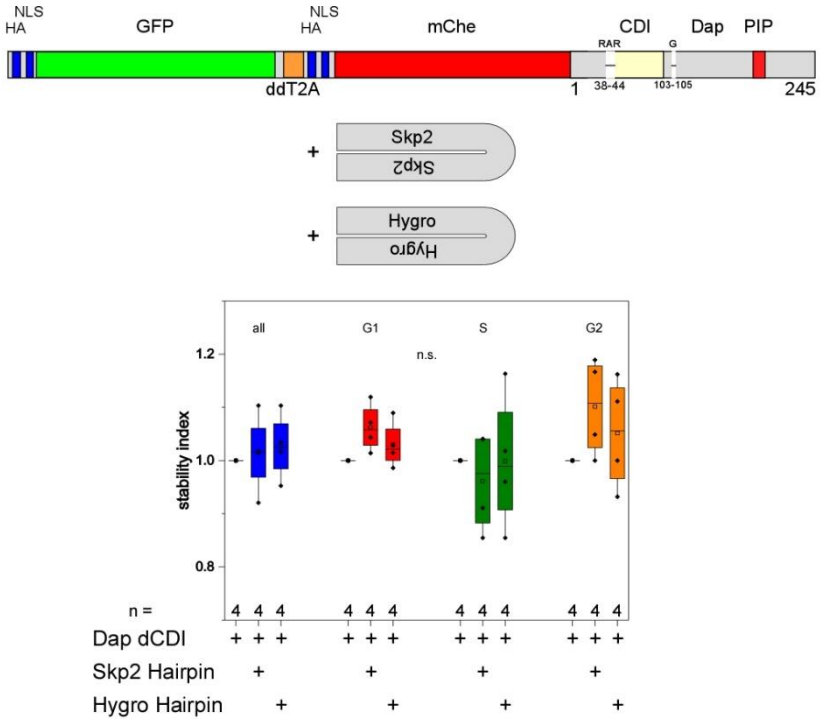

Figure 24 Stability of Dap dCDI upon Skp2 knockdown
Flow cytometric analysis of Dap dCDI stability with Skp2 downregulation. In comparison to Hygro hairpin, Skp2 hairpin does not influence Dap dCDI stability. n.s. = $p > 0.05$, t-test for equal variances.

5.3.5. Dap is not regulated by Skp2, even if the PIP mediated degradation pathway is eliminated

Since Dap dCDI is still degraded by $CRL4^{Cdt2}$ via the PIP-degron in S-Phase and since this is probably the principal way of its degradation, any effects that Skp2 may have are probably hard to detect. To overcome this issue, Dap dCDI dPIPa was used. This Dap version still lacked the ability to interact with CycE/Cdk2 and did not influence the cell cycle (Figure 19 compare E and F). Furthermore, the N-terminal part of the PIP-Box was deleted, resulting in a construct that was no longer degraded in S-Phase. Importantly though, earlier results in the lab showed it is still unstable in G1, a potential Skp2 degradation may still be in place (Christina Grasmüller, 6-week internship).

Dap dCDI dPIPa was significantly stabilized by 4xFLAG Skp2 overexpression (Figure 25A, one sample t-test, $p < 0.05$) with the exception of G2-Phase, where levels stayed normal (one sample t-test, $p > 0.05$). CycE overexpression did not change Dap dCDI dPIPa stability in a significant way (one sample t-test, $p > 0.05$). Overexpression of both components led to a significant stabilization in all, S and G2 cells (one sample t-test, $p < 0.05$) but not in G1-Phase (one sample t-test, $p > 0.05$).

Using Skp2 4xFLAG led to similar results. Dap dCDI dPIPa stability was significantly stabilized in all and G1 cells (Figure 25B, one sample t-test, $p < 0.05$ or $p < 0.01$), but not in S and G2 cells (one sample t-test, $p > 0.05$). CycE overexpression did not significantly change the stability (one sample t-test, $p > 0.05$) in concordance with the results obtained from 4xFLAG Skp2. Combined overexpression stabilized Dap dCDI dPIPa in S and G2 cells (one sample t-test, $p < 0.05$), but not in all and G1 cells (one sample t-test, $p > 0.05$).

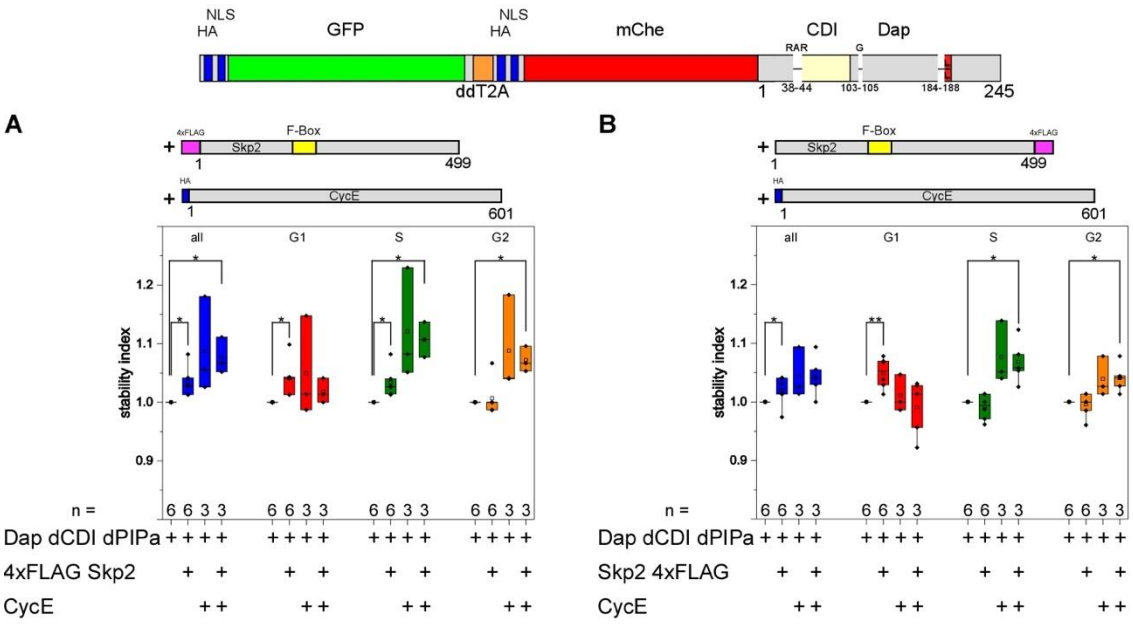

Figure 25 Dap dCDI dPIPa stability upon overexpression of 4xFLAG Skp2, Skp2 4xFLAG and CycE
Flow cytometric protein stability data of Dap dCDI dPIPa. (A) 4xFLAG Skp2 and 4xFLAG Skp2 plus CycE overexpression stabilizes Dap dCDI dPIPa, CycE overexpression has no effect. (B) Skp2 4xFLAG also has a stabilizing effect on Dap dCDI dPIPa in all and G1 cells, CycE does also have no effect and the combined overexpression leads to stabilization in S and G2. * = $p < 0.05$, ** = $p < 0.01$, one sample t-test. Only significant changes are indicated.

Dap dCDI dPIPa stability was also measured under Skp2 knockdown conditions. Skp2 knockdown led to a significant stabilization in comparison to the control knockdown with Hygro Hairpin in all and G1 cells (Figure 26, t-test for equal variances, $p < 0.05$).

Dap dCDI dPIPa neither did influence the cell cycle, nor did $CRL4^{Cdt2}$ mark it for degradation in S-Phase. Since any disturbing effects were shut down in this construct, possible degradation effects by Skp2 should have been easily visible. Yet, even in this case, Dacapo was not degraded by Skp2 overexpression. Instead, just as before, the only effect that Skp2 overexpression had was a stabilizing one. Skp2 knockdown on the other hand did lead to a stabilization of Dap dCDI dPIPa.

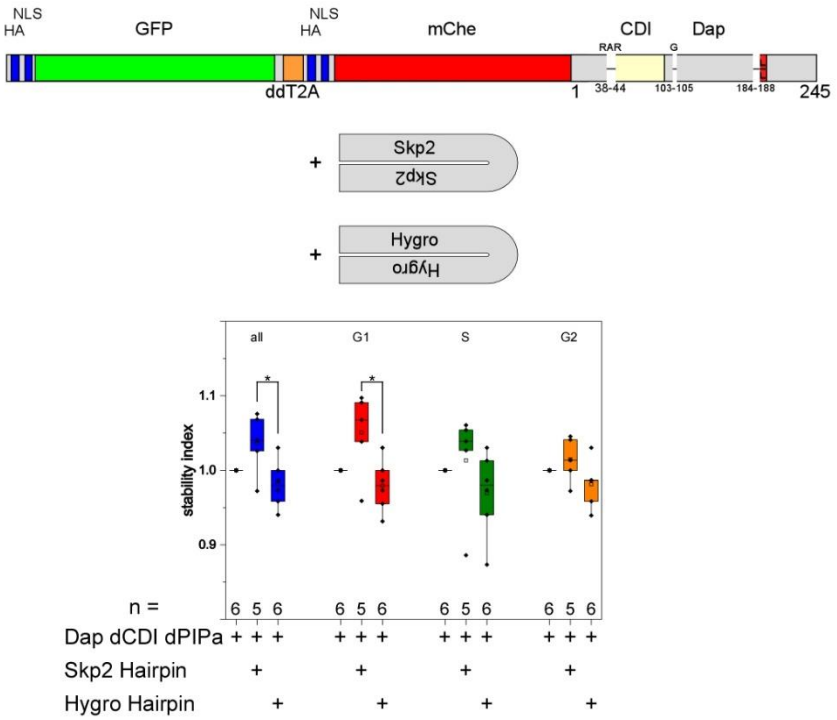

Figure 26 Stability of Dap dCDI dPIPa upon Skp2 knockdown
Measurement of Dap dCDI dPIPa stability with flow cytometry under Skp2 knockdown conditions. Skp2 knockdown significantly stabilizes Dap dCDI dPIPa in all and G1 cells in comparison to the control knockdown. * = $p < 0.05$, t-test for equal variances. Only significant changes are indicated.

5.3.6. Tests for biochemical interaction between Dacapo and Skp2 are ambiguous

According to the flow cytometric data, Skp2 was not responsible for Dacapo degradation. However, biochemical interaction between Skp2 and Dap has been reported previously (Dui et al., 2013). Biochemical interaction was therefore also analyzed. This was performed by co-immunoprecipitations. Tagged versions of both proteins were overexpressed in S2R+-cells. After 48 hours incubation, cells were lysed and one of the two proteins was precipitated with antibodies and agarose beads. Western Blot analysis showed if the precipitation was successful and if the other protein was co-immunoprecipitated.

Dui et al. (2013) showed that Skp2 FLAG interacted with 4xMyc Dap. This interaction is boosted if Cks85A is also overexpressed. It was tried to reproduce this result using differently tagged Skp2 constructs and HA-tagged Dap. Different combinations of tags, constructs and pull downs were tested. Figure 27 shows the used constructs. Full length Dacapo was either tagged with 4xFLAG or HA, Dap dCDI was tagged with 4xFLAG. Myc Dacapo, used in Dui et al, 2013, could not be used, since Myc antibody was not present in the lab. Skp2 was tagged either N-terminally with HA or 3xHA, or C-terminally with 4xFLAG. Cks85A was always used untagged. In all experiments, positive controls were always performed, but are not shown here for reasons of clarity.

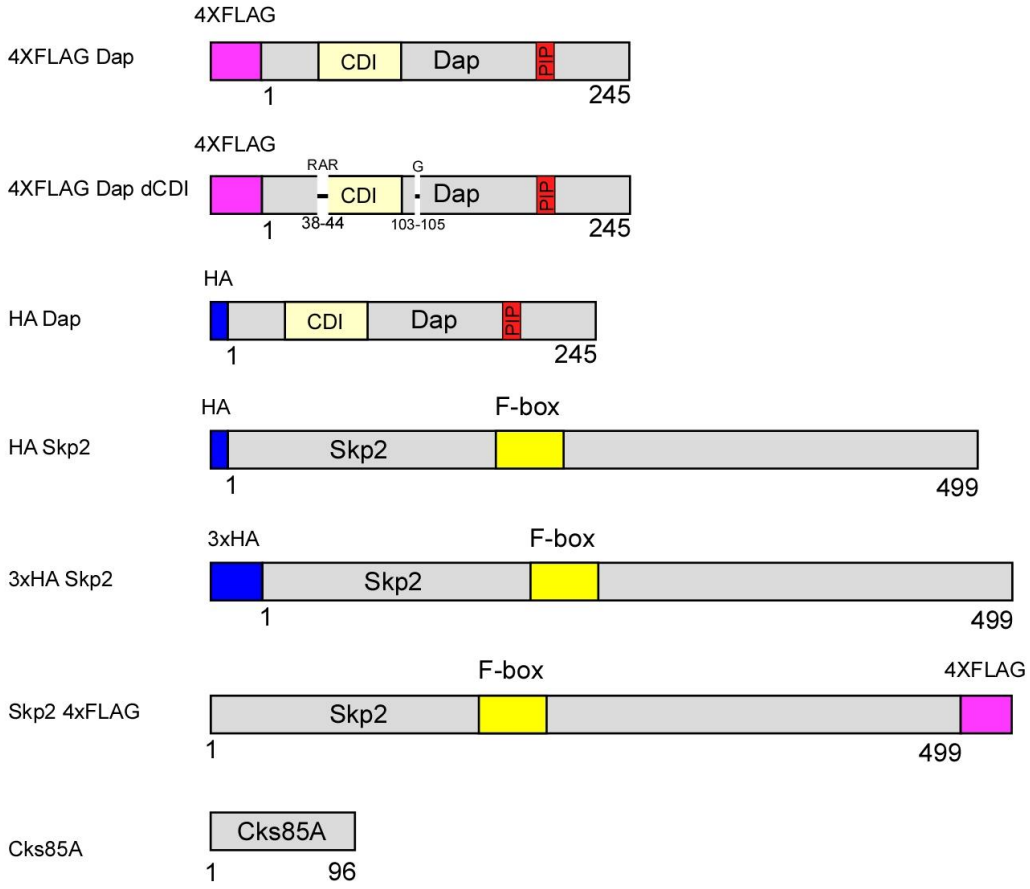

Figure 27 Different constructs used for Co-IP studies
Skp2, Dap and Cks85A constructs with various different immunotags used for Co-IP interaction studies.

In the beginning, it was tried to reproduce the experiment of Dui et al. (2013). Skp2 4xFLAG was pulled down by a FLAG antibody and HA Dap was detected by an HA antibody. Cks85A was also overexpressed for reproduction of the boosting effect. Skp2 4xFLAG was expressed and precipitation worked well (Figure 28, left side). Dacapo was also expressed, yet the detected amounts were low. The co-precipitation showed a smear of bands, especially in the negative control, where only HA-Dap was overexpressed. Luckily, though, it could be observed that HA-Dap was not binding unspecifically to the beads. Nonetheless, HA-Dap bands could not be detected when Skp2 4xFLAG was overexpressed. This was also not changed by overexpression of Cks85A that should actually boost the interaction between Skp2 and Dap (Figure 28, right side). According to this experiment, Skp2 and Dap did not interact with each other.

Since it was not possible to reproduce the biochemical interaction of Skp2 and Dap in this way, the experiment was modified. This time, the tags were switched, Skp2 was N-terminally tagged with 3xHA (3xHA Skp2) and the 4xFLAG tag was used on Dap (4xFLAG Dap). Since the FLAG antibody is stronger, the advantage was an enhanced signal intensity for the target protein. Furthermore, the HA-tag on Dap could prevent the interaction with Skp2. In this case, precipitation of Skp2 was performed with HA antibody.

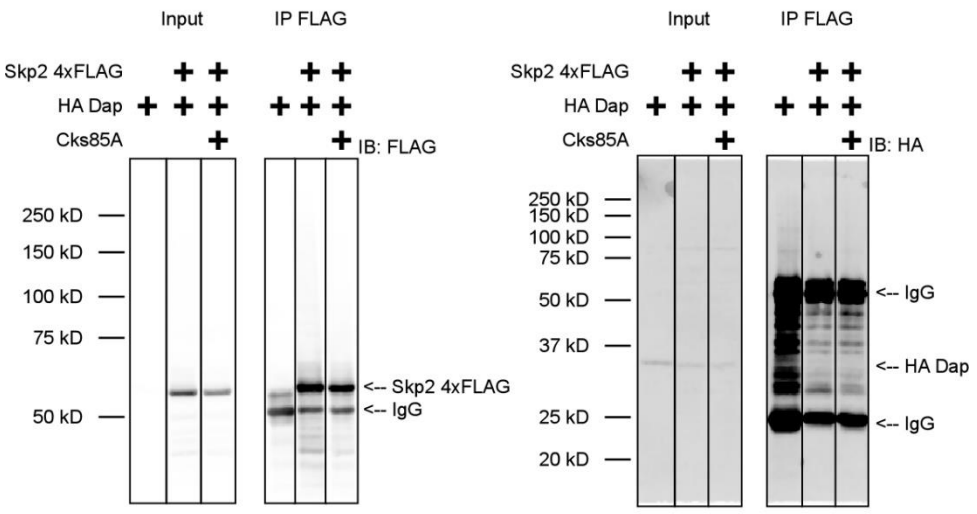

Figure 28 Co-IP between Skp2 4xFLAG and HA Dap
Co-Immunoprecipitation of Skp2 4xFLAG and HA Dacapo for testing of biochemical interaction. FLAG antibody was used for precipitation, FLAG or HA antibody for detection. Left: FLAG Blot for control of expression and precipitation of Skp2 4xFLAG. Right: HA Blot for expression and interaction test of HA Dap. Cks85A overexpression should strengthen the interaction. No biochemical interaction is detectable.

3xHA Skp2 was well expressed and precipitated (Figure 29, left). 4xFLAG Dacapo was also expressed well, in this case though, unspecific binding occurred in the negative control (Figure 29, right, first lane of the IP). Co-immunoprecipitation of 4xFLAG Dap with 3xHA Skp2 did not result in a band that was stronger than the background level, excluding interaction. Simultaneous overexpression of Cks85A did also not show a change in band intensity (Figure 29, right). Therefore, Skp2 and Dap were not interacting with each other, even with changed immuno-tags.

Finally, a different setup was tried. Instead of Skp2, Dap was precipitated and Skp2 was used as the target protein. Furthermore, besides full length Dacapo, Dap dCDI was also used. The Dap G1 stop may influence potential binding to Skp2, a factor that was turned off with Dap dCDI. Besides, Dap dCDI allowed to draw a conclusion if the potential interaction with Skp2 was direct or indirect (see 6.3).

4xFLAG Dap or 4xFLAG Dap dCDI was overexpressed together with HA Skp2. Precipitation was performed with FLAG-antibody. Expression of both Dap versions was relatively low. Yet, precipitation worked well (Figure 30, left). Skp2 expression was moderate and unfortunately HA Skp2 also bound unspecifically to the Protein G beads. However, the band intensity was stronger when Dap or Dap dCDI was also expressed (Figure 30, right), indicating biochemical interaction.

Together, these results indicated that Skp2 and Dap might have interacted with each other, but such an interaction was only seen in one experiment. In all other experiments, using differently tagged versions, no specific interaction was detected. Importantly, all tagged versions of Skp2 and Dap showed biological activity (data not shown). Overall, a specific interaction between Dap and Skp2 remained questionable.

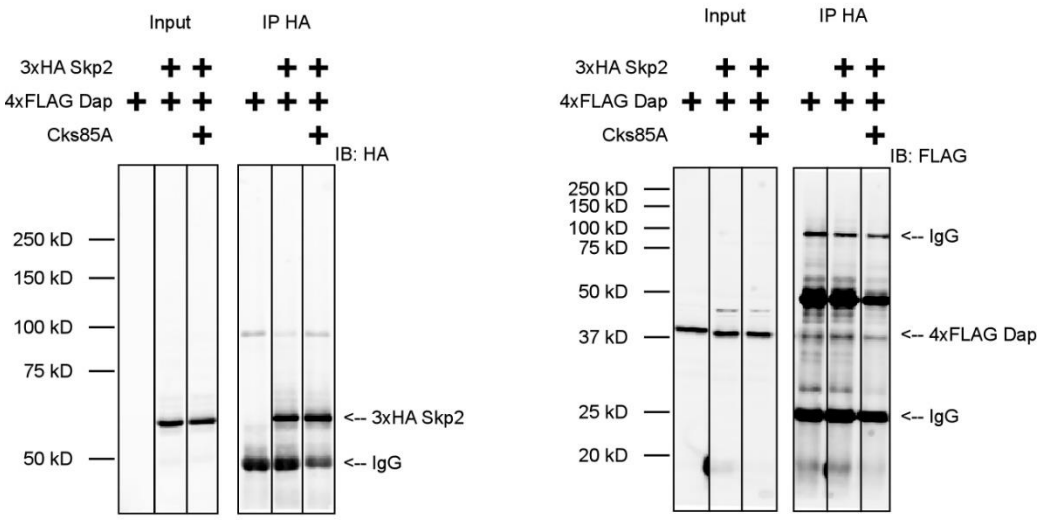

Figure 29 Co-IP between 3xHA Skp2 and 4xFLAG Dap

Co-Immunoprecipitation of 3xHA Skp2 and 4xFLAG Dacapo. HA antibody was used for precipitation, HA or FLAG antibody for detection. Left: HA Blot for control of expression and precipitation of 3xHA Skp2. Right: FLAG Blot for expression and interaction test of 4xFLAG Dap. 4xFLAG Dap shows unspecific binding to the Protein G beads. Cks85A overexpression should strengthen the interaction. No biochemical interaction is detectable.

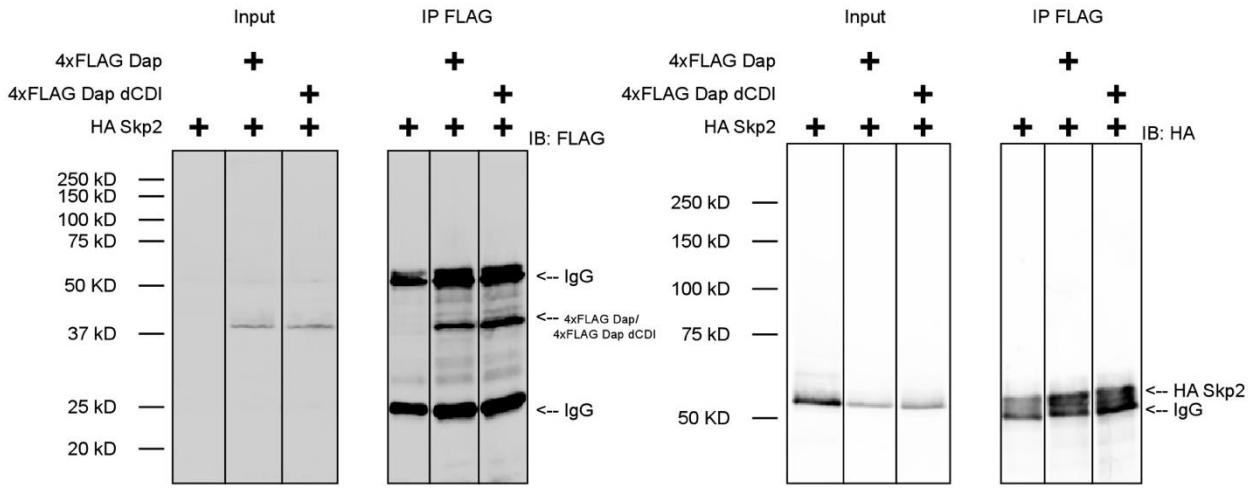

Figure 30 Co-IP between 4xFLAG Dap or 4xFLAG Dap dCDI and HA Skp2

Co-Immunoprecipitation of 4xFLAG Dap or 4xFLAG Dap dCDI and HA Skp2. FLAG antibody was used for precipitation, FLAG or HA antibody for detection. Left: FLAG Blot for control of expression and precipitation of both Dap constructs. Right: HA Blot for expression and interaction test of HA Skp2. HA Skp2 shows unspecific binding to the Protein G beads. Skp2 bands are stronger with simultaneous Dap or Dap dCDI overexpression, indicating biochemical interaction between Dap or Dap dCDI and Skp2.

5.3.7. Skp2 overexpression does not rescue, but enhance the Dap G1-stop

Besides flow cytometric protein stability determination and tests for biochemical interaction, it was also analyzed if Skp2 overexpression did influence the Dap phenotype in cells. Dacapo overexpression, under a strong promotor, did lead to a stop in G1-Phase (Figure 19B,C). Likewise, Skp2 overexpression resulted

in a slight shift to G1-Phase (Figure 11B,E). It was analyzed what effect both overexpressions had on the cell cycle. If Skp2 would play a role in the degradation of Dap, its overexpression should have resulted in reduced Dap levels and would thereby have diminished the G1-arrest phenotype caused by the overexpression of Dap.

Strong overexpression of Dacapo results in cells residing mostly in G1. Any effects that Skp2 may have, especially if they are not strong, may be masked by the Dap overexpression phenotype. Therefore, a situation was searched for, in which Dap levels are high enough to see a significant accumulation of cells in G1 without causing a complete G1-arrest. In order to achieve this situation, a GFP-tagged version of Dap was cloned into a vector with a shortened actin promoter, resulting in lower expression levels. 3xCherry served as the transfection control in this experiment, only cherry positive cells are shown.

Figure 31A shows the characteristic cell cycle distribution of S2R+-cells. Overexpression of Skp2 led to the already described effect of a weak cell accumulation in G1 (Figure 31B). As planned, Dap expression under the control of the short actin promoter did lead to an accumulation into G1, but only weakly (Figure 31C). Most importantly, combined overexpression did lead to even more cells in G1, a result that is not consistent with Skp2 downregulating Dap protein levels (Figure 31D). Figure 31E shows all four cell cycle distributions overlaid and normalized to their respective G1-peaks for oversight.

To conclude this chapter, Dacapo protein stability was not diminished upon Skp2 overexpression as measured by flow cytometric protein stability analysis. This held also true if components were overexpressed that should enhance the ability of Skp2 to recognize its substrate (CycE and Cks85A). Conversely, Skp2 seemed to have a stabilizing effect on the Dacapo protein in some cases. Skp2 dF-Box, a Skp2 version with a deleted F-Box, did also not exert a dominant-negative effect on Dap stability. Furthermore, usage of Skp2 knockdown did not alter Dap stability, with the exception of Dap dCDI dPIPa that was more stable in certain cell cycle phases if Skp2 was knocked down. Experiments were performed with different Dap versions that should diminish any disturbing effects of Dap (either cell cycle effects or alternate degradation pathways). Yet, overall the results stayed the same, regardless of the used Dap construct. Biochemical interaction was not easy to determine and a reproduction of the literature turned out impossible. Finally, Skp2 did not reduce an intermediate Dap overexpression phenotype in Schneider cells but actually enhanced it.

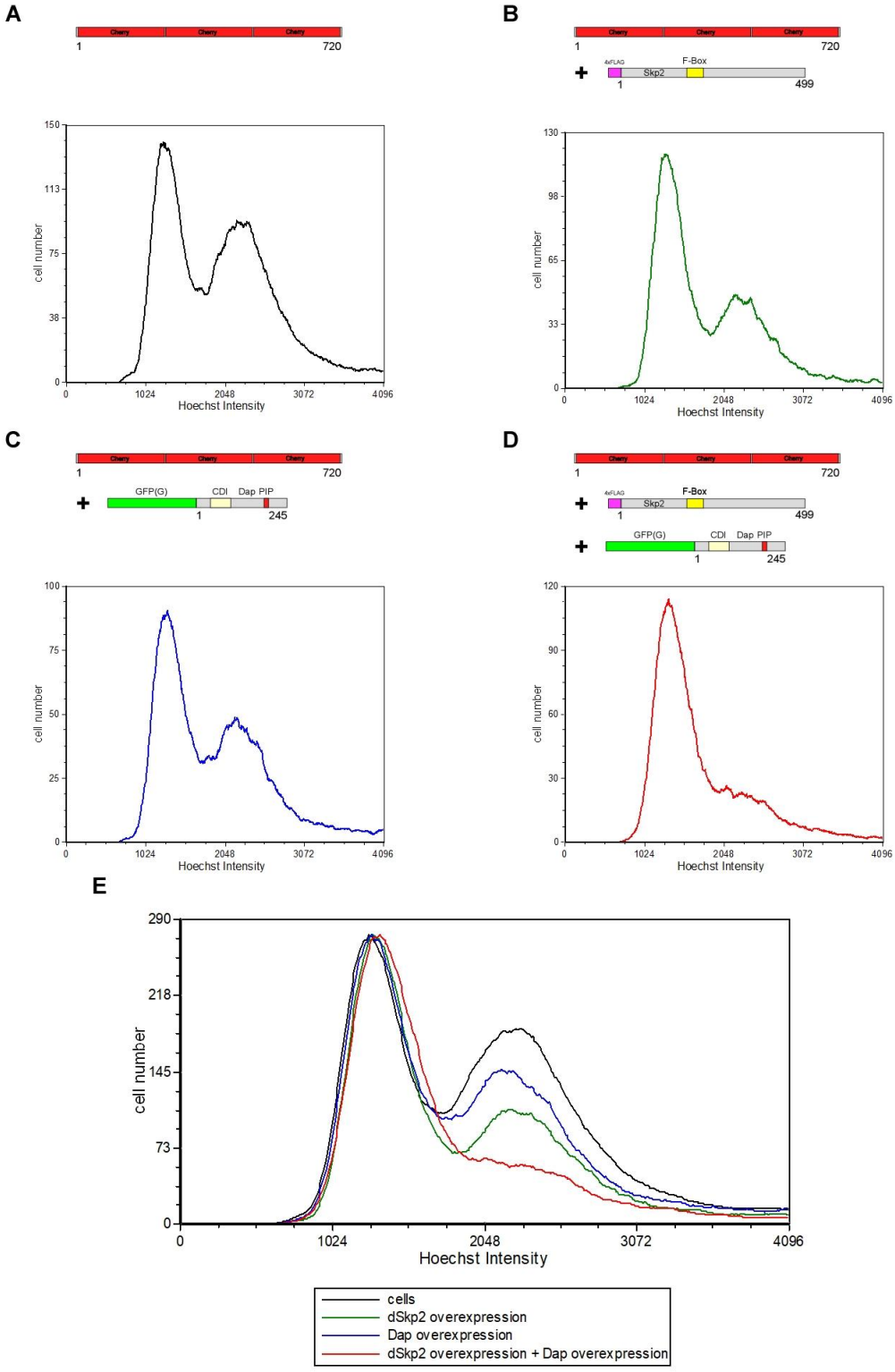

Figure 31 Skp2 does not rescue the Dap phenotype

Cell cycle distributions of Skp2 and/or Dap overexpression. 3xChe serves as the transfection control, only Cherry cells are shown (A) Cell cycle profile of 3xCherry positive cells. (B) Skp2 overexpression leads to a shift in G1-Phase. (C) Dap overexpression leads to a shift in G1-Phase. This construct was specifically created to cause a weaker Dap phenotype. (D) Skp2 and Dap overexpression does not lead to a rescue but rather to a stronger G1-shift. (E) Overlay of all cell cycle distributions. Histograms are normalized to the G1-peak. All presented cell cycle distributions are representative.

5.4. Cdt1 stability is regulated by SCF^{Skp2} depending on its phosphorylation

5.4.1. Overview

The experiments so far have not provided a biologically relevant substrate of the SCF^{Skp2} ubiquitin ligase. The aim of this thesis was to understand the phenotype of Skp2 in Schneider cells and to identify relevant substrates of SCF^{Skp2}. Cdt1 was one of the most promising candidates: it is a substrate of the human SCF^{Skp2} complex (Heo et al., 2016) and its role in DNA replication seemed in agreement with the observed phenotypes of Skp2.

Cdt1 has a homologue in *D. melanogaster*, the gene *double parked* or Dup. Dup is conserved in flies and fulfills the same molecular function in directing the MCM-complex to the origins of replications (Whittaker et al., 2000). Just like its human homologue, Dup has a Geminin-binding and an MCM-binding domain. Geminin binds and inhibits Dup, thereby regulating its function. The MCM-binding domain is responsible for transporting the MCM helicase to the origin of replications. Finally, Dup also possesses a PIP-degron that is responsible for degradation in S-Phase by $CRL4^{Cdt2}$, just like Dacapo. Since Dup had extensive influence on the cell cycle and was degraded in S-Phase, a version was created that minimized the effects on the cell cycle and was not degraded by $CRL4^{Cdt2}$. This was necessary to diminish the disturbances on the cycle by Dup overexpression and to concentrate only on the effects that Skp2 may had in degradation, an approach identical to the Dap experiments.

To prevent confusion between Dup (double-parked) and Dap (Dacapo), from now on only Cdt1 will be used in the text for the Dup protein if not explicitly mentioned otherwise.

Cdt1 protein stability was analyzed by flow cytometry in dependence of Skp2, Skp2 dF-Box and CycE overexpression or Skp2 knockdown respectively. This analysis indicated that Cdt1, if phosphorylated, was indeed a substrate of SCF^{Skp2}. In a next step, it was tried to map the important phosphorylation sites responsible for Cdt1-Skp2 binding. This was done by truncation of the protein and site directed mutation of conserved phospho-sites. Furthermore, biochemical interaction between Skp2 and Cdt1 was analyzed by Co-IP studies and finally the phenotypic effects on the cell cycle of Cdt1 and Skp2 overexpression and knockdown was examined.

5.4.2. Cell cycle effects of different Cdt1 versions

Cdt1 overexpression had a strong effect on the cell cycle of Schneider cells. Overexpressing full length Cdt1 led to overreplicating cells in comparison to the cell cycle of the control construct (Figure 32A and B, note the cell distribution after fluorescence unit 2024 on the x-axis). Interestingly, deletion of the N-terminal PIP-degron (created by truncating the first 15 amino acids) changed the phenotype. In this case, a G2-peak was no longer visible but only one single peak. The maximum of this peak was shifted to the right in comparison to the control, indicating an elevated number of S-Phase cells, therefore this population probably consisted of very late G1-/early S-Phase cells (Figure 32C). Figure 32D shows the overlay of all three cell cycle distributions, normalized to the G1-peak.

Just like in the case of Dap, it was advantageous to work with a Cdt1 version with a diminished influence on the cell cycle. Otherwise, any seen effects might be the result of the abnormal cell cycle phases and not of Skp2. Therefore, the last 143 amino acids, comprising the MCM-binding domain, were deleted, resulting in the construct Cdt1 15-600. Since this construct was no longer able to recruit MCM to the ORCs, the phenotypic effect of the overexpression should be turned off.

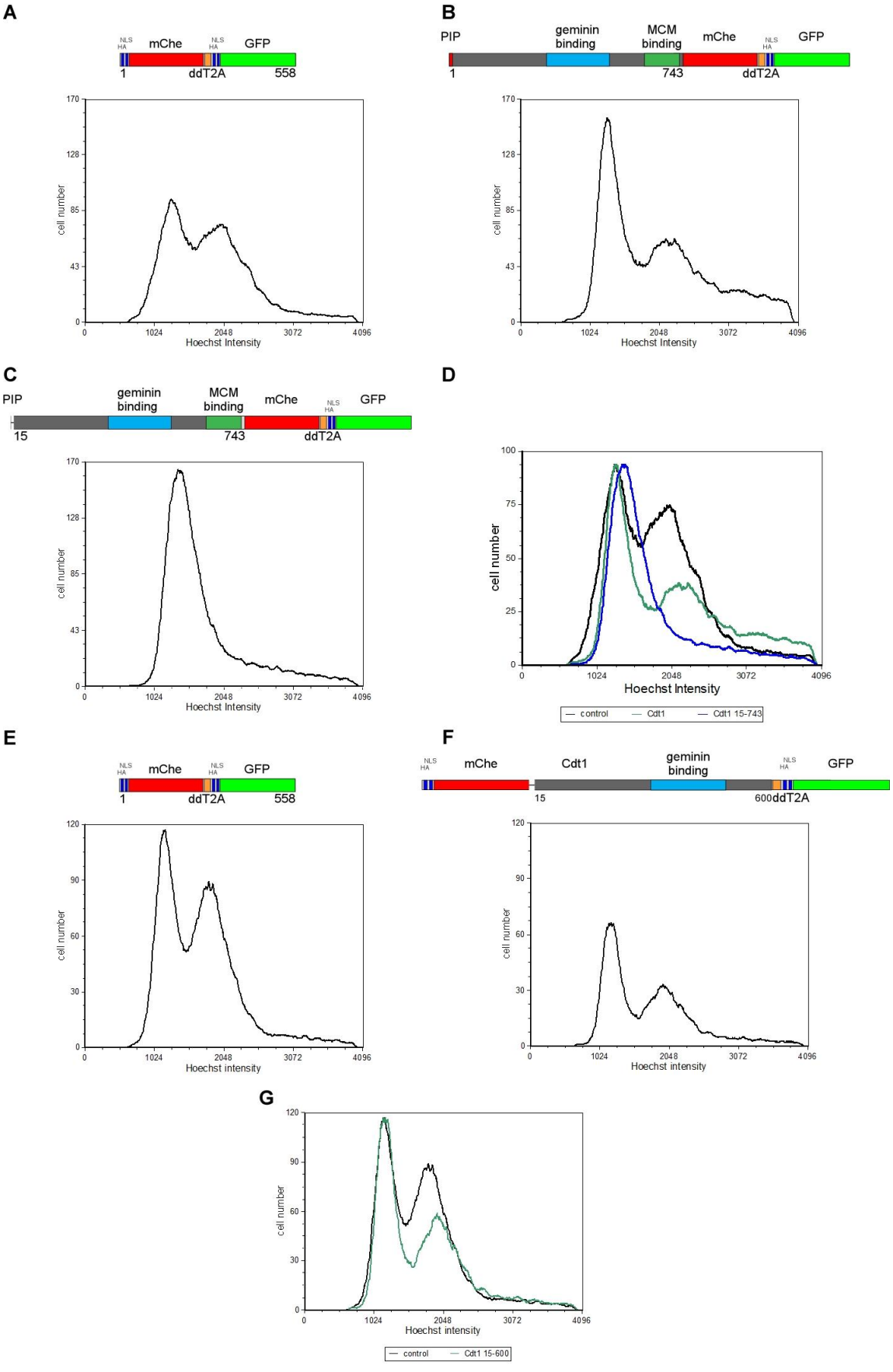
A
NLS HA
mChe
NLS HA
GFP
1
ddT2A
558
cell number
Hoechst Intensity
B
PIP
geminin binding
MCM binding
mChe
NLS HA
GFP
1
743
ddT2A
C
PIP
geminin binding
MCM binding
mChe
NLS HA
GFP
15
743
ddT2A
D
cell number
Hoechst Intensity
control
Cdt1
Cdt1 15-743
E
NLS HA
mChe
NLS HA
GFP
1
ddT2A
558
cell number
Hoechst intensity
F
NLS HA
mChe
Cdt1
geminin binding
NLS HA
GFP
15
600ddT2A
cell number
Hoechst intensity
G
cell number
Hoechst intensity
control
Cdt1 15-600

Figure 32 Cell cycle effects of different Cdt1 versions
Cell cycle distribution of cells transfected with different Cdt1 versions. GFP serves as the transfection control, only GFP positive cells are shown. (A,E) Cell cycle distribution of the control T2A construct. (B) Overexpression of Cdt1 full length leads to overreplicating cells. (C) Overexpression of Cdt1 15-763 (lacking the N-terminal PIP-degron) leads to accumulation of cells in very late G1-/S-Phase. (D) Overlay of cell cycle curves of control, Cdt1 full length and Cdt1 15-763 overexpression. (F) Overexpression of Cdt1 15-600 (lacking the C-terminal MCM-binding domain) leads to an accumulation of cells in G1. (G) Overlay of the cell cycle of control and Cdt1 15-600. Overlays are normalized to the G1-peak. All presented cell cycle distributions are representative.

Cdt1 15-600 did not show the overreplication of cells compared to Cdt1 full length. However, overexpression of Cdt1 15-600 resulted in a slight accumulation of cells in G1 in comparison to the control (Figure 32E, F and G). Nonetheless, since the cell cycle effects were modest, this construct was the starting point of Cdt1 flow cytometric protein stability analysis.

5.4.3. GFP Cdt1 1-600 is destabilized by Skp2

In order to analyze if Skp2 destabilized Cdt1, the relative stability of GFP Cdt1 1-600 was analyzed by flow cytometry. This construct still contained the PIP-degron, in theory resulting typically in S-Phase degradation. This degradation pathway may have covered any effect that Skp2 may had on Cdt1 stability. However, since the PIP-degron is positioned right at the beginning of the N-terminus, any major N-terminal tag (in this case HA-NLS-GFP) is disturbing the function of the PIP-degron (Senga et al., 2006); S-Phase degradation was probably not working.

The analysis of relative protein stability experiments was already described in the Dacapo section (see 5.3.3). The four distinct conditions (all, G1-Phase, S-Phase, and G2-Phase) were again analyzed. Expression levels of the reference protein between logarithmic fluorescence units 2.00 – 2.75 were used. Data was normalized to the stability of Cdt1 1-600. Influence of the overexpressed components on GFP and mCherry was checked in all cases, yet no influence could be detected.

GFP Cdt1 1-600 showed the same G1 shift of cells as mChe Cdt1 15-600 (Figure 33A,B,C). GFP Cdt1 1-600 stability was reduced upon Skp2 overexpression in all, G1 and G2 cells (Figure 33D, one sample t-test, $p < 0.01$), but not in S-Phase (one sample t-test, $p > 0.05$). However, the Cdt1 version seemed to be indifferent to CycE overexpression, protein stability remained stable in all cases (one sample t-test, $p > 0.05$). Combined overexpression of Skp2 and CycE did also lead to decreased protein stability of all and G1 cells (one sample t-test, $p < 0.01$); however, the effect was not increased in comparison to Skp2 overexpression alone. Furthermore, in this case Cdt1 instability was visible even in S cells (one sample t-test, $p < 0.01$). In G2 cells however, no significant effect was seen upon coexpression of Skp2 and CycE (one sample t-test, $p > 0.05$).

It was also analyzed what effect a Skp2 knockdown on the GFP Cdt1 1-600 stability had. In comparison to the control knockdown with the Hygro Hairpin construct, the Skp2 Hairpin construct led to a statistically significant stabilization of Cdt1 in all, G1- and S-Phase cells (Figure 34, t-test for unequal variances, $p < 0.01$ or $p < 0.05$) but not in G2 cells (t-test for unequal variances, $p > 0.05$).

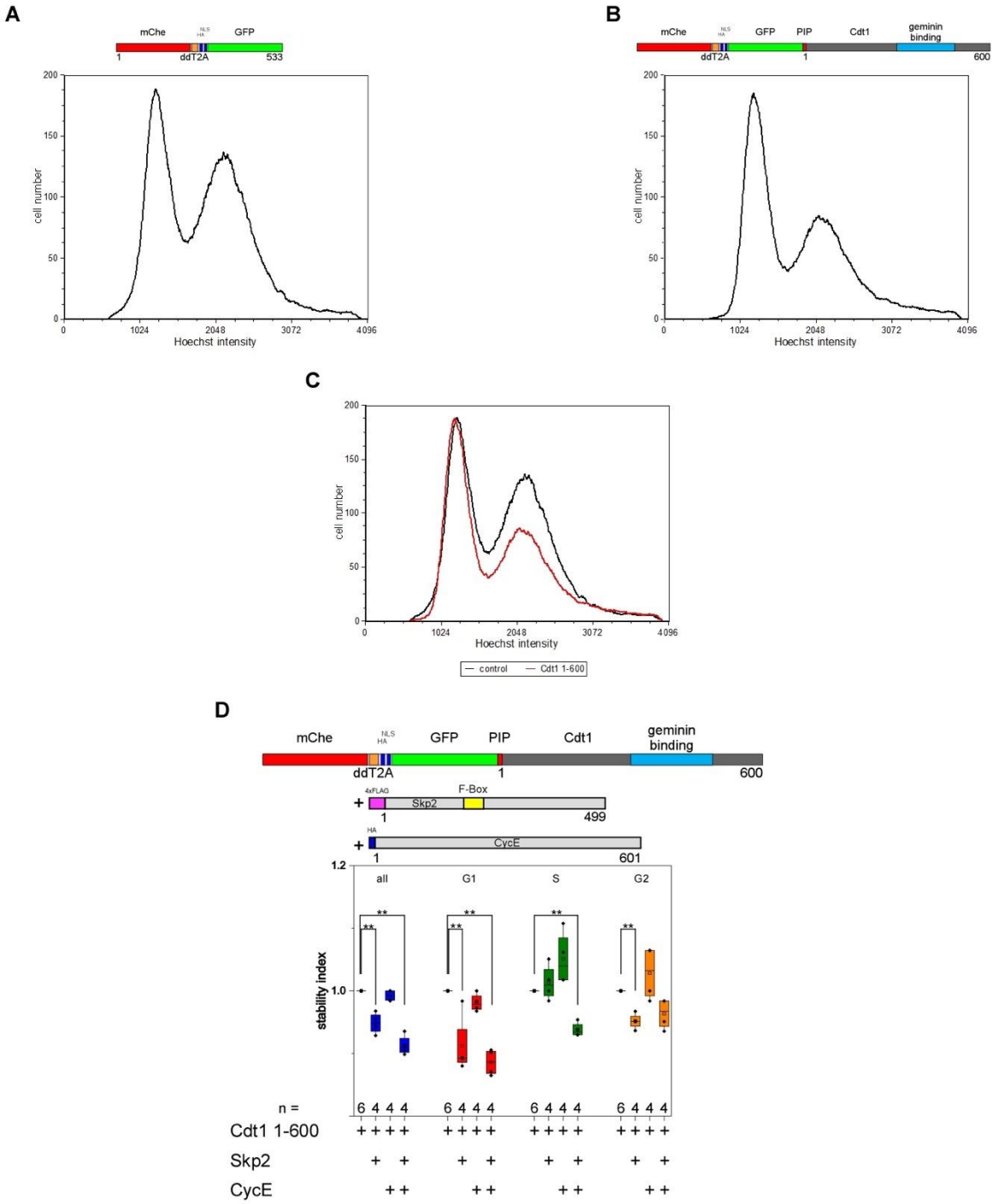

Figure 33 Cell cycle effects and stability of GFP Cdt1 1-600

Cell cycle distribution and stability data of GFP Cdt1 1-600. (A) Cell cycle of the control vector. (B) GFP Cdt1 1-600 shows cell accumulation in G1. (C) Overlay of control and GFP Cdt1 1-600 overexpression. Overlay is normalized to the G1-peak. In all cases, only mCherry positive cells are shown. All presented cell cycle distributions are representative. (D) Skp2 overexpression destabilizes Cdt1 1-600 in all, G1 and G2. CycE overexpression alone does not influence the stability. Combined overexpression leads to instability in all, G1 and S but not in G2. However, CycE does not enhance the Skp2 degradation in all and G1. ** = $p < 0.01$, one sample t-test. Only significant changes are indicated.

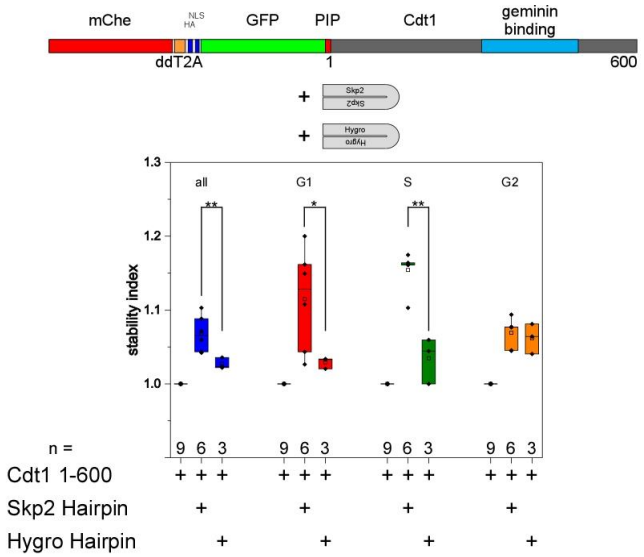

Figure 34 GFP Cdt1 1-600 stability with Skp2 knockdown

Protein stability analysis of GFP Cdt1 1-600 under Skp2 knockdown conditions. Skp2 knockdown significantly destabilizesGFP Cdt1 1-600 in all, G1 and S if compared to the control knockdown. * = $p < 0.05$, ** = $p < 0.01$, t-test for unequal variances. Only significant changes are indicated.

5.4.4. Che Cdt1 15-600 is destabilized by Skp2 in dependency of CycE dependent kinase activity

The results of GFP Cdt1 1-600 indicated that it was indeed a substrate of SCF^{Skp2}: Skp2 overexpression led to destabilization, Skp2 knockdown to stabilization. It has to be considered though that the GFP tag is not optimal for these analysis since the Hoechst signal, used for determination of the single cell cycle phases (see 4.2.6.5), partly emits light into the GFP fluorescence channel. This weakens the explanatory power of this assay. In addition, GPF Cdt1 1-600 still contained the PIP-sequences, even though the PIP degron was likely inactivated by the GFP fusion. To overcome these issues, Cdt1 was tagged N-terminally with mChe and the PIP degron sequence was deleted, resulting in the mCHE Cdt1 15-600 construct.

All subsequent experiments were performed with N-terminally mChe tagged Cdt1 versions. Surprisingly, two effects emerged that complicated the analysis and interpretation of the data. First, in few cases, control experiments showed that the stability of the control proteins GFP and mChe alone were slightly influenced by overexpression of Skp2, Skp2 dF-Box and CycE. In these cases, the controls are also shown to document this effect (the same approach as in Figure 20B). Second and more surprising, it turned out that the observed effects varied in dependency of the expression level used for analysis. Routinely, all data was analyzed with two expression level ranges of the reference fluorescence protein, a higher range between 2.00 – 2.75 and a lower range between 1.25 – 2.00 logarithmic fluorescent units. In all previous shown data, the results between these two expression ranges were similar; however, the spread of the data was much lower in case of the higher level, which is the reason that exclusively this was shown. Since results differed strongly according to the expression level ranges in case of the mChe Cdt1 constructs, it was considered necessary to present the results of both expression levels. Hence, the subsequent figures show the protein stability of both levels as indicated.

First, the stability of mChe Cdt1 15-600 was analyzed upon Skp2 and Skp2 dF-Box overexpression. In case of the expression level 1.25 – 2.00, controls showed significant stabilization of mChe in G1- and S-Phase upon Skp2 dF-Box overexpression (Figure 35A, one-sample t-test, $p < 0.05$). Skp2 overexpression did lead to a significant destabilization of mChe Cdt1 15-600 in G1- and G2-Phase (Figure 35B, one-sample t-test, $p < 0.01$), but to stabilization in S (one-sample t-test, $p < 0.05$). Skp2 dF-Box led to stabilized Cdt1 in all and S-Phase cells (one-sample t-test, $p < 0.01$).

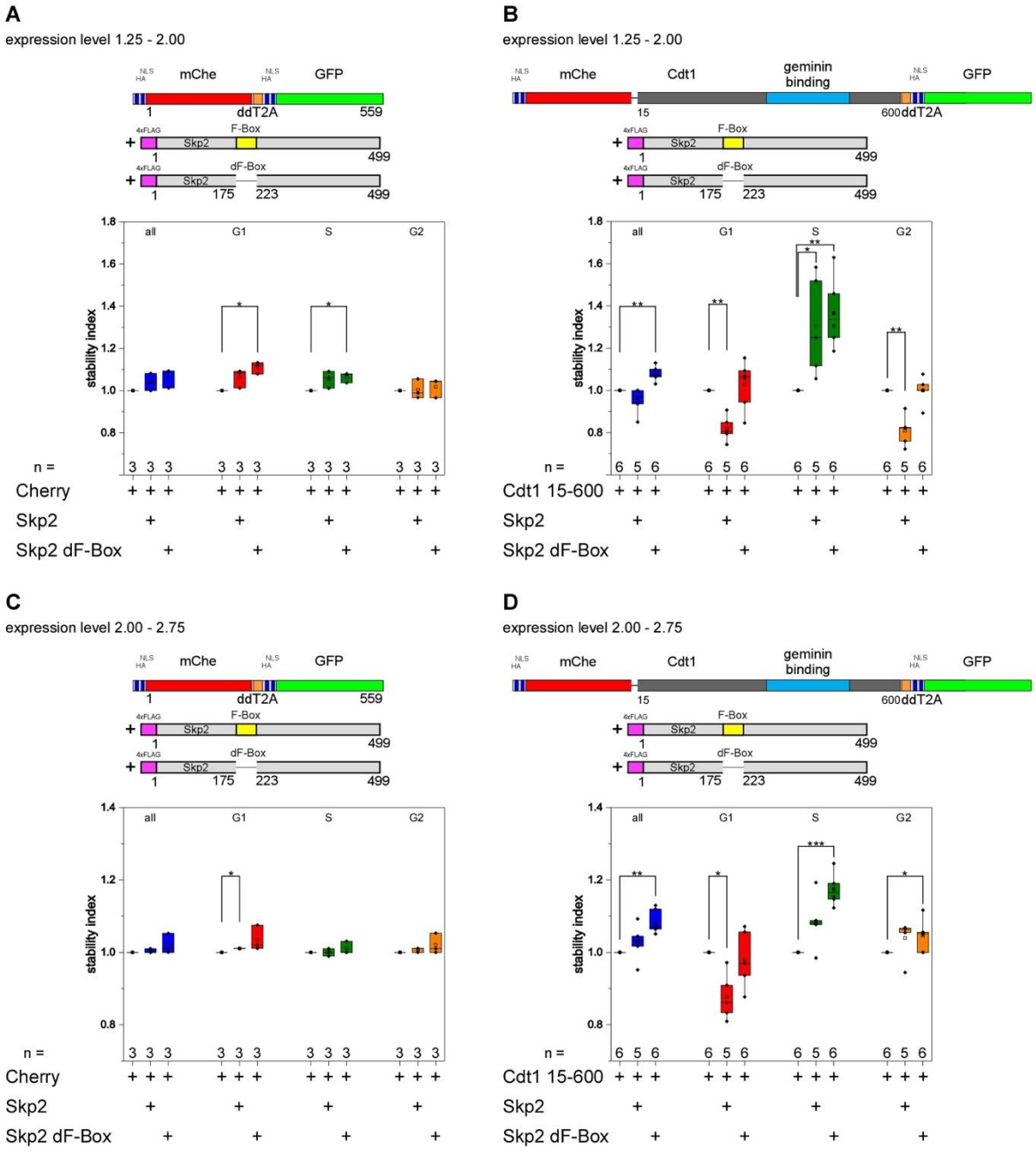

Figure 35 mChe Cdt1 15-600 stability with overexpression of Skp2 and Skp2 dF-Box

Flow cytometric protein stability analysis of mChe Cdt1 15-600 upon overexpression of Skp2 or Skp2 dF-Box. Expression level 1.25 – 2.00: (A) Skp2 dF-Box stabilizes mChe in G1 and S. (B) mChe Cdt1 15-600 is destabilized by Skp2 in G1 and G2 and stabilized in S, Skp2 dF-Box stabilizes Cdt1 15-600 in all and S. Expression level 2.00 – 2.75: (C) Skp2 stabilizes mChe in G1. (D) mChe Cdt1 15-

600 is destabilized in G1 upon Skp2 overexpression. Skp2 dF-Box leads to stabilization in all, S and G2 cells. * = $p < 0.05$, ** = $p < 0.01$, *** = $p < 0.001$, one sample t-test. Only significant changes are indicated.

The expression range 2.00 – 2.75 showed a significant stabilization of mChe protein upon Skp2 overexpression in G1 (Figure 35C, one-sample t-test, $p < 0.05$). Under these conditions, Cdt1 15-600 showed a significant destabilization only in G1-Phase if Skp2 was overexpressed (Figure 35D, one-sample t-test, $p < 0.05$). Skp2 dF-Box overexpression led to a stabilization in all, S and G2 cells (one-sample t-test, $p < 0.01$, $p < 0.001$ and $p < 0.05$).

Next, the stability in dependency of CycE dependent kinase activity was tested by overexpressing CycE. All data was normalized to the stability of mChe Cdt1 15-600 plus CycE overexpression for experimental reasons. In this case, control fluorescent proteins were not influenced by any overexpressed components (data not shown). With the expression range of 1.25 – 2.00, Skp2 overexpression did lead to a statistically significant decline of mChe Cdt1 15-600 stability in all distinct cases (Figure 36, one-sample t-test, $p < 0.001$). Expression of Skp2 dF-Box led conversely to a significant stabilization in all, G1 and S (one-sample t-test, $p < 0.05$), but not in G2 cells (one-sample t-test, $p > 0.05$).

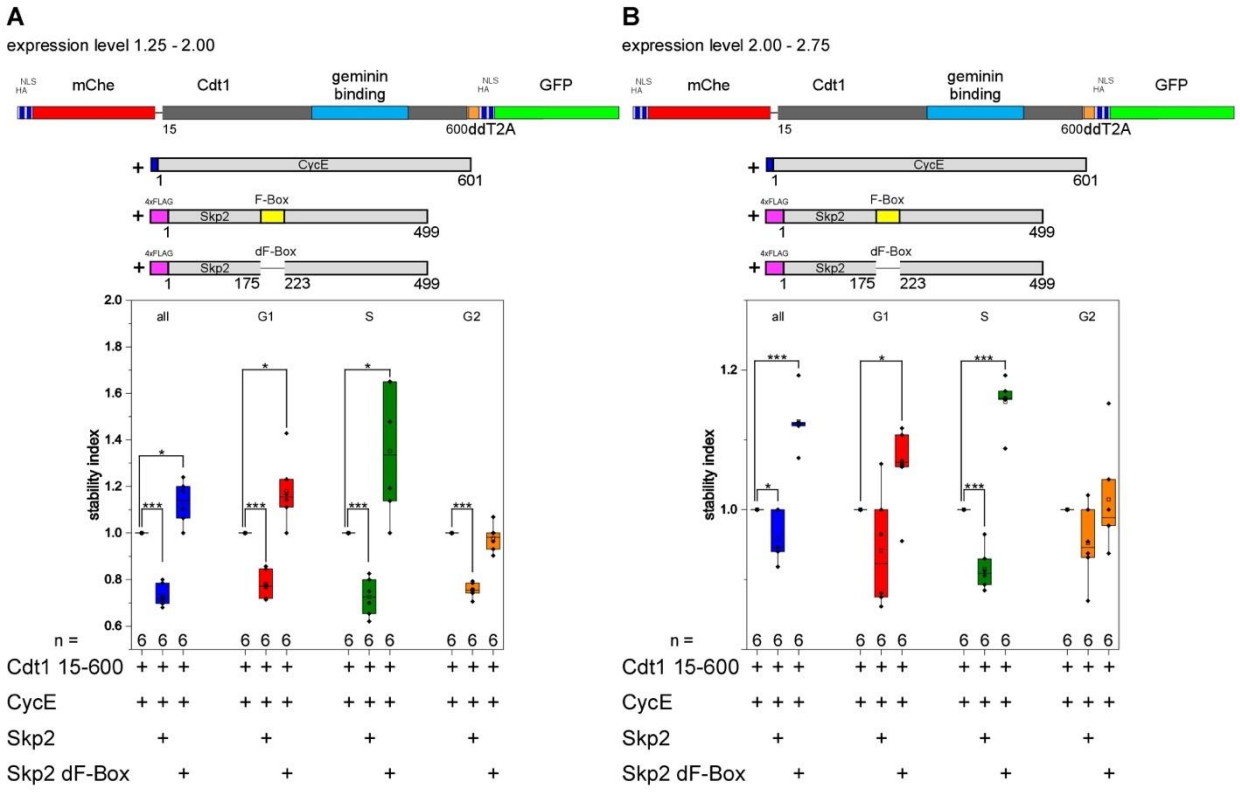

Figure 36 mChe Cdt1 15-600 stability upon overexpression of Skp2 or Skp2 dF-Box and CycE
Flow cytometric protein stability analysis of mChe Cdt1 15-600 upon overexpression of Skp2 or Skp2 dF-Box with CycE. (A) Expression level 1.25 – 2.00. Skp2 destabilizes mChe Cdt1 15-600, Skp2 dF-Box stabilizes Cdt1, excluding G2-Phase. (B) Expression level 2.00 – 2.75. Skp2 destabilizes mChe Cdt1 15-600 in all and S cells, Skp2 dF-Box stabilizes Cdt1, excluding G2-Phase. * = $p < 0.05$, *** = $p < 0.001$, one sample t-test. Only significant changes are indicated.

Analysis with the expression level 2.00 – 2.75 showed destabilization of mChe Cdt1 15-600 in all and in S-Phase under Skp2 overexpression (Figure 36B, one-sample t-test, $p < 0.05$ and $p < 0.001$). Just like before, Skp2 dF-Box stabilized mCdt1 15-600 in all, G1 and S (one-sample t-test, $p < 0.001$ and $p < 0.05$). CycE overexpression seemed to strengthen the effect that Skp2 had on Cdt1 15-600 stability.

Finally, the effect of Skp2 knockdown on mChe Cdt1 15-600 stability was analyzed. Analysis of the lower expression range showed a statistically significant stabilization of mChe Cdt1 15-600 upon Skp2 knockdown in comparison to the control (Figure 37A, t-test for unequal variances, $p < 0.001$). Likewise, if expression level 2.00 – 2.75 was analyzed, Skp2 hairpin showed stabilization of Cdt1 15-600 in all, S- and G2-Phase (Figure 37B, t-test for unequal variances, $p < 0.01$).

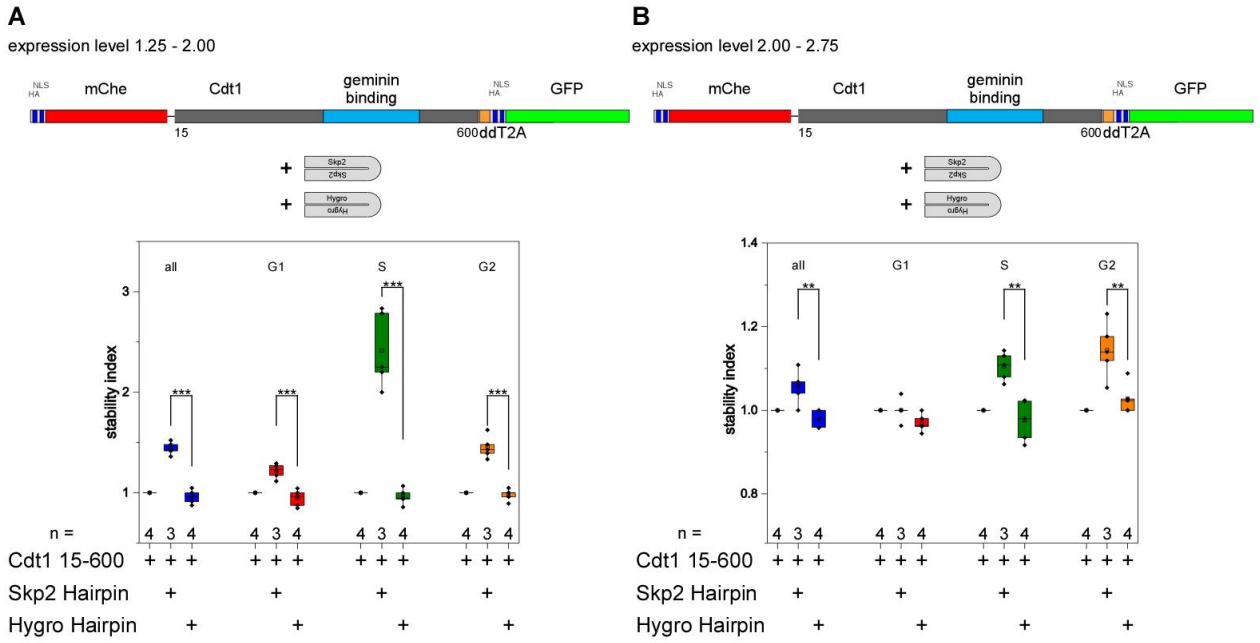

Figure 37 mChe Cdt1 15-600 stability upon Skp2 knockdown
Flow cytometric protein stability analysis of mChe Cdt1 15-600 upon Skp2 knockdown. (A) Analysis with expression level 1.25 – 2.00. Skp2 knockdown stabilizes Cdt1 15-600 in comparison to the control. (B) Analysis with expression level 2.00 – 2.75. Skp2 knockdown does also stabilize Cdt1 15-600 in this case. ** = $p < 0.01$, *** = $p < 0.001$, t-test for unequal variances. Only significant changes are indicated.

As a conclusion, Cdt1 stability seemed to be dependent upon Skp2 levels. Skp2 overexpression destabilized Cdt1, Skp2 dF-Box expression stabilized and protected Cdt1 from instability, CycE overexpression enhanced these effects and a Skp2 knockdown did lead to protein stabilization, all in concordance with Skp2 marking Cdt1 for degradation. The fact that CycE was necessary for an enhanced destabilization effect indicated that phosphorylation was important for Skp2 mediated degradation. In the following sections, different Cdt1 truncations and mutations were tested with the aim to localize phosphorylation sites important for Skp2 recognition.

5.4.5. Skp2 mediated Cdt1 degradation is independent of Geminin binding

In a straightforward approach for the identification of the phospho-sites, truncations of Cdt1 were created to confine the important regions for degradation by Skp2. The first tested truncation was Cdt1 15-300,

which did not contain the Geminin binding site any longer. As a side effect, it was also possible to analyze if Geminin binding influenced the degradation with this construct.

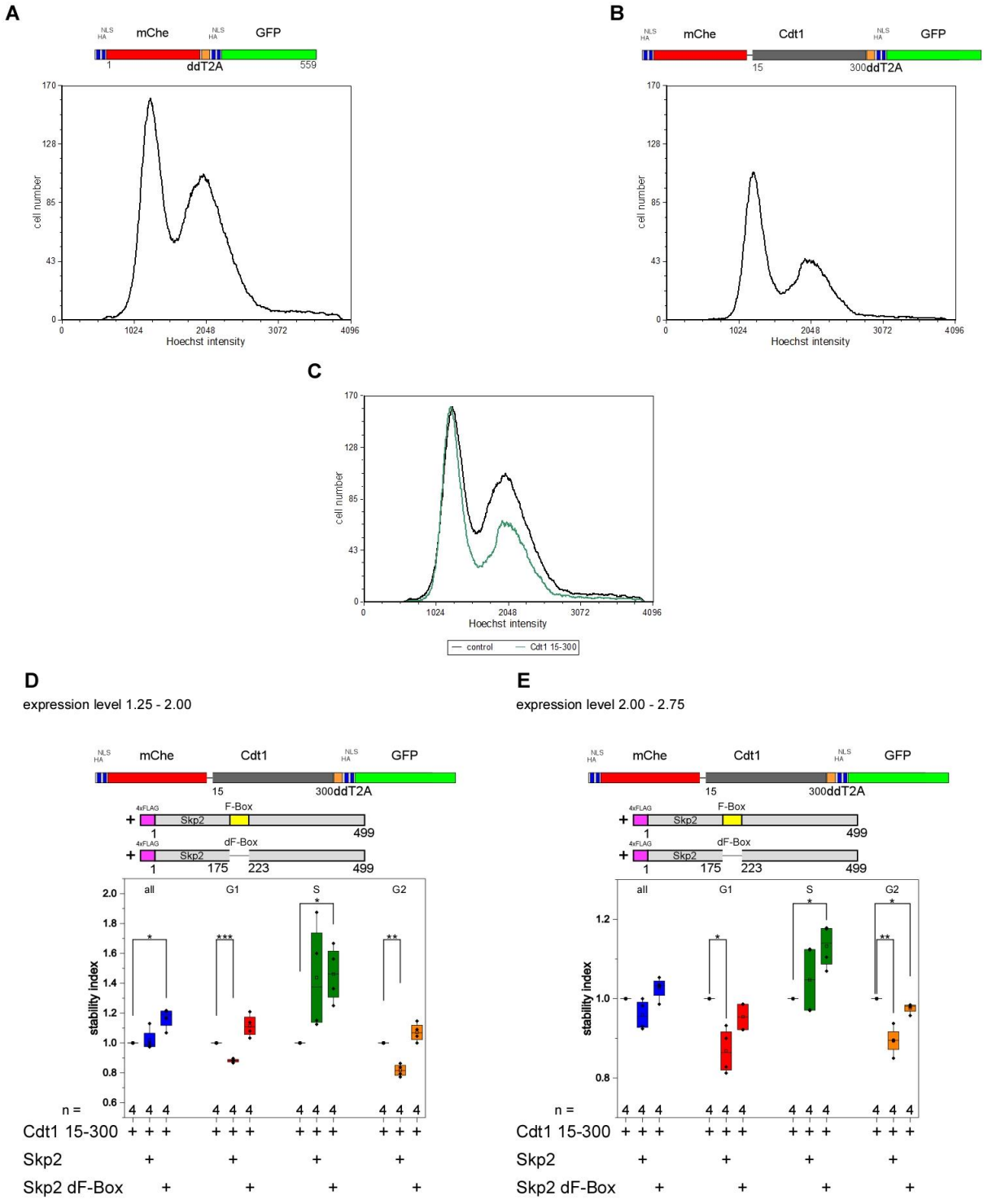

Figure 38 Cdt1 15-300 cell cycle effects and stability upon overexpression of Skp2 or Skp2 dF-Box

Cell cycle distribution and stability data of mChe Cdt1 15-300. (A) Cell cycle of the control vector. (B) Cdt1 15-300 shows accumulation of cells in G1. (C) Overlay of control and Cdt1 15-300 overexpression. Overlay is normalized to the G1-peak. In all cases, only GFP positive cells are shown. All presented cell cycle distributions are representative. (D) Expression level 1.25 – 2.00. Skp2 destabilizes Cdt1 15-300 in G1 and G2. Skp2 dF-Box expression leads to stabilization in all and S-Phase cells. (E) Expression

level 2.00 – 2.75. Skp2 destabilizes Cdt1 15-300 in G1 and G2. Skp2 dF-Box expression leads to stabilization in S-Phase and destabilization in G2-Phase. * = p < 0.05, ** = p < 0.01, *** = p < 0.001, one sample t-test. Only significant changes are indicated.

mChe Cdt1 15-300 showed a similar cell cycle effect than Cdt1 15-600, a shift into the G1-Phase (Figure 38A,B,C). By using expression level 1.25 – 2.00, Skp2 overexpression, destabilized Cdt1 15-300 only in G1 and G2-Phase (Figure 38D, one-sample t-test, $p < 0.001$ and $p < 0.01$), but not in all and S-Phase cells (one-sample t-test, $p > 0.05$). Skp2 dF-Box expression led to stabilization only in all and S-Phase cells (one-sample t-test, $p < 0.05$). Analysis of the higher range showed also a decrease in protein stability of Cdt1 15-300 in G1 and G2-Phase if Skp2 was overexpressed (Figure 38E, one-sample t-test, $p < 0.05$ and $p < 0.01$). Expression of Skp2 dF-Box on the other hand led to stabilization of Cdt1 15-300 in S-Phase (one-sample t-test, $p < 0.05$) and destabilization in G2-Phase (one-sample t-test, $p < 0.05$).

As it was the case with Cdt1 15-600, CycE overexpression did also strengthen the effects of Skp2 or Skp2 dF-Box respectively. With expression level 1.25 – 2.00, Cdt1 15-300 stability was statistically significant decreased upon Skp2 overexpression in all four distinct cases if CycE was simultaneously overexpressed (Figure 39A, one-sample t-test, $p < 0.01$ and $p < 0.05$). Cdt1 was stabilized in all, G1 and S if Skp2 dF-Box was used (one-sample t-test, $p < 0.01$ and $p < 0.05$), but there was no change in G2-Phase (one-sample t-test, $p > 0.05$). Using the higher expression level for analysis, Skp2 overexpression did result in reduced Cdt1 15-300 stability only in all, S and G2 cells (Figure 39B, one-sample t-test, $p < 0.05$ and $p < 0.01$), but not in G1-Phase Phase (one-sample t-test, $p > 0.05$). Skp2 dF-Box expression led to stabilization in all, S and G2 (one-sample t-test, $p < 0.01$).

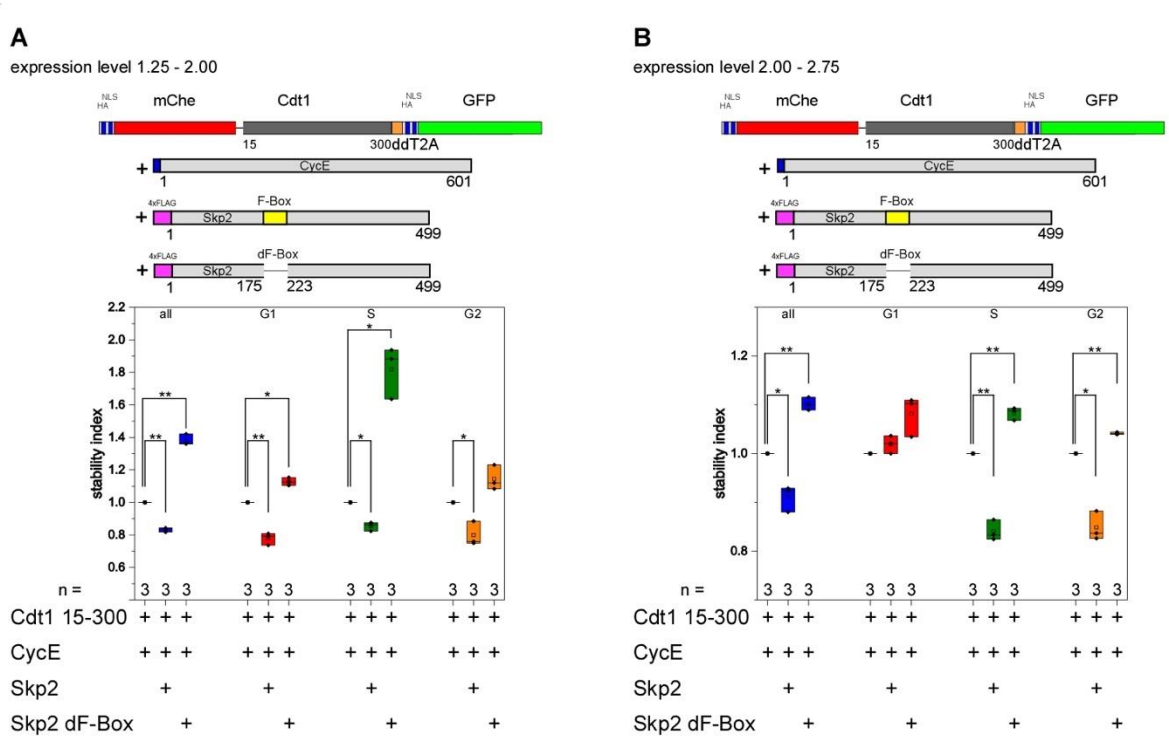

Figure 39 Cdt1 15-300 stability upon overexpression of Skp2 or Skp2 dF-Box and CycE
Protein stability of mChe Cdt1 15-300 with overexpressed Skp2, Skp2 dF-Box and CycE. (A) Expression level 1.25 – 2.00. Skp2 destabilizes mChe Cdt1 15-300 in all, G1, S and G2 cells. Skp2 dF-Box stabilizes Cdt1 15-300 in all, G1 and S. (B) Expression level

2.00 – 2.75. Skp2 destabilizes mChe Cdt1 15-300 in all, S and G2 cells. Skp2 dF-Box stabilizes Cdt1 15-300 in all, S and G2. * = $p < 0.05$, ** = $p < 0.01$, one sample t-test. Only significant changes are indicated.

To sum it up, Cdt1 15-300 did also show protein degradation in dependency of Skp2. The effects seen were similar to the observed effects of Cdt1 15-600 (degradation upon Skp2 overexpression, stabilization upon Skp2 dF-Box expression, intensified effects upon CycE overexpression). Important regions for degradation by Skp2 were not found yet and Cdt1 will be truncated further.

5.4.6. Stability of Cdt1 15-225 is regulated by Skp2 only weakly

Since Cdt1 15-300 was still destabilized by Skp2 and this destabilization was enhanced by CycE overexpression, crucial phospho-sites were likely present in this fragment. It is already known that phosphorylation dependent degradation relies upon one, some or all of 10 phospho-sites located in the first 300 amino acids of the protein. Mutation of all of these phospho-sites to alanine turns off the phospho-dependent degradation pathway (Thomer et al., 2004). Cdt1 was further truncated to narrow down the number of potential sites that would be mutated in a second step. The first version created was Cdt1 15-225, excluding the last six optimal phospho-sites.

Just like the other two constructs, mChe Cdt1 15-225 led to a shift of the cell cycle into G1 (Figure 40A,B,C). Analysis with expression level 1.25 – 2.00 surprisingly showed that Skp2 overexpression stabilized Cdt1 15-225 in all, G1 and S-Phase cells (Figure 40D, one-sample t-test, $p < 0.01$ and $p < 0.05$). Expression of Skp2 dF-Box did only in S-Phase lead to a significant stabilization (one-sample t-test, $p < 0.01$). Using expression level 2.00 – 2.75 changed this picture. Conversely, Skp2 overexpression led to destabilization but only in G2 (Figure 40E, one-sample t-test, $p < 0.05$), while Skp2 dF-Box did not affect the stability at all (one-sample t-test, $p > 0.05$).

Together with CycE overexpression, Skp2 did no longer significantly affect the stability of mChe Cdt1 15-225 at expression level 1.25 – 2.00. However, since the “stability index” (logarithmic mChe Cdt1 15-225 fluorescence intensity divided by the logarithmic GFP fluorescence intensity) was actually lower than one in this case, Skp2 indeed had a tendency of destabilisation on this Cdt1 version, although the effect was not statistically significant (Figure 41A, one-sample t-test, $p > 0.05$). Skp2 dF-Box did also not influence the stability in a significant way (one-sample t-test, $p > 0.05$). Nonetheless, this led to a tendency of protein stabilization, though again the difference was not significant. With expression level 2.00 – 2.75, Skp2 overexpression led to a statistically significant lower protein stability of Cdt1 15-225 in all cases (Figure 41B, one-sample t-test, $p < 0.05$ and $p < 0.01$). Skp2 dF-Box on the other hand did not influence the protein stability (one-sample t-test, $p > 0.05$).

Taken together, the data showed that the degradation of Cdt1 15-225 by Skp2 was weaker than Cdt1 15-300. Analysis without CycE overexpression showed no effect of Skp2 overexpression or even stabilization and the effects of Skp2 dF-Box did become no longer statistically significant for the most part. CycE overexpression eliminated the stabilization effect of Skp2, though destabilization of Cdt1 was not as pronounced and clear as with the other constructs. Again, Skp2 dF-Box did not execute any significant effect on the stability. According to these experiments, the residues between 225 and 300 were required for Skp2 mediated destabilization of Cdt1.

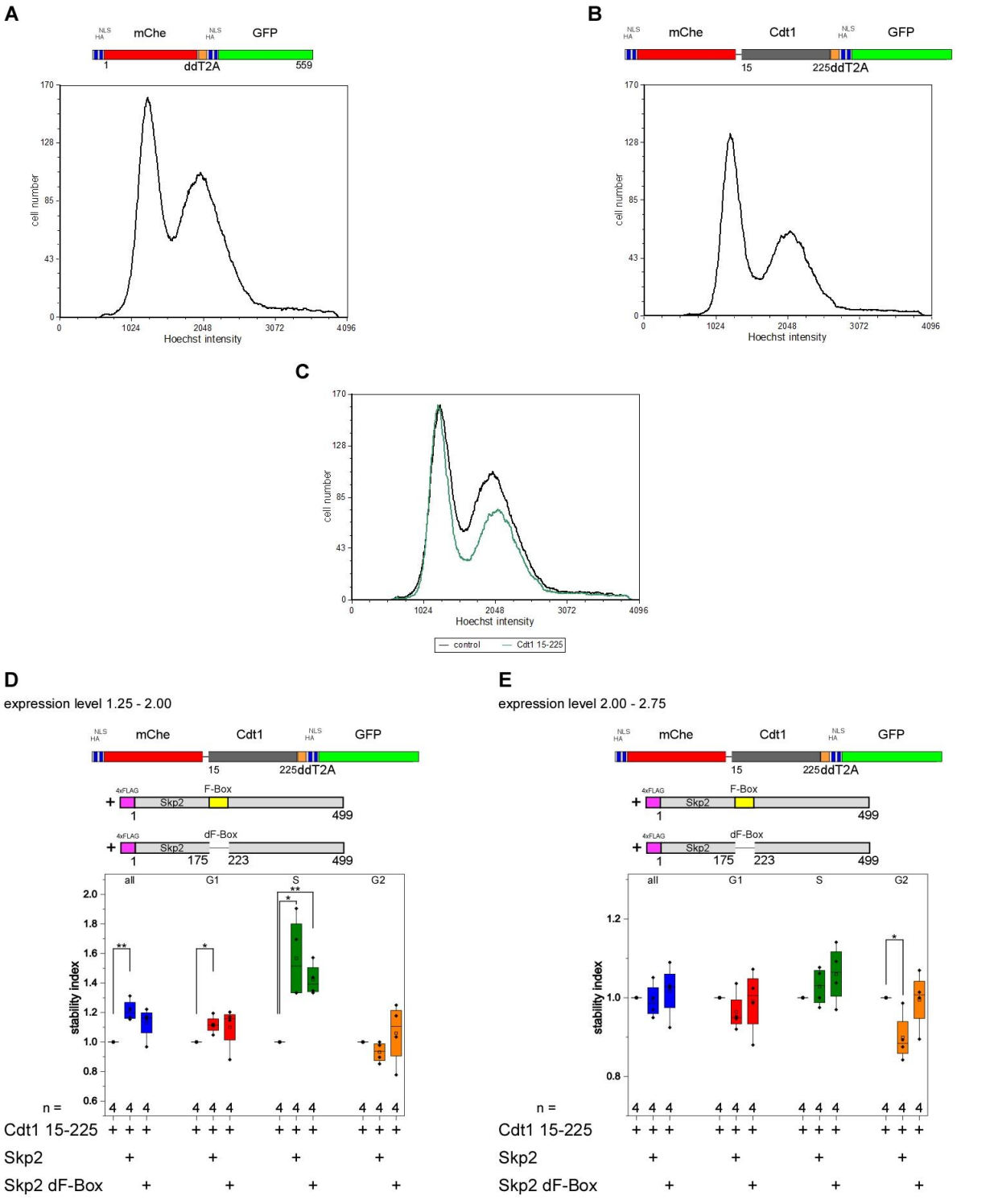

Figure 40 Cdt1 15-225 cell cycle effects and stability upon overexpression of Skp2 and Skp2 dF-Box

Cell cycle distribution and stability data of mCherry Cdt1 15-225. (A) Cell cycle of the control vector. (B) Cdt1 15-225 shows G1 accumulation of cells. (C) Overlay of control and Cdt1 15-225 overexpression. Overlay is normalized to the G1-peak. All presented cell cycle distributions are representative. Only GFP positive cells are shown. (D) Expression level 1.25 – 2.00. Skp2 stabilizes Cdt1 15-225 in all, G1 and S. Skp2 dF-Box acts stabilizing only in S-Phase. (E) Expression level 2.00 – 2.75. Skp2 destabilizes Cdt1 15-225 in G2. Skp2 dF-Box does not influence protein stability. * = $p < 0.05$, ** = $p < 0.01$, one sample t-test. Only significant changes are indicated.

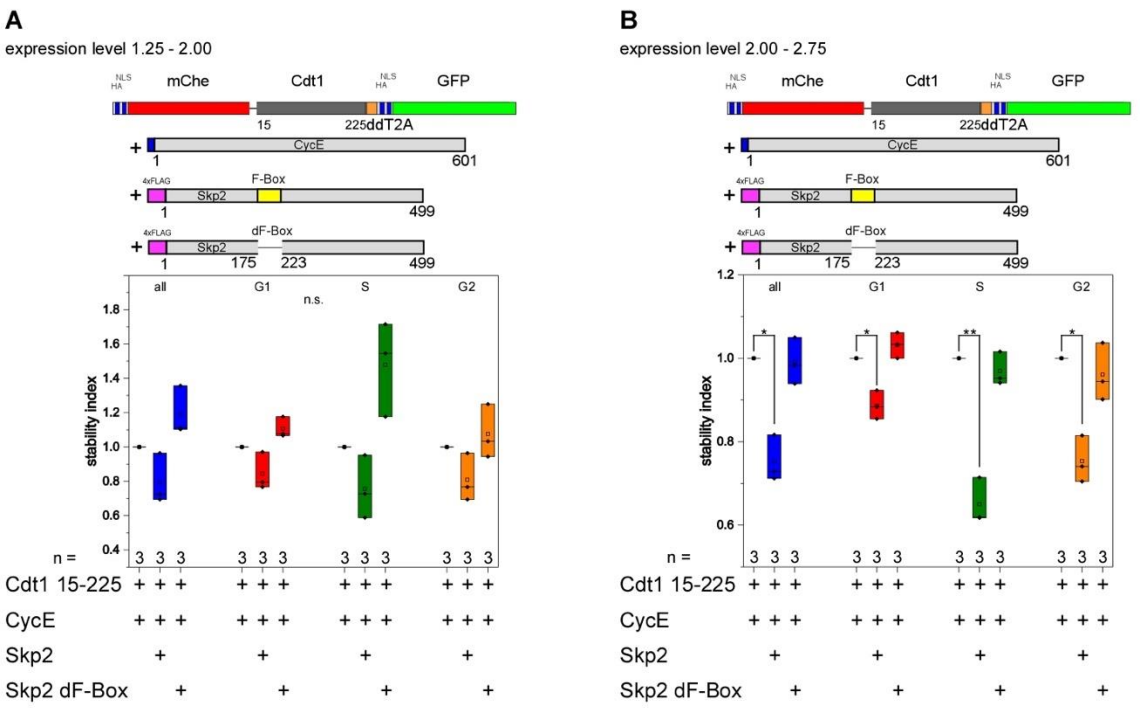

Figure 41 Cdt1 15-225 stability upon overexpression of Skp2 or Skp2 dF-Box and CycE
Protein stability of mChe Cdt1 15-225 with overexpressed Skp2, Skp2 dF-Box and CycE. (A) Expression level 1.25 – 2.00. Neither Skp2 nor Skp2 dF-Box changes Cdt1 15-225 stability in a significant way. The tendency of Skp2 overexpression is protein degradation and of Skp2 dF-Box expression stabilization, however. (B) Expression level 2.00 – 2.75. Skp2 destabilizes Cdt1 15-225 in all cases, while Skp2 dF-Box does not have any effect. n.s. = $p > 0.05$, * = $p < 0.05$, ** = $p < 0.01$, one sample t-test. Only significant changes are indicated.

5.4.7. Cdt1 15-263 is still a target for Skp2 regulation

In the region between 225 and 300 three optimal Cdk2 consensus phosphorylation sites are present. To identify potential phospho-sites important for Skp2 mediated degradation further, the version Cdt1 15-263 was created, lacking the last three known sites.

The cell cycle effect of mChe Cdt1 15-263 overexpression was similar to the other constructs, a G1 accumulation (Figure 42A,B,C). The stability of Cdt1 15-263 after Skp2 overexpression or Skp2 dF-Box expression was unaffected at the lower expression level (Figure 42D, one-sample t-test, $p > 0.05$). If the higher expression level was used, stability of Cdt1 15-263 was lowered only in G1 at Skp2 overexpression (Figure 42E, one-sample t-test, $p < 0.05$). Skp2 dF-Box did not seem to influence this truncation (one-sample t-test, $p > 0.05$).

Simultaneous CycE overexpression restored the ability of Skp2 to mark Cdt1 15-263 for degradation. At expression level 1.25 – 2.00 protein stability was significantly lower in all, S- and G2-Phase cells (Figure 43A, one-sample t-test, $p < 0.05$ and $p < 0.001$). Likewise, CycE overexpression resulted in stabilization of Cdt1 15-263 at Skp2 dF-Box expression in all and S cells (one-sample t-test, $p < 0.05$ an $p < 0.01$). Analysis with expression level 2.00 – 2.75 showed that Skp2 overexpression still significantly reduced Cdt1 15-263 stability in all, S and G2 cells (Figure 43B, one-sample t-test, $p < 0.05$ and $p < 0.01$), although Skp2 dF-Box did not affect the stability any more (one-sample t-test, $p > 0.05$).

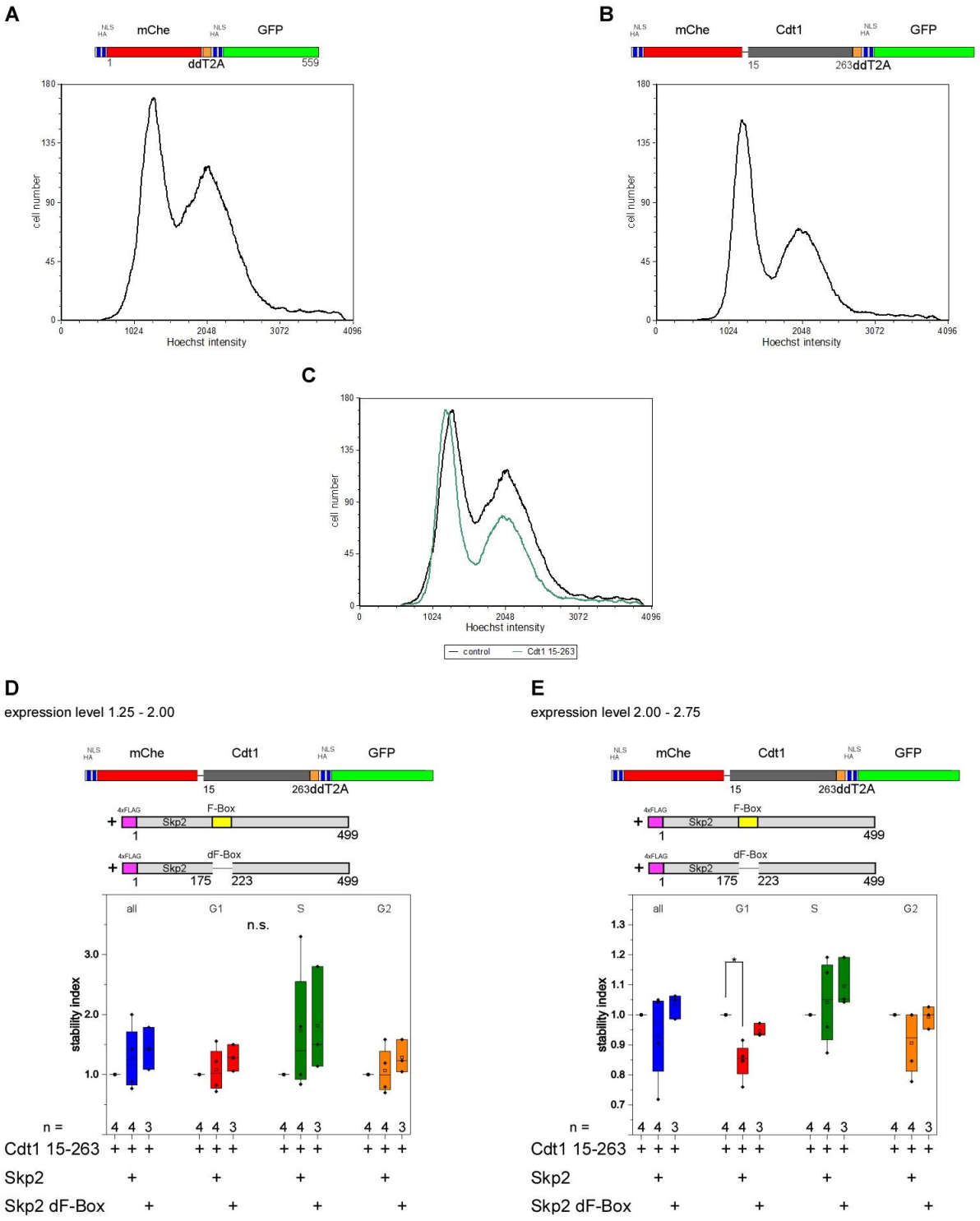

Figure 42 Cdt1 15-263 cell cycle effects and stability upon overexpression of Skp2 and Skp2 dF-Box

Cell cycle distribution and stability data of mCherry Cdt1 15-263. (A) Cell cycle of the control vector. (B) Cdt1 15-263 shows G1 accumulation of cells. (C) Overlay of control and Cdt1 15-225 overexpression. Overlay is normalized to the G1-peak. All presented cell cycle distributions are representative. Only GFP positive cells are shown. (D) Expression level 1.25 -2.00. Skp2 and Skp2 dF-Box overexpression do not alter Cdt1 15-263 stability. (E) Expression level 2.00 – 2.75. Skp2 degrades Cdt1 15-263 only in G1. Skp2 dF-Box does not influence the stability. n.s. = $p > 0.05$, * = $p < 0.05$, one sample t-test. Only significant changes are indicated.

Unlike Cdt1 15-225, 15-263 again showed the regulation by Skp2, however only after CycE overexpression. This construct still contained six optimal phosphorylation sites, which were, according to these results, potentially important for degradation through SCF^{Skp2}. In a next step, a Cdt1 version with a truncated N-terminus was created to screen for phospho-sites necessary for degradation in the N-terminus of the protein.

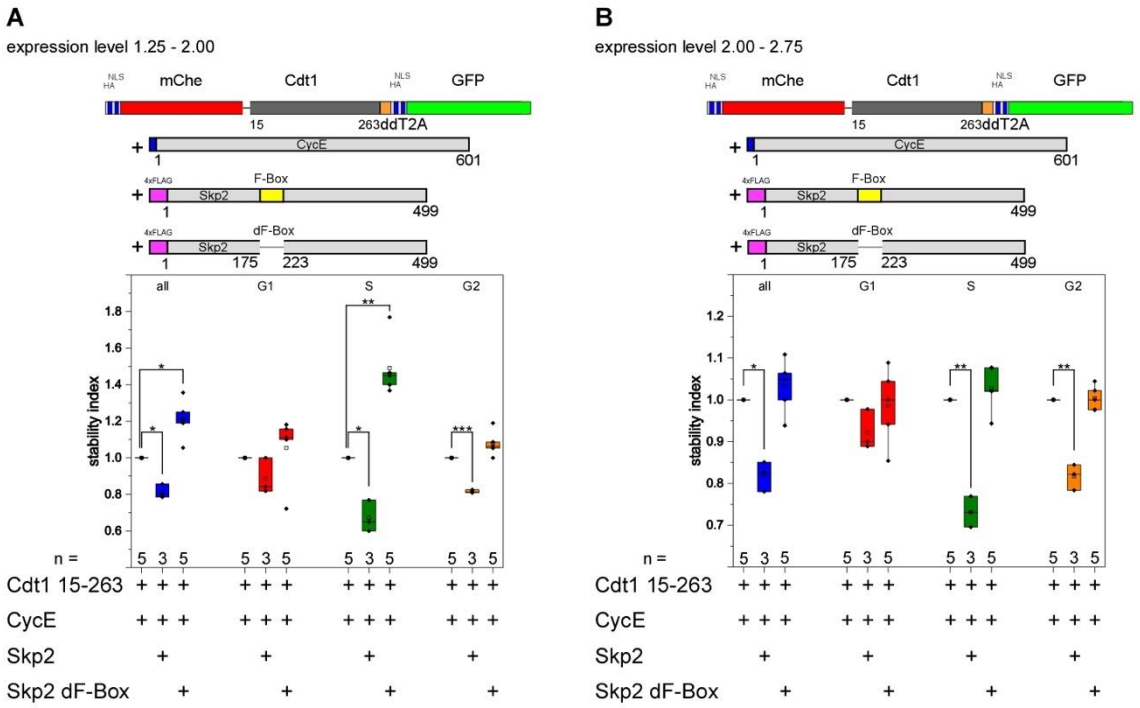

Figure 43 Cdt1 15-263 stability upon overexpression of Skp2 or Skp2 dF-Box and CycE
Protein stability of mChe Cdt1 15-263 with overexpressed Skp2, Skp2 dF-Box and CycE. (A) Expression level 1.25 – 2.00. Cdt1 15-263 is destabilized by Skp2 in all, S and G2. Skp2 dF-Box leads to stabilization in all and S. (B) Expression level 2.00 – 2.75. Skp2 destabilizes Cdt1 15-263 in all, S and G2. Skp2 dF-Box does not have any effect. * = $p < 0.05$, ** = $p < 0.01$, one sample t-test. Only significant changes are indicated.

5.4.8. The N-terminus of Cdt1 is necessary for Skp2 mediated degradation

To find out if the N-terminal 170 amino acids are important for the regulation, Cdt1 170 – 300 was created. This version excluded the first four of the already identified optimal phospho-sites.

Cdt1 170-300 also showed the G1-accumulation of Schneider cells (Figure 44A,B,C). With an expression level of 1.25 – 2.00, Cdt1 170-300 was not degraded upon Skp2 overexpression (Figure 44D, one sample t-test, $p > 0.05$). The only significant change was a stabilization of the protein in S-Phase (one sample t-test, $p < 0.05$). Skp2 dF-Box overexpression led to a statistically significant stabilization of the construct in all distinct phases (one sample t-test, $p < 0.01$ and $p < 0.05$). Analysis of expression level 2.00 – 2.75 showed that neither Skp2 nor Skp2 dF-Box overexpression resulted in a significant change of Cdt1 170-300 stability (Figure 44E, one sample t-test, $p > 0.05$), the only exception was a stabilization of the truncation in S-Phase with Skp2 dF-Box expression (one-sample t-test, $p < 0.05$).

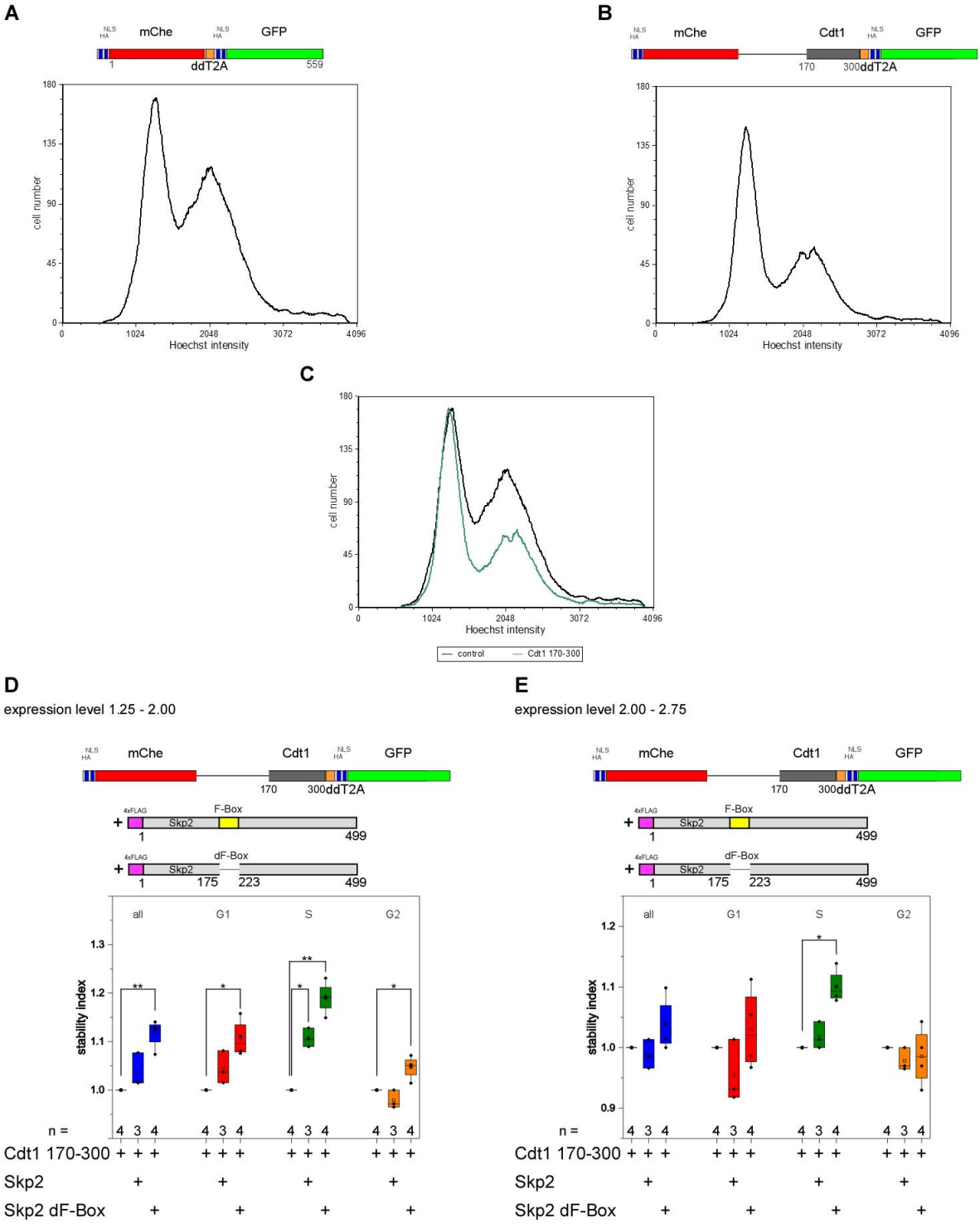

Figure 44 Cdt1 170-300 cell cycle effects and stability upon overexpression of Skp2 and Skp2 dF-Box

mChe Cdt1 170-300 cell cycle distribution and stability data. (A) Cell cycle of the control vector. (B) Cdt1 170-300 shows G1 accumulation of cells. (C) Overlay of control and Cdt1 170-300 overexpression. Overlay is normalized to the G1-peak. All presented cell cycle distributions are representative. Only GFP positive cells are shown. (D) Expression level 1.25 – 2.00. Skp2 overexpression has no effect on Cdt1 170-300, except a stabilization in S-Phase. Skp2 dF-Box stabilizes in all, G1, S and G2 cells. (E) Expression level 2.00 – 2.75. Skp2 does have no effect on Cdt1 170-300 stability. Skp2 dF-Box stabilizes Cdt1 170-300 only in S-Phase. * = $p < 0.05$, ** = $p < 0.01$, one sample t-test. Only significant changes are indicated.

Simultaneous CycE overexpression did not result in enhanced Skp2 effects. On the opposite, Skp2 showed no effect with expression level 1.25 – 2.00 (Figure 45A, one sample t-test, $p > 0.05$). Skp2 dF-Box overexpression showed stabilization in all and S-Phase cells (one sample t-test, $p < 0.05$). Expression level 2.00 – 2.75 showed also no significant effect of Skp2 overexpression on protein stability (Figure 45B, one sample t-test, $p > 0.05$). Skp2 dF-Box showed under these circumstances surprisingly a destabilization of Cdt1 170-300, although this happened only in G2 (one sample t-test, $p < 0.05$).

According to these results, Cdt1 170-300 was not a target for Skp2 mediated ubiquitination. Accordingly, the phospho-sites, deleted in this version, seemed to play a role for the recognition by Skp2. After evaluation of the truncated Cdt1 versions, it was decided to concentrate further on Cdt1 15-263, since it still showed degradation upon Skp2 overexpression if CycE was also overexpressed. Cdt1 170-300 and Cdt1 15-225 conversely showed no consistent degradation by Skp2 and CycE overexpression, and in some cases even a significant protein stabilization that did not fit into the data already gathered. These two truncations were consequently dropped from further analysis and only the phosphorylation sites in Cdt1 15-263 were analyzed.

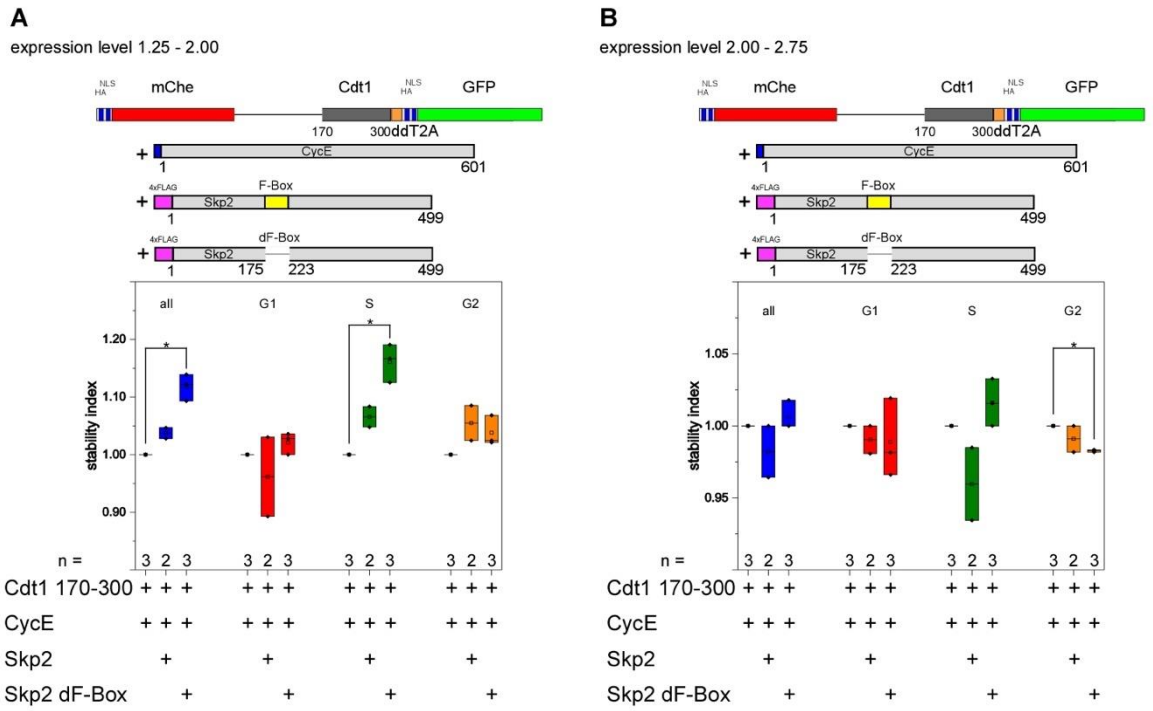

Figure 45 Cdt1 170-300 stability upon overexpression of Skp2 or Skp2 dF-Box and CycE
Protein stability of mChe Cdt1 170-300 with overexpressed Skp2, Skp2 dF-Box and CycE. (A) Expression level 1.25 – 2.00. Skp2 overexpression does not change the stability of Cdt1 170-300. Skp2 dF-Box overexpression leads to stabilization in all and S-Phase. (B) Expression level 2.00 – 2.75. Skp2 overexpression does not exhibit any effect on Cdt1 170-300. Skp2 dF-Box leads to a significant destabilization, but only in G2-Phase. * = $p < 0.05$, one sample t-test. Only significant changes are indicated.

Cdt1 15-263 contains seven possible phospho-sites, important for the ubiquitination by Skp2 (Thomer et al., 2004). The first one of these (S37) was excluded from further analysis, since it only has the minimal consensus site for phosphorylation (S-P). The remaining six amino acids (S111, T158, S168, S226, S249 and T256) have an optimal consensus sequence for phosphorylation (S/T-P-X-R/K) and it was decided to investigate their role for Cdt1 stability further.

5.4.9. Neither phospho-sites S111, S168 nor S226 are influencing the Cdt1 stability in dependency of Skp2

The region of Cdt1 between amino acids 15 and 263 harbors six optimal consensus Cdk phosphorylation sites (S/T-P-X-K/R sites; see Figure 46) according to Thomer et al. (2004). To illuminate the role of the six single phospho-sites, in vitro mutagenesis was performed to change these amino acids to alanine, which should prevent any phosphorylation. This was successful for S111, T158, S168 and S226. Unfortunately, mutations in the phospho-sites S249 and T256 could not be obtained by the in-vitro mutagenesis approach, despite several attempts and had to be dropped from the analysis because of time reasons. Additionally, T158 had to be excluded from the analysis, since expression of Cdt1 15-263 T158A resulted in a loss of GFP and mCherry signal over several consecutive trials (data not shown).

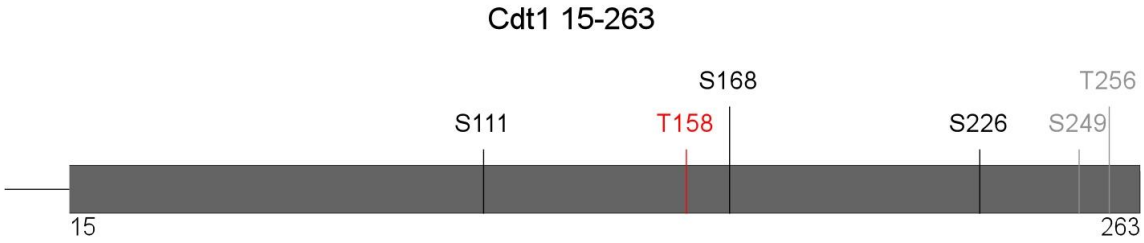

Figure 46 Schema of Cdt1 15-263 with the examined phospho-sites
Cdt1 fragment 15-263 with the six optimal phospho-sites (S111, T158, S268, S226, S249 and T256) considered important for degradation through SCF^{Skp2}. Mutation of T158 (red) resulted in a loss of GFP and mCherry fluorescence and could not be analyzed. S249 and T256 (grey) could not be mutated.

The stability of the remaining three constructs (S111, S168 and S226) was analyzed by flow cytometry. Analysis was performed with the respective construct under CycE overexpression conditions and with simultaneous overexpression of Skp2. If the mutated phospho-site would be important for Skp2 mediated degradation, Skp2 overexpression should not change the stability any longer if CycE is also overexpressed at the same time. Just like before, working with Cdt1 showed different results in dependency of the used expression levels. Therefore, again both levels are presented.

The first analyzed construct was Cdt1 15-263 S111A. At expression level 1.25 – 2.00, no influence of the expressed components on mCherry was visible, stability of the controls was inconspicuous (Figure 47A, one-sample t-test, $p > 0.05$). The Cdt1 mutation itself showed a statistically significant destabilization if Skp2 was overexpressed in all four cases (Figure 47B, one-sample t-test, $p < 0.01$, $p < 0.05$ and $p < 0.001$). If level 2.00 – 2.75 was analyzed, control experiments showed a significant effect on mChe upon Skp2 overexpression: mCherry was significantly destabilized in all and G1 cells (Figure 47C, one-sample t-test, $p < 0.05$). Cdt1 15-263 S111A showed a significant reduction of stability in all cells, as well as in S- and G2-Phase (Figure 47D, one-sample t-test, $p < 0.001$ and $p < 0.01$), but not in G1-Phase (one-sample t-test, $p > 0.05$).

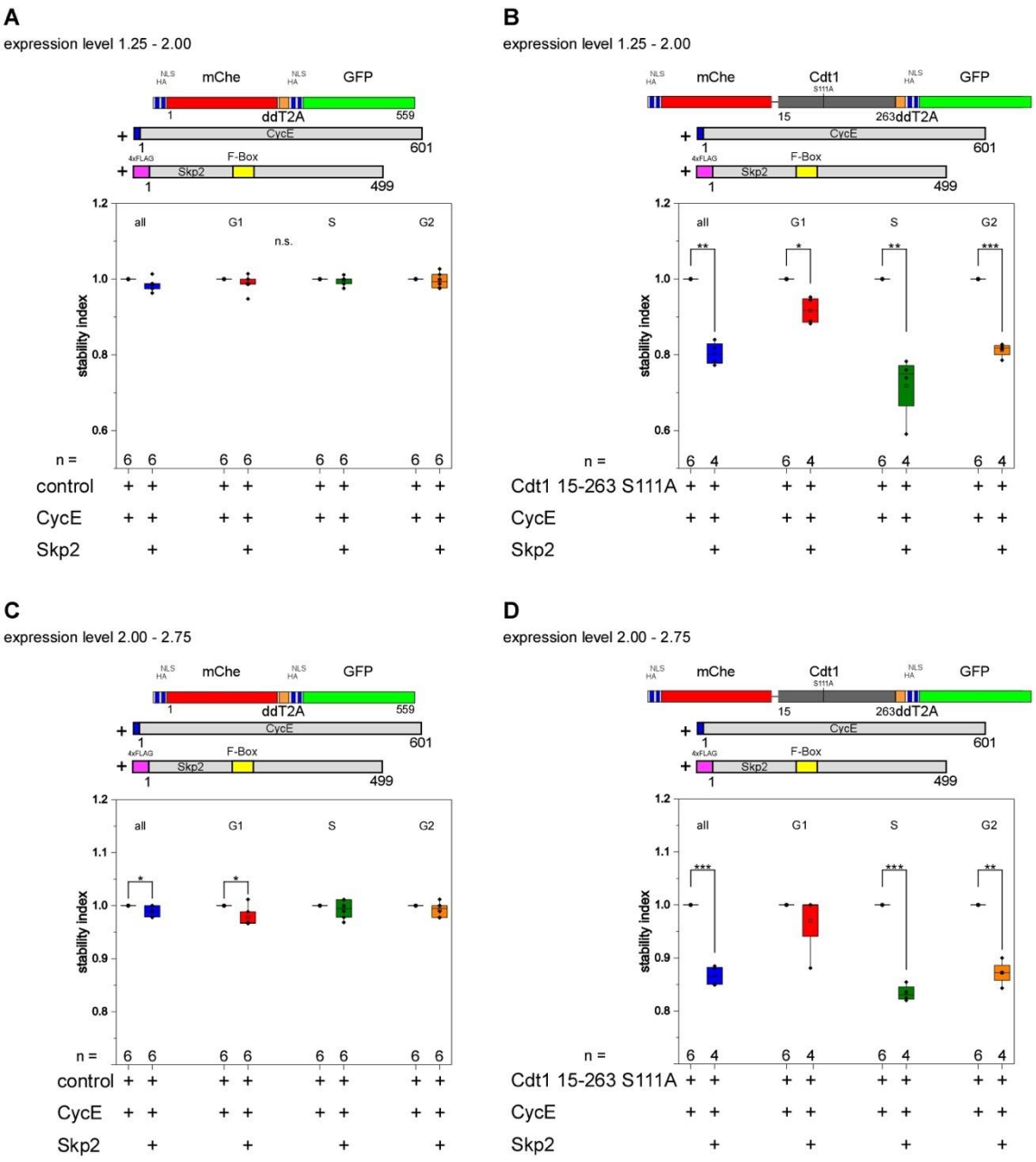

Figure 47 Stability of Cdt1 15-263 S111A upon CycE and Skp2 overexpression

Protein stability of Cdt1 15-263 S111A with overexpressed CycE and Skp2. Expression level 1.25 – 2.00: (A) Skp2 overexpression does not influence the stability of mCherry. (B) Skp2 overexpression leads to destabilization of Cdt1 15-263 S111A in all four cases. Expression level 2.00 – 2.75: (C) Skp2 overexpression results in a lower stability of mCherry in all and G1 cells. (D) Cdt1 15-263 S111A is destabilized in all, S- and G2-Phase cells upon Skp2-overexpression. n.s. = $p > 0.05$, * = $p < 0.05$, ** = $p < 0.01$, *** = $p < 0.001$, one sample t-test. Only significant changes are indicated.

The experiments with Cdt1 15-263 S168A showed that Skp2 overexpression had no influence on the controls, although the same vectors were used as above (data not shown). Skp2 destabilized Cdt1 15-263 S168A significantly in all, S and G2 cells (Figure 48A, one-sample t-test, $p < 0.01$) if analyzed with level

1.25 – 2.00 and under CycE overexpression conditions. The higher expression level showed a similar destabilization in all, S- and G2-Phase (Figure 48B, one-sample t-test, $p < 0.01$ and $p < 0.001$).

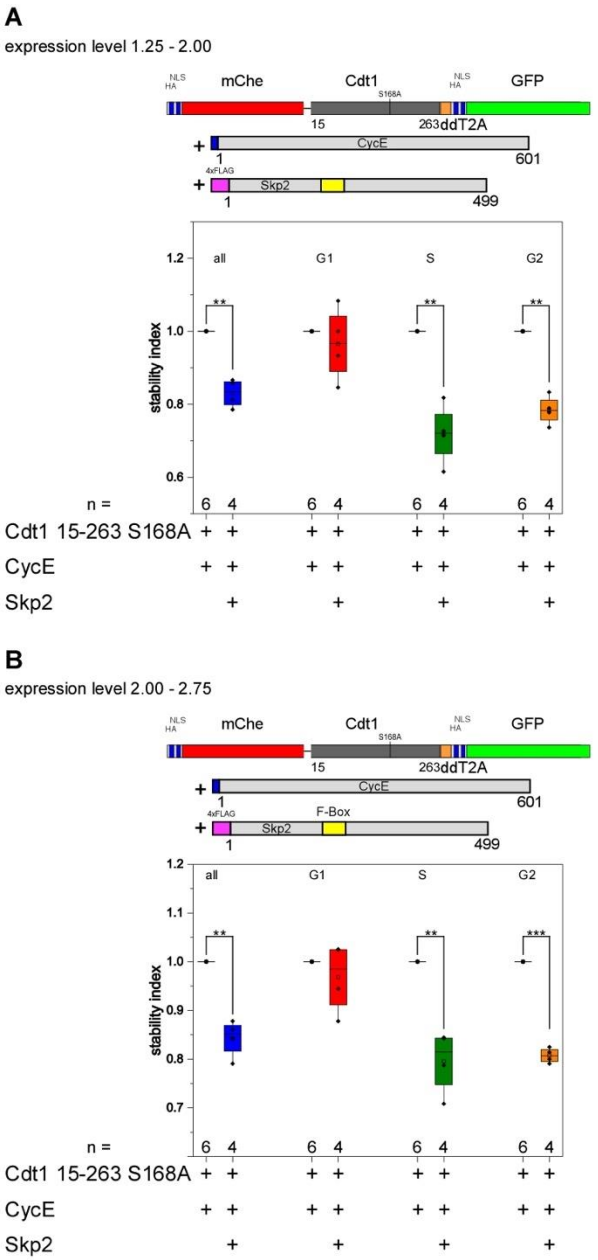

Figure 48 Stability of Cdt1 15-263 S168A upon CycE and Skp2 overexpression
Stability of Cdt1 15-263 S168A with overexpression of CycE and Skp2. (A) Expression level 1.25 – 2.00. Overexpressing Skp2 leads to increased instability of Cdt1 15-263 S168A in all, S and G2. (B) Expression level 2.00 – 2.75. Skp2 overexpression showed a similar degradation of the Cdt1 mutant in all, S and G2. ** = $p < 0.01$, *** = $p < 0.001$, one sample t-test. Only significant changes are indicated.

The last mutation tested was Cdt1 15-263 S226A. The control experiments showed no effect of Skp2 on mCherry under CycE overexpression conditions (data not shown). Analysis of the lower expression level showed that Cdt1 15-263 S226A was destabilized upon Skp2 overexpression in all and S-Phase (Figure 49A,

one-sample t-test, $p < 0.05$ and $p < 0.01$). Expression level 2.00 – 2.75 on the other hand showed a statistically significant degradation in all four cases (Figure 49B, one-sample t-test, $p < 0.05$ and $p < 0.01$).

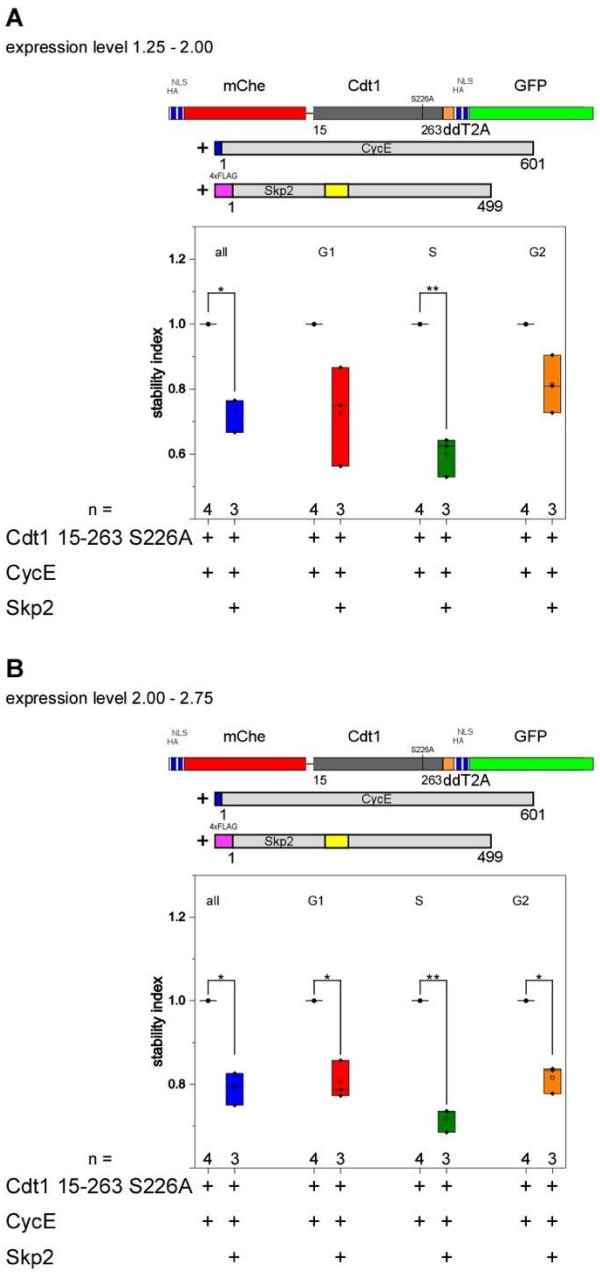

Figure 49 Cdt1 15-263 S226A stability upon CycE and Skp2 overexpression

Cdt1 15-263 S226A stability by CycE and Skp2 overexpression. (A) Expression level 1.25 – 2.00. Cdt1 15-263 is statistically significant destabilized in all and S. (B) Expression level 2.00 – 2.75. Skp2 overexpression destabilizes the Cdt1 mutant in all, G1, S and G2. * = $p < 0.01$, ** = $p < 0.01$, one sample t-test. Only significant changes are indicated.

To summarize these experiments, mutation of three phospho-sites alone (S111A, S168A and S226A) did not result in a different degradation pattern of Cdt1 upon Skp2 overexpression if CycE was also overexpressed.

5.4.10. Cdt1 shows biochemical interaction with Skp2

Flow cytometric protein stability analysis of Cdt1 suggested that it was a target of the SCF^{Skp2} complex in dependency of phosphorylation. To test for biochemical interaction between Cdt1 and Skp2, co-immunoprecipitation was performed. An HA-tagged version of Cdt1 15-600 was used to prevent any unwanted disturbances in the cell cycle and to exclude the PIP-mediated degradation. The pull down was performed with 4xFLAG Skp2.

Expression of 4xFLAG Skp2 in Schneider cells worked well. Skp2 was also efficiently precipitated (Figure 50, left). HA Cdt1 15-600 expression was also detectable. Cdt1 did not bind unspecifically to the IgG beads. The Co-IP itself showed a slight but visible Cdt1 band (Figure 50, right). Biochemical interaction between Cdt1 15-600 and Skp2 existed, therefore.

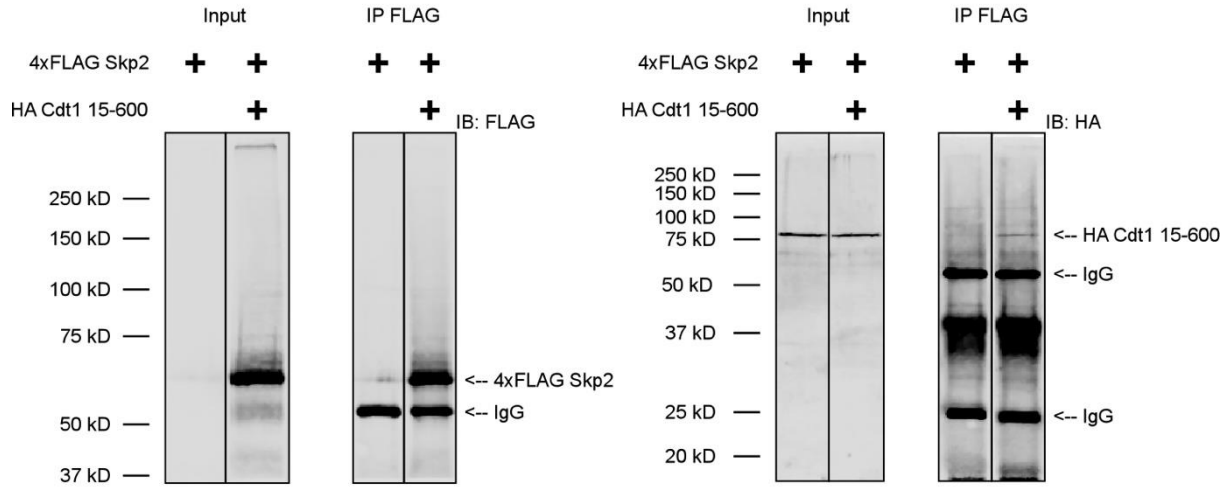

Figure 50 Co-IP between 4xFLAG Skp2 and HA Cdt1 15-600

Co-immunoprecipitation of 4xFLAG Skp2 and HA Cdt1 15-600 for analysis of biochemical interaction. FLAG antibody was used for precipitation, FLAG or HA antibody for detection. Left: FLAG Blot for control of expression and precipitation of 4xFLAG Skp2. Right: HA Blot for control of expression and interaction of HA Cdt1 15-600. Biochemical interaction is detected.

5.4.11. Skp2 modulates Cdt1 phenotypes in cells

According to the stability data and the Co-IP assays, Cdt1 was a substrate for the SCF^{Skp2} complex. If this was indeed the case, any Cdt1 phenotypes should have been susceptible to a modulation of the Skp2 levels. Cell cycle phenotypes of Cdt1 and Cdt1 dPIP overexpression were already described (see Figure 32B,C and D). Consequently, the effect of Skp2 overexpression or knockdown on these phenotypes was analyzed by flow cytometry.

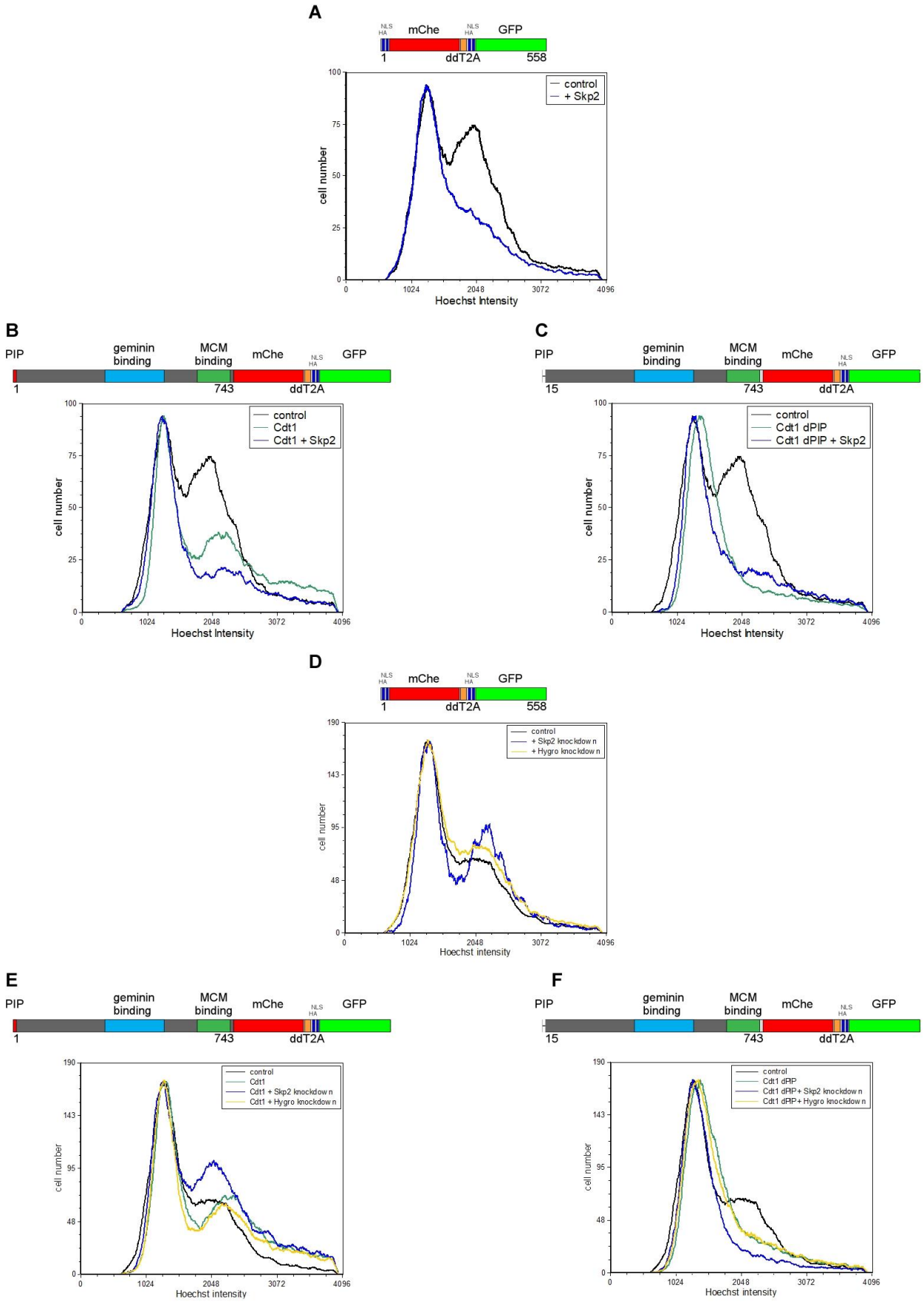
A
NLS HA
mChe
NLS HA
GFP
1
ddT2A
558
control
+ Skp2
cell number
Hoechst Intensity
B
PIP
geminin binding
MCM binding
mChe
NLS HA
GFP
1
743
ddT2A
control
Cdt1
Cdt1 + Skp2
cell number
Hoechst Intensity
C
PIP
geminin binding
MCM binding
mChe
NLS HA
GFP
15
743
ddT2A
control
Cdt1 dPIP
Cdt1 dPIP + Skp2
cell number
Hoechst Intensity
D
NLS HA
mChe
NLS HA
GFP
1
ddT2A
558
control
+ Skp2 knockdown
+ Hygro knockdown
cell number
Hoechst intensity
E
PIP
geminin binding
MCM binding
mChe
NLS HA
GFP
1
743
ddT2A
control
Cdt1
Cdt1 + Skp2 knockdown
Cdt1 + Hygro knockdown
cell number
Hoechst intensity
F
PIP
geminin binding
MCM binding
mChe
NLS HA
GFP
15
743
ddT2A
control
Cdt1 dPIP
Cdt1 dPIP+ Skp2 knockdown
Cdt1 dPIP+ Hygro knockdown
cell number
Hoechst intensity

Figure 51 Cell cycle distributions of the Cdt1-Skp2 rescue experiments if Cdt1 is overexpressed
Effects of Skp2 overexpression or knockdown if Cdt1 or Cdt1 dPIP is overexpressed. (A) Control experiment, Skp2 overexpression exhibits the already described G1 shift. (B) Skp2 overexpression reduces the amount of overreplicating cells caused by Cdt1 overexpression. (C) Skp2 overexpression weakens the effect of the Cdt1 dPIP overexpression. Distinct G1- and G2-peaks can be observed again. (D) Control experiment, Skp2 knockdown exhibits the already described G2 shift. (E) Skp2 knockdown enhances the G2 cell accumulation caused by Cdt1 overexpression. (F) Skp2 knockdown enhances the G1 shift caused by Cdt1 dPIP overexpression. GFP serves as the transfection control, only GFP cells are shown. All overlays are normalized to the G1-peaks. All presented cell cycle distributions are representative.

Cell cycle distribution of the control samples showed the already observed accumulation of G1 cells in comparison to the control if Skp2 is overexpressed (Figure 51A). Cdt1 overexpression led to overreplication of Schneider cells (Figure 51B) as described before. Skp2 overexpression rescued this phenotype, the amount of overreplicating cells was restored to the level in the control experiment.

An even more interesting result was achieved by using Cdt1 dPIP. As already observed, Cdt1 dPIP resulted in an accumulation of cells in very late G1 or probably in early S-Phase (Figure 51C). Skp2 overexpression also rescued this phenotype. The maximum of the peak shifted back, restoring the G1-peak. Most importantly, a distinct G2-peak emerged, that was not seen when Cdt1 dPIP was overexpressed. It is important to point out that this Skp2 overexpression effect was very unusual. Skp2 overexpression showed in all observed cases in this thesis always cell cycle shifts in the direction of the G1-Phase. Only if Cdt1 dPIP was overexpressed, a Skp2 overexpression led to a more pronounced G2-Phase. This speaks strongly for a rescue effect of Skp2 on the Cdt1 dPIP cell cycle distribution phenotype.

Beside these rescue experiments, it was also analyzed what happened to the Cdt1 phenotypes if Skp2 was knocked down. If Cdt1 is a substrate of SCF^{Skp2}, this knockdown should lead to stronger effects. Again, the control experiments showed the already described phenotype of the Skp2 knockdown, an accumulation of cells in G2-Phase in comparison to a Hygro knockdown (Figure 51D).

The control Hygro knockdown did not influence the effects of Cdt1 overexpression (Figure 51E). Knockdown of Skp2 led to an increased accumulation of cells in G2-Phase if Cdt1 was overexpressed, although there was no increase in the amount of overreplicating cells visible. The Cdt1 dPIP phenotype was also not influenced by the Hygro knockdown (Figure 51F). In this case, though, the Skp2 knockdown resulted in a stronger shift into late G1-/S-Phase, an enhancement of the Cdt1 dPIP effect. Again, this effect of modulated Skp2 levels under Cdt1 dPIP overexpression conditions was unique, since knockdown of Skp2 led typically to a G2 shift of cells in this thesis.

It was also tested if the effects of a Cdt1 knockdown were influenced by changing Skp2 levels. Cdt1 knockdown was performed by in vitro synthesized dsRNA and not by a hairpin construct. Hence, Amp dsRNA was used as a control. The S2R+-cells in this experiment showed a slight G2-shift for unknown reasons (Figure 52A). Nonetheless, the control Amp knockdown did not show any effect on this cell cycle. Cdt1 knockdown showed a cell shift into G1-Phase. Even sub-G1 cells (cells with a DNA content smaller than 2C) could be observed (Figure 52B). Skp2 knockdown resulted in the already familiar shift into G2 cells (Figure 52C). Consequently, it was tested what effects an additional Skp2 knockdown or overexpression had if Cdt1 was knocked down. The Skp2 knockdown rescued the effect partially. The number of sub-G1 cells was reduced and more G2 cells were visible (Figure 52D). The effects of Skp2 overexpression in this case was mixed however. Though in theory, this constellation should lead to a

stronger effect, the number of sub-G1 cells was decreased instead (Figure 52E). Conversely, the number of G2 cells was also decreased in this case, showing a stronger effect than Cdt1 knockdown alone.

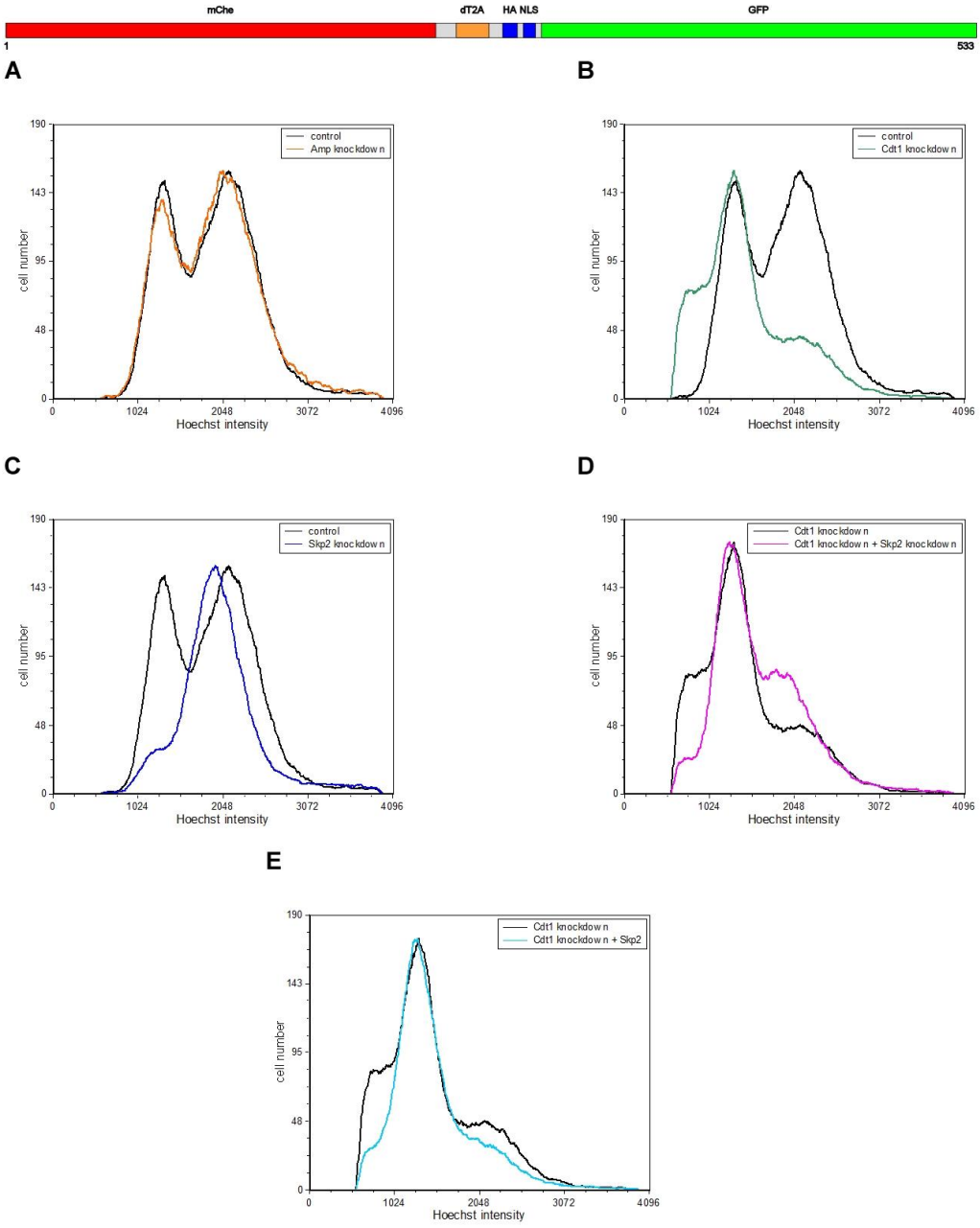

Figure 52 Cell cycle distributions of the Cdt1-Skp2 rescue experiments if Cdt1 is knocked down

Effects of Skp2 knockdown or overexpression if Cdt1 is knocked down. (A) Amp knockdown exhibits no effect on the cell cycle. (B) Cdt1 knockdown results in a G1 cell shift and cells with a DNA content smaller than 2C (Sub-G1 cells). (C) Skp2 knockdown shows the already observed shift into G2-Phase. (D) Simultaneous knockdown of Cdt1 and Skp2 weakens the Cdt1 effects, less Sub-G1 cells and more G2 cells could be observed. (E) If Skp2 is overexpressed, the number of Sub-G1 cells is also reduced, but the G2 effect is exacerbated. All overlays are normalized, A and C to the G2-peak, B,D and E to the G1-peak. All presented cell cycle distributions are representative.

As a conclusion, the performed experiments hinted that Cdt1 was a substrate of SCF^{Skp2} in *D. melanogaster*. Cdt1 was degraded in S2R+-cells if CycE was also overexpressed, indicating that phosphorylation was important for Skp2 dependent degradation. Overexpression of Skp2 dF-Box stabilized Cdt1. This was in accordance with a dominant negative effect that F-Box proteins with a deleted F-Box have on their substrates. Furthermore, Skp2 knockdown did lead to a stabilization of Cdt1.

Experiments were also performed to identify the phospho-sites in Cdt1 important for its binding to Skp2. Cdt1 truncations narrowed the analysis down to the amino acids S111, T158, S168, S226, S249 and T256. Mutations ruled out that S111, S168 or S226 alone were responsible for the recognition by Skp2.

Cdt1 did also show biochemical interaction with Skp2, as seen by a Co-IP experiment.

Finally, effects of Cdt1 overexpression or knockdown could be rescued or enhanced by Skp2 knockdown or overexpression, respectively.

5.5. Regulation of CycE through Skp2 is questionable

5.5.1. Overview

Besides Dacapo and Cdt1, CycE was another potential substrate that was tested. CycE is responsible for the entry into S-Phase. CycE overexpression shows very strong effects on the cell cycle. Furthermore, it is also efficiently degraded in S-Phase by SCF^{Ago}. These factors make working with CycE difficult. Therefore, the analysis of CycE was only basic and far from complete. CycE stability was analyzed by flow cytometry and a Co-IP study was also performed.

5.5.2. Cell cycle effects of CycE and artificial stop in G1

Overexpression of mChe CycE resulted in a dramatic shift of cells into G2-Phase (Figure 53, compare cell cycle curves of A and C). Furthermore, Figure 53C shows that CycE was extremely unstable. There was almost no signal detectable in the Cherry fluorescence channel. It is unreliable to perform the flow cytometric protein stability analysis in this case. The massive effect of CycE on the cell cycle prevented a precise determination of the distinct cell cycle phases and the extremely low basic stability made detection and calculation of the stability difficult.

A solution was found to overcome these issues. Cells were artificially kept in G1-Phase. The G1-Stop was performed by overexpression of Dacapo under a strong promotor (Figure 53B). This resulted in a cell cycle with distinct G1-, S- and G2/M-Phases that were again possible to define (Figure 53D). Since cells did not transit rapidly into S-Phase any longer, the degradation of CycE by SCF^{Ago} was also diminished and a mChe CycE signal was detectable (Figure 53D). A positive side effect of this assay was that mostly effects of Skp2 on CycE were analyzed since the competing SCF^{Ago} degradation pathway was not able to target its substrates in G1-Phase.

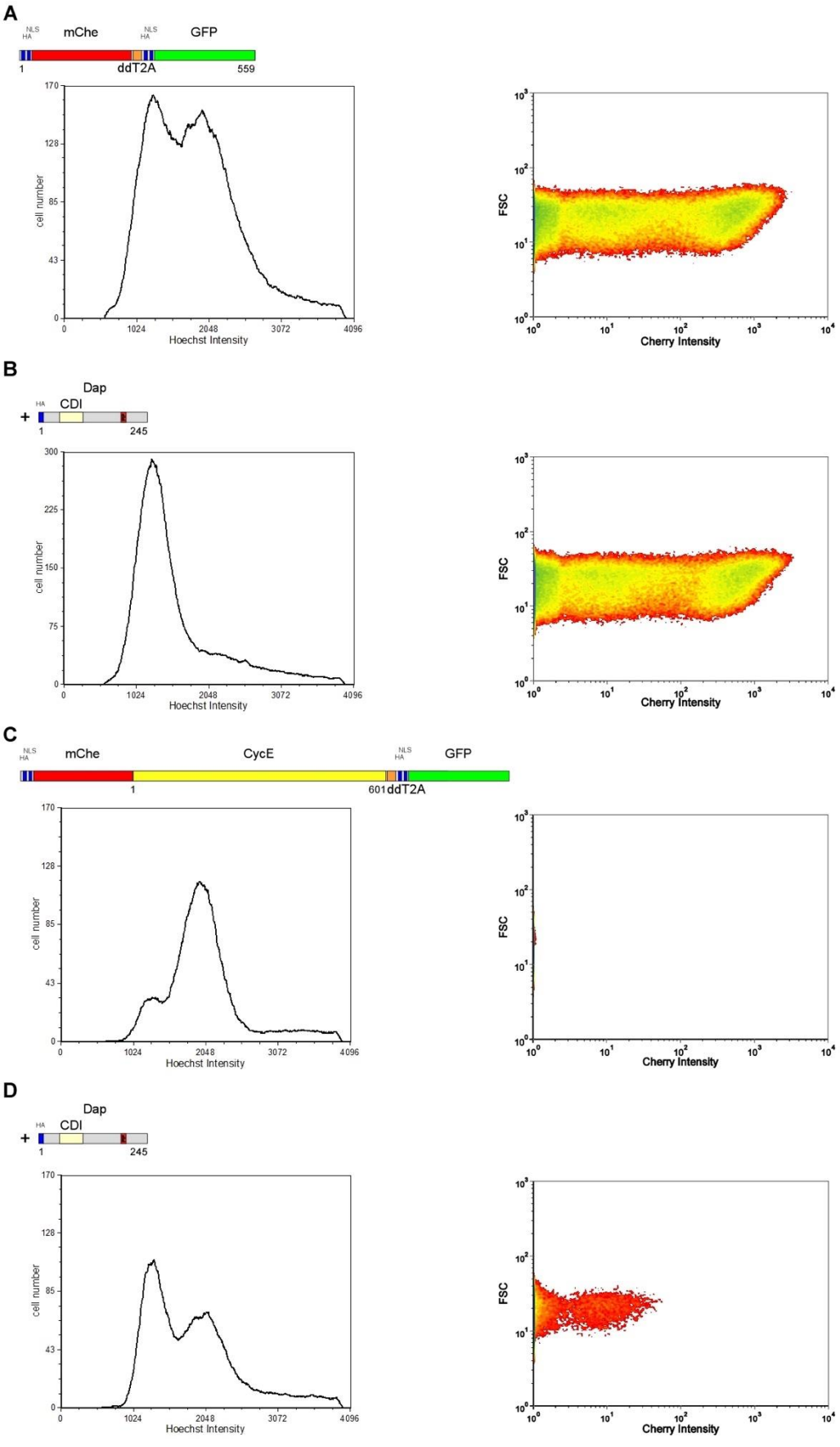
A
NLS
HA
mChe
NLS
HA
GFP
1
ddT2A
559
cell number
Hoechst Intensity
FSC
Cherry Intensity
B
Dap
+
HA
CDI
1
245
cell number
Hoechst Intensity
FSC
Cherry Intensity
C
NLS
HA
mChe
CycE
NLS
HA
GFP
1
601ddT2A
cell number
Hoechst Intensity
FSC
Cherry Intensity
D
Dap
+
HA
CDI
1
245
cell number
Hoechst Intensity
FSC
Cherry Intensity

Figure 53 Cell cycle effects of CycE with and without artificial G1 arrest
Cell cycle distributions of mChe CycE and simultaneous Dap overexpression. (A) *Left:* Cell cycle of control cells. *Right:* intensity of the corresponding Cherry signal (B) *Left:* Cell cycle of cells overexpressing Dap, resulting in a G1 arrest. *Right:* intensity of the corresponding Cherry signal (C) *Left:* CycE leads to a strong G2-shift. *Right:* mChe-CycE is efficiently degraded during the cell cycle, almost no signal is detectable in the red fluorescent channel. (D) *Left:* simultaneous overexpression of CycE and Dap still arrests the cells in G1. *Right:* the G1 arrest stabilizes mChe-CycE, the Cherry signal is again detectable. GFP serves as the transfection control, only GFP cells are shown All depicted graphs are representative.

5.5.3. Stability of CycE is not influenced by Skp2 levels

Flow cytometric stability analysis was conducted with and without Dap G1 arrest. If the G1 arrest was not used, stability was only analyzed for all cells (regardless of the cell cycle phases) and G2-Phase, since G1- and S-Phase were no longer identifiable with the used method. Stability data was stabilized to CycE or CycE + Dap respectively. GFP and mCherry controls were not influenced by overexpression of Skp2. Only expression level 2.00 – 2.75 is depicted.

Stability of CycE was not influenced by Skp2 overexpression (Figure 54, one-sample t-test, $p > 0.05$) neither in all cells nor in G2-Phase. This still held true if cells were arrested in G1, regardless of the cell cycle phase (one-sample t-test, $p > 0.05$). It has to be noted that standard deviation in some of these cases was unusually high.

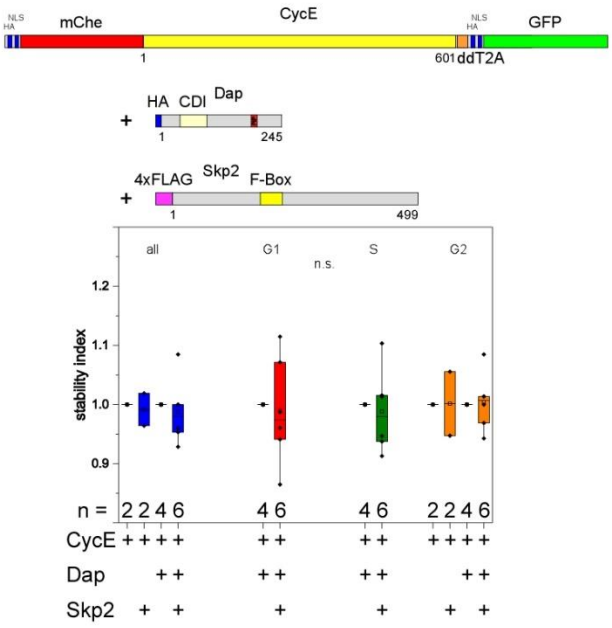

Figure 54 Stability of CycE upon Skp2 overexpression and G1 arrest
Flow cytometric stability data of CycE. Skp2 overexpression does not change the stability of CycE. This is also the case if cells are arrested in G1-Phase by Dap overexpression. n.s. = $p > 0.05$, one-sample t-test

CycE stability was also analyzed if Skp2 was knocked down. Analysis was performed as described above. In case of the G1 arrest, no control Hygro Hairpin tests were performed because there were not enough wells on the 12-well plate available.

CycE stability was not changed upon Skp2 knockdown in comparison to the Hygro knockdown (Figure 55, t-test for equal variances, $p > 0.05$). The Dap G1 arrest did also not change this result: CycE stability was not influenced by Skp2 knockdown (t-test for equal variances, $p > 0.05$). Since the Hygro Hairpin control was lacking, the comparison was performed between CycE and CycE + Skp2 Hairpin in this case.

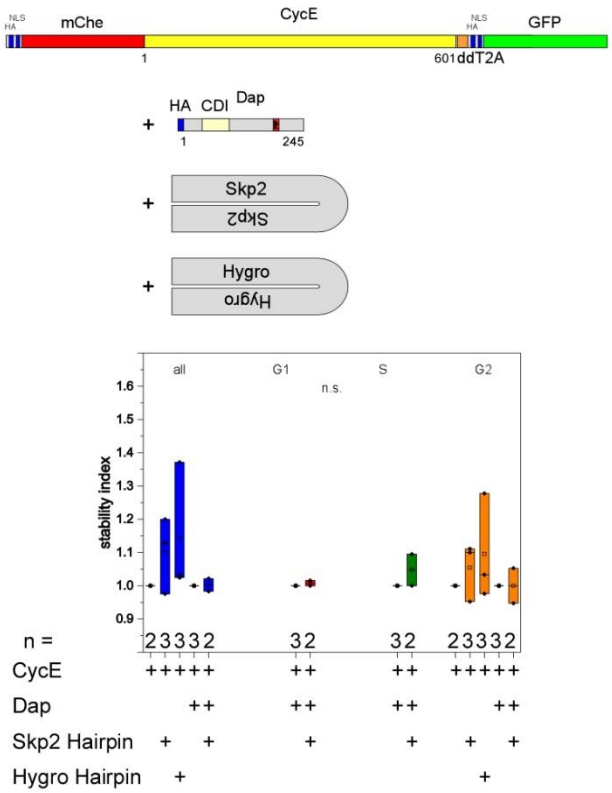

Figure 55 Stability of CycE upon Skp2 knockdown and G1 arrest
CycE protein stability data upon Skp2 knockdown. Skp2 knockdown has no influence on the CycE stability, regardless of a G1 arrest created by Dap overexpression. n.s. = $p > 0.05$, t-test for equal variances

5.5.4. CycE interacts biochemically with Skp2

A Co-IP was performed to test for interaction between CycE and Skp2. Skp2 was tagged N-terminally with 4xFLAG. CycE was tagged with GFP and expressed under an actin promotor instead of a polyubiquitin promotor. 4xFLAG Skp2 was again well expressed and precipitated efficiently (Figure 56, left). Expression of GFP CycE was visible though weaker than 4xFLAG Skp2, corresponding to the weaker promotor. A weak, but visible band could be seen if GFP CycE was co-immunoprecipitated with 4xFLAG Skp2, indicating a biochemical interaction between both proteins (Figure 56, right).

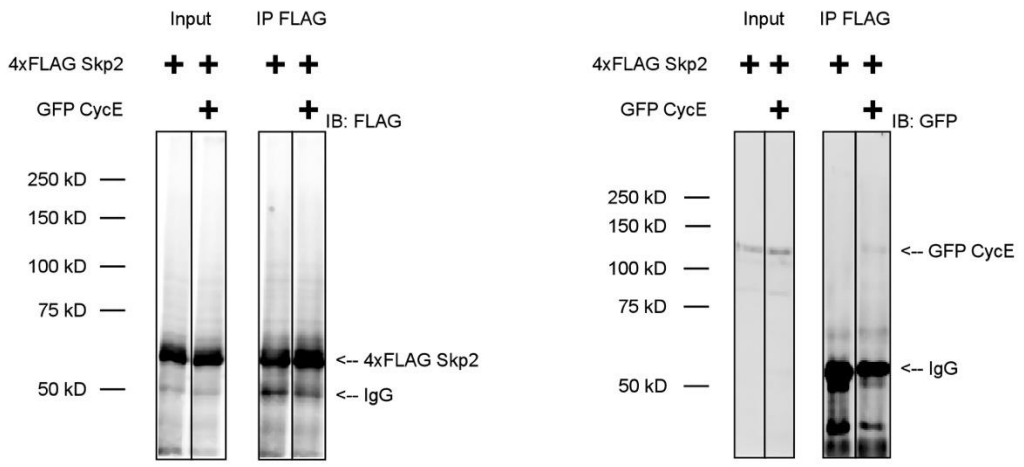

Figure 56 Co-IP between 4xFLAG Skp2 and GFP CycE
Co-immunoprecipitation of 4xFLAG Skp2 and GFP CycE for testing of biochemical interaction. FLAG antibody was used for precipitation, FLAG and GFP antibody was used for detection. Left: FLAG Blot for control of expression and precipitation of 4xFLAG Skp2. Right: GFP Blot for control of expression and interaction of GFP CycE. Biochemical interaction is detected.

To summarize this chapter, a definite conclusion if CycE is a substrate of SCF^{Skp2} could not be made. Flow cytometric stability analysis did not show an effect of Skp2 overexpression or knockdown on CycE stability. However, the validity of these assays is questionable because of the dramatic interventions on the cell cycle that had to be undertaken. On the other hand, biochemical analysis indeed showed interaction between CycE and Skp2.

5.6. Mass spectrometric analysis of Skp2 binding partners did not show any obvious substrates for cell cycle regulation

So far, substrates for Skp2 were tested if homologues showed Skp2 mediated regulation in higher eukaryotes. Mass-spectrometric analysis however was also performed. This could potentially not only confirm already obtained results, but also lead to new potential substrates. 4xFLAG Skp2 was overexpressed in Schneider cells and precipitated. As a control, wild type cells were also lysed and treated with FLAG-tagged agarose beads. These samples were analyzed by mass-spectrometry (see 4.2.5). The resulting hits were compared to the *Drosophila* proteins in the UniProt database.

Originally, 222 proteins were found in the 4xFLAG Skp2 sample that could be identified without reasonable doubt. After comparison with the control, to exclude unspecifically bound proteins, 154 remained (see Table 27). These potential hits were identified in the FlyBase database and ordered according to the biological processes they are involved in. The most prominent categories were proteins related to ubiquitin-proteasomal degradation (14 hits), ribosomal proteins (12 hits) and cell cycle proteins (7 hits). A large amount (24 hits) were proteins involved in as yet unidentified processes.

Some important hits are specified here: Skp2, as the bait protein, was found in first place with a score of 6115.9, proving that precipitation indeed worked. SkpA was found with a score of 498.5. This showed that at least some portion of the precipitated Skp2 was incorporated into the SCF-complex. The finding of Cul1 (score 273.6, under the name lin19-RC) hinted also in this direction. Another interesting hit was Cdk2 with a score of 103. Table 18 does summarize these hits.

Table 18 Interesting proteins identified in mass spec analysis

Protein	Score	No. of peptides	Sequence coverage (%)
Skp2 (Bait)	6115.9	58	62.1
SkpA	498.5	7	54.9
Cul1 (= lin19)	273.6	5	8.8
Cdk2	103.0	3	14.0

It is important to note that neither Dap, nor Cdt1 or CycE could be found in the mass spec analysis. Furthermore, the number of cell cycle proteins were altogether low, only 7 of 154 hits (or 4.5%) were connected to the cell cycle. To sum it up, mass spectrometric analysis did not help to identify new substrates of Skp2 regarding cell cycle control.

6 Discussion

6.1.Establishment of Skp2 phenotypes in Schneider cells

6.1.1. Skp2 overexpression

The aim of this thesis was to identify new substrates of the SCF^{Skp2} complex in *Drosophila melanogaster*. Schneider cells were primarily used for this purpose, since they could be easily genetically manipulated, and results could be obtained rapidly. In the beginning of the investigation, Skp2 phenotypes in the cell culture were observed and analyzed as a basis for further analysis. This was necessary, since up to now only effects of Skp2 knockdown are described in *Drosophila* tissues (Dui et al., 2013; Ghorbani et al., 2011). Cell cycle profiles of Schneider cells with changed Skp2 levels are as to this date not published.

Fluorescence-activated cell scanning (FACS) analysis of cell cycle distributions revealed that Skp2 overexpression led to an accumulation of Schneider cells in G1-Phase (Figure 11B,E). In most of the presented experiments, Skp2 was tagged with the 4xFLAG tag. The cell cycle shift was present, regardless if the tag was positioned N- or C-terminally. In mammalian cells, the effects of Skp2 overexpression are different. For example, in Rat-1 cells, Skp2 overexpression leads to an accumulation of cells in G2-Phase (Sutterluty et al., 1999). This is also true for Rat-6 cells when they are in a non-adherent state (Carrano and Pagano, 2001). In CCD18-Co cells, Skp2 overexpression leads to accumulation in S-Phase (Fujita et al., 2008). It seems that Skp2 has different roles in cell cycle regulation in different cell types.

A potential Skp2 overexpression phenotype was also analyzed in *Drosophila* wings using the engrailed driver for expression in the posterior part of the wing. In this case, Skp2 overexpression had no visible effect on wing morphology in comparison to the control. Wing area as well as direction, number and distance between the wing hairs all were inconspicuous upon Skp2 overexpression (Figure 11G,H). However, all these parameters show an effect upon Skp2 knockdown (Ghorbani et al., 2011). As mentioned, Skp2 overexpression showed only a weak G1 accumulation in S2R+-cells. Further experiments in the Sprenger group showed that cell cycle effects of Skp2 overexpression in wing imaginal disc cells are comparable; the accumulation of cells in G1 is also not a strong phenotype (Hirsch, 2018). The absence of an associated phenotype in wing morphology and wing hairs is probably explainable by compensation of cell cycle regulatory mechanisms in the course of the wing development.

The overexpression phenotype was analyzed further, and live cell imaging experiments resulted in a possible explanation for the cell accumulation in G1-Phase (Figure 12). Cells remained in G1 for a longer time if Skp2 is overexpressed, the transition to S-Phase was procrastinated, resulting in a G1 cell cycle shift.

Skp2 is a well-known F-Box protein, though it could not be ruled out that it still has more tasks in the cell. It was important to ascertain that the described effects were indeed dependent on the F-Box of Skp2 that is responsible for the binding to the SkpA-Cul1-Rbx1 complex (Hao et al., 2005; Yu et al., 1998). Since Skp2 dF-Box did not show a change in the cell cycle profile (Figure 13B), it is reasonable that the Skp2 overexpression phenotype was caused by the ubiquitination activity of the SCF^{Skp2} complex. Furthermore, Skp2 dF-Box was also used later for the analysis of possible Skp2 substrates.

6.1.2. Skp2 knockdown

Overexpression studies are always challenging. Though easy to perform, the interpretation of the results has to be done carefully. Overexpression of Skp2 means to flood the cell with Skp2 molecules, which could

have unforeseen effects on various cell mechanisms (some of these issues will be discussed later, see 6.2). Therefore, besides overexpression studies Skp2 was also knocked down in cells.

Skp2 knockdown resulted in a shift into G2-Phase, regardless if dsRNA (Figure 14) or a hairpin construct (Figure 16) was used. The effect of the Skp2 hairpin construct was weaker in comparison to the dsRNA. There are two explanations for this outcome. First, the used parts of the Skp2 sequence for the different kinds of knockdowns varied in position and size. The dsRNA was transcribed from the C-terminal Skp2 coding region and was 893 bp long. The hairpin construct on the other hand was created from the first 500 bp of the N-terminus. It may be possible that length and position of the knockdown fragments influenced the efficiency of downregulation. The second explanation is that the promotor of the hairpin construct, though a polyubiquitin promotor, the strongest promotor available in the lab, is too weak to precisely imitate the effect of the high concentrated dsRNA. Regardless of this observation, both approaches resulted in principal in the same effect. It was also confirmed that knockdown with both methods is directed against Skp2, since both methods resulted in a downregulation of GFP-Skp2 in control experiments (Jan Polz, 6-week internship; Damian Mikietyn, 6-week internship).

The specificity of the knockdown was controlled with Amp dsRNA, Hygro dsRNA or Hygro Hairpin, in dependency of the respective experiment. These control knockdowns did not show a significant effect on the cell cycle distribution or stability of GFP and mCherry, indicating that the observed effects are specific. One caveat might be that the Hygro Hairpin construct had a weaker promotor (metallotheonine promoter) than the Skp2 hairpin construct (polyubiquitin promotor). However, recently in the course of a bachelor thesis, a polyubiquitin Hygro Hairpin was successfully cloned, and expression of this hairpin does at least not change the cell cycle distribution of S2R+-cells (Tremmel, 2018). According to the dsCheck program (Naito et al., 2005) neither the used dsRNAs nor the hairpins had any off-target effects.

The reason for the G2-shift under knockdown conditions was a shortened G1-Phase, as determined by live cell imaging (Figure 15).

The G2-shift upon Skp2 knockdown is the reciprocal effect of the G1-shift upon Skp2 overexpression. These effects are also typical for a tumor suppressor that induce G1-S transition and subsequent cell accumulation in G2 when mutated. Therefore, potential substrates of Skp2 in *D. melanogaster* will likely induce or support a transition from G1 to S. The effect of Skp2 knockdown in wing imaginal discs is also a cell accumulation in G2/M-Phase (Liang et al., 2014), in concordance with the knockdown effect in S2R+-cells. In contrast to these results, Skp2 knockdown in higher eukaryotes leads to an accumulation of cells in G0/G1 and not in G2 (Ding et al., 2017; Liu and Yamauchi, 2009; Schuler et al., 2011; Wei et al., 2004). However, other reports state the opposite, a shift into G2-Phase upon Skp2 knockdown (Hu and Aplin, 2008). Again, it seems that the role that Skp2 plays depends upon the cell type.

According to the results presented here, the effect of both Skp2 overexpression and knockdown does differ between different species and cell types. Skp2 seems to have many targets in mammalians, affecting different processes from cell cycle control, to DNA replication, DNA repair, gene transcription and more (Frescas and Pagano, 2008). Conversely, in flies only the CKI Dacapo is a proposed target (Dui et al., 2013), though data presented here argue against Dap being a substrate (discussed in 6.3). One may speculate that Skp2 has primordial substrates that are targeted in both flies and mammals. During evolution, Skp2 may have earned additional substrates and functions in higher organisms, resulting in different effects that Skp2 exercises on the cell cycle. More data needs to be gathered to pursue this theory though.

Another explanation is that, as already noted, Skp2 function seems to differ in different cell - or tissue types. Another peculiarity from the mammalian system hints in this direction. In mammalians, Skp2 substrates are both, positive and negative regulators of the cell cycle. Indeed, it was shown recently that Skp2 has different effects on cell cycle distribution and gene transcription in dependency of the observed cell line (Krishnan et al., 2017). The authors speculate that Skp2 plays a role in different checkpoints in strong dependency of the used cells. The effects on the *Drosophila* cell cycle of Skp2 are at least similar in Schneider cells (this thesis) and wing imaginal discs (Hirsch, 2018). Therefore, it is possible that the results presented here are not strictly restricted to S2R+-cells.

Knockout of Skp2 does lead to polyploidy in cells of the wing imaginal disc (Ghorbani et al., 2011). Skp2 knockdown did not show any visible overreplication effect in S2R+-cells when analyzed 48 hours after addition of dsRNA (Figure 14C). One possibility was that Skp2 knockdown had to be conducted for a longer time period to observe any effects. Indeed, a prolonged exposure of cells to Skp2 dsRNA led to an increase of overreplication (Figure 17). Besides, cells were also enlarged in this case. Furthermore, it has to be said that the cell number in these experiments were altogether low (compare the scale of the y-axes of control, Amp dsRNA and Skp2 dsRNA in this figure). This may be a hint that Skp2 knockdown led to more cell death or apoptosis, which is in accordance with results seen in wing imaginal discs if Skp2 is knocked out (Ghorbani et al., 2011).

Polyploidy associated with Skp2 depletion is also described in mammalians: mouse hepatocytes showed distinct peaks with 8C and 16C if Skp2 is knocked out (Nakayama et al., 2000). Skp2 knockdown in fly imaginal discs was also analyzed in the Sprenger group, with the result of overreplication in these cells (Hirsch, 2018). Thus, Skp2 knockdown does lead to overreplication in *Drosophila*, altogether. The data from the S2R+-cells suggest that reduction of Skp2 results in the beginning in accumulation in G2. The observed overreplication might then originate from uncoordinated DNA-replication starting in G2. This results in overerreplicating cells and finally polyploidy for reasons as yet unknown. A possible mechanism may involve Cdt1. The results of this thesis allow the conclusion that Skp2 regulates Cdt1 (see 6.4), which is indeed important for DNA replication. Consequently, Skp2 knockdown will lead to higher Cdt1 levels in the cell. This may result in refiring of replication origins, especially in G2-Phase, where low Cdk activity allows Cdc6 to reaccumulate in the cell cycle, which is the second factor besides Cdt1 that regulates origin licensing. Perhaps, apoptosis is also induced in these cells, resulting in a lower density which could lead to the described wing hair spacing phenotype (Ghorbani et al., 2011).

6.2. Change of Skp2 levels in cells does not influence the availability of free SkpA-Cul1-Rbx1 complex

Overexpression or knockdown experiments can be tricky to interpret. Flooding or depletion of cells with proteins may lead to observable effects. However, if these effects are a direct result of the changed protein levels or only experimental artifacts for example by influencing the availability of certain complexes has to be considered. F-Box proteins are part of the SCF-complex. The SCF is able to bind various different F-Box proteins (Skp2, Rca1, Morgue, Slimb and many more) which means that it plays a role in many different cellular processes.

Overexpression or knockdown of F-Box proteins could influence the availability of free SkpA-Cul1-Rbx1-complex. Therefore, the ability of other F-Box proteins to bind to SkpA-Cul1-Rbx1 and fulfill their respective roles in the cell may be altered. Any observed effect in this case would not be caused by the changed level

of the protein of interest but more by a different composition of SCF-complexes in comparison to a wild type situation.

Since the focus of this thesis was Skp2, it was analyzed if the overexpression or knockdown of this F-Box protein was problematic in this respect. The ability of the artificial F-Box protein slmb-vhhGFP4 to specifically bind and ubiquitinate GFP or GFP-tagged proteins was used (Caussinus et al., 2011). Overexpression of both slmb-vhhGFP4 and GFP re-enacted the regulation of a protein by the SCF-complex. Indeed, GFP stability was lowered if slmb-vhhGFP4 was expressed simultaneously (Figure 18B). This result showed that there was enough unoccupied SkpA-Cul1-Rbx1 complex in Schneider cells, so that the overexpression of slmb-vhhGFP4 can perform GFP degradation. It seems that the amount of unoccupied SkpA-Cul1-Rbx1 complex is not the rate limiting factor, at least if only one F-Box protein is overexpressed.

Conversely, the overexpression of two F-Box proteins, slmb-vhhGFP4 and Skp2, did result in stabilization of GFP. One conclusion is that the massive overexpression of two F-Box proteins creates a situation in Schneider cells, where competition for the binding to the SkpA-Cul1-Rbx1 complex occurs. Slmb-vhhGFP4 is no longer able to degrade GFP under these circumstances. It has to be said that all experiments presented in this thesis regarding overexpression studies were done by overexpression of only one F-Box protein. Therefore, it can be assumed that competition for SkpA-Cul1-Rbx1 was not a disturbing factor in these experiments.

Knockdown of Skp2 on the other hand did not result in a statistically significant change of GFP stability in comparison to the control knockdown. Probably, there already is enough unoccupied SkpA-Cul1-Rbx1 so that the knockdown of an F-Box protein does not create opportunities for other F-Box proteins to bind to the complex and perform their functions to a higher degree.

A caveat of these experiments that is already stated in the original publication is that GFP alone is only inefficiently degraded by slmb-vhhGFP4 (Caussinus et al., 2011). The reason is that either GFP cannot be tagged easily by ubiquitin due to its structure, or because the protein is too small to span the gap between the F-Box Protein and the E2-ubiquitin-ligase bound to SCF. To resolve this issue, a GFP-tagged protein can be used, being more susceptible for ubiquitination and bigger. This protein would however need certain requirements for the presented assay: it must not influence the cell cycle and cannot be a substrate of SCF^{Skp2}. It has to be said that GFP-tagged proteins, namely GFP-CycB and GFP-Dap, were already tested, but did only show small improvements on the degradation-ability of slmb-vhhGFP4 (Serena Herzinger, 6-week internship). Nonetheless, usage of a GFP tagged protein that may be degraded by slmb-vhh even stronger than GFP alone, could lead to more accurate results.

To conclude this section, neither the overexpression nor the knockdown of an F-Box protein did influence the availability of free SkpA-Cul1-Rbx1. Competition seemed to occur only if two F-Box proteins were overexpressed simultaneously, which was never done in the presented experiments. Therefore, all observed effects of both overexpression and knockdown were considered direct effects that Skp2 had on cell cycle distribution or protein stability.

6.3.Dacapo stability is not negatively regulated by Skp2

The first potential Skp2 substrate tested was Dacapo (Dap) the *Drosophila* homologue of p21, p27 and p57. Dap is a cyclin dependent kinase inhibitor (CKI), responsible for inhibition of CycE/Cdk2 activity (Lane et al., 1996). Overexpression of Dap leads to a stop of the cell cycle in G1-Phase since the transition from G1 to S is no longer taking place (de Nooij et al., 1996; Lane et al., 1996; Reis and Edgar, 2004). This well-

known stop in G1-Phase was also visible in the analyzed S2R+-cells (Figure 19B). In mammalian cells, p21, p27 and p57 are targets of Skp2 and their degradation causes a shift into S-Phase.

In *Drosophila*, Skp2 overexpression resulted in a transition of the cell cycle distribution to G1-Phase. Skp2 knockdown had the adverse effect of shifting the cells towards G2. The overexpression effect is not comprehensible with Dap degradation that should result in more CycE/Cdk2 activity and consequently entry into S-Phase. Likewise, Skp2 knockdown should lead under these circumstances to more Dap and consequently to cells remaining in G1-Phase. Thus, the results seen in *Drosophila* are the exact opposite to the expected effects if Dap would be regulated by Skp2. This suggests that Dap is not a target of Skp2 in *D. melanogaster*.

Stability analysis of Dap full length by flow cytometry did also not show any hints for Skp2 mediated degradation. To get an overview, Table 19 summarizes the results of all experiments with Dap full length. A destabilization of Dap is marked by "-" and a black box, stabilization by "+" and a white box and if no statistically significant effect was seen a "0" is inserted into the table and the box was colored grey.

Table 19 Summary of flow cytometric protein stability analysis of Dacapo
+ and white box = stabilization; 0 and grey box = no effect

Dacapo full length				
Expressed constructs	all	G1	S	G2
4xFLAG Skp2	0	0	0	+
CycE	0	0	0	0
4xFLAG Skp2 + CycE	0	0	0	0
Skp2 4xFLAG	0	0	0	0
CycE	+	0	0	0
Skp2 4xFLAG + CycE	0	0	0	0
Cks85A	0	0	0	0
4xFLAG Skp2 + Cks85A	0	0	0	0
CycE + Cks85A	0	0	0	0
4xFLAG Skp2 + CycE + Cks85A	0	0	0	0
4xFLAG Skp2	0	0	0	0
4xFLAG Skp2 dF-Box	0	0	0	0
Skp2 Hairpin vs. Hygro Hairpin	0	0	+	0

Since overexpression of Dap (full length) results in a strong arrest of cells in G1-Phase, the interpretation of these results is challenging. The G1 stop disturbs the cell cycle and the cells do not resemble a wild type situation. A conclusion of the natural processes in a cell is impossible to make in this case. Therefore, the experiments were also performed with Dap dCDI, which is not able to inhibit the activity of CycE/Cdk2 any longer and thereby does not impair the cell cycle distribution. Table 20 summarizes the results of the flow cytometric protein stability experiments of Dap dCDI.

Table 20 Summary of flow cytometric protein stability analysis of Dacapo dCDI
- and black box = destabilization; + and white box = stabilization; 0 and grey box = no effect; n.a. = not applicable

Dacapo dCDI				
Expressed constructs	all	G1	S	G2
4xFLAG Skp2	+	+	+	0
CycE	-	-	-	0
4xFLAG Skp2 + CycE	0	0	0	+
Skp2 4xFLAG	+	+	+	+
CycE	-	-	0	0
Skp2 4xFLAG + CycE	0	0	0	+
Cks85A	0	0	+	+
4xFLAG Skp2 + Cks85A	n.a.	n.a.	n.a.	n.a.
CycE + Cks85A	-	-	0	+
4xFLAG Skp2 + CycE + Cks85A	0	0	+	+
4xFLAG Skp2	+	+	+	+
4xFLAG Skp2 dF-Box	+	0	+	+
Skp2 Hairpin vs. Hygro Hairpin	0	0	0	0

While Dap dCDI does no longer have an effect on the cell cycle, it is still degraded in S-Phase by $CRL4^{Cdt2}$ because of its PIP-degron. Since this degradation mechanism may cover the effects that Skp2 might have, the mutant Dap dCDI dPIPa was also used. This version is no longer degraded in S-Phase by $CRL4^{Cdt2}$ via its PIP-box, which makes it possible to emphasize on potential Skp2 effects. A summary of the results of the protein stability analysis can be found in Table 21.

Table 21 Summary of flow cytometric protein stability analysis of Dacapo dCDI dPIPa
- and black box = destabilization; + and white box = stabilization; 0 and grey box = no effect

Dacapo dCDI dPIPa				
Expressed constructs	all	G1	S	G2
4xFLAG Skp2	+	+	+	0
CycE	0	0	0	0
4xFLAG Skp2 + CycE	+	0	+	+
Skp2 4xFLAG	+	+	0	0
CycE	0	0	0	0
Skp2 4xFLAG + CycE	0	0	+	+
Skp2 Hairpin vs. Hygro Hairpin	+	+	0	0

The following sections will deal with a comparison of the effects of the different treatments on the three Dacapo versions. Overexpression of Skp2 (regardless of the position of the FLAG tag) did not have a destabilizing effect on Dacapo (full length). Both Skp2 versions did also not have a destabilizing effect on Dap dCDI. Instead, stabilization was observed in this case. This data is not in concordance with the results of Dui et al. (2013), who saw reduced levels of Dap upon Skp2 overexpression. Since overexpressing Skp2 led to longer G1-Phases in S2R+-cells, it is possible that the stabilization of Dap dCDI was derived by reduced degradation in S-Phase. However, the construct Dap dCDI dPIPa that is not targeted by $CRL4^{Cdt2}$ in S-Phase did also show stabilization upon Skp2 overexpression. If the stabilization of Dap by Skp2

overexpression was derived from the reduction of S-Phase cells, this construct should have no longer shown this effect. Skp2 overexpression apparently caused stabilization of Dacapo by other means.

Another explanation for the stabilization would be that SCF^{Skp2} is indeed targeting Dap dCDI for ubiquitination, but in this case, this would not be a signal for proteasomal degradation. Instead, it may have another effect on Dap, perhaps activation or induction of complex formation with a Dap partner. This effect may have been not seen with Dap (full length) but the G1-arrested cells could have behaved differently. It is already known that SCF^{Skp2} can have other effects than marking target proteins for degradation. Skp2 ubiquitinates LKB1, an important kinase for various different cell processes, for example energy metabolism, apoptosis, proliferation and cell polarity. Ubiquitination of LKB1 by Skp2 does not mark the protein for proteasomal degradation but leads instead to the complex formation with activators of LKB1 and subsequent protein activity (Lee et al., 2015). A similar mechanism may also exist in case of Dacapo.

If this would be indeed the case, overexpression of a Skp2 variant without a functional F-Box should exert the dominant-negative effect of either insensitivity or even destabilization on Dap. The deletion of the F-Box does not impair the binding of the F-Box protein to its respective substrate. However, since the recruitment onto the SkpA-Cul1-Rbx1 complex is no longer possible and the substrates cannot be bound from two F-Box proteins at the same time, they are protected from ubiquitination and subsequent processes. The detection of a dominant-negative effect under these circumstances is one possibility to identify substrates of F-Box proteins (Carrano et al., 1999). In this respect, results with Skp2 dF-Box overexpression argue against an impact of Skp2 on Dap. The effects of Skp2 dF-Box on Dap (full length) and Dap dCDI were altogether comparable to the overexpression of Skp2. A dominant negative effect was not observed, which would be a sign for regulation by Skp2. This is another argument that Dap is not a substrate of Skp2.

It is possible that Skp2 is indirectly affecting the stability of Dap by influencing mechanisms that are responsible for Dap degradation. The PIP-mediated degradation pathway cannot be the only way for Dap regulation in the cell. An initial degradation has to take place for the transition into S-Phase. Therefore, it may be possible that Skp2 overexpression changes activities of proteins that control Dap stability at the G1-S transition.

CycE overexpression did also not have any destabilizing effect on Dap (full length). This is unexpected at first glance, since CycE overexpression should bring the cells in S-Phase were Dap degradation takes place, mediated by its PIP-degron. The explanation for the absence of this effect is that under these experimental conditions, Dacapo overexpression resulted in G1 cell arrest that could not be overcome by CycE overexpression (Figure 53D). Thus, the rapid cell cycle shift into S-Phase did not take place and the PIP-mediated degradation pathway, that can only happen in S-Phase, was not intensified. In contrast, Dap dCDI was destabilized if CycE was overexpressed. This was the expected outcome, since Dap dCDI does no longer influence the cell cycle (Figure 19E,F) and was degraded by the PIP-degron mechanism upon the rapid transition into S-Phase, caused by CycE overexpression. Dap dCDI dPIPa on the other hand did no longer react to CycE overexpression, since the PIP-degron is no longer active.

Biochemical analysis in Dui et al. (2013) shows that binding between Skp2 and Dap is greatly enhanced by Cks85A overexpression. In opposition to this result, overexpression of Cks85A neither alone, nor in combination with 4xFLAG Skp2 or CycE or both proteins combined did influence the stability of Dap (full length) measured by flow cytometry. In case of Dap dCDI, overexpressing Cks85A did also not lead to

protein instability. For the combined overexpression of 4xFLAG Skp2 and Cks85A only one set of data was available, hence, no conclusion could be drawn from this experiment. Combined overexpression of the three components Cks85A, CycE and 4xFLAG Skp2 did also not result in the degradation of Dap dCDI. In conclusion, Cks85A did not decrease the stability of the two Dap versions. Therefore, it was considered very unlikely that Cks85A is exerting a negative effect on Dap stability in combination with Skp2. Consequently, it was dropped from the stability analysis of Dap dCDI dPIPa.

It is known that Skp2 uses phosphorylation for substrate recognition (Skaar et al., 2013). To include this aspect, Skp2 and CycE were simultaneously expressed. This should lead to phosphorylation of the expressed Dap versions, which may help to make them accessible for Skp2 recognition. However, this approach did also not lead to a significant change in Dap (full length) stability, regardless of the position of the FLAG tag at Skp2. In the experiments with Dap dCDI however, a peculiarity of the data was that the overexpression of both components did not change the stability any longer, while the overexpression of the single proteins did indeed lead to either stabilization (overexpression of Skp2 versions) or destabilization (CycE overexpression) respectively (Table 20). This effect was not seen for Dap dCDI dPIPa, where overexpression of both components all in all showed the same effect as the overexpression of Skp2, a stabilization of the Dap dCDI dPIPa protein. One possible interpretation of these differing results is that the stabilization of Skp2 overexpression and destabilization of CycE overexpression are independently compensating each other in the case of Dap dCDI. This cannot work any longer in the case of Dap dCDI dPIPa, since CycE overexpression does no longer exercise the destabilizing effect.

Knockdown of Skp2 did not change the stability of Dap (full length), except in S-Phase, were stability increased. If this was a real effect or an artifact of the Dap G1 cell cycle stop or the experimental procedure (see later) is not sure though. In case of Dap dCDI, Skp2 knockdown did not have any significant effect on protein stability, speaking against Dap being a substrate for SCF^{Skp2}. Remarkably Skp2 knockdown did lead to a stabilization of Dap dCDI dPIPa, at least in all and G1-cells. The stabilization of Dap dCDI dPIPa after Skp2 knockdown could point to Skp2 being directly involved in Dap protein stability, but all other experiments did not support this idea. It should be also noted that Skp2 overexpression resulted in partial stabilization of Dap dCDI dPIPa in S- and G2-Phase. Skp2 overexpression should have the opposite effect in comparison to the Skp2 knockdown, in this case destabilization of Dap dCDI dPIPa. These inconsistencies make the conclusion that Skp2 is responsible for direct Dap regulation doubtful. One explanation would be that Skp2 is degrading an unknown component, responsible for Dap stabilization. Another explanation can be hypothesized based on the cell cycle changes of Skp2 knockdown and regulation of stability of Dap dCDI dPIPa. Dap degradation probably must start in G1-Phase, since CycE/Cdk2 activity has to be strongly increased so that the transition to S can be performed. This thesis argues against Skp2 being responsible for this step. Indeed, another thesis in the Sprenger group found that the F-Box protein Rca1, the fly homologue to Emi1, is responsible for Dap degradation in G1 (Kies, 2017). Skp2 knockdown did lead to a faster transition from G1 to S. It is possible that this shortened G1-Phase did not offer enough time for a normal Dap degradation through SCF^{Rca1}. Consequently, the amount of Dap dCDI dPIPa was higher than normal. The fact that Dap dCDI did not show stabilization if Skp2 is knocked down does not speak against this theory, since in this case, the excess protein will be efficiently degraded by the proteasome because of ubiquitination by $CRL4^{Cdt2}$. Since this degradation pathway was shut off in Dap dCDI dPIPa, the protein accumulated, resulting in “stabilization” when analyzed. One caveat of this hypothesis is that the observed G2-shift of the Skp2 hairpin construct was weak, making it at least questionable that the length of G1-Phase was strongly affected. A live cell imaging experiment, as already described (see 4.2.7) might give deeper insight into the exact effect of Skp2 hairpin on G1-length.

To conclude this section about the Dacapo protein stability, determined by flow cytometric analysis, it can be stated that the majority of the protein stability data gathered speak against Dacapo being a substrate of SCF^{Skp2} for negative regulation. Various different approaches were undertaken to incorporate different factors: phenotypic effects and alternative regulatory pathways of Dap, substrate modification by phosphorylation and the presence of an additional supporter protein. Furthermore, not only overexpression experiments were performed but also knockdowns and approaches with a dF-Box version of Skp2. Yet, only the stabilization of Dap dCDI dPIPa under Skp2 knockdown conditions showed a hint for Dap being degraded upon Skp2 ubiquitination, and this result is explainable in different ways. Contrary, some results seemed to indicate that Skp2 activity actually contributed to Dacapo stabilization.

These results are in contrast to the publication of Dui et al. (2013), which stated that Dap protein levels are diminished if Skp2 is overexpressed in Schneider cells and fly eyes. On the other hand, Ghorbani et al. (2011) found that Dap levels were not elevated in larvae and extracts from brain/imaginal discs of Skp2 knock out flies, speaking against a Skp2 dependent regulation of Dap. The results of the protein stability assays in this thesis strengthen this notion.

Additionally, the results regarding the cell cycle shifts of Skp2 knockdown presented here may explain some of the effects seen in Ghorbani et al. (2011). In this investigation, a knockout of Skp2 led to decreasing levels of endogenous Dap in mitotic tissues. The result of the live cell imaging experiments showed that cells exited G1-Phase faster under Skp2 knockdown conditions (see 6.1.2) and since Dap is efficiently degraded in S-Phase mediated by its PIP-degron, it seems reasonable that the faster transition into S-Phase results in increased Dap degradation.

It is important to note that the determination of protein stability by flow cytometry is a new approach in the Sprenger group. Although the assay seems to work in principle (Polz, 2017) experience is limited and the method and even the handling of the flow cytometer is still improved. Future refinements will probably give results with greater precision. One of the critical points is the definition of the G1-, S- and G2-cell population. The set boundaries, based upon Hoechst intensity (see 4.2.6.5 and Figure 9), are educated guesses, derived from operating experience. A better approach would be to visualize directly the S-Phase cell population for example by EdU or BrdU assays. Specified algorithms and programs, like Modfit LT (Verity Software House), can then use this data to give a more sophisticated estimation of the different cell cycle phases. Especially the determination of S-Phase is debatable, since Schneider cells do not show a clear S-Phase plateau in the flow cytometer and S-Phase cells overlap with the G1- and G2-peak. This is possibly also the explanation of a peculiarity in the data regarding the stability of Dap dCDI. In the majority of these experiments, Dap dCDI was not degraded in S-Phase, which it must be, because degradation depends on PCNA, present exclusively in S during DNA replication. This was probably an artifact of the flow cytometric protein stability assay. Experiments already showed that the population of cells called “G1” actually also contains cells in early S-Phase, whereas the population called “S” is composed of cells in the middle of S-Phase in this setup (Heimbucher, 6-week internship). These inaccuracies should be kept in mind in the interpretation of protein stability in the three distinct cell cycle phases.

Lastly, the statistical analysis of individual experiments with large sets of data might be improved by using alternative methods, for example an ANOVA (analysis of variances). The applied statistical analysis might also explain why the control experiments sometimes showed a statistically significant effect on mCherry stability upon overexpression of different components (see Figure 20C, Figure 35A and C and Figure 47C). In all other cases, stability of the control fluorescent proteins stayed unaltered, regardless of any

overexpression. Nonetheless, with the knowledge of the time point of writing this thesis, Skp2 did not negatively regulate Dap stability.

Beside protein stability assays, co-immunoprecipitations with Skp2 and Dap were performed to test for biochemical interaction. Most Co-IPs showed no interaction between these two proteins, although many parameters were changed during the thesis. Interaction of Skp2 4xFLAG with HA Dap was never seen. Furthermore, the simultaneous overexpression of Cks85A did also not result in protein interaction. To test if the tags were critical for this potential interaction, they were swapped. Yet, an interaction between 3xHA Skp2 and 4xFLAG Dap was also not visible, regardless of the presence of Cks85A.

This was in contrast to the published observation that Skp2 interacts with Dap in S2 cells and that overexpressing Cks85A does lead to a boost of this effect (Dui et al., 2013). All versions of Skp2 tested here showed very strong interaction with Cks85A (which was used as a positive control in all Co-IP experiments and not shown). Furthermore, the used versions of all proteins, regardless of Skp2 or Dap, resulted in principle in the expected cell cycle changes and stability. This is a hint that these proteins are in fact active, ruling out this potential source of misinterpretation.

Finally, some interaction could be observed if 4xFLAG Dap or 4XFLAG-Dap-dCDI was precipitated and HA Skp2 detected. However, unspecific binding of HA-Skp2 was also observed and the validity of this result has to be considered carefully. Since both Dap and Dap dCDI showed interaction with Skp2, it can be ruled out that the interaction was indirect. It was a possibility that Skp2 binds indirectly to Dap through interaction with Cks85A (Ghorbani et al., 2011), which binds to CycE/Cdk2 (Ghorbani et al, 2011), which is the target of Dap binding (Lane et al., 1996). Precipitating Dap may lead to a co-precipitation of all other components, so that Skp2 is detectable on the Western Blot without actual direct interaction, therefore. Dap dCDI is no longer binding to CycE/Cdk2 however, and this theory can be rejected.

Mass-spectrometric analysis of 4xFLAG Skp2 interaction partners also failed to detect Dap (see 6.6). In addition, another MS-analysis was performed the Sprenger group with the aim to identify interaction partners of 4xFLAG Dap dCDI dPIPa. Skp2 is also not found in this analysis with a significant score (Kies, 2017), another hint that there does not exist an interaction between both proteins.

In conclusion, it was not possible to detect a robust biochemical interaction between Dap and Skp2 in the presented results. While it is difficult to rule out technical aspects, this data is in agreement with the stability analysis of Dap and the biological assays (G1-rescue, see below). Furthermore, biochemical interaction does not automatically mean ubiquitination, and ubiquitination does not mean degradation. As already mentioned, it is known, at least in one case, that Skp2 mediated ubiquitination leads to protein activity (Lee et al., 2015). Co-IPs alone can therefore not prove negative regulation of Dap by Skp2.

Lastly, the biological effect of Skp2 on the Dap G1 arrest also argues against an involvement of Skp2 in Dap degradation. The combined overexpression of Dap and Skp2 led to an even greater accumulation of cells in G1-Phase and not to a rescue of the accumulation in G1. It is hard to say if this result can be traced back to an independent function of both proteins or if both overexpressions were working synergistically to excel the single effects. Anyway, a rescue was by all means not detectable, speaking again against a degradation of Dap triggered through binding to Skp2.

Until now, there are two sources differing in their results regarding the regulation of Dap by Skp2 in *Drosophila*. While Ghorbani et al. (2011) did not see Dap being a substrate for SCF^{Skp2}, Dui et al. (2013) saw evidence for this relationship. One aim of this thesis was to solve this discrepancy. The majority of the

gathered results showed that it is very unlikely that Dap is negatively regulated by Skp2 in flies. The only result speaking for this theory, the stabilization of Dap dCDI dPIPa upon Skp2 knockdown, can be explained alternatively. There were minor hints for stabilization of Dap through Skp2 activity. Dap dCDI showed stabilization if Skp2 was overexpressed and biochemical interaction was detected, albeit this result was not without doubt. Therefore, it is questionable if this relationship can be confirmed. More experiments have to be undertaken to make a clear conclusion. Negative regulators for Dap may be, as already mentioned, Rca1 (Kies, 2017) or other unconsidered F-Box proteins. In this regard, it should be mentioned that p27 is at least in NIH 3T3 cells and mouse embryonic fibroblasts, not only degraded by SCF^{Skp2} and $CRL4^{Cdt2}$ but also by the Kip1 ubiquitination-promoting complex KPC (Kamura et al., 2004), opening the possibility for additional regulators of Dap.

The question remains why Dui et al. (2013) did see a Skp2 dependent degradation of Dap and biochemical interaction between both proteins. Some of these results can be explained in an alternative way. Since the authors used Dap full length for their assays, the cell cycle of the used Schneider cells was deeply disturbed. This may have a wide range of effects on the processes in a cell with uncontrollable outcome for the molecular mechanisms. For example, it is well known that the Dap homologue p27 needs to be phosphorylated in order to get ubiquitinated (Montagnoli et al., 1999). This may also be the case in *D. melanogaster*. Dap overexpression means less CycE/Cdk2 activity and consequently less phosphorylation of Dap, making it unlikely to become a target for SCF^{Skp2}. Another example is their result that Skp2 knockdown leads to more Dap protein. Skp2 knockdown however led to a prominent accumulation of cells in G2-Phase were Dap is no longer a target of degradation, resulting in stabilization. Since the results presented in this thesis are from Dap mutations that do not affect the cell cycle any longer and are not degraded by $CRL4^{Cdt2}$, these possible sources of misinterpretation are diminished and the presented analysis is much more precise.

One difference in the Co-IP experiments was the tag of the Dacapo protein. The experiments performed in this thesis were done with a HA tagged and not Myc tagged Dap as in the publication and it may be that the HA tag is preventing Skp2 to bind to Dap. On the other side, the HA tag does not prevent Dap from being recognized by Rca1, another F-Box protein (Kies, 2017). An additional aspect that differed were the buffer conditions, though it has to be said that positive controls in general worked with the used buffers and, more importantly, that interaction between Skp2 and other potential substrates could be seen with this setup (see 6.4 and 6.5).

Another possible explanation is that the used cell lines are different and Skp2 behaves differently in this case. Dui et al. (2013) used S2 cells, while the cells used in this thesis were S2R+. This may on the first glance not make a big difference but it is known that different Schneider cell lines show high diversification and different transcription patterns (Cherbas and Gong, 2014). Furthermore, it is known that, at least in certain rat cells, the function of Skp2 is dependent upon cell adhesion. Skp2 overexpression did lead in these cells to more incorporation of BrdU, equivalent to more S-Phase cells. Yet, this effect could only be observed in non-adherent Rat-6 cells, adherent cells did not show any effect on Skp2 overexpression (Carrano and Pagano, 2001). This is interesting, since one difference between the two *Drosophila* cell lines is in fact that S2R+-cells are more adherent than S2. Non-adherent cells are not included in the assays since the sample preparation protocols (see 4.2.6.2) in the Sprenger group discard the medium before any experiments, only cells sticking on the bottom of the well are analyzed. This may also underline the assumption made in mammalian cells that Skp2 function is dependent of the cell type (Krishnan et al., 2017).

6.4.Cdt1 stability is regulated by SCF^{Skp2} in *D. melanogaster*

Cdt1 is an important regulator of DNA replication and a known substrate of SCF^{Skp2} in mammalian cells (Li et al., 2003). Skp2 mediated ubiquitination marks Cdt1 for proteasomal degradation, which is one way for regulation of Cdt1 activity during the cell cycle. Overexpression of Cdt1 results in rereplication in human cells (Liu et al., 2007) and fly cells (see Figure 32). Rereplicating cells were also seen upon prolonged Skp2 knockdown (see 6.1.1), making it possible that Cdt1 is a substrate of Skp2. These hints led to an investigation if SCF^{Skp2} also targets Cdt1 in flies.

Cdt1 overexpression showed rereplication (Figure 32B). This resembles the results of Cdt1 overexpression in some human cancer cell lines (H1299 and U2OS) that also exhibit rereplication under these treatments. It has to be said though that the effect of Cdt1 overexpression is dependent upon the used cell line. Only human cancer cell lines exhibit rereplication if Cdt1 is overexpressed. Non-cancer cell lines respond to Cdt1 overexpression alone only weakly (Liu et al., 2007). Yet, a simultaneous overexpression with Cdc6 leads to rereplication also in these cases (Sugimoto et al., 2009).

Overexpression of Cdt1 dPIP that is no longer targeted by $CRL4^{Cdt2}$ for ubiquitination in S2R+-cells exhibited a stop of the cell cycle, possibly not in G1- but in early S-Phase, since the peak of the distribution curve was slightly shifted (Figure 32C). This hypothesis should be investigated further, for example by using S-Phase cell cycle markers or the incorporation of BrdU in the DNA during DNA-synthesis. Both assays would give reassurance of the S-Phase cell cycle stop. The described Cdt1 dPIP overexpression effects in S2R+-cells are similar to the results of a study that also used a PIP-Box-deleted Cdt1 version in *Drosophila* embryos (Lee et al., 2010). Overexpression of this Cdt1 dPIP version did also lead to a stop of the cell cycle in S-Phase in epidermal cells of fly embryos. The authors speculated that turning off the PIP-mediated degradation of Cdt1 leads to high levels in S-Phase, resulting in reinitiation of replication origins. Thereby, DNA damage occurs and a checkpoint is activated, which stops the cell cycle. This study also found that ubiquitous expression of Cdt1 dPIP led to embryonic death and that the PIP-Box dependent degradation of Cdt1 is exclusively important for the proliferating tissues; cells that perform endocycles are not disturbed. The situation in higher eukaryotes seems to be similar. A stabilized version of Cdt1, lacking the first 32 amino acids including the PIP-Box, was overexpressed in HeLa cells. In this case, cells accumulate for a prolonged period in G1-Phase, and furthermore subsequent S-Phase is longer as well (Takeda et al., 2005). Deactivating the prominent PIP-degradation pathway of Cdt1 probably results in protein accumulation. Another example are human U2OS cells, where an accumulation of Cdt1 leads to activation of cell cycle checkpoints, resulting in a stop in S-/G2-Phase (Klotz-Noack et al., 2012).

Rereplication of S2R+-cells was not observed in this thesis if Cdt1 dPIP was overexpressed. This is also in concordance with Takeda et al. (2005), since the authors showed that the capability of their truncated Cdt1 version to trigger rereplicaton is abolished.

Working with full length Cdt1 is challenging since cell cycle effects and PIP-degron dependent degradation are making the interpretation of the results difficult. Cdt1 15-600 was created by deleting the PIP-degron and the MCM binding domain, eliminating these factors. The effect of Cdt1 15-600 on the cell cycle was greatly diminished, yet, there still was a slight shift into G1-Phase visible (Figure 32F,G). Further truncations of Cdt1 with a deleted Geminin binding domain showed similar effects, excluding an involvement of Geminin in this cell cycle shift (Figure 38B,C). The cause of this shift therefore is unknown and requires further analysis.

In order to analyze if Skp2 mediates degradation of Cdt1 the first set of experiments were performed with GFP Cdt1 1-600. Table 22 summarizes the results of the flow cytometric stability analysis. In concordance with the assumption that Cdt1 is regulated by Skp2, stability was reduced by overexpression of Skp2 and Skp2 and CycE combined. Likewise, Skp2 knockdown led to stabilization of GFP Cdt1 1-600. These were only preliminary results, however, since Hoechst fluorescence, necessary for determining the cell cycle distribution, is interfering with the GFP signal, diminishing the accuracy of the stability. In this Cdt1 version, the N-terminal PIP-degron motive is not deleted. However, it seems reasonable that the PIP-degron is not active in this construct, since fusing large protein tags to the N-terminus of Cdt1 impedes this degradation pathway (Senga et al., 2006). To exclude this possibility completely, all further experiments with mChe tagged versions of Cdt1 featured a deleted PIP-Box.

Table 22 Summary of flow cytometric protein stability analysis of GFP Cdt1 1-600
- and black box = destabilization; + and white box = stabilization; 0 and grey box = no effect

GFP Cdt1 1-600				
Expressed constructs	all	G1	S	G2
Skp2	-	-	0	-
CycE	0	0	0	0
Skp2 + CycE	-	-	-	0
Skp2 Hairpin vs. Hygro Hairpin	+	+	+	0

Subsequent experiments were performed with mChe tagged versions of Cdt1. One caveat in all mChe Cdt1 experiments was that analysis of different expression levels showed strong differences in protein stability. This effect had probably something to do with Cdt1, since it was not observed in any of the other experiments in this thesis. A speculative explanation is that the expression levels of Skp2 (or Skp2 hairpin in case of knockdown experiments) were not proportional to the expression of mChe Cdt1. In other words, the ratio of Skp2 to Cdt1 protein may not always be identical in both expression levels, which will of course affect the stability of Cdt1. This effect was not seen in experiments with Dacapo (see section 6.3) or CycE (see section 6.5) to a great extent, probably because these proteins did not show regulation by Skp2 in the flow cytomentric protein stability assay.

Stability analysis of mChe Cdt1 15-600 (Table 23) showed a distinct destabilization effect of Skp2 overexpression only if CycE was also overexpressed. CycE overexpression corresponds to more Cdk2 activity and consequently to more phosphorylation. It is already known that *Drosophila* Cdt1 is phosphorylated by CycE/Cdk2 activity (Thomer et al., 2004). Furthermore, it could be shown that at least one of the used constructs (Cdt1 15-263) is phosphorylated upon CycE overexpression by using a PhosTag enriched SDS-PAGE gel (Heimbucher, 6-week internship). It is also well known that substrates have to be phosphorylated for the recognition by Skp2 (Skaar et al., 2013).

Furthermore, Skp2 dF-Box stabilized Cdt1 15-600 under CycE overexpression conditions and exhibited a dominant-negative effect thereby. This is an approach used routinely for identifying new substrates of F-Box proteins (Carrano et al., 1999). Skp2 knockdown did also have a stabilizing effect on mChe Cdt1 15-600, another argument for Skp2 dependent regulation. The conclusion drawn from these experiments was that Cdt1 is indeed a substrate for SCF^{Skp2} in *D. melanogaster*, its recognition by Skp2 dependent on the phosphorylation status.

Table 23 Summary of flow cytometric protein stability analysis of mChe Cdt1 15-600
- and black box = destabilization; + and white box = stabilization; 0 and grey box = no effect

Che Cdt1 15-600								
	Expression level: 1.25 – 2.00				Expression level: 2.00 – 2.75			
Expressed constructs	all	G1	S	G2	all	G1	S	G2
Skp2	0	-	+	-	0	-	0	0
Skp2 dF-Box	+	0	+	0	+	0	+	+
Che Cdt1 15-600 + CycE								
Skp2	-	-	-	-	-	0	-	0
Skp2 dF-box	+	+	+	0	+	+	+	0
Che Cdt1 15-600								
Skp2 Hairpin vs. Hygro Hairpin	+	+	+	+	+	0	+	+

Interestingly, the study of Cdt1 dPIP effects in embryos (Lee et al., 2010) did not find a stabilization of Cdt1 if regulation by both degradation pathways are eliminated. By combining their PIP-Box deletion with the 10A version of Thomer et al. (2004), which probably also eliminates the Skp2 mediated degradation, the authors created a Cdt1 version that should be in theory stable in the cell cycle. Yet, the result of this experiment is that the additional 10A mutations, eliminating the phospho-sites that are presumably important for the degradation by the SCF^{Skp2}-complex, do not increase the Cdt1 stability, speaking against a phospho-dependent regulation through SCF^{Skp2}. One possibility is, of course, that Cdt1 regulation differs in embryos in comparison to S2R+-cells. It could also be that the method to determine protein stability in this case was imprecise. The authors used BrdU staining to identify S-Phase cells in embryos and applied immunostainings against their Cdt1 versions to find out if Cdt1 is absent in S-Phase cells. This is however not a fitting method to determine gradual or modest changes in protein stability. The assays used in this thesis are probably more sensitive in this respect.

Various truncations of Cdt1 were created with the aim to identify the phosphorylation sites necessary for recognition by Skp2. In a first step, mChe Cdt1 15-300 was created, deleting the Geminin-binding site. Results of flow cytometric protein stability analysis were for the most part comparable to Cdt1 15-600, destabilization was seen if Skp2 and CycE were overexpressed simultaneously (Table 24). Likewise, Skp2 dF-Box overexpression led to stabilization of Cdt1 15-300 under these conditions. It seems that Skp2 and CycE overexpression did not affect Cdt1 15-600 in G2-Phase in the higher expression level, yet, Cdt1 15-300 was degraded by the same treatment. This corresponds to the situation in human cells, were one task of Geminin is to protect Cdt1 from proteasomal degradation in G2 and M (Ballabeni et al., 2004). Later on, it was shown that Geminin protects Cdt1 explicitly from the recognition by Skp2 and degradation in mitosis (Tsunematsu et al., 2013). The presented data hints that this may also be the case in *D. melanogaster*. It should be noted however that this effect was only visible if higher expression levels were analyzed. The experiments did not show any difference in case of the lower expression level and more experiments have to be performed to make a clear statement about a potential protective function of Geminin in *Drosophila*. In any case, since Cdt1 15-300 still reacted to Skp2 and Skp2 dF-Box overexpression, the phosphorylation sites were still present in this fragment. Therefore, Geminin seems to play no part in this degradation pathway.

Table 24 Summary of flow cytometric protein stability analysis of mChe Cdt1 15-300
- and black box = destabilization; + and white box = stabilization; 0 and grey box = no effect

Che Cdt1 15-300								
	Expression level: 1.25 – 2.00				Expression level: 2.00 – 2.75			
Expressed constructs	all	G1	S	G2	all	G1	S	G2
Skp2	0	-	0	-	0	-	0	-
Skp2 dF-Box	+	0	+	0	0	0	+	-
Che Cdt1 15-300 + CycE								
Skp2	-	-	-	-	-	0	-	-
Skp2 dF-box	+	+	+	0	+	0	+	+

The stability and phosphorylation sites of *Drosophila* Cdt1 were already investigated. As mentioned before, Thomer et al. (2004) found that Cdt1 stability is partly dependent upon 10 phosphorylation sites residing within the first 300 amino acids of the protein. Mutating all 10 phospho-sites results in partial stabilization of this fragment. The authors of this paper assume that a second, phosphorylation independent way of degradation exists. Probably, this is the degradation by $CRL4^{Cdt2}$, mediated by the PIP-degron in Cdt1, since the function of the PIP-degron was not known back in 2004.

Table 25 Summary of flow cytometric protein stability analysis of mChe Cdt1 15-225, Cdt1 15-263 and Cdt1 170-300
- and black box = destabilization; + and white box = stabilization; 0 and grey box = no effect

Che Cdt1 15-225								
	Expression level: 1.25 – 2.00				Expression level: 2.00 – 2.75			
Expressed constructs	all	G1	S	G2	all	G1	S	G2
Skp2	+	+	+	0	0	0	0	-
Skp2 dF-Box	0	0	+	0	0	0	0	0
Che Cdt1 15-225 + CycE								
Skp2	0	0	0	0	-	-	-	-
Skp2 dF-box	0	0	0	0	0	0	0	0
Che Cdt1 15-263								
	Expression level: 1.25 – 2.00				Expression level: 2.00 – 2.75			
Skp2	0	0	0	0	0	-	0	0
Skp2 dF-Box	0	0	0	0	0	0	0	0
Che Cdt1 15-263 + CycE								
Skp2	-	0	-	-	-	0	-	-
Skp2 dF-box	+	0	+	0	0	0	0	0
Che Cdt1 170-300								
	Expression level: 1.25 – 2.00				Expression level: 2.00 – 2.75			
Skp2	0	0	+	0	0	0	0	0
Skp2 dF-Box	+	+	+	+	0	0	+	0
Che Cdt1 170-300 + CycE								
Skp2	0	0	0	0	0	0	0	0
Skp2 dF-Box	+	0	+	0	0	0	0	-

Regarding the state of knowledge, one can assume that SCF^{Skp2} needs either one, a subset or all of these 10 phosphorylation sites to recognize Cdt1 as its substrate. Consequently, these 10 phospho-sites were closer analyzed. To minimize the mutations needed for this analysis, three truncations of the N-terminal part were analyzed beforehand.

From the three tested truncations, only mChe Cdt1 15-263 showed a degradation pattern resembling that of Cdt1 15-600 (Table 25). mChe Cdt1 15-225 was not degraded under CycE overexpression conditions if the lower expression level was analyzed and stabilization upon Skp2 dF-Box expression was never seen. Furthermore, Skp2 overexpression alone led to stabilization, which is very unusual, disqualifying this fragment for further analysis. Cdt1 170-300 on the other hand was never degraded upon Skp2 overexpression.

Cdt1 15-263 still contained six optimal phosphorylation sites, S111, T158, S168, S226, S249 and T256 (Thomer et al., 2004), four of which were mutated. The mutation Cdt1 15-263 T158A was not expressed in S2R+-cells for unknown reasons and was also dropped from analysis.

Cdt1 15-263 S111A, S168A and S226A were analyzed and all showed destabilization after CycE and Skp2 overexpression like Cdt1 15-600 (Table 26).

Table 26 Summary of flow cytometric protein stability analysis of mChe Cdt1 15-263 S111A, S168A and S226A
- and black box = destabilization; + and white box = stabilization; 0 and grey box = no effect

Che Cdt1 15-263 S111A + CycE								
	Expression level: 1.25 – 2.00				Expression level: 2.00 – 2.75			
Expressed constructs	all	G1	S	G2	all	G1	S	G2
Skp2	-	-	-	-	-	0	-	-
Che Cdt1 15-263 S168A + CycE								
Skp2	-	0	-	-	-	0	-	-
Che Cdt1 15-263 S226A + CycE								
Skp2	-	0	-	0	-	-	-	-

Thus, critical phosphorylation sites responsible for recognition by Skp2 could not be identified, yet. It may well be that the remaining unmutated sites are responsible for the interaction with Skp2. Another possibility would be that beside the optimal phosphorylation sites, the minimal consensus sites (with the motive S/T-P) might also play a role in the recognition by SCF^{Skp2}. On the other hand, single mutations might not lead to a loss of the interaction with Skp2 and stabilization. Indeed, in human Cdt1 it is assumed that two sites, T29 and S31, might have to be phosphorylated for Skp2 binding (Nishitani et al., 2006). T29 is at least confirmed as important in this regard (Takeda et al., 2005). The authors of the same paper also state that up to their knowledge all SCF^{Skp2} substrates are phosphorylated at a threonine for recognition, making the Cdt1 T158A and T256A mutations a worthy subject of further investigation. Besides mutating the last two phospho-sites, another rewarding approach would be to create a Cdt1 6A version, were all six relevant sites are phosphorylated. This might lead to insensitivity of Cdt1 toward Skp2 overexpression, confirming the importance of the selected phospho-sites. Further analysis using a combination of single mutations or mutating other phosphorylation sites might be necessary to unravel critical phosphorylation sites.

Biochemical interaction between Skp2 and Cdt1 15-600 could also be detected, though according to the signal intensity, this interaction was only weak (Figure 50). It is possible that the majority of ubiquitinated

Cdt1 is rapidly degraded by the proteasome. Using a proteasomal inhibitor (e.g. MG132 or Bortezomib) may stabilize Cdt1 and lead to stronger signals. However, a direct physical binding between Skp2 and its substrates may be extremely short and therefore hard to detect in a Co-IP assay (Frank Sprenger, personal communication).

As mentioned, overexpression of Cdt1 or Cdt1 dPIP in S2R+-cells led to changes in the cell cycle distribution. Cdt1 overexpression resulted in accumulation in G2-Phase and rereplication, while overexpressing Cdt1 dPIP showed more cells in G1- or early S-Phase. Modulating the amount of Skp2 protein did influence the cell cycle phenotypes of Cdt1 overexpression and knockdown (Figure 51 and Figure 52). This is a hint for genetical interaction between both proteins. Skp2 overexpression reduced the rereplication caused by Cdt1, possibly because the excess amount of Cdt1 could be controlled by the higher amount of SCF^{Skp2} in this case. The cell accumulation in G1 or early S-Phase upon Cdt1 dPIP overexpression was also weakened upon Skp2 overexpression. Remarkably, Skp2 overexpression resulted in a reappearance of a G2 cell peak, in accordance with an increased degradation of Cdt1 dPIP. Skp2 overexpression effects observed in this thesis were always an accumulation of cells in G1. Therefore, the reappearance of G2 peak was not connected to other functions of Skp2 and a strong hint for a direct effect of Skp2 on Cdt1 dPIP. Both observations also underline that Skp2 regulation worked independently from PIP-box mediated degradation of Cdt1. Likewise, Skp2 knockdown did intensify the G2 cell accumulation of the Cdt1 overexpression, probably because the cell was lacking the ability to regulate Cdt1 by SCF^{Skp2} in this case. Importantly, Skp2 knockdown did also strengthen the stop at the G1/S boundary upon Cdt1 dPIP overexpression. This is remarkable, since Skp2 knockdown normally did always lead to more cells in the G2-Phase. This reversal is strong evidence for a direct effect of Skp2 on Cdt1 and in concordance with the equally unusual cell cycle effect of Skp2 overexpression, when Cdt1 dPIP is also overexpressed (see above). It cannot be explained by the effect that Skp2 knockdown may have on other cell cycle proteins since only under Cdt1 dPIP overexpression conditions did Skp2 knockdown led to G1 cell accumulation.

Cdt1 knockdown led to a stop of the cell cycle in G1-Phase and to cells with a smaller DNA content than 2C (Figure 52B). This corresponds to effects found in *Drosophila* Schneider 2D cells. Cdt1 knockdown does also lead to a sub-G1 cell population in this case (Mihaylov et al., 2002). The authors speculated that Cdt1 knockdown leads to uncoupling of mitosis and DNA replication, leading to cell division during G1-Phase. As a result, unusually small cells with a DNA content smaller than 2C will occur. This is not a general phenomenon though, HeLa cells do not show any visible cell cycle effect upon Cdt1 knockdown (Sugimoto et al., 2011), though HeLa cells, as a non-cancerous cell line, may be insensitive at least to Cdt1 overexpression. Simultaneous Skp2 knockdown rescued the Cdt1 knockdown partly (Figure 52D), another hint for genetic interaction between these two proteins.

In accordance with Skp2 being a regulator of Cdt1, the overexpression strengthened the Cdt1 knockdown phenotype, G1 cell accumulation was more pronounced, though this was only a minor effect (Figure 52E). Conversely, the number of cells smaller than 2C was also reduced, although a strengthening of the effect was expected. Perhaps this effect was the result of Skp2 regulation of as yet unidentified cell cycle regulators in *Drosophila*.

As a conclusion, the data presented in this thesis strongly hinted that *Drosophila* Cdt1 is regulated by the activity of SCF^{Skp2}. As a prerequisite for this regulation, Cdt1 has to be phosphorylated by CycE/Cdk2. This differs from data gathered in mammalian cells, were CycA/Cdk1 is the kinase responsible for Cdt1 phosphorylation (Pozo and Cook, 2016). However, CycE/Cdk2 is already discovered as the kinase responsible for Cdt1 phosphorylation in flies (Thomer et al., 2004) and this thesis underlines this fact. CycA

might still play a role though and further experiments may show if CycA/Cdk1 does also phosphorylate Cdt1 in *D. melanogaster*.

Considering the effect strength of modulated Skp2 levels on Cdt1 stability, it can be argued that Skp2 is not the main pathway for Cdt1 regulation. Indeed, Cdt1 is strongly regulated in the cell, since it is one of the key regulators of DNA replication (Pozo and Cook, 2016). There exist at least three more proteasomal degradation pathways to regulate Cdt1 stability: ubiquitination by SCF^{Fbxo31}, regulating Cdt1 in G2. Regulation by APC/C^{Cdh1}, necessary if cells enter G0 state. And of course, PIP-mediated ubiquitination by $CRL4^{Cdt2}$, responsible for S-Phase degradation or if DNA damage occurred (Hernandez-Carralero et al., 2018). Indeed, it is already shown in HeLa cells that Skp2 mediated degradation is not the main pathway for Cdt1 regulation. If the Skp2 recognition of Cdt1 is excluded by mutation of the responsible phospho-sites, Cdt1 is still efficiently degraded, probably by $CRL4^{Cdt2}$ (Takeda et al., 2005). All stability data in this thesis was gathered with Cdt1 versions that did not possess a functioning PIP-degron to concentrate solely on the effect of Skp2. Skp2 represents only one of several ways of Cdt1 regulation, and may only work as a supporter or back-up system. Another idea that already was proposed is that ubiquitination and subsequent degradation of Cdt1 by $CRL4^{Cdt2}$ cannot start directly in S-Phase, since it is dependent upon binding of PCNA on DNA. Consequently, there exists a time span until DNA replication starts and PCNA is recruited to the DNA, were Cdt1 would not be regulated and reinitiation of the replication origins could occur, with severe consequences for the replication machinery. Skp2 dependent degradation may keep Cdt1 activity under control in the beginning of S-Phase when DNA replication has not started and $CRL4^{Cdt2}$ cannot execute its regulatory function yet (Havens and Walter, 2011). Furthermore, Skp2 may also play a role to regulate Cdt1 levels after S-Phase, since uncontrolled activity may lead to origin firing and erroneous DNA replication. Interestingly, Ghorbani et al. (2011), the paper that identified Skp2 in *D. melanogaster*, did not see a regulation of Cdt1 by Skp2. Western Blots showed that the amount of Cdt1 protein either in whole 3rd instar larvae or in mitotic tissue (brains and imaginal discs) is not affected by Skp2 knock out. This is no contradiction to the conclusions of this thesis though, since endogenous Cdt1 is still degraded in S-Phase by $CRL4^{Cdt2}$, underlining the point that Skp2 has supporting function in Cdt1 regulation.

6.5.Results regarding Skp2 regulation of CycE are ambiguous

Flow cytometric analysis showed that CycE overexpression led to a dramatic shift of the cell cycle into G2-Phase and that CycE was unstable (Figure 53C). This shift is a result of the biological function of CycE; it binds and activates Cdk2, which ultimately leads to gene transcription of S-Phase genes and consequently to a rapid transition from G1- to S-Phase. The high instability is derived from proteasomal degradation in S-Phase by ubiquitination through SCF^{Ago} (Moberg et al., 2001). Skp2 is also identified in the mammalian system as a cause for CycE instability (Nakayama et al., 2000). In this thesis, experiments were conducted to test if CycE stability is influenced by Skp2 in the fly system. According to the data of the flow cytometric protein stability analysis, Skp2 overexpression or knockdown did not influence the stability of CycE (Figure 53). However, the strong instability of CycE, likely mediated by SCF^{Ago}, and the strong influence of CycE on the cell cycle made this analysis difficult to interpret.

It was tried to overcome the S-Phase dependent degradation and the CycE cell cycle effect by strong Dap overexpression. This resulted in a constant inhibition of CycE/Cdk2 activity and partial normalization of the cell cycle distribution. The possibility that Skp2 will interact with the ectopically expressed Dap was rejected because of the data regarding Skp2 regulation of Dacapo already gathered (see 6.3).

Dap overexpression did indeed lead to a cell cycle with distinguishable phases and to CycE stabilization (Figure 53D). However, experiments with Skp2 overexpression and knockdown in this setup did also not show any effect on CycE stability. It is striking that the standard deviation was unusually high in these cases. This may be a hint that some factor, perhaps CycE stability or Skp2 activity, was reacting differently to the Dap G1 arrest in the different replications. Possibly the G1 arrest was disturbing the cell cycle in such a fierce way that the normal processes are no longer working reliably. These data may be considered as also not reliable therefore.

Conversely, it is already known that SCF^{Skp2} is regulating CycE in mouse and human cells (Nakayama et al., 2000). In these cases, Skp2 targets specifically free, unbound CycE. Indeed, it was possible to detect biochemical interaction between Skp2 and CycE in flies with a Co-IP assay (Figure 56), which hints towards Skp2 dependent regulation. Furthermore, the observed cell cycle shifts upon changed Skp2 levels (Figure 11B,E; Figure 14C) are in concordance to the theory that Skp2 regulates CycE.

While the Co-IP experiment pointed to CycE being a substrate of Skp2, the flow cytometric protein stability analysis did not support this notion. A final conclusion is not possible, therefore. One way to tackle this challenge is to create a CycE mutant that is no longer capable of Cdk2-binding. Overexpression of this mutant will no longer perturb the cell cycle. Protein stability of this mutant will presumably also be higher than wild type CycE since cells are not progressing rapidly to S-Phase any longer, minimizing the influence of the SCF^{Ago} dependent degradation. Furthermore, this CycE version would exclude the possibility that Cdk2 protects it from Skp2 recognition. This could help to focus solely on the Skp2 effects regarding stability in the analysis. Indeed, recently such CycE mutants were generated in the lab, called CycE-deltaN-E340A and CycE-deltaN-K311A. Preliminary experiments showed that these versions are showing slight stabilization upon Skp2 knockdown (Serena Herzinger, personal communication), indicating that Skp2 may after all play a role in the regulation of CycE in *D. melanogaster*.

6.6. Mass spectrometric analysis revealed interaction of Skp2 with Cdk2 but did not identify interaction partners

Mass spectrometric analysis of 4xFLAG Skp2 binding partners showed that SkpA and Cul1 were interacting with this Skp2 version (Table 18). This is important, since it proved that the ectopically expressed 4xFLAG Skp2 was indeed incorporated in a SCF-complex. 4xFLAG Skp2 can perform its biological function of binding substrates to an E3 ubiquitin ligase therefore.

Another interesting hit was Cdk2. Indeed, it is already known that Skp2 biochemically interacts with Cdk2 through a Co-IP assay in *Drosophila* (Ghorbani et al., 2011). It is unlikely that Cdk2 is a target of SCF^{Skp2} ubiquitination and proteasomal degradation. In general, Cdks are stable proteins that are not regulated in the course of a cell cycle. Instead, Cdk activity is regulated by binding of cyclins and cyclins are the primary target of various cell cycle regulation mechanisms. Cdk2 is marked by the E3 ubiquitin ligase KLHL6 however, leading to proteasomal degradation. Yet, this does not happen during the cell cycle. Instead, proteasomal degradation of Cdk2 is a way for a cell to permanently exit the cell cycle and start cell differentiation (Ying et al., 2018). It is highly unlikely therefore, that Skp2 targets Cdk2 for ubiquitination and consequent proteasomal degradation during the cell cycle.

Another hypothesis is that Skp2 binds to Cdk2 to efficiently find and bind its targets. As already mentioned, Skp2 targets normally have to be phosphorylated. This phosphorylation is at least partly performed by the CycE/Cdk2 complex. If Skp2 is bound to Cdk2 during the phosphorylation of the substrate, Skp2 and its

substrate are located close together, allowing for efficient binding and ubiquitination of the substrate. This leads to a maximization of the ability of Skp2 to regulate its substrates. The fact that F-Box protein substrates need to be bound on a cyclin/Cdk complex for ubiquitination is indeed already known. I-κB for example can only be recognized by F-Box proteins if complexed with a cyclin/Cdk complex (Yaron et al., 1997). More interestingly, that kind of mechanism is also already known for p27 and Skp2 in HeLa cells. In order for p27 being recognized by Skp2, this protein has to be not only phosphorylated but also bound to Cyclin E/Cdk2 (Montagnoli et al., 1999). Later on, a model was created of how this mechanism works. p27 is bound to Cyclin E/Cdk2 and phosphorylated (Xu et al., 2007). Cks1 (human homologue to Cks85A in flies) is also interacting with CycE/Cdk2, were it helps to recruit substrates to the complex (Bourne et al., 1996). Skp2 can be recruited to the complex by binding to Cks1, indeed Cks1 has three distinct binding sites, one for phosphorylated substrates, one for binding to cyclin/Cdks and one for interaction with Skp2 (Bourne et al., 1996; Hao et al., 2005). Furthermore, it is already shown that it is not uncommon for human Skp2 to bind to Cyclin/Cdk complexes. Skp2 can interact with the Cyclin A/Cdk2 complex through a novel Cyclin A binding domain. The amino acids necessary for that interaction are highly conserved, even in fly Skp2 (Ji et al., 2006; Ji et al., 2007). Indeed, it already is proposed that binding of p27 to Cyclin A/Cdk2 stimulates the ubiquitination through SCF^{Skp2} (Hao et al., 2005). Xu et al. (2007) proposed that after Skp2 is bound to the CycE/Cdk2 complex, p27 spans with its C-terminus onto Skp2 while still in contact with the cyclin-Cdk complex. Skp2 can therefore immediately bind its substrate after all components are grouped around Cdk2 and the SCF complex starts the attachment of ubiquitin.

A similar mechanism seems possible in *D. melanogaster* and the interaction with Cdk2 seen in this thesis and in Ghorbani et al. (2011) makes this a worthwhile field of study. For a start, *in vitro* experiments can show if Skp2 is principally interacting with a substrate (for example Cdt1) in the absence of Cdk2. It has to be said though that heterologous gene expression and purification of the various different *Drosophila* proteins necessary for this assay, may be complicated and time consuming. For *in vivo* studies, Co-IPs can be performed where it is not only tested if for example, Cdt1 co-precipitates with Skp2 but also Cdk2. However, these assays also have their disadvantages, since it is not possible to determine if all three proteins build one ternary complex or if Skp2 interacts with both Cdt1 and Cdk2 independently. Furthermore, it is always possible that protein interaction is lost during the process of a Co-IP (Shyu et al., 2008). A worthwhile experiment for the detection of a ternary multi protein complex could be the combination of Bimolecular Fluorescence Complementation (BiFC) and Förster Resonance Energy Transmission (FRET). BiFC is based on two fragments of a fluorescent protein both fused to potential interaction partners. If the potential partners indeed interact with each other, the fragments are in close proximity and will form a complete, functioning fluorescence protein. Interaction can be seen by the appearance of a fluorescene signal therefore (Hu et al., 2002; Shyu et al., 2006). For FRET assays, two functioning fluorescence proteins are fused to the potential partners. If the partners interact, both fluorescent proteins are in close proximity to each other. One of them, the so-called donor, will be excited and the light that is emitted will be used by the second fluorescent protein, the so-called acceptor, for excitation. Consequently, interaction can be seen by the appearance of the fluorescent signal of the acceptor molecule (Jares-Erijman and Jovin, 2006). BiFC-FRET combines both assays, to analyze protein interaction in a ternary complex. Two proteins are tagged with the two fragments of the fluorescent protein of the BiFC assay, that itself serves as the acceptor protein. The donor protein is fused to the third interaction partner. If all three proteins interact, the donor protein can be excited and will transmit its emission energy to the now built acceptor protein, whose emission can be detected (Shyu et al., 2008).

This assay represents an elegant method to elucidate a potential supporting role of Cdk2 in the binding of Skp2 to its substrates.

It is important to note that by comparison, only a small number of proteins were found by mass spectrometric analysis. An MS analysis of Rca1 binding partners performed in the same way (Kies, 2017), shows 1294 hits against only 154 hits in the presented data. Moreover, while 176 proteins with a function in the cell cycle are identified in the Rca1 assay, only seven were identified here. What is more, no prominent Skp2 interaction partner, neither Dap nor Cdt1, CycE or the homologues of the various interaction partners in vertebrates, were found. One possibility is a weak binding between Skp2 and its substrates making it impossible to detect the interaction with endogenous levels, rendering mass spectrometric analysis unfit for substrate identification. Indeed, it was already tried to strengthen the connection between Skp2 and its substrates by fusing Skp2 with a UBA-domain. This leads on the one hand to a tighter connection between both proteins and prevents on the other hand the substrates from proteasomal degradation (Mark et al., 2014). Results of the MS-analysis were comparable to 4xFLAG Skp2 however and this data was not shown. It seems that MS-analysis with the constructs used in this thesis is not an appropriate tool for identification of new Skp2 substrates in *D. melanogaster*.

7 Supplement

7.1. Sources

Abbas, T. and Dutta, A., 2009. p21 in cancer: intricate networks and multiple activities. Nat Rev Cancer. 9, 400-14.

Abbas, T. and Dutta, A., 2011. CRL4Cdt2: master coordinator of cell cycle progression and genome stability. Cell Cycle. 10, 241-9.

Abbas, T., Sivaprasad, U., Terai, K., Amador, V., Pagano, M. and Dutta, A., 2008. PCNA-dependent regulation of p21 ubiquitylation and degradation via the CRL4Cdt2 ubiquitin ligase complex. Genes Dev. 22, 2496-506.

Amador, V., Ge, S., Santamaria, P.G., Guardavaccaro, D. and Pagano, M., 2007. APC/C(Cdc20) controls the ubiquitin-mediated degradation of p21 in prometaphase. Mol Cell. 27, 462-73.

Arbabi Ghahroudi, M., Desmyter, A., Wyns, L., Hamers, R. and Muyldermans, S., 1997. Selection and identification of single domain antibody fragments from camel heavy-chain antibodies. FEBS Lett. 414, 521-6.

Arentson, E., Faloon, P., Seo, J., Moon, E., Studts, J.M., Fremont, D.H. and Choi, K., 2002. Oncogenic potential of the DNA replication licensing protein CDT1. Oncogene. 21, 1150-8.

Arooz, T., Yam, C.H., Siu, W.Y., Lau, A., Li, K.K. and Poon, R.Y., 2000. On the concentrations of cyclins and cyclin-dependent kinases in extracts of cultured human cells. Biochemistry. 39, 9494-501.

Ballabeni, A., Melixetian, M., Zamponi, R., Masiero, L., Marinoni, F. and Helin, K., 2004. Human geminin promotes pre-RC formation and DNA replication by stabilizing CDT1 in mitosis. EMBO J. 23, 3122-32.

Bashir, T., Dorrello, N.V., Amador, V., Guardavaccaro, D. and Pagano, M., 2004. Control of the SCF(Skp2-Cks1) ubiquitin ligase by the APC/C(Cdh1) ubiquitin ligase. Nature. 428, 190-3.

Bassermann, F., Eichner, R. and Pagano, M., 2014. The ubiquitin proteasome system - implications for cell cycle control and the targeted treatment of cancer. Biochim Biophys Acta. 1843, 150-62.

Bauer, M., 2011. Analyse von G1/S-Regulatoren in Drosophila-Schneiderzellen (master thesis).

Berghammer, H. and Auer, B., 1993. "Easypreps": fast and easy plasmid minipreparation for analysis of recombinant clones in E. coli. Biotechniques. 14, 524, 528.

Bertoli, C., Skotheim, J.M. and de Bruin, R.A., 2013. Control of cell cycle transcription during G1 and S phases. Nat Rev Mol Cell Biol. 14, 518-28.

Bienkiewicz, E.A., Adkins, J.N. and Lumb, K.J., 2002. Functional consequences of preorganized helical structure in the intrinsically disordered cell-cycle inhibitor p27(Kip1). Biochemistry. 41, 752-9.

Bocca, S.N., Muzzopappa, M., Silberstein, S. and Wappner, P., 2001. Occurrence of a putative SCF ubiquitin ligase complex in Drosophila. Biochem Biophys Res Commun. 286, 357-64.

Bornstein, G., Bloom, J., Sitry-Shevah, D., Nakayama, K., Pagano, M. and Hershko, A., 2003. Role of the SCFSkp2 ubiquitin ligase in the degradation of p21Cip1 in S phase. J Biol Chem. 278, 25752-7.

Bourne, Y., Watson, M.H., Hickey, M.J., Holmes, W., Rocque, W., Reed, S.I. and Tainer, J.A., 1996. Crystal structure and mutational analysis of the human CDK2 kinase complex with cell cycle-regulatory protein CksHs1. Cell. 84, 863-74.

Carrano, A.C., Eytan, E., Hershko, A. and Pagano, M., 1999. SKP2 is required for ubiquitin-mediated degradation of the CDK inhibitor p27. Nat Cell Biol. 1, 193-9.

Carrano, A.C. and Pagano, M., 2001. Role of the F-box protein Skp2 in adhesion-dependent cell cycle progression. J Cell Biol. 153, 1381-90.

Caussinus, E., Kanca, O. and Affolter, M., 2011. Fluorescent fusion protein knockout mediated by anti-GFP nanobody. Nat Struct Mol Biol. 19, 117-21.

Chan, C.H., Lee, S.W., Wang, J. and Lin, H.K., 2010. Regulation of Skp2 expression and activity and its role in cancer progression. ScientificWorldJournal. 10, 1001-15.

Chan, C.H., Morrow, J.K., Li, C.F., Gao, Y., Jin, G., Moten, A., Stagg, L.J., Ladbury, J.E., Cai, Z., Xu, D., Logothetis, C.J., Hung, M.C., Zhang, S. and Lin, H.K., 2013. Pharmacological inactivation of Skp2 SCF ubiquitin ligase restricts cancer stem cell traits and cancer progression. Cell. 154, 556-68.

Cherbas, L. and Gong, L., 2014. Cell lines. Methods. 68, 74-81.

Clurman, B.E., Sheaff, R.J., Thress, K., Groudine, M. and Roberts, J.M., 1996. Turnover of cyclin E by the ubiquitin-proteasome pathway is regulated by cdk2 binding and cyclin phosphorylation. Genes & Development. 10, 1979-1990.

Cottee, P.A., Abs, E.L.O.Y.G., Nisbet, A.J. and Gasser, R.B., 2006. Ubiquitin-conjugating enzyme genes in Oesophagostomum dentatum. Parasitol Res. 99, 119-25.

de Nooij, J.C., Graber, K.H. and Hariharan, I.K., 2000. Expression of the cyclin-dependent kinase inhibitor Dacapo is regulated by cyclin E. Mech Dev. 97, 73-83.

de Nooij, J.C., Letendre, M.A. and Hariharan, I.K., 1996. A cyclin-dependent kinase inhibitor, Dacapo, is necessary for timely exit from the cell cycle during Drosophila embryogenesis. Cell. 87, 1237-47.

Deshaies, R.J., 1999. SCF and Cullin/Ring H2-based ubiquitin ligases. Annu Rev Cell Dev Biol. 15, 435-67.

Devault, A., Vallen, E.A., Yuan, T., Green, S., Bensimon, A. and Schwob, E., 2002. Identification of Tah11/Sid2 as the ortholog of the replication licensing factor Cdt1 in Saccharomyces cerevisiae. Curr Biol. 12, 689-94.

Ding, L., Li, R., Han, X., Zhou, Y., Zhang, H., Cui, Y., Wang, W. and Bai, J., 2017. Inhibition of Skp2 suppresses the proliferation and invasion of osteosarcoma cells. Oncol Rep. 38, 933-940.

Dui, W., Wei, B., He, F., Lu, W., Li, C., Liang, X., Ma, J. and Jiao, R., 2013. The Drosophila F-box protein dSkp2 regulates cell proliferation by targeting Dacapo for degradation. Molecular biology of the cell. 24, 1676-87, S1-7.

Dulic, V., Stein, G.H., Far, D.F. and Reed, S.I., 1998. Nuclear accumulation of p21Cip1 at the onset of mitosis: a role at the G2/M-phase transition. Mol Cell Biol. 18, 546-57.

Duronio, R.J., Brook, A., Dyson, N. and O'Farrell, P.H., 1996. E2F-induced S phase requires cyclin E. Genes Dev. 10, 2505-13.

Dyson, N., 1998. The regulation of E2F by pRB-family proteins. Genes Dev. 12, 2245-62.

Fang, G., Yu, H. and Kirschner, M.W., 1998. Direct binding of CDC20 protein family members activates the anaphase-promoting complex in mitosis and G1. Mol Cell. 2, 163-71.

Feldman, R.M., Correll, C.C., Kaplan, K.B. and Deshaies, R.J., 1997. A complex of Cdc4p, Skp1p, and Cdc53p/cullin catalyzes ubiquitination of the phosphorylated CDK inhibitor Sic1p. Cell. 91, 221-30.

Frank, M., 2013. Analyse der F-box-Funktion von Rca1 in Drosophila melanogaster (Ph.D. Thesis).

Frescas, D. and Pagano, M., 2008. Deregulated proteolysis by the F-box proteins SKP2 and beta-TrCP: tipping the scales of cancer. Nat Rev Cancer. 8, 438-49.

Fujita, T., Liu, W., Doihara, H. and Wan, Y., 2008. Regulation of Skp2-p27 axis by the Cdh1/anaphase-promoting complex pathway in colorectal tumorigenesis. Am J Pathol. 173, 217-28.

Ganoth, D., Bornstein, G., Ko, T.K., Larsen, B., Tyers, M., Pagano, M. and Hershko, A., 2001. The cell-cycle regulatory protein Cks1 is required for SCF(Skp2)-mediated ubiquitinylation of p27. Nature cell biology. 3, 321-4.

Gaubatz, S., Lees, J.A., Lindeman, G.J. and Livingston, D.M., 2001. E2F4 is exported from the nucleus in a CRM1-dependent manner. Mol Cell Biol. 21, 1384-92.

Geng, Y., Lee, Y.M., Welcker, M., Swanger, J., Zagozdzon, A., Winer, J.D., Roberts, J.M., Kaldis, P., Clurman, B.E. and Sicinski, P., 2007. Kinase-independent function of cyclin E. Mol Cell. 25, 127-39.

Geng, Y., Yu, Q., Sicinska, E., Das, M., Schneider, J.E., Bhattacharya, S., Rideout, W.M., Bronson, R.T., Gardner, H. and Sicinski, P., 2003. Cyclin E ablation in the mouse. Cell. 114, 431-43.

Ghorbani, M., Vasavan, B., Kraja, E. and Swan, A., 2011. Cks85A and Skp2 interact to maintain diploidy and promote growth in Drosophila. Developmental biology. 358, 213-23.

Glotzer, M., Murray, A.W. and Kirschner, M.W., 1991. Cyclin is degraded by the ubiquitin pathway. Nature. 349, 132-8.
Goldstein, G., Scheid, M., Hammerling, U., Schlesinger, D.H., Niall, H.D. and Boyse, E.A., 1975. Isolation of a polypeptide that has lymphocyte-differentiating properties and is probably represented universally in living cells. Proc Natl Acad Sci U S A. 72, 11-5.
Guarino, E., Shepherd, M.E., Salguero, I., Hua, H., Deegan, R.S. and Kearsey, S.E., 2011. Cdt1 proteolysis is promoted by dual PIP degrons and is modulated by PCNA ubiquitylation. Nucleic Acids Res. 39, 5978-90.
Hall, J.R., Lee, H.O., Bunker, B.D., Dorn, E.S., Rogers, G.C., Duronio, R.J. and Cook, J.G., 2008. Cdt1 and Cdc6 are destabilized by rereplication-induced DNA damage. J Biol Chem. 283, 25356-63.
Hammer, Ø., Harper, D.A.T. and Ryan, P.D., 2001. Past: Paleontological statistics software package for education and data analysis. Palaeontologia Electronica. 4, 9.
Hao, B., Zheng, N., Schulman, B.A., Wu, G., Miller, J.J., Pagano, M. and Pavletich, N.P., 2005. Structural basis of the Cks1-dependent recognition of p27(Kip1) by the SCF(Skp2) ubiquitin ligase. Molecular cell. 20, 9-19.
Harper, J.W., Adami, G.R., Wei, N., Keyomarsi, K. and Elledge, S.J., 1993. The p21 Cdk-interacting protein Cip1 is a potent inhibitor of G1 cyclin-dependent kinases. Cell. 75, 805-16.
Havens, C.G. and Walter, J.C., 2009. Docking of a specialized PIP Box onto chromatin-bound PCNA creates a degron for the ubiquitin ligase CRL4Cdt2. Mol Cell. 35, 93-104.
Havens, C.G. and Walter, J.C., 2011. Mechanism of CRL4(Cdt2), a PCNA-dependent E3 ubiquitin ligase. Genes Dev. 25, 1568-82.
Helin, K., 1998. Regulation of cell proliferation by the E2F transcription factors. Curr Opin Genet Dev. 8, 28-35.
Heo, J., Eki, R. and Abbas, T., 2016. Deregulation of F-box proteins and its consequence on cancer development, progression and metastasis. Seminars in cancer biology. 36, 33-51.
Hernandez-Carralero, E., Cabrera, E., Alonso-de Vega, I., Hernandez-Perez, S., Smits, V.A.J. and Freire, R., 2018. Control of DNA Replication Initiation by Ubiquitin. Cells. 7.
Higa, L.A., Yang, X., Zheng, J., Banks, D., Wu, M., Ghosh, P., Sun, H. and Zhang, H., 2006. Involvement of CUL4 ubiquitin E3 ligases in regulating CDK inhibitors Dacapo/p27Kip1 and cyclin E degradation. Cell cycle. 5, 71-7.
Hirsch, F., 2018. Interplay between Skp2 and Cdt1 in *Drosophila melanogaster* (master thesis).
Hochegger, H., Takeda, S. and Hunt, T., 2008. Cyclin-dependent kinases and cell-cycle transitions: does one fit all? Nat Rev Mol Cell Biol. 9, 910-6.
Hofmann, J.F. and Beach, D., 1994. cdt1 is an essential target of the Cdc10/Sct1 transcription factor: requirement for DNA replication and inhibition of mitosis. EMBO J. 13, 425-34.
Hu, C.D., Chinenov, Y. and Kerppola, T.K., 2002. Visualization of interactions among bZIP and Rel family proteins in living cells using bimolecular fluorescence complementation. Mol Cell. 9, 789-98.
Hu, D., Liu, W., Wu, G. and Wan, Y., 2011. Nuclear translocation of Skp2 facilitates its destruction in response to TGFbeta signaling. Cell cycle. 10, 285-92.
Hu, R. and Aplin, A.E., 2008. Skp2 regulates G2/M progression in a p53-dependent manner. Mol Biol Cell. 19, 4602-10.
Huang, L., Kinnucan, E., Wang, G., Beaudenon, S., Howley, P.M., Huibregtse, J.M. and Pavletich, N.P., 1999. Structure of an E6AP-UbcH7 complex: insights into ubiquitination by the E2-E3 enzyme cascade. Science. 286, 1321-6.
Ikeda, F. and Dikic, I., 2008. Atypical ubiquitin chains: new molecular signals. 'Protein Modifications: Beyond the Usual Suspects' review series. EMBO reports. 9, 536-42.
Jamal, A., Swarnalatha, M., Sultana, S., Joshi, P., Panda, S.K. and Kumar, V., 2015. The G1 phase E3 ubiquitin ligase TRUSS that gets deregulated in human cancers is a novel substrate of the S-phase E3 ubiquitin ligase Skp2. Cell cycle. 14, 2688-700.

Jares-Erijman, E.A. and Jovin, T.M., 2006. Imaging molecular interactions in living cells by FRET microscopy. Curr Opin Chem Biol. 10, 409-16.
Jentsch, S., Seufert, W. and Hauser, H.P., 1991. Genetic analysis of the ubiquitin system. Biochim Biophys Acta. 1089, 127-39.
Ji, P., Goldin, L., Ren, H., Sun, D., Guardavaccaro, D., Pagano, M. and Zhu, L., 2006. Skp2 contains a novel cyclin A binding domain that directly protects cyclin A from inhibition by p27Kip1. The Journal of biological chemistry. 281, 24058-69.
Ji, P., Sun, D., Wang, H., Bauzon, F. and Zhu, L., 2007. Disrupting Skp2-cyclin A interaction with a blocking peptide induces selective cancer cell killing. Molecular cancer therapeutics. 6, 684-91.
Jones, D., Crowe, E., Stevens, T.A. and Candido, E.P., 2002. Functional and phylogenetic analysis of the ubiquitylation system in Caenorhabditis elegans: ubiquitin-conjugating enzymes, ubiquitin-activating enzymes, and ubiquitin-like proteins. Genome Biol. 3, RESEARCH0002.
Kamura, T., Hara, T., Kotoshiba, S., Yada, M., Ishida, N., Imaki, H., Hatakeyama, S., Nakayama, K. and Nakayama, K.I., 2003. Degradation of p57Kip2 mediated by SCFSkp2-dependent ubiquitylation. Proc Natl Acad Sci U S A. 100, 10231-6.
Kamura, T., Hara, T., Matsumoto, M., Ishida, N., Okumura, F., Hatakeyama, S., Yoshida, M., Nakayama, K. and Nakayama, K.I., 2004. Cytoplasmic ubiquitin ligase KPC regulates proteolysis of p27(Kip1) at G1 phase. Nat Cell Biol. 6, 1229-35.
Karakaidos, P., Taraviras, S., Vassiliou, L.V., Zacharatos, P., Kastrinakis, N.G., Kougiou, D., Kouloukoussa, M., Nishitani, H., Papavassiliou, A.G., Lygerou, Z. and Gorgoulis, V.G., 2004. Overexpression of the replication licensing regulators hCdt1 and hCdc6 characterizes a subset of non-small-cell lung carcinomas: synergistic effect with mutant p53 on tumor growth and chromosomal instability--evidence of E2F-1 transcriptional control over hCdt1. Am J Pathol. 165, 1351-65.
Kies, M., 2017. Dual regulation of APC/C activity by Rca1 (PhD thesis).
Kim, Y., Starostina, N.G. and Kipreos, E.T., 2008. The CRL4Cdt2 ubiquitin ligase targets the degradation of p21Cip1 to control replication licensing. Genes Dev. 22, 2507-19.
Kipreos, E.T. and Pagano, M., 2000. The F-box protein family. Genome Biol. 1, REVIEWS3002.
Klotz-Noack, K., McIntosh, D., Schurch, N., Pratt, N. and Blow, J.J., 2012. Re-replication induced by geminin depletion occurs from G2 and is enhanced by checkpoint activation. J Cell Sci. 125, 2436-45.
Knoblich, J.A., 2010. Asymmetric cell division: recent developments and their implications for tumour biology. Nat Rev Mol Cell Biol. 11, 849-60.
Knoblich, J.A., Sauer, K., Jones, L., Richardson, H., Saint, R. and Lehner, C.F., 1994. Cyclin E controls S phase progression and its down-regulation during Drosophila embryogenesis is required for the arrest of cell proliferation. Cell. 77, 107-20.
Koepp, D.M., Schaefer, L.K., Ye, X., Keyomarsi, K., Chu, C., Harper, J.W. and Elledge, S.J., 2001. Phosphorylation-dependent ubiquitination of cyclin E by the SCFFbw7 ubiquitin ligase. Science. 294, 173-7.
Koff, A., Cross, F., Fisher, A., Schumacher, J., Leguellec, K., Philippe, M. and Roberts, J.M., 1991. Human cyclin E, a new cyclin that interacts with two members of the CDC2 gene family. Cell. 66, 1217-28.
Koff, A., Giordano, A., Desai, D., Yamashita, K., Harper, J.W., Elledge, S., Nishimoto, T., Morgan, D.O., Franza, B.R. and Roberts, J.M., 1992. Formation and activation of a cyclin E-cdk2 complex during the G1 phase of the human cell cycle. Science. 257, 1689-94.
Komander, D., 2009. The emerging complexity of protein ubiquitination. Biochem Soc Trans. 37, 937-53.
Kraus, B., Pohlschmidt, M., Leung, A.L., Germino, G.G., Snarey, A., Schneider, M.C., Reeders, S.T. and Frischauf, A.M., 1994. A novel cyclin gene (CCNF) in the region of the polycystic kidney disease gene (PKD1). Genomics. 24, 27-33.

Krishnan, A., K, D., Babu, P.S.S., Jagadeeshan, S., Prasad, M. and Nair, S.A., 2017. Oncogenic Actions of SKP2 Involves Deregulation of CDK1 Turnover Mediated by FOXM1. J Cell Biochem. 118, 797-807.
Kroeger, P.T., Jr., Shoue, D.A., Mezzacappa, F.M., Gerlach, G.F., Wingert, R.A. and Schulz, R.A., 2013. Knockdown of SCF(Skp2) function causes double-parked accumulation in the nucleus and DNA re-replication in Drosophila plasmatocytes. PloS one. 8, e79019.
Kurland, J.F. and Tansey, W.P., 2004. Crashing waves of destruction: the cell cycle and APC(Cdh1) regulation of SCF(Skp2). Cancer Cell. 5, 305-6.
Lane, M.E., Sauer, K., Wallace, K., Jan, Y.N., Lehner, C.F. and Vaessin, H., 1996. Dacapo, a cyclin-dependent kinase inhibitor, stops cell proliferation during Drosophila development. Cell. 87, 1225-35.
Lee, H.O., Zacharek, S.J., Xiong, Y. and Duronio, R.J., 2010. Cell type-dependent requirement for PIP box-regulated Cdt1 destruction during S phase. Mol Biol Cell. 21, 3639-53.
Lee, S.W., Li, C.F., Jin, G.X., Cai, Z., Han, F., Chan, C.H., Yang, W.L., Li, B.K., Rezaeian, A.H., Li, H.Y., Huang, H.Y. and Lin, H.K., 2015. Skp2-Dependent Ubiquitination and Activation of LKB1 Is Essential for Cancer Cell Survival under Energy Stress. Molecular cell. 57, 1022-1033.
Lees, J.A., Saito, M., Vidal, M., Valentine, M., Look, T., Harlow, E., Dyson, N. and Helin, K., 1993. The retinoblastoma protein binds to a family of E2F transcription factors. Mol Cell Biol. 13, 7813-25.
Li, W., Bengtson, M.H., Ulbrich, A., Matsuda, A., Reddy, V.A., Orth, A., Chanda, S.K., Batalov, S. and Joazeiro, C.A., 2008. Genome-wide and functional annotation of human E3 ubiquitin ligases identifies MULAN, a mitochondrial E3 that regulates the organelle's dynamics and signaling. PLoS One. 3, e1487.
Li, X., Zhao, Q., Liao, R., Sun, P. and Wu, X., 2003. The SCF(Skp2) ubiquitin ligase complex interacts with the human replication licensing factor Cdt1 and regulates Cdt1 degradation. The Journal of biological chemistry. 278, 30854-8.
Liang, L., Haug, J.S., Seidel, C.W. and Gibson, M.C., 2014. Functional genomic analysis of the periodic transcriptome in the developing Drosophila wing. Developmental cell. 29, 112-27.
Lim, M.S., Adamson, A., Lin, Z., Perez-Ordonez, B., Jordan, R.C., Tripp, S., Perkins, S.L. and Elenitoba-Johnson, K.S., 2002. Expression of Skp2, a p27(Kip1) ubiquitin ligase, in malignant lymphoma: correlation with p27(Kip1) and proliferation index. Blood. 100, 2950-6.
Lin, H.C., Wu, J.T., Tan, B.C. and Chien, C.T., 2009a. Cul4 and DDB1 regulate Orc2 localization, BrdU incorporation and Dup stability during gene amplification in Drosophila follicle cells. J Cell Sci. 122, 2393-401.
Lin, H.K., Wang, G., Chen, Z., Teruya-Feldstein, J., Liu, Y., Chan, C.H., Yang, W.L., Erdjument-Bromage, H., Nakayama, K.I., Nimer, S., Tempst, P. and Pandolfi, P.P., 2009b. Phosphorylation-dependent regulation of cytosolic localization and oncogenic function of Skp2 by Akt/PKB. Nature cell biology. 11, 420-32.
Liontos, M., Koutsami, M., Sideridou, M., Evangelou, K., Kletsas, D., Levy, B., Kotsinas, A., Nahum, O., Zoumpourlis, V., Kouloukoussa, M., Lygerou, Z., Taraviras, S., Kittas, C., Bartkova, J., Papavassiliou, A.G., Bartek, J., Halazonetis, T.D. and Gorgoulis, V.G., 2007. Deregulated overexpression of hCdt1 and hCdc6 promotes malignant behavior. Cancer Res. 67, 10899-909.
Liu, E., Lee, A.Y., Chiba, T., Olson, E., Sun, P. and Wu, X., 2007. The ATR-mediated S phase checkpoint prevents rereplication in mammalian cells when licensing control is disrupted. J Cell Biol. 179, 643-57.
Liu, S. and Yamauchi, H., 2009. p27-Associated G1 arrest induced by hinokitiol in human malignant melanoma cells is mediated via down-regulation of pRb, Skp2 ubiquitin ligase, and impairment of Cdk2 function. Cancer Lett. 286, 240-9.
Lu, Z. and Hunter, T., 2010. Ubiquitylation and proteasomal degradation of the p21(Cip1), p27(Kip1) and p57(Kip2) CDK inhibitors. Cell cycle. 9, 2342-52.

Mahadevappa, R., Neves, H., Yuen, S.M., Bai, Y., McCrudden, C.M., Yuen, H.F., Wen, Q., Zhang, S.D. and Kwok, H.F., 2017. The prognostic significance of Cdc6 and Cdt1 in breast cancer. Sci Rep. 7, 985.
Mailand, N. and Diffley, J.F., 2005. CDKs promote DNA replication origin licensing in human cells by protecting Cdc6 from APC/C-dependent proteolysis. Cell. 122, 915-26.
Maiorano, D., Moreau, J. and Mechali, M., 2000. XCDT1 is required for the assembly of pre-replicative complexes in Xenopus laevis. Nature. 404, 622-5.
Mandal, S., Freije, W.A., Guptan, P. and Banerjee, U., 2010. Metabolic control of G1-S transition: cyclin E degradation by p53-induced activation of the ubiquitin-proteasome system. The Journal of cell biology. 188, 473-9.
Mark, K.G., Simonetta, M., Maiolica, A., Seller, C.A. and Toczyski, D.P., 2014. Ubiquitin ligase trapping identifies an SCF(Saf1) pathway targeting unprocessed vacuolar/lysosomal proteins. Molecular cell. 53, 148-61.
Marti, A., Wirbelauer, C., Scheffner, M. and Krek, W., 1999. Interaction between ubiquitin-protein ligase SCFSKP2 and E2F-1 underlies the regulation of E2F-1 degradation. Nat Cell Biol. 1, 14-9.
Masai, H., Matsumoto, S., You, Z., Yoshizawa-Sugata, N. and Oda, M., 2010. Eukaryotic chromosome DNA replication: where, when, and how? Annu Rev Biochem. 79, 89-130.
Matsuoka, S., Edwards, M.C., Bai, C., Parker, S., Zhang, P., Baldini, A., Harper, J.W. and Elledge, S.J., 1995. p57KIP2, a structurally distinct member of the p21CIP1 Cdk inhibitor family, is a candidate tumor suppressor gene. Genes Dev. 9, 650-62.
McLean, J.R., Chaix, D., Ohi, M.D. and Gould, K.L., 2011. State of the APC/C: organization, function, and structure. Crit Rev Biochem Mol Biol. 46, 118-36.
Mendez, J., Zou-Yang, X.H., Kim, S.Y., Hidaka, M., Tansey, W.P. and Stillman, B., 2002. Human origin recognition complex large subunit is degraded by ubiquitin-mediated proteolysis after initiation of DNA replication. Mol Cell. 9, 481-91.
Metzger, M.B., Hristova, V.A. and Weissman, A.M., 2012. HECT and RING finger families of E3 ubiquitin ligases at a glance. J Cell Sci. 125, 531-7.
Mihaylov, I.S., Kondo, T., Jones, L., Ryzhikov, S., Tanaka, J., Zheng, J., Higa, L.A., Minamino, N., Cooley, L. and Zhang, H., 2002. Control of DNA replication and chromosome ploidy by geminin and cyclin A. Mol Cell Biol. 22, 1868-80.
Minella, A.C., Loeb, K.R., Knecht, A., Welcker, M., Varnum-Finney, B.J., Bernstein, I.D., Roberts, J.M. and Clurman, B.E., 2008. Cyclin E phosphorylation regulates cell proliferation in hematopoietic and epithelial lineages in vivo. Genes Dev. 22, 1677-89.
Moberg, K.H., Bell, D.W., Wahrer, D.C., Haber, D.A. and Hariharan, I.K., 2001. Archipelago regulates Cyclin E levels in Drosophila and is mutated in human cancer cell lines. Nature. 413, 311-6.
Montagnoli, A., Fiore, F., Eytan, E., Carrano, A.C., Draetta, G.F., Hershko, A. and Pagano, M., 1999. Ubiquitination of p27 is regulated by Cdk-dependent phosphorylation and trimeric complex formation. Genes Dev. 13, 1181-9.
Morgan, D.O., 1995. Principles of CDK regulation. Nature. 374, 131-4.
Morgan, D.O., 2007. The cell cycle: principles of control, Published by New Science Press in association with Oxford University Press; Distributed inside North America by Sinauer Associates, Publishers, London, Sunderland, MA.
Munoz, S., Bua, S., Rodriguez-Acebes, S., Megias, D., Ortega, S., de Martino, A. and Mendez, J., 2017. In Vivo DNA Re-replication Elicits Lethal Tissue Dysplasias. Cell Rep. 19, 928-938.
Naito, Y., Yamada, T., Matsumiya, T., Ui-Tei, K., Saigo, K. and Morishita, S., 2005. dsCheck: highly sensitive off-target search software for double-stranded RNA-mediated RNA interference. Nucleic acids research. 33, W589-91.
Nakayama, K., Nagahama, H., Minamishima, Y.A., Matsumoto, M., Nakamichi, I., Kitagawa, K., Shirane, M., Tsunematsu, R., Tsukiyama, T., Ishida, N., Kitagawa, M. and Hatakeyama, S., 2000. Targeted

disruption of Skp2 results in accumulation of cyclin E and p27(Kip1), polyploidy and centrosome overduplication. The EMBO journal. 19, 2069-81.
Nelson, D.E., Randle, S.J. and Laman, H., 2013. Beyond ubiquitination: the atypical functions of Fbxo7 and other F-box proteins. Open Biol. 3, 130131.
Nishitani, H., Lygerou, Z., Nishimoto, T. and Nurse, P., 2000. The Cdt1 protein is required to license DNA for replication in fission yeast. Nature. 404, 625-8.
Nishitani, H., Shiomi, Y., Iida, H., Michishita, M., Takami, T. and Tsurimoto, T., 2008. CDK inhibitor p21 is degraded by a proliferating cell nuclear antigen-coupled Cul4-DDB1Cdt2 pathway during S phase and after UV irradiation. J Biol Chem. 283, 29045-52.
Nishitani, H., Sugimoto, N., Roukos, V., Nakanishi, Y., Saijo, M., Obuse, C., Tsurimoto, T., Nakayama, K.I., Nakayama, K., Fujita, M., Lygerou, Z. and Nishimoto, T., 2006. Two E3 ubiquitin ligases, SCF-Skp2 and DDB1-Cul4, target human Cdt1 for proteolysis. EMBO J. 25, 1126-36.
Nishitani, H., Taraviras, S., Lygerou, Z. and Nishimoto, T., 2001. The human licensing factor for DNA replication Cdt1 accumulates in G1 and is destabilized after initiation of S-phase. J Biol Chem. 276, 44905-11.
Ohtani, K., DeGregori, J. and Nevins, J.R., 1995. Regulation of the cyclin E gene by transcription factor E2F1. Proc Natl Acad Sci U S A. 92, 12146-50.
Ohtsubo, M. and Roberts, J.M., 1993. Cyclin-dependent regulation of G1 in mammalian fibroblasts. Science. 259, 1908-12.
Peters, J.M., 2002. The anaphase-promoting complex: proteolysis in mitosis and beyond. Mol Cell. 9, 931-43.
Polyak, K., Kato, J.Y., Solomon, M.J., Sherr, C.J., Massague, J., Roberts, J.M. and Koff, A., 1994. p27Kip1, a cyclin-Cdk inhibitor, links transforming growth factor-beta and contact inhibition to cell cycle arrest. Genes Dev. 8, 9-22.
Polz, J., 2017. Establishment of the T2A-system for protein stability analysis of cell cycle proteins by flow cytometry (master thesis). Master Thesis.
Pozo, P.N. and Cook, J.G., 2016. Regulation and Function of Cdt1; A Key Factor in Cell Proliferation and Genome Stability. Genes (Basel). 8.
Quinn, L.M., Herr, A., McGarry, T.J. and Richardson, H., 2001. The Drosophila Geminin homolog: roles for Geminin in limiting DNA replication, in anaphase and in neurogenesis. Genes Dev. 15, 2741-54.
Randell, J.C., Bowers, J.L., Rodriguez, H.K. and Bell, S.P., 2006. Sequential ATP hydrolysis by Cdc6 and ORC directs loading of the Mcm2-7 helicase. Mol Cell. 21, 29-39.
Reis, T. and Edgar, B.A., 2004. Negative regulation of dE2F1 by cyclin-dependent kinases controls cell cycle timing. Cell. 117, 253-64.
Rizzardi, L.F. and Cook, J.G., 2012. Flipping the switch from g1 to s phase with e3 ubiquitin ligases. Genes & cancer. 3, 634-48.
Roubinet, C. and Cabernard, C., 2014. Control of asymmetric cell division. Curr Opin Cell Biol. 31, 84-91.
Rubin, S.M., Gall, A.L., Zheng, N. and Pavletich, N.P., 2005. Structure of the Rb C-terminal domain bound to E2F1-DP1: a mechanism for phosphorylation-induced E2F release. Cell. 123, 1093-106.
Russo, A.A., Jeffrey, P.D., Patten, A.K., Massague, J. and Pavletich, N.P., 1996. Crystal structure of the p27Kip1 cyclin-dependent-kinase inhibitor bound to the cyclin A-Cdk2 complex. Nature. 382, 325-31.
Saeki, Y., 2017. Ubiquitin recognition by the proteasome. J Biochem. 161, 113-124.
Saha, P., Chen, J., Thome, K.C., Lawlis, S.J., Hou, Z.H., Hendricks, M., Parvin, J.D. and Dutta, A., 1998. Human CDC6/Cdc18 associates with Orc1 and cyclin-cdk and is selectively eliminated from the nucleus at the onset of S phase. Mol Cell Biol. 18, 2758-67.
Schneider, C.A., Rasband, W.S. and Eliceiri, K.W., 2012. NIH Image to ImageJ: 25 years of image analysis. Nat Methods. 9, 671-5.

Schuler, S., Diersch, S., Hamacher, R., Schmid, R.M., Saur, D. and Schneider, G., 2011. SKP2 confers resistance of pancreatic cancer cells towards TRAIL-induced apoptosis. Int J Oncol. 38, 219-25.
Schulman, B.A., Carrano, A.C., Jeffrey, P.D., Bowen, Z., Kinnucan, E.R., Finnin, M.S., Elledge, S.J., Harper, J.W., Pagano, M. and Pavletich, N.P., 2000. Insights into SCF ubiquitin ligases from the structure of the Skp1-Skp2 complex. Nature. 408, 381-6.
Schulman, B.A. and Harper, J.W., 2009. Ubiquitin-like protein activation by E1 enzymes: the apex for downstream signalling pathways. Nat Rev Mol Cell Biol. 10, 319-31.
Senga, T., Sivaprasad, U., Zhu, W., Park, J.H., Arias, E.E., Walter, J.C. and Dutta, A., 2006. PCNA is a cofactor for Cdt1 degradation by CUL4/DDB1-mediated N-terminal ubiquitination. J Biol Chem. 281, 6246-52.
Seo, J., Chung, Y.S., Sharma, G.G., Moon, E., Burack, W.R., Pandita, T.K. and Choi, K., 2005. Cdt1 transgenic mice develop lymphoblastic lymphoma in the absence of p53. Oncogene. 24, 8176-86.
Sheaff, R.J., Groudine, M., Gordon, M., Roberts, J.M. and Clurman, B.E., 1997. Cyclin E-CDK2 is a regulator of p27Kip1. Genes Dev. 11, 1464-78.
Sherr, C.J. and Roberts, J.M., 1999. CDK inhibitors: positive and negative regulators of G1-phase progression. Genes Dev. 13, 1501-12.
Sheu, Y.J. and Stillman, B., 2006. Cdc7-Dbf4 phosphorylates MCM proteins via a docking site-mediated mechanism to promote S phase progression. Mol Cell. 24, 101-13.
Shi, Q., Gu, S., Yu, X.S., White, T.W., Banks, E.A. and Jiang, J.X., 2015. Connexin Controls Cell-Cycle Exit and Cell Differentiation by Directly Promoting Cytosolic Localization and Degradation of E3 Ligase Skp2. Developmental cell. 35, 483-96.
Shibutani, S.T., de la Cruz, A.F., Tran, V., Turbyfill, W.J., 3rd, Reis, T., Edgar, B.A. and Duronio, R.J., 2008. Intrinsic negative cell cycle regulation provided by PIP box- and Cul4Cdt2-mediated destruction of E2f1 during S phase. Dev Cell. 15, 890-900.
Shyu, Y.J., Liu, H., Deng, X. and Hu, C.D., 2006. Identification of new fluorescent protein fragments for bimolecular fluorescence complementation analysis under physiological conditions. Biotechniques. 40, 61-6.
Shyu, Y.J., Suarez, C.D. and Hu, C.D., 2008. Visualization of ternary complexes in living cells by using a BiFC-based FRET assay. Nat Protoc. 3, 1693-702.
Siu, K.T., Rosner, M.R. and Minella, A.C., 2012. An integrated view of cyclin E function and regulation. Cell Cycle. 11, 57-64.
Sivakumar, S. and Gorbsky, G.J., 2015. Spatiotemporal regulation of the anaphase-promoting complex in mitosis. Nat Rev Mol Cell Biol. 16, 82-94.
Skaar, J.R., Pagan, J.K. and Pagano, M., 2009. SnapShot: F box proteins I. Cell. 137, 1160-1160 e1.
Skaar, J.R., Pagan, J.K. and Pagano, M., 2013. Mechanisms and function of substrate recruitment by F-box proteins. Nat Rev Mol Cell Biol. 14, 369-81.
Skaar, J.R. and Pagano, M., 2009. Control of cell growth by the SCF and APC/C ubiquitin ligases. Curr Opin Cell Biol. 21, 816-24.
Skowyra, D., Craig, K.L., Tyers, M., Elledge, S.J. and Harper, J.W., 1997. F-box proteins are receptors that recruit phosphorylated substrates to the SCF ubiquitin-ligase complex. Cell. 91, 209-19.
Spruck, C., Strohmaier, H., Watson, M., Smith, A.P., Ryan, A., Krek, T.W. and Reed, S.I., 2001. A CDK-independent function of mammalian Cks1: targeting of SCF(Skp2) to the CDK inhibitor p27Kip1. Mol Cell. 7, 639-50.
Spruck, C.H., Won, K.A. and Reed, S.I., 1999. Deregulated cyclin E induces chromosome instability. Nature. 401, 297-300.
Starostina, N.G. and Kipreos, E.T., 2012. Multiple degradation pathways regulate versatile CIP/KIP CDK inhibitors. Trends Cell Biol. 22, 33-41.

Strohmaier, H., Spruck, C.H., Kaiser, P., Won, K.A., Sangfelt, O. and Reed, S.I., 2001. Human F-box protein hCdc4 targets cyclin E for proteolysis and is mutated in a breast cancer cell line. Nature. 413, 316-22.

Sugimoto, N., Tatsumi, Y., Tsurumi, T., Matsukage, A., Kiyono, T., Nishitani, H. and Fujita, M., 2004. Cdt1 phosphorylation by cyclin A-dependent kinases negatively regulates its function without affecting geminin binding. J Biol Chem. 279, 19691-7.

Sugimoto, N., Yoshida, K., Tatsumi, Y., Yugawa, T., Narisawa-Saito, M., Waga, S., Kiyono, T. and Fujita, M., 2009. Redundant and differential regulation of multiple licensing factors ensures prevention of re-replication in normal human cells. J Cell Sci. 122, 1184-91.

Sugimoto, N., Yugawa, T., Iizuka, M., Kiyono, T. and Fujita, M., 2011. Chromatin remodeler sucrose nonfermenting 2 homolog (SNF2H) is recruited onto DNA replication origins through interaction with Cdc10 protein-dependent transcript 1 (Cdt1) and promotes pre-replication complex formation. J Biol Chem. 286, 39200-10.

Sutterluty, H., Chatelain, E., Marti, A., Wirbelauer, C., Senften, M., Muller, U. and Krek, W., 1999. p45SKP2 promotes p27Kip1 degradation and induces S phase in quiescent cells. Nat Cell Biol. 1, 207-14.

Swanson, C.I., Meserve, J.H., McCarter, P.C., Thieme, A., Mathew, T., Elston, T.C. and Duronio, R.J., 2015. Expression of an S phase-stabilized version of the CDK inhibitor Dacapo can alter endoreplication. Development. 142, 4288-98.

Szuplewski, S., Sandmann, T., Hietakangas, V. and Cohen, S.M., 2009. Drosophila Minus is required for cell proliferation and influences Cyclin E turnover. Genes Dev. 23, 1998-2003.

Takeda, D.Y., Parvin, J.D. and Dutta, A., 2005. Degradation of Cdt1 during S phase is Skp2-independent and is required for efficient progression of mammalian cells through S phase. J Biol Chem. 280, 23416-23.

Thomer, M., May, N.R., Aggarwal, B.D., Kwok, G. and Calvi, B.R., 2004. Drosophila double-parked is sufficient to induce re-replication during development and is regulated by cyclin E/CDK2. Development. 131, 4807-18.

Tremmel, K., 2018. Synthese verschiedener RNAi-Tools für den knockdown des Drosophila Gens rca1 (bachelor thesis).

Tsunematsu, T., Takihara, Y., Ishimaru, N., Pagano, M., Takata, T. and Kudo, Y., 2013. Aurora-A controls pre-replicative complex assembly and DNA replication by stabilizing geminin in mitosis. Nat Commun. 4, 1885.

Vosper, J., Masuccio, A., Kullmann, M., Ploner, C., Geley, S. and Hengst, L., 2015. Statin-induced depletion of geranylgeranyl pyrophosphate inhibits cell proliferation by a novel pathway of Skp2 degradation. Oncotarget. 6, 2889-902.

Wang, J., Huang, Y., Guan, Z., Zhang, J.L., Su, H.K., Zhang, W., Yue, C.F., Yan, M., Guan, S. and Liu, Q.Q., 2014. E3-ligase Skp2 predicts poor prognosis and maintains cancer stem cell pool in nasopharyngeal carcinoma. Oncotarget. 5, 5591-601.

Wei, W., Ayad, N.G., Wan, Y., Zhang, G.J., Kirschner, M.W. and Kaelin, W.G., Jr., 2004. Degradation of the SCF component Skp2 in cell-cycle phase G1 by the anaphase-promoting complex. Nature. 428, 194-8.

Wei, Z., Jiang, X., Liu, F., Qiao, H., Zhou, B., Zhai, B., Zhang, L., Zhang, X., Han, L., Jiang, H., Krissansen, G.W. and Sun, X., 2013. Downregulation of Skp2 inhibits the growth and metastasis of gastric cancer cells in vitro and in vivo. Tumour Biol. 34, 181-92.

Weiner, M.P., Costa, G.L., Schoettlin, W., Cline, J., Mathur, E. and Bauer, J.C., 1994. Site-directed mutagenesis of double-stranded DNA by the polymerase chain reaction. Gene. 151, 119-23.

Whittaker, A.J., Royzman, I. and Orr-Weaver, T.L., 2000. Drosophila double parked: a conserved, essential replication protein that colocalizes with the origin recognition complex and links DNA replication with mitosis and the down-regulation of S phase transcripts. Genes Dev. 14, 1765-76.

Wilkinson, K.D., 2005. The discovery of ubiquitin-dependent proteolysis. Proc Natl Acad Sci U S A. 102, 15280-2.
Willems, A.R., Schwab, M. and Tyers, M., 2004. A hitchhiker's guide to the cullin ubiquitin ligases: SCF and its kin. Biochim Biophys Acta. 1695, 133-70.
Wohlschlegel, J.A., Dwyer, B.T., Dhar, S.K., Cvetic, C., Walter, J.C. and Dutta, A., 2000. Inhibition of eukaryotic DNA replication by geminin binding to Cdt1. Science. 290, 2309-12.
Won, K.A. and Reed, S.I., 1996. Activation of cyclin E/CDK2 is coupled to site-specific autophosphorylation and ubiquitin-dependent degradation of cyclin E. Embo Journal. 15, 4182-4193.
Xu, S., Abbasian, M., Patel, P., Jensen-Pergakes, K., Lombardo, C.R., Cathers, B.E., Xie, W., Mercurio, F., Pagano, M., Giegel, D. and Cox, S., 2007. Substrate recognition and ubiquitination of SCFSkp2/Cks1 ubiquitin-protein isopeptide ligase. J Biol Chem. 282, 15462-70.
Yaron, A., Gonen, H., Alkalay, I., Hatzubai, A., Jung, S., Beyth, S., Mercurio, F., Manning, A.M., Ciechanover, A. and Ben-Neriah, Y., 1997. Inhibition of NF-kappa-B cellular function via specific targeting of the I-kappa-B-ubiquitin ligase. EMBO J. 16, 6486-94.
Ye, Y. and Rape, M., 2009. Building ubiquitin chains: E2 enzymes at work. Nat Rev Mol Cell Biol. 10, 755-64.
Ying, M., Shao, X., Jing, H., Liu, Y., Qi, X., Cao, J., Chen, Y., Xiang, S., Song, H., Hu, R., Wei, G., Yang, B. and He, Q., 2018. Ubiquitin-dependent degradation of CDK2 drives the therapeutic differentiation of AML by targeting PRDX2. Blood. 131, 2698-2711.
Yu, Z.K., Gervais, J.L. and Zhang, H., 1998. Human CUL-1 associates with the SKP1/SKP2 complex and regulates p21(CIP1/WAF1) and cyclin D proteins. Proc Natl Acad Sci U S A. 95, 11324-9.
Zhang, H., Kobayashi, R., Galaktionov, K. and Beach, D., 1995. p19Skp1 and p45Skp2 are essential elements of the cyclin A-CDK2 S phase kinase. Cell. 82, 915-25.
Zhang, W., Cao, L., Sun, Z., Xu, J., Tang, L., Chen, W., Luo, J., Yang, F., Wang, Y. and Guan, X., 2016. Skp2 is over-expressed in breast cancer and promotes breast cancer cell proliferation. Cell Cycle. 15, 1344-51.
Zheng, N., Wang, Z. and Wei, W., 2016. Ubiquitination-mediated degradation of cell cycle-related proteins by F-box proteins. Int J Biochem Cell Biol. 73, 99-110.
Zhong, W., Feng, H., Santiago, F.E. and Kipreos, E.T., 2003. CUL-4 ubiquitin ligase maintains genome stability by restraining DNA-replication licensing. Nature. 423, 885-9.
Zhu, C.Q., Blackhall, F.H., Pintilie, M., Iyengar, P., Liu, N., Ho, J., Chomiak, T., Lau, D., Winton, T., Shepherd, F.A. and Tsao, M.S., 2004. Skp2 gene copy number aberrations are common in non-small cell lung carcinoma, and its overexpression in tumors with ras mutation is a poor prognostic marker. Clin Cancer Res. 10, 1984-91.
Zielke, N., Kim, K.J., Tran, V., Shibutani, S.T., Bravo, M.J., Nagarajan, S., van Straaten, M., Woods, B., von Dassow, G., Rottig, C., Lehner, C.F., Grewal, S.S., Duronio, R.J. and Edgar, B.A., 2011. Control of Drosophila endocycles by E2F and CRL4(CDT2). Nature. 480, 123-7.

7.2.Complete results of the mass spectrometric analysis

Table 27 Results of the mass spectrometric analysis of Skp2 binding partners

Complete list of all hits of the mass spectrometric analysis of binding partners of Skp2. Analysis was performed as described in 4.2.5.2. Depicted are the name of the protein, the number of found peptides, the sequence coverage (SC) in percent and the score.

Protein	Number of Peptides	SC [%]	Score
Skp2	58	62.1	6115.9
Hsc70-4	51	60.8	4199
Hsp70Ab	40	55.5	3270
Hrb98DE	31	56.0	2927.3
Hsp70Bbb	34	55.2	2550.1
zip	40	25.3	2415.4
Hsp68	30	50.7	2356.8
FI05241p	22	45.0	1577.7
bel	24	41.7	1410.8
CG30122	20	23.9	1362.9
βTub56D	21	47.0	1087.8
Hsc70-3	15	21.3	1024.1
Hsp23	14	66.7	987.5
αTub84D	15	44.2	879.6
Act5C	13	43.1	757.6
msk	15	18.8	708
βTub60D	12	23.8	635.7
Lam	11	24.8	618.6
Chc	13	10.8	544.9
His2A	5	54.8	532.7
Karyβ3	12	16.5	529.2
Hsp26	8	53.4	525.9
Rpt5	11	32.5	504.6
SkpA	7	54.9	498.5
14-3-3ε	8	32.4	487.2
lig	7	7.5	487.1
Rpt2	9	26.7	484.4
Act57B	9	30.3	481.4
hyd	12	6.0	478.9
Rpn2	10	16.6	461.5
ZAP3	9	14.1	442.5
Rpn1	11	17.3	431.1
ref(2)P	6	15.7	411.8
cher	10	6.0	393.8
Hsp27	6	35.2	374.8
Rpn5	8	19.9	368.3
CG5787	8	11.5	356.7
Rpt4	7	26.2	349
Hsc70Cb	7	13.7	331.8
Ubi-p63E	5	61.8	330.2

Rpn9	5	18.3	320.4
Rpn3	6	17.0	309.1
eIF4G1	7	6.5	302.1
nop5	8	23.9	302
Rm62	6	11.0	299.3
RpL3	4	17.5	297.4
tral	5	13.3	288
Rpn13	6	30.7	281.6
lin19 (Cul1)	5	8.8	273.6
DnaJ-1	5	20.4	271.4
Pp2A-29B	5	12.0	268.9
Tep4	6	5.4	268.1
Rpt6	6	14.6	267.4
fmt	7	11.6	260.3
Rpt1	5	17.3	251.6
eIF4a	7	22.8	248.4
Rpt3	5	25.4	234.8
CCT3	6	14.9	233.7
CG9590	4	23.2	231.5
Kap-α3	3	8.8	223.4
RpA-70	4	8.5	217.5
Klp61F	6	8.3	210.1
rin	5	11.7	203.7
eIF2α	4	15.0	198.4
RpL30	5	53.2	197.7
RpS15Aa	4	40.8	196.8
RpL4	4	16.5	195.2
Rpn6	5	18.0	193.5
CG32165	5	5.5	190.6
Prosα6	4	23.7	186.6
Strica	4	10.4	182.4
rept	4	9.6	181.9
CG8963	3	7.1	179.9
CG5728	5	4.7	179.8
CG4747	5	12.5	178.7
ssx	4	10.9	177.8
Rpn8	5	22.8	174
Hsp22	3	21.8	170
Gfat2	3	5.7	166.9
RpS2	4	21.0	166
CG9684	3	7.0	162.1
eIF3m	3	10.1	161.4
CCT2	4	12.9	161.2
Rpn7	5	15.2	160.3
Rpn12	2	11.0	154.4
GEO07404p1	4	29.1	153.9
Pen	4	14.4	153.5

RpL23A	3	13.0	152.9
RpL23	2	18.6	147.4
Nup75	3	7.0	141.1
sqh	3	12.6	139.6
Rack1	3	10.1	139.6
Tom70	3	8.0	138.9
αCOP	4	3.6	137.6
RpL12	2	21.2	136.2
CNBP	2	22.4	133.8
RpS24	2	20.6	132.8
ACC	3	2.1	132.7
blp	2	22.7	131.4
awd	2	20.3	128.6
Gapdh1	2	4.2	127.7
sds22	3	14.4	124.6
blanks	3	11.5	124.4
CaMKII	3	9.4	124.2
Unc-76	3	14.9	123.4
RpS11	3	23.8	123.1
RpS6	3	13.3	122.7
Usp7	3	3.8	122.4
Rpn10	3	14.1	122
l(2)37Cc	3	13.8	120.4
CG2396	3	6.8	120
CG7546	3	5.0	119.8
Top2	3	2.8	119.2
Nup358	4	2.7	117.6
CCT7	3	7.7	115.4
Nop56	2	12.6	115.1
stwl	2	2.7	113.9
RpL22	3	7.7	113.3
Tnpo	2	4.4	112.1
tyf	3	3.1	112
Prosα4	3	16.5	110
Prosβ1	2	14.7	108.1
CG3071	2	5.2	107.8
Atx2	2	5.4	107.4
koi	2	3.4	107.2
Vap33	2	15.7	106.9
RpL36	2	17.4	106.4
RpL5	3	10.4	106.4
pod1	3	7.2	105.7
GEO11434p1	1	12.5	105.4
Nap1	3	12.2	105.3
GEO10457p1	2	15.5	104.9
MED17	3	8.6	104.7
SdhA	2	3.8	104.5

eIF4E1	1	9.3	104.2
Cdk2	3	14.0	103
RpL18	3	23.4	102.5
Gp210	2	1.5	101.5

7.3.List of figures

7.4.List of tables

8 Danksagung

Zunächst möchte ich Professor Dr. Frank Sprenger danken, der mir die Chance gegeben hat diese Arbeit in seiner Arbeitsgruppe durchführen zu dürfen und der im Laufe der Doktorarbeit und bei der Erstellung dieser Dissertation immer wieder hilfreiche Einfälle hatte.

Ich muss auch den jetzigen und ehemaligen Mitgliedern der AG Sprenger danken, auf deren Arbeit ich aufbauen konnte, um mein eigenes Projekt voranzutreiben. Ich hoffe, der Input den ich eingebracht habe war ebenso nützlich. Im Besonderen danke ich hierbei: Christiane Sprenger, für die Betreuung der Zellkultur und Hilfestellungen im Labor. Serena Herzinger, für ihre Mithilfe bei der Etablierung des Slmb-vhh Assay in ihrer Zeit als Praktikantin. Florian Hirsch, der sich in seiner Masterarbeit auf Effekte von Skp2 in Fliegengeweben konzentriert und damit das gesamte Themengebiet in der AG Sprenger erweitert hat und der mit seiner gründlichen und exakten Arbeitsweise eine echte Bereicherung war.

Im Laufe der Zeit durfte ich viele Studenten, seien es Bachelorarbeiten oder Projektpraktika, betreuen, die alle auf irgendeine Weise einen Beitrag an dieser Arbeit hatten. Ganz besonders bedanken möchte ich mich bei: Janina Narloch, die meine erste Bachelorstudentin war und eine der engagiertesten, fähigsten und ehrlichsten Menschen ist, die ich an der Universität Regensburg getroffen haben. Nicole Kabella, für ihre Arbeiten an CycE und für ihren nie nachlassenden Einsatz. Simon Eder, der die grundlegenden Arbeiten mit Cdt1 begonnen hat. Johanna „Jojo“ Heimbucher, die sich ebenfalls mit Cdt1 befasst hat und viele Experimente vorbereitet hat, die ich am Ende schließlich durchführen und mit aufnehmen konnte und die sich als sehr geschätzte Laborpartnerin und Kollegin erwiesen hat.

Der gesamten Hefe-Arbeitsgruppe, insbesondere Lea, Kathi, Franzi, Wolfgang und Phillip, möchte ich danken für die nette und freundliche Aufnahme, zahllose Hilfen, und die unkomplizierte Zusammenarbeit. Dank auch an die Hefe-TAs (Andrea, Adelheid und Antje), die verschiedene allgemeine Aufgaben im Labor übernahmen (Autoklavieren, Herstellung kompetenter Zellen, usw.), was eine große Unterstützung war. Arlette Hirsch danke ich für die immer kompetente und nette Hilfe in allen organisatorischen Sachen. Nina Weber und Sebastian Höckner danke ich dafür, mich auf die freie Stelle in der AG Sprenger überhaupt erst aufmerksam gemacht zu haben.

Frau Dr. Astrid Bruckmann und ihrem Team danke ich für die freundliche Unterstützung bei der Durchführung der MS-Analyse. Die entsprechenden Proben wurden in ihrem Labor aufbereitet und analysiert und die erste Auswertung wurde ebenfalls von ihr übernommen.

Dem Lehrstuhl Schneuwly, v.a. Dr. Susanne Fischer und Dr. Matthias Rass, danke ich für die Beantwortung von Fragen über die Fliegenarbeit, dem Bereitstellen verschiedenster Materialien wie z.B. DPX und der Benutzung des Stereomikroskops. Herrn Professor Dr. Stephan Schneuwly danke ich dafür, dass er die Rolle meines 2. Mentors übernommen hat.

Den Mitgliedern der AG Krahn, Giada Dogliotti, Olga Panichkina, Barbara Schwertner, Daniela Sparrer, Rui Sun und Lars Kullmann, danke ich für die gemeinsame Zeit und Zusammenarbeit, sowohl während als auch nachdem ich Teil dieser AG war. Bestimmte Erfahrungen verbinden. Arnab Sen danke ich für die Einarbeitungszeit. Ein Großteil meines methodischen Wissens durfte ich von ihm erlernen.

Schließlich danke ich noch Kinga Ay für die immer freundliche und kompetente Hilfe bei allen Fragen, die mit RIGeL zu tun hatten.

9 Widmung

Die letzten Jahre, seit ich diese Doktorarbeit begonnen habe, waren wohl mit die aufreibendsten und anstrengendsten, die ich bisher erlebt habe. Eine ganze Reihe Personen war daran beteiligt, dass ich trotz aller Rückschläge diese Arbeit zu Ende bringen konnte.

Meine Familie hat es mir überhaupt erst ermöglicht ohne Komplikationen zu studieren und mich auch während der Doktorarbeit weiter unterstützt. Außerdem haben sie mich auch in den schwierigeren Zeiten ertragen, was keine Kleinigkeit ist.

Sabine Feicht hat nicht nur erfolgreich Kupplerin gespielt, sie hat mir auch in der wahrscheinlich schlimmsten Zeit zugehört und mir dabei geholfen etwas zurück zu bekommen, was ich in dieser Zeit verloren hatte: einen anderen Blickwinkel.

Ina Hallstein, die wahrscheinlich die beste Freundin ist, die man sich nur wünschen kann, hat mir ebenfalls aus dieser Zeit geholfen. Ich kann nicht aufzählen wie wertvoll die Zeit mit ihr und ihre Ratschläge sind, sowohl innerhalb als auch außerhalb der Arbeit, und meine Hoffnung ist, dass ich ein wenig davon zurückgeben kann.

Und wie immer am Ende kommen natürlich Sybille „Bille“ Bauer, Oliver Edenharter und Christoph Schmidt, die mit mir einige der besten und auch einige der schlimmsten Zeiten durchgemacht haben, die immer ein offenes Ohr haben und auf die ich mich immer verlassen konnte.

All diese Menschen haben mir aufgeholfen, wenn ich gestrauchelt bin; haben mir den Weg gewiesen, wenn ich verloren war und haben mir Rat gegeben, wenn ich ratlos war. Ohne sie wäre diese Arbeit nicht zu Stande gekommen. Deswegen ist sie ihnen gewidmet.

Frage dich, wo des Menschen Ruhm beginnt und endet. Und sieh, dass sich mein Ruhm nur auf meine Freunde gründet.

William Butler Yeats

Danke